ISSN: 2067-3809

ACTA TECHNICA CORVINIENSIS
BULLETIN OF ENGINEERING

fascicule 3
[July-September]

TOME VI
[2013]

ACTA TECHNICA CORVINIENSIS
– BULLETIN of ENGINEERING
ISSN: 2067-3809 [CD-Rom, online]

http://acta.fih.upt.ro

UNIVERSITY "POLITEHNICA" TIMISOARA

FACULTY OF ENGINEERING – HUNEDOARA

5, Revolutiei,
331128 – Hunedoara,
ROMANIA

ACTA TECHNICA CORVINIENSIS – Bulletin of Engineering
Tome VI (Year 2013) – FASCICULE 3 [July–September]
ISSN 2067–3809

Aims & Scope

General Aims:

ACTA TECHNICA CORVINIENSIS – BULLETIN OF ENGINEERING is an international and interdisciplinary journal which reports on scientific and technical contributions.

Every year, in four online issues (fascicules 1 – 4), ACTA TECHNICA CORVINIENSIS – Bulletin of Engineering [e-ISSN: 2067-3809] publishes a series of reviews covering the most exciting and developing areas of engineering. Each issue contains papers reviewed by international researchers who are experts in their fields. The result is a journal that gives the scientists and engineers the opportunity to keep informed of all the current developments in their own, and related, areas of research, ensuring the new ideas across an increasingly the interdisciplinary field.

ACTA TECHNICA CORVINIENSIS – BULLETIN OF ENGINEERING publishes invited review papers covering the full spectrum of engineering. The reviews, both experimental and theoretical, provide general background information as well as a critical assessment on topics in a state of flux. We are primarily interested in those contributions which bring new insights, and papers will be selected on the basis of the importance of the new knowledge they provide.

Topical reviews in materials science and engineering, each including:

- *surveys of work accomplished to date*
- *current trends in research and applications*
- *future prospects.*

As an open-access journal ACTA TECHNICA CORVINIENSIS – Bulletin of Engineering will serve the whole engineering research community, offering a stimulating combination of the following:

- *Research Papers - concise, high impact original research articles,*
- *Scientific Papers - concise, high impact original theoretical articles,*
- *Perspectives - commissioned commentaries highlighting the impact and wider implications of research appearing in the journal.*

ACTA TECHNICA CORVINIENSIS – BULLETIN OF ENGINEERING encourages the submission of comments on papers published particularly in our journal. The journal publishes articles focused on topics of current interest within the scope of the journal and coordinated by invited guest editors. Interested authors are invited to contact one of the Editors for further details.

ACTA TECHNICA CORVINIENSIS – Bulletin of Engineering has been published since 2008, as an online supplement of the ANNALS OF FACULTY ENGINEERING HUNEDOARA – INTERNATIONAL JOURNAL OF ENGINEERING.

Now, the ACTA TECHNICA CORVINIENSIS – Bulletin of Engineering is a free-access, online, international and multidisciplinary publication of the Faculty of Engineering Hunedoara.

ACTA TECHNICA CORVINIENSIS – BULLETIN OF ENGINEERING exchange similar publications with similar institutions of our country and from abroad.

Audience & Coverage:

Scientists and engineers with an interest in the respective interfaces of engineering fields, technology and materials, information processes, research in various industrial applications. It publishes articles of interest to researchers and engineers and to other scientists involved with materials phenomena and computational modeling.

ACTA TECHNICA CORVINIENSIS – Bulletin of Engineering is a good opportunity for the researchers to exchange information and to present the results of their research activity. Scientists and engineers with an interest in the respective interfaces of engineering fields, technology and materials, information processes, research in various industrial applications are the target and audience of ACTA TECHNICA CORVINIENSIS – Bulletin of Engineering. It publishes articles of interest to researchers and engineers and to other scientists involved with materials phenomena and computational modeling.

The journal's coverage will reflect the increasingly interdisciplinary nature of engineering, recognizing wide-ranging contributions to the development of methods, tools and evaluation strategies relevant to the field. Numerical modeling or simulation, as well as theoretical and experimental approaches to engineering will form the core of ACTA TECHNICA CORVINIENSIS – Bulletin of Engineering's content, however approaches from a range of environmental science and economics are strongly encouraged.

ACTA TECHNICA CORVINIENSIS – Bulletin of Engineering appear in four issues per year and is open to the reviews, papers, short communications and breakings news inserted as Scientific Events, in the field of engineering.

Mission:

ACTA TECHNICA CORVINIENSIS – Bulletin of Engineering is an international and interdisciplinary journal which reports on scientific and technical contributions. The ACTA TECHNICA CORVINIENSIS – Bulletin of Engineering advances the understanding of both the fundamentals of engineering science and its application to the solution of challenges and problems in engineering and management, dedicated to the publication of high quality papers on all aspects of the engineering sciences and the management.

You are invited to contribute review or research papers as well as opinion in the fields of science and technology including engineering. We accept contributions (full papers) in the fields of applied sciences and technology including all branches of engineering and management.
Submission of a paper implies that the work described has not been published previously (except in the form of an abstract or as part of a published lecture or academic thesis) that it is not under consideration for publication elsewhere. It is not accepted to submit materials which in any way violate copyrights of third persons or law rights. An author is fully responsible ethically and legally for breaking given conditions or misleading the Editor or the Publisher.
The Editor reserves the right to return papers that do not conform to the instructions for paper preparation and template as well as papers that do not fit the scope of the journal, prior to refereeing. The Editor reserves the right not to accept the paper for print in the case of a negative review made by reviewers and also in the case of not paying the required fees if such will be fixed and in the case time of waiting for the publication of the paper would extend the period fixed by the Editor as a result of too big number of papers waiting for print. The decision of the Editor in that matter is irrevocable and their aim is care about the high content-related level of that journal.
The mission of the ACTA TECHNICA CORVINIENSIS - Bulletin of Engineering is to disseminate academic knowledge across the scientific realms and to provide applied research knowledge to the appropriate stakeholders. We are keen to receive original contributions from researchers representing any Science related field.
We strongly believe that the open access model will spur research across the world especially as researchers gain unrestricted access to high quality research articles. Being an Open Access Publisher, Academic Journals does not receive payment for subscription as the journals are freely accessible over the internet.

General Topics:

ENGINEERING
- ☐ Mechanical Engineering
- ☐ Metallurgical Engineering
- ☐ Agricultural Engineering
- ☐ Control Engineering
- ☐ Electrical Engineering
- ☐ Civil Engineering
- ☐ Biomedical Engineering
- ☐ Transport Engineering
- ☐ Nanoengineering

CHEMISTRY
- ☐ General Chemistry
- ☐ Analytical Chemistry
- ☐ Inorganic Chemistry
- ☐ Materials Science & Metallography
- ☐ Polymer Chemistry
- ☐ Spectroscopy
- ☐ Thermo-chemistry

ECONOMICS
- ☐ Agricultural Economics
- ☐ Development Economics
- ☐ Environmental Economics
- ☐ Industrial Organization
- ☐ Mathematical Economics
- ☐ Monetary Economics
- ☐ Resource Economics
- ☐ Transport Economics
- ☐ General Management
- ☐ Managerial Economics
- ☐ Logistics

AGRICULTURE
- ☐ Agricultural & Biological Engineering
- ☐ Food Science & Engineering
- ☐ Horticulture

COMPUTER & INFORMATION SCIENCES
- ☐ Computer Science
- ☐ Information Science

EARTH SCIENCES
- ☐ Geodesy
- ☐ Geology
- ☐ Hydrology
- ☐ Seismology
- ☐ Soil science

ENVIRONMENTAL
- ☐ Environmental Chemistry
- ☐ Environmental Science & Ecology
- ☐ Environmental Soil Science
- ☐ Environmental Health

BIOMECHANICS & BIOTECHNOLOGY
- ☐ Biomechanics
- ☐ Biotechnology
- ☐ Biomaterials

MATHEMATICS
- ☐ Applied mathematics
- ☐ Modeling & Optimization
- ☐ Foundations & Methods

Invitation:

We are looking forward to a fruitful collaboration and we welcome you to publish in our ACTA TECHNICA CORVINIENSIS - Bulletin of Engineering. You are invited to contribute review or research papers as well as opinion in the fields of science and technology including engineering. We accept contributions (full papers) in the fields of applied sciences and technology including all branches of engineering and management.
Submission of a paper implies that the work described has not been published previously (except in the form of an abstract or as part of a published lecture or academic thesis) that it is not under consideration for publication elsewhere. It is not accepted to submit materials which in any way violate copyrights of third persons or law rights. An author is fully responsible ethically and legally for breaking given conditions or misleading the Editor or the Publisher.

5th Anniversary Celebration:

We are very pleased to inform that our journal ACTA TECHNICA CORVINIENSIS - Bulletin of Engineering completed its five years of publication successfully [2008-2012, Tome I-V]. In a very short period it has acquired global presence and scholars from all over the world have taken it with great enthusiasm.
We are extremely grateful and heartily acknowledge the kind of support and encouragement from all contributors and all collaborators!

ACTA TECHNICA CORVINIENSIS - BULLETIN of ENGINEERING

ISSN: 2067-3809 [CD-Rom, online]

ACTA TECHNICA CORVINIENSIS – Bulletin of Engineering
Tome VI (Year 2013) – FASCICULE 3 [July–September]
ISSN 2067–3809

Editorial & Advisory Board

Review process & Editorial Policy

ACTA TECHNICA CORVINIENSIS - Bulletin of Engineering is dedicated to publishing material of the highest engineering interest, and to this end we have assembled a distinguished Editorial Board and Scientific Committee of academics, professors and researchers.

ACTA TECHNICA CORVINIENSIS - Bulletin of Engineering publishes invited review papers covering the full spectrum of engineering. The reviews, both experimental and theoretical, provide general background information as well as a critical assessment on topics in a state of flux. We are primarily interested in those contributions which bring new insights, and papers will be selected on the basis of the importance of the new knowledge they provide.

The editorial policy of ACTA TECHNICA CORVINIENSIS - Bulletin of Engineering is to serve its readership in two ways. Firstly, it provides a critical overview of the current issues in a well-defined area of immediate interest to materials scientists. Secondly, each review contains an extensive list of references thus providing an invaluable pointer to the primary research literature available on the topic. This policy is implemented by the Editorial Board which consists of outstanding scientists in their respective disciplines. The Board identifies the topics of interest and subsequently invites qualified authors. In order to ensure speedy publication, each material will be report to authors, separately, thought Report of the Scientific Committee. For an overview of recent dispatched issues, see the ACTA TECHNICA CORVINIENSIS - Bulletin of Engineering issues.

ACTA TECHNICA CORVINIENSIS - Bulletin of Engineering encourages the submission of comments on papers published particularly in our journal. The journal publishes articles focused on topics of current interest within the scope of the journal and coordinated by invited guest editors. Interested authors are invited to contact one of the Editors for further details.

The members of the Editorial Board may serve as reviewers. The reports of the referees and the Decision of the Editors regarding the publication will be sent to the corresponding authors.

The evaluated paper may be recommended for:

- *Acceptance without any changes - in that case the authors will be asked to send the paper electronically in the required .doc format according to authors' instructions;*
- *Acceptance with minor changes - if the authors follow the conditions imposed by referees the paper will be sent in the required .doc format;*
- *Acceptance with major changes - if the authors follow completely the conditions imposed by referees the paper will be sent in the required .doc format;*
- *Rejection - in that case the reasons for rejection will be transmitted to authors along with some suggestions for future improvements (if that will be considered necessary).*

The manuscript accepted for publication will be published in the next issue of ACTA TECHNICA CORVINIENSIS - Bulletin of Engineering after the acceptance date.

ACTA TECHNICA CORVINIENSIS - Bulletin of Engineering accept for publication unpublished manuscripts on the understanding that the same manuscript is not under simultaneous consideration of other journals. Publication of a part of the data as the abstract of conference proceedings is exempted.

All the authors and the corresponding author in particular take the responsibility to ensure that the text of the article does not contain portions copied from any other published material which amounts to plagiarism. We also request the authors to familiarize themselves with the good publication ethics principles before finalizing their manuscripts.

Manuscripts submitted (original articles, technical notes, brief communications and case studies) will be subject to peer review by the members of the Editorial Board or by qualified outside reviewers. Only papers of high scientific quality will be accepted for publication. Manuscripts are accepted for review only when they report unpublished work that is not being considered for publication elsewhere.

ACTA TECHNICA CORVINIENSIS - BULLETIN of ENGINEERING

ISSN: 2067-3809 [CD-Rom, online]

ACTA TECHNICA CORVINIENSIS – Bulletin of Engineering
Tome VI (Year 2013) – FASCICULE 3 [July–September]
ISSN 2067–3809

Regional Associate Editors & Collaborators

The Editor and editorial board members do not receive any remuneration. These positions are voluntary.
We are very pleased to inform that our journal ACTA TECHNICA CORVINIENSIS - BULLETIN of ENGINEERING is going to complete its five years of publication successfully. In a very short period it has acquired global presence and scholars from all over the world have taken it with great enthusiasm. We are extremely grateful and heartily acknowledge the kind of support and encouragement from you.
ACTA TECHNICA CORVINIENSIS - BULLETIN of ENGINEERING is seeking qualified researchers as members of the editorial team. Like our other journals, ACTA TECHNICA CORVINIENSIS - BULLETIN of ENGINEERING will serve as a great resource for researchers and students across the globe. We ask you to support this initiative by joining our editorial team. If you are interested in serving as a member of the editorial team, kindly send us your resume to redactie@fih.upt.ro.

ACTA TECHNICA CORVINIENSIS - BULLETIN of ENGINEERING

ISSN: 2067-3809 [CD-Rom, online]

ACTA TECHNICA CORVINIENSIS – Bulletin of Engineering
Tome VI (Year 2013) – FASCICULE 3 [July–September]
ISSN 2067–3809

Scientific Committee Members & Reviewers

Members from SLOVAKIA

Štefan NIZNIK
Technical University of KOŠICE, Faculty of Metallurgy, Department of Materials Science - KOŠICE
Karol VELIŠEK
Slovak University of Technology BRATISLAVA, Faculty Materials Science & Technology - TRNAVA
Peter KOŠTÁL
Slovak University of Technology - BRATISLAVA, Faculty Materials Science & Technology - TRNAVA
Juraj ŠPALEK
University of ZILINA, Faculty of Electrical Engineering - ZILINA
Vladimir MODRAK
Technical University of KOSICE, Faculty of Manufacturing Technologies - PRESOV
Michal HAVRILA
Technical University of KOSICE, Faculty of Manufacturing Technologies - PRESOV
Jozef NOVAK-MARČINCIN
Technical University of KOSICE, Faculty of Manufacturing Technologies - PRESOV
Ľubomir ŠOOŠ
Slovak University of Technology in BRATISLAVA, Faculty of Mechanical Engineering - BRATISLAVA
Miroslav BADIDA
Technical University of KOŠICE, Faculty of Mechanical Engineering - KOŠICE
Ervin LUMNITZER
Technical University of KOŠICE, Faculty of Mechanical Engineering - KOŠICE
Tibor KVAČKAJ
Technical University KOŠICE, Faculty of Metallurgy - KOŠICE
Ľudovít KOLLÁTH
Slovak University of Technology in BRATISLAVA, Manufacturing Systems Institute - BRATISLAVA
Ladislav GULAN
Slovak University of Technology, Institute of Transport Technology & Designing - BRATISLAVA
Dušan HUSKA
Slovak Agricultural University, Faculty of European studies & Regional Development - NITRA
Miroslav VEREŠ
Slovak University of Technology in BRATISLAVA, Faculty of Mechanical Engineering - BRATISLAVA
Milan SAGA
University of ŽILINA, Faculty of Mechanical Engineering - ŽILINA
Imrich KISS
Institute of Economic & Environmental Security, University of Security Management - KOŠICE
Otakav BOKŮVKA
University of ŽILINA, Faculty of Mechanical Engineering - ŽILINA
Michal CEHLÁR
Technical University KOSICE, Faculty of Mining, Ecology, Process Control & Geotechnologies - KOSICE
Pavel NEČAS
Armed Forces Academy of General Milan Rastislav Stefanik - LIPTOVSKÝ MIKULÁŠ
Milan DADO
University of ŽILINA, Faculty of Electrical Engineering - ŽILINA
Jozef PILC
University of ŽILINA, Faculty of Mechanical Engineering - ŽILINA

Members from ITALY

Alessandro GASPARETTO
University of UDINE, Faculty of Engineering - UDINE
Alessandro RUGGIERO
University of SALERNO, Department of Mechanical Engineering - SALERNO
Adolfo SENATORE
University of SALERNO, Department of Mechanical Engineering - SALERNO

ACTA TECHNICA CORVINIENSIS – Bulletin of Engineering
Tome VI (Year 2013) – FASCICULE 3 [July–September]
ISSN 2067–3809

CONTENT of FASCICULE 3 / 2013 [JULY–SEPTEMBER]

Abstract: The value of pH is an important quality control parameter measured in industry and research. The quality of the measurement process can be evaluated in the same manner as any manufacturing process. The aim of submitted work is to analyze the quality of pH measurement. MSA, analysis of uncertainty, t-test and ANOVA were used. Four appraisers measured pH of 10 solutions of HCl and HNO_3. The pH meter GRYF 208L with standard electrode THETA 90 HC 113 were used as measurement equipment. Analyzed the process of pH measurement is capable according to MSA. The fine discrimination and high accuracy of used equipment and high pH variability of measured solutions are reasons of high process capability. Low value of index %AV witness good competence of all appraisers. Positive effect of appraisers on the capability was confirmed by t-test and ANOVA.

Abstract: In today's world, since the rise of internet most of the communication and information sharing is done over the web. With the increasing unauthorized access of confidential data, information security is of utmost importance. Thus, a big issue now a day is to reduce the chances of information detection during transmission. Cryptography deals with encryption of message but its presence arouse suspicion about the communication, on the other hand, Steganography hides the existence of message in such a way that no one can even guess about the communication going on between two parties. A large variety of Steganographic techniques exists for hiding data in digital images. In this paper, an overview on Steganography is presented and it also covers different existing techniques on Image Steganography and their relative strong and weak points. Steganography benefits and applications are also discussed.

Abstract: Among metallic matrices, Aluminum based matrix remains the most explored metal matrix material for the development of MMCs. This is primarily due to the broad spectrum of properties offered by aluminum based matrix composites at low processing cost. The mechanical behavior of aluminum alloy (6063) - alumina particulate composites developed using two step stir casting was investigated. AA 6063 - Al_2O_3 particulate composites having 6, 9, 15, and 18 volume percent of Al_2O_3 were produced. It is observed that AA 6063/Al_2O_{3p} composites having low porosity levels (≤ 3.51 %porosity) and a good uniform distribution of the alumina particulates in the matrix of the AA 6063 were produced. The tensile strength, yield strength, and hardness increased with increase in alumina volume percent while the strain to fracture and fracture toughness decreased with increasing volume percent alumina.

Abstract: When a transformer is energized by the supply voltage, a high current called transient inrush current which it may raise to ten times of the transformer full load current could be drawn by the primary winding. This paper discusses a microcontroller circuit with the intention of controlling and limiting the inrush current for a transformer by the method of ramping up the supply voltage feeding to the transformer primary. Simulations and the experimental results show a significant reduction of inrush current when the ramping up voltage is applied to the three-phase transformer load. Inrush current could be almost eliminated if choosing a correct switching step rate.

Abstract: The steady flow of an electrically conducting, incompressible micropolar fluid in a narrow gap between two concentric rotating vertical cylinders, with porous lining on inside of outer cylinder, under an imposed axial magnetic field is studied. Beavers and Joseph slip condition is taken at the porous lining boundary. The velocity profiles, coefficient of skin friction on the cylinders are calculated. The effects of Hartmann number, the porous lining thickness parameter, coupling number, couple stress parameters and Reynolds number on azimuthal velocity, micro-rotation component and coefficient of skin friction on cylinders are depicted through graphs.

Abstract: An article deals with the experimental determination of milling model for thin-walled parts. The determination of milling model is one of basic characteristics for calculating cutting forces and chip thickness. The calculation of milling model is analytically and numerically by finite element method. Experiment is performed with modal hammer. With modal hammer is determined dynamic elasticity for work-piece and tool. In the first section is summarized the basic knowledge of thin-walled parts. Inn experimental part is described Frequency Response Function and application of this technique. The last part of this work is to evaluate the experiment, which compared different techniques to determinate milling model during machining thin-walled parts.

Abstract: This paper analyzes effect of biodiesel on engine power, fuel consumption, emissions: nitrogen oxides (NOx) and particulate matter (PM) while the effective power is maintain constant. Biodiesel is a renewable, alternative diesel fuel of domestic origin derived from a variety of fats and oils by a transesterification reaction. Considering global energy policies, more and more governments try to increase the usability of biodiesel for powering motor vehicles. Cars manufacturing companies and private users are reluctant in using biodiesel, especially in current engines. Because of this, it is difficult to achieve the targets of increases the usage of biodiesel in ICE. There is a lack of knowledge on emissions of an engine what is fueled with biodiesel. An advantage of biodiesel is its potential to significantly reduce most regulated exhaust emissions, including particulate matter (PM), with the exception of nitrogen oxides (NO_x).

ACTA TECHNICA CORVINIENSIS – Bulletin of Engineering, Fascicule 3/2013 [July-September/2013] *includes scientific papers presented in the sections of Conference on:*

- *THE INTERNATIONAL SYMPOSIUM ON ENVIRONMENTAL MANAGEMENT AND MATERIAL FLOW MANAGEMENT – EMFM2012, organized in Zenica, BOSNIA & HERZEGOVINA (7-9 June 2012), jointly by the Technical Faculty in Bor, University of Belgrade (SERBIA), Faculty of Mechanical Engineering, University of Zenica (BOSNIA & HERZEGOVINA) and Environmental Campus Birkenfeld, University of Applied Sciences Trier (GERMANY). The new current identification numbers of papers are #1-4, in the content list.*
- *THE CHINESE - ROMANIAN CONFERENCE on APPLIED SCIENCES in DEFENCE – ASD 2012, organized in Hunedoara, ROMANIA (15 – 16 June 2012), jointly by the Faculty of Engineering Hunedoara, University "Politehnica" of Timisoara, ROMANIA and Military Economics Academy of Wuhan, CHINA, in cooperation with Scientific Interdisciplinary Values for Education and Research Society, Timisoara, ROMANIA. The current identification number of paper is #14, in the content list.*
- *THE INTERNATIONAL CONFERENCE MOTOR VEHICLE & TRANSPORTATION – MVT 2012, organized in Timisoara, ROMANIA (7-9 November 2012), hosted by the "Politehnica" University of Timisoara, Mechanical Engineering Faculty, Road Vehicles and Transportation Department, under SIAR (Society of Automotive Engineers of Romania) support. The new current identification numbers of papers are #9-13 and #22-24, in the content list.*

Also, ***ACTA TECHNICA CORVINIENSIS – Bulletin of Engineering, Fascicule 3/2013 [July-September/2013]*** *includes, also, original papers submitted to the Editorial Board, directly by authors or by the regional collaborators of the Journal [papers # 5 – 8, # 15 - 21 and # 25].*

ACTA TECHNICA CORVINIENSIS – BULLETIN of ENGINEERING

ISSN: 2067-3809 [CD-Rom, online]

ACTA TECHNICA CORVINIENSIS – Bulletin of Engineering
Tome VI (Year 2013) – FASCICULE 3 [July–September]
ISSN 2067–3809

[1.] Šefket GOLETIĆ, [2.] Nusret IMAMOVIĆ, [3.] Heidy SCHWARCZOVÁ

THE DUST EMISSION CONTROL IN PRODUCTION OF FERROALLOYS BY APPLICATION OF BEST AVAILABLE TECHNICS

[1,2.] FACULTY OF MECHANICAL ENGINEERING, UNIVERSITY OF ZENICA, BOSNIA & HERZEGOVINA
[3.] UNIVERSITY OF CENTRAL EUROPE IN SKALICA, KRÁL'OVSKÁ 386/11, 909 01 SKALICA, SLOVAKIA

ABSTRACT: In the production ferosilicon alloys produced as a byproduct of a very fine gray dust, which consists of spherical amorphous particles non cristalic silicon dioxide (SiO_2). Created in the process of reduction of quartz in the metallic silicon electrical furnace by adding a reducing carbon materials (wood chips, coal, metallurgical coke and coal) at a temperature of about 2000^{0}C. This paper presents the results of application of best available techniques to control dust emissions in the production of ferroalloys in the example plant "Steelmin BH" in Jajce, Bosnia. The new technical solution drainage and purification of flue gases is reduced emissions of dust behind the filters below 5 mg/m^3, which is the threshold limit values for emissions of SiO_2 and its connections to the national environmental standards and BAT EU recommendations.
KEYWORDS: ferroalloys, the emission of dust, the filter system

INTRODUCTION

In the production ferosilicon alloys produced as a byproduct of a very fine gray dust, which consists of non cristalic spherical particles of amorphous silicon dioxide (SiO_2). Created in the process of reduction of quartz in the metallic silicon electrical furnace by adding a reducing ugljeničkih materials (wood chips, coal, metallurgical coke and coal) at a temperature of about 2000 ^{0}C [1].

BiH has a centuries-old tradition in the production of ferroalloys and another from 1908 it was present on the European market as a significant producer of Silicon. The company "Elektrobosna" Jajce was one of the major European manufacturers of Silicon (FeSi) and silicon metal (Si-metal) until the termination of the 1992. As part of this company was the production of ferro-alloy plant with electric-furnace 4 and 5, which was built and put into operation during the period between the 1970 and 1973. Electric-furnace 4, installed power 30 [MVA] and the construction of "Ing Leone Tagliaferri" of Milan, was put into operation 1971. Electric-furnace 5, power 48 [MVA] and the construction of "ELKEM" from Oslo, was put into operation. The maximum annual production capacity totaled 41,000 tons of ferro-alloys.

Investment capital through the company's Steel Minerals (Steelmin), Perth, Western Australia purchased a drive with electro-reductive furnace 4 and 5 in order to start production of ferroalloys in the newly formed company "BH Steelmin" Jajce.

This company has initiated activities to revitalize this facility provided that the application of efficient waste gas dedusting solutions based on the best available techniques (BAT recommendations of the EU). The goal is to achieve the emission of dust behind the filters below 5 mg/m^3, which is permissible emission limit value for SiO_2 and its connections to the national environmental standards and recommendations of the EU BAT [2].

Feasibility study and study on the effects on the environment have shown a technological, economic and environmental revitalization of the justification of this facility and existing facilities, the application of specific measures for the technological and environmental improvements, the production of ferroalloys has perspective and important area of product placement in the European market. The existing industrial infrastructure, natural stocks of raw materials in the environment, human resources and acquired a tradition in the production of ferro-alloys constitute a solid basis for the revitalization and start production in the respective facility for the production of ferroalloys. Applying the most effective technical solutions for waste gas treatment based on BAT for the non-metal industry towards achieving this goal.

BASIC TECHNICAL AND TECHNOLOGICAL CHARACTERISTICS OF FERROALLOYS PRODUCTION IN FACILITY "BH STEELMIN" JAJCE

Ferroalloys production will take place in two existing electro-reduction furnace that will revitalize and improve the technological application of efficient technical systems for sewage and waste gases. Otherwise, the electric reducing furnace is a complex

technical and technological system for the production of ferroalloys, which contains the following basic technological equipment:

1. *Equipment for supplying electricity and electrical equipment to create a network port, which encompasses a system of electrodes and electrode carrier,*
2. *Equipment to add (dosage) of feedstock, such as quartz, reduction material and other necessary components,*
3. *The body of an electric arc furnace with Shaft, bushing and cap that protects the furnace equipment toplotng of radiation,*
4. *Equipment for removal of dissolved material and slag from the furnace,*
5. *The system of sewerage and waste flue gases from the furnace.*

Ferroalloys production begins by preparing raw materials (quartz, wood chips, coal, coal, metallurgical coke, iron filings, etc.). Raw materials are mixed together in previously technology defined stoichiometric relationship. Mixed batch is added to the electro-reduction furnace in which the reagents warm up to temperatures around 2000°C by passing electric current through a batch furnace. The melting furnace is made of quartz at a temperature of about 2000°C using three graphite electrodes powered electricity, ie electric arc that forms between the electrodes (by passing electricity through a batch furnace).

Ferroalloy production process is based on the direct reduction of quartz or quartzite in the furnace by adding carbon materials: wood chips, coal, lignite mining and metallurgical coke. When raw materials are heated to the required temperature chemical reactions take place with quartz reduction of carbon from carbon materials. The production process takes place in the oven continuously dosing (filling) mixtures of feed materials from the furnace through the dosing silo tubes arranged around the rim caps furnace. Obtained ferroalloys (eg. Silicon) is collected at the bottom of the furnace and electrical discharges into the transmission pan. Then drain opening in the furnace is closed with a clay cap, a process in the furnace continues to cyclic and continuous dosing of raw materials into the furnace creates a new volume of the product (liquid ferro-alloys) which is fed back to the aperture opening oven for about an hour. During this time, drain the pot is filled with liquid and shipment of ferroalloys in the cooling and processing of commercial grain. The technological processes of production are added is shown in Figure 1.

In the process of melting quartz ore in a reducing furnace electro-generated waste flue gases with high content of fine dust, which is taken in the ventilation system in order to bag filter dust separation from gases. Makes a very fine dust dispersed, amorphous SiO_2. Individual particles of SiO_2 are extremely small, 50-100 times smaller than cement particles and have an average size of 0.1 to 0.2 μm. If these particles are removed from waste gases, can cause significant environmental and health effects in humans and ecosystems in the region.

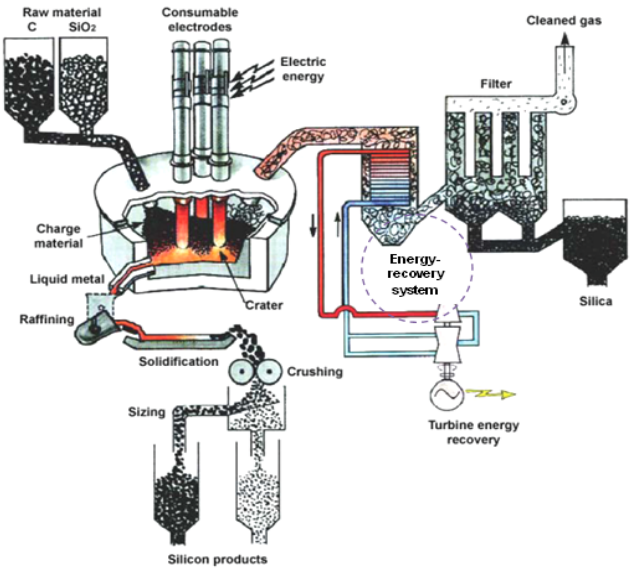

Figure 1. Elements of electro-reduction process ferro-silicon [2]

It is assumed that emissions of dust and gases from the electric furnace are about 94% of the total emissions from the plant for production of ferroalloys. Unloading, internal transportation and manipulation of raw materials may appear uncontrolled emissions of dust, which can have an impact only in the workplace [2].

IMPROVING THE EFFICIENCY OF TECHNICAL SYSTEMS WASTE GASES TREATMENT

Technical system for purification of waste gases generated in the electric furnace is a reducing type CEAG - dust collector with a conventional filter bags in which to perform purification of waste gases before their release into the ambient air. The efficiency of this filter system does not meet the new regulations on the allowable emission limit values. The values for emissions during operation of the plant usually varied between 50 and 100 mg/Nm^3, which is well above the allowable emission limit value presented from 5 mg/Nm^3. In order to improve the efficiency of the existing technical system for dedusting the waste gases (bag filter with the preliminary separators for separation of larger particles and sparks) and reduction of dust emissions below the specified limit access to a new conceptual design solutions to upgrade certain structural elements and improve the technical efficiency of existing treatment systems waste gases generated in a reducing electric furnaces.

A new technical solution drainage and purification waste gases is based on applying the best technical solutions given in the BAT for non-metallic industry. New technical systems for waste gas purification have the following main technical characteristics:

- *total volume of the exhaust flue gases is Vo = 589 000 Nm^3/h,*
- *load on the filter surface is 30.51 m^3/m^2 x h,*
- *flue gas temperature is max. 240 °C*
- *P_{gas} = 5016 Pa,*
- *NMct = 3 MW,*
- *filter system has 14 chambers and each chamber was built at 288 filter bag measuring 149 m^2 per bag,*

- *filter bags are manufactured from materials provided by a mixture of glass fibers with a PTFE membrane (Microporous Teflon Membrane), which have a guaranteed minimum efficiency of 99.99%, because their membranes have a pore size below 2 μm,*
- *length is 10.5 m and each sack was supplied with 10 rings, which give the bag shape,*
- *the life of the bag is about 10 years,*
- *lower power consumption,*
- *such a filter chamber was provided container for collecting dust, which is transported in the pneumatic pipeline tower pelleting and storage to loading into trucks for delivery to customers as a secondary raw material,*
- *dust collection hopper holds approximately 225 m^3,*
- *accumulation of dust is provided for approximately 16 h,*
- *cleaned gases from the filter system drains through the stack into the surrounding air,*
- *content of dust in the rest of the purified gases behind the filters is max. 2-5 mg/Nm^3*
- *control dust emissions is done by installing automatic measuring device for the continuous registration of dust concentration in the stack,*
- *management of work filter system is fully automated and computer driven.*

Waste gases resulting in a reducing electric furnaces is transported 160 pipeline length of his specially designed filter system in front of which there is a cyclone separator. Each furnace has its own pipeline to transport of smoke (waste) gases into the filter system and on the two pipelines is one cyclone for preliminary separation of larger particles and sparks (as it would damage the bags).

The pipeline is made by cooling the gas. Gases due to pass through the filter system of bags and cleaned so it drains through the stack into the ambient air. Bags are made of glass fiber and virtually retain the smallest particles of dust, so that the concentration of particles on the mechanical output from the filters below 5 mg/m^3, which is the projected value of this type of technical systems for dust collection.

Limit values for emissions of SiO_2 and its compounds is 5 mg/m^3 at a mass flow rate greater than 25 g/h, according to national regulations and BAT for non-metal industry.

The dust is retained in the bag and shakes the bag with air-powered fan (who shall in turn release and withdrawal of air) and deposited in a receiving tank for collecting dust each chamber (14 chambers). From these tanks the dust is still transported via screw conveyors in the plant for palletizing. Pelleted dust, known as microsilica, is used as secondary raw materials.

Performance management systems filter is fully automated. The degree of efficiency of the new (improved) CEAG technical system for dedusting of smoke gases is very high and under normal conditions is approximately 99.99%.

Emission of dust behind this filter is 2-5 mg/m^3, which is below the limit values according to national regulations and BAT [2,3]. The total dust emission varies between 0.2 and 0.3 kg/t of ferro-alloys, which is within the limits specified in the Reference Document on Best Available Techniques in the Non Ferrous Metals Industries, December, 2001.

The prescribed criteria for the emission of dust 5 mg/m^3 as a matter of good practice in facilities that operate in the European Union, such as: FERROATLANTICA, ELKEM, FESIL, VA POCKING, etc.). This criterion is taken as a national standard for the emission of dust SiO_2 in B&H [3].

Fabric filter systems are widely used and recommended within the industrial sector for the production of ferroalloys, due to their high efficiency in controlling emissions of fine particles that are produced in the smelting operations. Numerous commercial filters designed using different types of filtration bags which in principle should realize low emission levels below 5 mg/m^3. It primarily depends on the filter mode, filtering surface, the way of maintenance, as well as the temperature of smoke gas that filters the quality is up to max. 280°C. Providing better maintenance prolongs the working life of the bag about 10 years, and the pressure drop is about 2.5 kPa.

Featured in the bag filter dust is gray, which consists of very fine dispersed, amorphous SiO_2 particles, size <45 um. This dust is happiness in the literature under various names: mikrosilica, condensed silica fume (CSF), silica fume (SF), etc. Microsilica is actually a commercial name for SiO_2 dust. It consists of a non cristalic spherical particles of amorphous SiO_2. Because of the fineness of particles, large surface area, and high content of SiO_2, microsilica is highly valued secondary raw materials used in the manufacture of cement, concrete waterproofing, special materials for the repair of damaged buildings, refractory materials and other specialty building materials. Quality Microsilica specified in ASTM C 1240, the Norwegian Standard NS3045, CAN/CSA-A23.5-M Canadian standards and European standards.

Amounts of dust (microsilica) that separates the process of production of ferro-alloys is about 200 to 300 kg SiO2/1.000 kg, depending on the type of raw materials, products and technology of applied. Thus, for maximum production of 41 000 t/y of ferro-alloys can be expected around 8200-12300 t/microsilica, which is prepared and used as a secondary raw material for production of construction materials.

Since the gaseous pollutants are emitted dominantly CO_2 in ambient air and the exhaust flue gases do not contain significant quantities of SO_2, NOx, CO, HF, polycyclic aromatic hydrogen (PAH) and volatile organic compounds (VOCs). Air emissions can be significantly reduced by improvements (process redesign) the production of ferroalloys [4,5].

CONCLUSIONS

The following table shows the air emissions in relation to the design techniques of charging electric furnace.

Table 1. Air emissions from the standpoint of design techniques to fill according to BAT [2].

Pollutant	Emission (per ton of product)			
	Unit	The standard technique of filling	Improved technique of filling	Improved technique of filling + High temperature gas drainage
CO	kg/t	4.8	3.5	0.5
PCDD/F	μg/t	5.5	1.1	0.2
NOx	kg/t	-	7	8.3
PAH	g/t	1.21	0.01	0.01

The presented results show that the use of technological improvements and controlled management process significantly reduces the emission of gaseous pollutants.

REFERENCES

[1.] Goletić, Š., Imamović, N.: Plan aktivnosti sa mjerama i rokovima za postupno smanjenje emisija odnosno uticaja na okoliš i za usaglašavanje sa najboljom raspoloživom tehnikom za pogone i postrojenja za proizvodnju ferolegura firme "Steelmin BH" Jajce, Univerzitet u Zenici, 2011.

[2.] Integrated Pollution Prevention and Control (IPPC): Reference Document on Best Available Techniques in the Non Ferrous Metals Industries, European Comission, December 2001.

[3.] Pravilnik o graničnim vrijednostima emisije zagađujućih materija u zrak ("Službene novine Federacije BiH", broj: 12/05).

[4.] Smjernice za najbolje raspoložive tehnike-mjerenje emisija i korištenje podataka o emisijama, Mjerenje emisija i korištenje podataka o emisijama, Projekt CARDS 2004.

[5.] A Driver for Environmental Performance in Industry, European Conference on "The Sevilla Process, Energy use and process integrated BAT measures illustrated by examples from the Non Ferrous Metals Industries BREF Ludwig Finkeldei European IPPC Bureau Stuttgart, 6 and 7 April 2000.

ISSN: 2067-3809 [CD-Rom, online]

ACTA TECHNICA CORVINIENSIS – Bulletin of Engineering
Tome VI (Year 2013) – FASCICULE 3 [July–September]
ISSN 2067–3809

[1.] Vladimir CVETKOVSKI, [2.] Silvana DIMITRIJEVIC, [3.] Vesna CONIC,
[4.] Suzana DRAGULOVIC, [5.] Zdenka STANOJEVIC-SIMSIC, [6.] Ruzica LEKOVSKI

DISTRIBUTION OF ARSINE IN THE PROCESS OF COPPER CEMENTATION

[1-6.] MINING AND METALLURGY INSTITUTE BOR, ZELENI BULEVAR 35, BOR, SERBIA

ABSTRACT: The paper presents results of the of arsine distribution in the process of cementation of copper from the underground mining water and waste metallurgical solutions and the possibility of appearance of toxic gas arsine. Investigations were conducted on synthetic solutions similar to the solutions used in copper cementation. It was found that the more rigorous conditions than the limit (the acidity of water at the entrance to the cementation plant of pH = 1.5 and arsenic content of 1 g/dm^3) arsine does not separated from the processes of cementation. Investigations have been showed that there no conditions for toxic arsine emissions into the atmosphere, during the copper cementation from underground mine water and waste solution. Investigation is necessary to be continued for determining maximal content of arsenic and acidity of cementation solution, which should not be exceed, with aim to prevent arsine emissions into the atmosphere. In the same time it was explained, that presence of arsenic in the cement-copper is a result of arsenic ions cementation on iron scrap.
KEYWORDS: copper cementation, arsenic, underground mining water

INTRODUCTION

Based on theoretical and experimental data [1,2], it should be expected the release of the arsine in the cementation process of copper from underground mining waters and metallurgical waste solution and waste waters, for the defined boundary conditions. Starting from this conclusion, it was laboratory investigated possibility of extraction arsenic paired solution from plant for copper-sulfate; underground mining water and prepared solution with the desired acidity and arsenic content. Next phases of work were investigated:

- ☐ Change the content of arsenic in water cementation with decreasing acidity.
- ☐ Release arsenic for these boundary conditions cementation.
- ☐ Cementation of arsenic on the iron scrap.

CHANGES OF ARSENIC CONTENT IN CEMENTATION WATER - Characteristics of water for cementation

Department of cementation in the service mining shaft processed underground mining water in a quantity of 130 m^3/h, with the content (g/dm^3): Cu = 0.1-0.2; As = 0.001; Fe = 0.2; pH = 2.9-3.1 and metallurgy waste solution in a quantity of 1.5 m^3/h, with copper and harmful content of impurities (g/dm^3): Cu = 1.0-4.5; H_2SO_4 = 20-35; As = 0.01-0.07. Those results are obtained by measuring flow rate by Thomson's spillway at the entrance to cementation. Waters are mixed and put in the process with acidity pH = 2.3-2.6 and the arsenic content of 0.002 g/dm^3. The maximum arsenic content in the entrance at the cementation is 0.004 g/dm^3 and it can be achieved when the arsenic content in the waste solution electrolysis reached a value of 0.2 g/dm^3.

Change the content of arsenic in arsenic salt solution - Usage of sodium-arsenate solutions

For experimental work synthetic arsenic solution has been prepared. For the preparation of 0.25dm^3 aqueous sodium, C_{As} = 2.0g/dm^3 As, 0.66g As_2O_3 is used. Arsenic trioxide was dissolved in water in the presence of 0.40g NaOH at temperature of 50°C, by the reactions:

$$As_2O_3 + 2NaOH = 2NaAsO_2 + H_2O \quad (1)$$

By this way aqueous solution of sodium arsenic concentrations 2 g/dm^3 As was prepared. It was used as the initial solution for laboratory experiments.

Change the content of arsenic in solution with decreasing acidity

Sodium-arsenate, with the concentration of As 2.0g/dm^3, was used for getting solution with a concentration of arsenic of 0.50g/dm^3. The initial alkalinity of pH = 9.8 was reduced to pH = 2, with the addition of sulfuric acid solution. Sodium arsenate hydrolyzed by the reaction:

$$NaAsO_2 + H_2O = As_2O_3 + 2NaOH \quad (2)$$

Reaction (2) is dependent on the pH of the solution, and the reaction of the arsenic acid is followed by the release of OH^- ions, which are neutralized:

$$2NaOH + H_2SO_4 = Na_2SO_4 + 2H_2O \quad (3)$$

But for the acidity and concentration of Arsenic in the solution, arsenic acid is stable and As_2O_3 does not precipitate. Acidity of the resulting solution is then reduced by addition of sodium-hydroxide solution in the first stage to pH = 4.5 and in the second stage to pH = 7.5 by the following reactions:

$$2NaOH + HAsO_2 = NaAsO_2 + H_2O \quad (4)$$

In both cases a hydrolytic precipitate does not existed.

Change the content of arsenic in solution with increasing Ferro ion concentration

By the addition of sulfuric acid, pH of the solution is reduced to 2.5, which is the acidity of input waters in copper cementation plant. Decopperisated water from cementation was added to the solution and acidity was adjusted to pH = 3.5. Solution with 0.125 g/dm^3 As was obtained. Arsenic compounds were not precipitated. With addition of $Ca(OH)_2$ at the same time with $Fe_2(SO_4)_3$ pH is adjusted to 9.8. The content of arsenic after neutralization was 3.0mg/dm^3. Arsenic from synthetic solutions is precipitated by the following reactions:

$$NaAsO_2 + Ca(OH)_2 = Ca(AsO_2)_2 + H_2O \quad (5)$$

$$2NaAsO_2 + 3Ca(OH)_2 + Fe_2(SO_4)_3 = FeAsO_3 + 3CaSO_4 + 4H_2O \quad (6)$$

Arsine extraction in cementation of copper

Boundary conditions for arsine release are defined in the works related to the cementation of copper underground mining water (to which is added waste electrolysis solutions) [3,4]. The first boundary condition refers to the minimum acidity of the solution at the entrance of cementation which is pH = 1.5, for the existing content of arsenic in water with copper. The other condition is the maximum allowed concentration of arsenic of 1 g/dm^3 for the acidity of water with copper about pH=2.3-2.6, at the entrance to cementation.

In the aim to check these settings, in laboratory conditions, cementation of copper from the copper solution experiments were performed. The realization of these experimental three samples was used. Table 1 shows the list of these samples. The content of released arsine in cementation products, for each tested sample, is shown in Table 2.

Table 1. The tested copper solutions

Sample	pH	C_{As} (g/dm^3)	C_{Cu} (g/dm^3)
Underground mining water with sulfuric acid	1.4	0.02	0.2
Underground mining water with arsenic	2.4	1.14	0.2
Solution from $CuSO_4$ production plant	3.0	1.12	25

Table 2. Results released arsenic

Sample	C_{As} (g/dm^3) in sample	Release of arsenic (quantitatively)
Underground mining water with sulfuric acid	0.02	-
Underground mining water with arsenic	1.14	-
Solution from $CuSO_4$ production plant	1.12	+

In the first experiment, a prepared sample of water from mining had 0.02 g/dm^3 As, and acidity of pH=l.4, in the cementation with an iron plate, arsine was not detected.

In the second experiment sample was prepared with 1.14g/dm^3 As, acidity was pH = 2.4, and in the process of cementation arsine also was not detected.

In the third experiment the original vaporized electrolyte from the copper sulphate production plant with 300 g/dm^3 H_2SO_4, 25 g/dm^3 Cu and 12 g/dm^3 As, in the cementation with iron staple, arsine was detected.

Copper cementation reaction is represented by the chemical reaction:

$$2Fe + Cu^{2+} + H^+ = Cu + 2Fe^{2+} + H_2 \quad (7)$$

Reactions of arsine release reactions are presented by the chemical reaction:

$$AsO_2^- + 7H^+ = AsH_3 + 2H_2O \quad (8)$$

$$AsO_4^- + 11H^+ = AsH_3 + 4H_2O \quad (9)$$

Elementary hydrogen that is released in the cementation has reductive properties, so that ions with AsO_2^- and AsO_4^- in contact with it realize arsine (5). Results of the analyze are presented in Table 2.

Cementation of arsenic from the solution

The solution prepared from 0.5 g/dm^3 As acidity and pH = 5, cementation of arsenic was performed with iron staple. The relatively low acidity of the solution was taken for favoring arsenic cementation. After one hour of process, the acidity of the solution is slightly reduced at pH = 5.5 and the content of arsenic in solution to 0.34 g/dm^3. On this basis, it may be adopted that the cementation caused by the reaction of arsenic:

$$2HAsO_2 + 6H^+ + 3Fe = 2As + 3Fe^{2+} + 4H_2O \quad (10)$$

This reduction is thermodynamically possible because in this case (as in the case of copper) electrochemical potential of the iron $E_{Fe/Fe2+}$ = –0.41V, is more negative then of arsenic, which is $E_{As/AsO+}$ = +0.25V. Similar reactions can be expected in the case of bismuth and antimony, whose ions are also present in copper water, and whose electrochemical potentials are:

$$E_{Bi/BiO+} = 0{,}32V \text{ and } E_{Sb/SbO+} = 0{,}21V \quad (11)$$

CONCLUSIONS

This research has shown that there are no conditions for the release of toxic arsenic in operation of copper cementation from mining waste waters and the electrolysis solution. However, further research is needed to determine maximum allowed content of arsenic in water and its acidity, which should not be exceeded in order to prevent the occurrence arsine emision. At the same time it was explained that the presence of arsenic in cement slurries is the consequence of arsenic ions cementation on the iron staple.

ACKNOWLEDGMENT

This work has resulted from the project funded by the Ministry of Education and Science of the Republic of Serbia, No. 34004 on which the authors of this occasion want to thank.

REFERENCES

[1.] I. Filipović i S. Lipanović: Opća i anorganska hemija, Školska knjiga, Zagreb, 1982.
[2.] Melod: Moderna Melorova neorganska hemija, popravljeno izdanje, G.D. Parkes-a, Drugo izdanje, Naučna knjiga, Beograd, 1964.
[3.] B. Nešić: Elaborat o raspodeli arsena u procesu cementacije bakra gvožđem, Institut za bakar, Bor, 1993.
[4.] S. Živković: Studija o izvorima opasnosti i štetnostima u postrojenju cementacija, Institut za bakar. Bor, 1993.
[5.] F.P. Tredvel: Kvantitativna hemijska analiza, Naučna knjiga, Beograd, 1949.
[6.] K. Biswas, G. Davenport: Extractve Metallurgy of Copper, Second Edition, Pergamon Press, Oxford, 1976.

ACTA TECHNICA CORVINIENSIS – Bulletin of Engineering
Tome VI (Year 2013) – FASCICULE 3 [July–September]
ISSN 2067–3809

[1.] Sanda MIDŽIĆ KURTAGIĆ, [2.] Irem SILAJDŽIĆ, [3.] Branko VUČIJAK

IMPROVEMENT OF RESOURCE EFFICIENCY IN METAL INDUSTRY

[1,3.] MECHANICAL FACULTY, UNIVERSITY OF SARAJEVO, VILSONOVO ŠETALIŠTE BR. 9, SARAJEVO, BOSNA & HERZEGOVINA
[2.] HYDRO-ENGINEERING INSTITUTE, STJEPANA TOMIĆA 1, SARAJEVO, BOSNA & HERZEGOVINA

ABSTRACT: The principle of "polluter pays" implies that industrial companies are legally and financially responsible for the safe treatment of waste and emission control, for creating the preconditions for their minimization at source, and the efficient and rational use of energy and natural resources. Opportunities to improve resource efficiency by applying preventive techniques are studied in three production facilities of metal industries, with different characteristics, the type of production process and capacity, size and mode of production. The fact that there are joint auxiliary processes, asked for careful diagnosis in determining the consumption of resources, particularly water and energy. It showed that if there is no measurement in the process units, it is difficult to determine those data. A special approach to the characterization of waste streams is required, because both sewage and treatment systems are common for all production units, and there are no records of waste streams. The objective of determination of these waste streams and resource consumption by processes is evaluation of resource efficiency and determination of emission sources in the technological processes in order to recognized possible measures of prevention or minimization. The application of preventive techniques in three selected plants clearly demonstrated that pollution prevention can be financially viable. Economic benefit from cleaner production is the main motivation for most companies. The cost of ancillary materials is huge, so any loss of raw materials represents a financial loss for companies.
KEYWORDS: resource efficiency, pollution prevention, metal industry

INTRODUCTION

The principle of "polluter pays" implies that industrial companies are legally and financially responsible for the safe disposal of waste and emission control waste, creating the preconditions for their minimization at source, and the efficient and rational use of energy and natural resources. In accordance with the principle of "polluter pays" plant operator that causes damage to the environment must ultimately provide the means to repair the damage done. Responsibility that is in our traditional practice was responsibility of a "society", are now the burden of the facility operator, which brings additional responsibilities and additional financial burden. Therefore, it is clear that industrial enterprises need expert assistance in identifying opportunities for pollution prevention in an economically profitable way. Based on the experience of other countries that have been or are in the process of transition, it is obvious that the investment funds should focus on improving manufacturing processes and preventing or minimizing pollution at source in order to reduce the need for treatment and treatment costs at the end of the production cycle, or "end-of-pipe" treatment [1].

Table 1. Characteristics of plant metal industry involved in research

Type section of the	Mark and to	Number of employees	Capacity (t / day)
Production of wire	P-1	262	250
Surface treatment of yards of soil will	P-2	252	30
Metalwork	P-3	152	3

Possibilities to improve resource efficiency by applying preventive techniques are studied in three metal industries, with different characteristics in terms of the type of production process and capacity, the company's size (Table 1).

METHODOLOGY

A "Method of Identifying Preventive Techniques-MIP" (Table 2) [11] was used to select preventive techniques. The MIP method accepts and elaborates on the steps of Cleaner production (CP) assessment methods [2], and takes the idea of form and approach to data collection methods from the Minimisation Opportunities Environmental Diagnosis (MOED)[3].

With the aim of integrating the principles of prevention in the business policy the method is amended with functions Shewhart-Deming's circle [4]. The phase „Process Analysis" is extended with analysis of the problem (Plan), and with connection with the identified problems and establishing goals to be achieved, in this case those relating to resource efficiency and reducing environmental impacts. The phase "Do" corresponds to the phase of "Improvement", however a preparation of the proposals for measures to prevent pollution is shifted in phase "Planning-Analysis", because the proposal is still not an improvement but requires analysis relating to techno-economic feasibility and the expected environmental and economic improvements. The phase "Control" measures the results of application of selected preventive measures, and monitors compliance of the results with goals set out

in the planning stage. In case of deviation of the results and set goals, the correction follows through further improvements of the process in phase "Act" This phase in the CP assessment method is called "Integration".

Table 2. The methodological phases and steps, MIP methods

PDSA circle	Phase of MIP method	Step no.	Description of steps	DPSIR Indicator
Plan	Assessment	I	Overview of products, regimes of work, organization and staffing	D, S
		II	Overview of production and auxiliary facilities, and the technological processes, with an understanding of their chemical and physical aspects	D
		III	Review of consumption of raw materials, auxiliary materials, energy and water by plants, and associated costs	P
		IV	Review the types and quantities of generated waste streams, and associated costs for their management, show the input-output flows and the amounts on the process diagram	P
	Analysis	V	Situation analysis, problem identification and determination of the objectives	S, I
		V	Making lists of proposed measures to prevent and / or minimize pollution	R
		VII	Analysis of technical feasibility of the proposed measures	
		VIII	Analysis of economic feasibility of the proposed measures	
		IX	Evaluation of the techniques according to the criteria and ranking	
Do	Improvement	X	Selection of measures	
		XI	Implementation of measures	
Control	Integration	XII	Monitoring of the results	
Act		XIII	Corrections and / or documenting	

In the planning stage, with the aim of identifying problems, the MIP method is based on the DPSIR method [4]. "D-driving force" can production capacity of certain product, where the "P-pressure", can be emissions of wastes. If the production and emissions are taken as functions of eco-efficiency of technologies and techniques applied, then the improved eco-efficiency can reduce pressure, although the driving force can remain the same even increased. Emission of waste contributes to a "S-state of the environment", which in dependence of environmental carrying capacity causes some "I-impact on the environment." In this way we can follow a series of "causes-impacts", and recognize the need and the "R-response of society", i.e, in the context of industrial production, the measures that a company should take to reduce emissions.

PRODUCTION PROCESS CHARACTERISTICS AND STATE OF ENVIRONMENTAL PERFORMANCE

The wire production process, in the I-1 plant, the basic material that comes to drawing in most cases comes as rolled or bonded. Such material has not always uniform structure, nor the same mechanical properties along its entire length. There is thicker or thinner oxide layer on the surface, which should be removed, and to prepare the wire for drawing.

Tabela 3. Indicators of emissions and resource efficiency in instalations I-1, I-2 and I-3 [11]

Installation		Resource efficiency indicators	Environmental efficiency indicators
Wire production	P-1	Water efficiency: 14.5 m^3/t Energy efficiency: 448.91 KWh/t Efficiency of gas consumption: 180.2 m3/t	Wastewater indicator 0.55 m^3/t; 1.6 PE/t, Specific water pollution load 1.5 kg/ t Burnt coke 0.2 kg/t Asbestos rope 21.0 t/god Organic waste, packaging waste, paper, cartridge, paper…
Surface treatment	P-2	Water efficiency: 5.7 m^3/t; Energy efficiency: 614.09 KWh/t	Wastewater indicator 3.1 m^3/t 0.23 EBS/t Specific water pollution load 100 t/god Zinc waste (ash) 75 t/god Solid Zinc 2 t/god Ferrum oxide dust 20.3 t/god Organic waste, packaging waste, paper, cartridge, paper… 56 t Wastewater sludge rich with heavy metals Fe(OH)3L
Production of barrels, hydrophors and boilers	P-3	Water efficiency: 18.35 m^3/t; Energy efficiency: 192.5 KWh/t	Wastewater indicator 11.9 m^3/t 3.6 EBS/t, Specific water pollution load 0.7 t/god Zinc waste 18 t/god Waste acid 0.6 t/god Mineral wool 0.8 t/god Waste paint 33 t/god Organic waste, packaging waste, paper, cartridge, paper, etc 20 t/god Metal Sheet waste

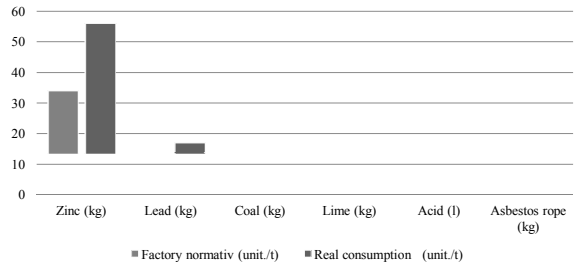

Figure 1. Factory normative and real consumption I-1[9,10]

The mechanical cleaning of blasting technology is applied at the plant P-1. The introduction of blasting technology is one of the earlier projects of cleaner production in the plant P-1, which has replaced the chemical process of preparing with mechanical wires, and thus excluded the emergence of wastewater from this process. Although the investment for the implementation of preventive measures amounted to 594 870 KM, savings on basic raw materials, water, steam, electricity, waste water neutralization, and fees for wastewater discharge, amounted 295 414 KM. The rate of return was 2 years [6].

Indicators of specific consumption of plant P-1 (Table 3) refer to the total consumption of all consumers, because there is no possibility of measuring the unit production process. Comparison with the specific values determined in other plants of the same

technology is not possible, because the literature reports on spending by individual technological processes and expressed as the amount of water consumed in relation to the surface-treated metals, while in the facility P-1 data on production capacity recorded in the tons of galvanized construction. For example, Nordic Council report on the consumption of 50 L/m2 galvanized surfaces [7], and the French regulations concerning metal finishing require consumption of 40 L/m2, 5 stages of rinsing [8].

Given the impossibility of comparing the values of indicators, analysis of the burden of production in financial terms. Water consumption and energy cost burden products with 120.7 KM / t, which accounts for about 20-30% high-carbon wire cost and low carbon wire cost. Since the galvanization dominant consumer of water, energy and basic raw materials, the analyzes of the possibilities of application of preventive measures, was focused on one of the galvanizing lines capacity of 1665 t / yr. Measurements showed that the consumption of raw materials is greater than the prescribed factory normative (Figure 1).

The installation I-2 provide metal finishing services by coating metal with zinc, as well as production and finishing of tin plates for transmission lines, and production and finishing of iron profiles for transmission line construction. In the technological process of hot coating, the waste material is generated while cleaning the zinc bath.

Wastewater from the zinc bath contains solid and ash zinc which is approximately 40% of the zinc used for production on annual basis. The company is located on the river bank, thus periodical increases of groundwater level are observed causing flooding of production halls. In order to prevent flooding, pumping wells were constructed to decrease level of ground water. Water is pumped in the sewage system.

The analysis of water, energy and zinc cost share in the unit price shows that these costs make product price less concurrent on the market and that costs must be reduced. One of the reasons for high electricity consumption is its use in the peak consumption period when several consumers are connected at the same time to the system. It is determined that water in the cooling process is used uncontrollably. Cooling bath has continuous flow required to maintain low temperatures, while flow required to keep the temperature down is not controlled. The bath with the acid solution (HCl) is changed 2 times per month which requires large quantities of water for preparation, while technological water after cooling is discharged unused. Beside potential use for preparation of acid solution, technological cooling water can be reused for rinsing after treatment with HCl. Pumped ground water is discharged unused while drinking water is used for technological purposes.

In the installation P-3, the problem with increased number of returned final product from the tin barrel line is observed. Total of 2.4% of final products (479 pieces) is returned annually, which increases need for refinishing thus increasing consumption of raw material (paint and diluent) and energy (naphtha and electricity), and generating additional quantities of wastewater. In the production of barrels, hydrophors and boilers, majority of technological operations is common. All production steps were analysed, from purchase of raw materials to dispatch of final product, and concluded that cause for damage on the barrels is inadequate storage space.

Final products are stored on open space under influence of climatic factors which causes problems with paint fixation. From environmental aspect, greater impact on environment is generated in zinc coating and painting processes. Beside these main operations, auxiliary operation of galvanisation with cadmium for anticorrosion protection is applied. Cadmium is very toxic and costly metal.

ENVIRONMENTAL AND ECONOMIC BENEFITS OF IMPLEMENTED MEASURES

In the installation I-1, zinc coating process line of 1665 t/y capacity, two gas measurement devices are installed (in the preheating line and annealing line) as well as two water meters (in the washing line after treating with basic solutions and zinc coating line) (Table 4).

Table 4. Introduced prevention and minimisation measures [11]

Measure	I-1	I-2	I-3
Product change	-	Reducing zinc coating temperature to average temperature of 447 °C and obtaining the same quality of product with thinner coating, thus reducing overall zinc consumption	-
Technological measures	Two measurement devices for gas and two for water installed in the zinc coating line.	Installation of thermostat in cooling baths and automatic valve for adjustment of water flow from the public water supply system.	Construction of covered storage space for protecting the barrels
		Installation of pumps in the groundwater draw-down system with the purpose of cooling the construction after zinc coating with pumped water	
		Installation of device for regulation of engaged power i.e. peak energy consumption	
Reuse and recycling	Excess of heat from zinc bath used for drying of wire after fluxing process.	Extraction of zinc ash by sieving to obtain zinc to be reused in the process.	-
		Reuse of cooling water for acid preparation and neutralisation processes	-
Good housekeeping	Recording of auxiliary material consumption to achieve their rational use.	Planning of the production with the purpose of taking advantage of lower energy tariff and avoiding simultaneous connection of several energy consumers	-

Continuous 15-day measurements of energy and water use indicated consumption of 11,4 m^3/t. The zinc coating process was technically improved by introducing an additional pipe for excess heat removal above the zinc bath.

This heat was conveyed to the drying chamber. Resources management and cost analysis system was introduced. Consumption was measured daily using installed devices. Other measurements such as acid, coal, azbest rope consumption were recorded by

weighting. Data obtained were recorded in tables per cost centres for easier analysis and tracking the costs. With above mentioned measures, the company reduced consumption of water for 71%, gas for 10%, zinc for 57%, and lead for 31%. Total savings were 526,747 KM with immediate return of investment (Picture 2).

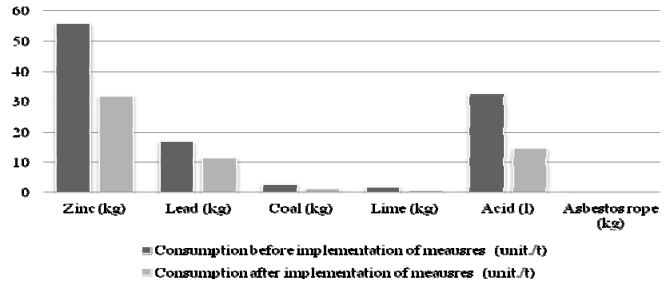

Picture 2. The effects of prevention measures at the zinc coating line of capacity of 1665 t/y at the I-1 installation

In the installation I-2, changes in product are introduced by reducing temperature of zinc coating to average temperature of 447°C. This measure at the same time increased resource efficiency by rationalisation of zinc and acid consumption. These technological measures (Table 4) reduced water and energy consumption as well. By implementing group of measured, the I-2 installation reduced consumption of energy for 9%, water for 83% and waste zinc for 85%/ton of end product. This resulted in savings of 391,839 KM with investment pay-back period being less then 1 month.

In the installation I-3, construction of covered storage space enabled better paint fixation for the barrel and reduced number of barrels returned by the customers. This resulted in reduction of raw material, auxiliary materials, energy and water (Table 6). Pay-back period for this investment was 4 years and 9 months.

Total savings obtained in all three installations amounted to 924,227.80 KM, while total investments amounted to 33,400.00 KM (Table 5). These results were achieved at the time when water and sewerage tariffs were subsidized meaning that costs were not calculated based on the real costs of water production while wastewater treatment plan was not in function. In case the installation had wastewater treatment costs and that cost of auxiliary resources were based on economic calculation, annual savings would be greater. Implementation of these measure produced not only economical but also environmental benefits expressed through reduction in consumption per unit product and reduction of emission to environment (Table 6).

Table 5. Overview of investments and savings [11]

Installation	Investment	Savings
I-1	1.000.0	525.747.0
I-2	1.000.0	391.839.0
I-3	31.400.0	6.641.8
Ukupno	33.400.00	924.227.80

Table 6. Savings in energy. water and reduction in waste generated [11]

Installation	Energy	Water	Waste
	kWh/y	m^3/y	t/y
I-3	2.479	155.4	0
I-2	4.559	22.050	123
I-1	0	13.647	0
Total	7.038	35.852.4	123

CONCLUSIONS

The fact that common auxiliary processes exist asked to pay special attention while doing diagnosis on resources consumption, especially water and energy. It is demonstrated that these data are hard to obtain unless measurement per process line is performed. Special approach was also required in characterization of waste flows since wastewater discharge systems are usually common for process and sanitary wastewater. Recording of the waste flow qualities is also not present. The purpose of waste flow determination and determination of resources consumption per process is to evaluate resource efficiency and recognise parts of the process where flows are generated. This makes selection of prevention and minimisation options easier. The use of prevention techniques in three installations selected clearly showed that pollution prevention can be financially sustainable. Economic gain from cleaner production was the main motivation for majority of companies. Cost share of auxiliary materials is significant so any waste of material represent big financial loss for a company.

REFERENCES

[1.] *S. Midžić, I.Silajdžić, at all (2006). «Possibilities for Application of Cleaner Production in Transition Countries - Experiences from the LIFE project "Capacity Building in Cleaner Production in Bosnia and Herzegovina", International Scientific Conference, Brno, May 2006, proceedings. pgs 133-140*

[2.] *L. Nilsson, at all (2007). Cleaner Production. Technologies and Tools for Resource Efficient Production. The Baltic University Press. ISBN 91-975526-1-5. 2007*

[3.] *MOED- Minimisation Opporunities Environmental Diagnosis, ISBN 84-363-5127-5. Regional Activity Center for Cleaner Production. UNEP. Spain. Ministry for Environment. 504.06: 628.5*

[4.] *Moen. R. D., Nolan. T. W., (1987). Process improvement. Quality Progress. ASQC. September. pp. 62-68.*

[5.] *P. Kristensen (2004), The DPSIR Framework, Paper presented at the 27-29 September 2004 workshop on a comprehensive / detailed assessment of the vulnerability of water resources to environmental change in Africa using river basin approach. UNEP Headquarters. Nairobi, Kenya*

[6.] *Pollution Prevention, Case Study in Metalworking Industry no.80. Bosnia and Herzegovina. Greco Med Clean Report Overview. Published by Regional Activity Centre for Cleaner Production. 2008.*

[7.] *Nordic-Council (2002), "DEA- an aid for identification of BAT in the inorganic surface treatment industry", Tema Nord, Nordic Council of Ministers, Tema Nord 2002:525.*

[8.] *France. T. (2003), "French regulations for surface treatment activities".*

[9.] *Omerbegović Z., Midžić S., Džajić M. (2006), Model for Cost and Management of Natural Resources and Cleaner Production. Proceedings IX International Symposia for Waste Management. Zagreb;15(4):378-383*

[10.] *Omerbegović. Z., (2005) Development of the Model for Cost Management as Sub-System of the Quality System, Master Thesis. Mechanical Faculty. University of Sarajevo 2005.*

[11.] *Midžić Kurtagić. S., (2012) Instruments of best Available techniques in function of Sustainable Development - Food Industry Case, Doctoral Thesis, Mechanical Faculty, University of Sarajevo, 2012*

ACTA TECHNICA CORVINIENSIS – Bulletin of Engineering
Tome VI (Year 2013) – FASCICULE 3 [July–September]
ISSN 2067–3809

[1.] Mirjana STOJANOVIĆ, [2.] Zorica LOPIČIĆ, [3.] Marija MIHAJLOVIĆ,
[4.] Marija PETROVIĆ, [5.] Dragan RADULOVIĆ, [6.] Jelena MILOJKOVIĆ

NEW URANIUM REMEDIATION APPROACH BASED ON MINERAL ROW MATERIALS AND PHYTOACUMULATORS

[1-6.] INSTITUTE FOR TECHNOLOGY OF NUCLEAR AND OTHER MINERAL RAW MATERIALS, BELGRADE, SERBIA

ABSTRACT: Environmental uranium contamination based on human activity is a serious problem worldwide. Widespread use of nuclear energy, application of weapons with depleted uranium, nuclear testing, coal combustion, oil and gas production, production and application of phosphoric fertilizer, mineral processing and formation radioactive waste landfill, improper waste storage practices and uranium tailings are the main anthropogenic sources of uranium entering the environment. State of the environment and the concept of sustainable development require the development of new technological solutions that would reduce impact of human activities on the environment. The subject of this paper is a development new concept hybrid, combined, remediation technology for cleanup uranium contaminated soils which includes: i) proper selection of hyperaccumulating plants, with the ability to accumulate an exceptionally high uranium content in the shoots, ii) application of amendments: synthetic and nature organic agents with aim of improving the mobilization of uranium and increasing the efficiency of phytoextraction and iii) application reactive materials (adsorbents) based on aluminosilicate minerals for immobilization and transformation of excess uranium, that plant didn't accept. Subject of this research was determination the effectiveness of mobilization of uranium, with natural and modified zeolite, apatite, diatomite and bentonite, individually and in mixtures. The use of adsorbents with faster and stable action, together with the materials with slower acting, provide synergistic effect of reactive materials mixtures for in situ stabilization of uranium ions. Such a treatment would provide a prevention of inclusion of uranium in the food chain and protection of the population from ionizing radiation.
KEYWORDS: uranium remediation, mineral row materials, phytormediation

INTRODUCTION

Widespread use of nuclear energy, application of weapons with depleted uranium, nuclear testing, coal combustion, oil and gas production, production and application of phosphoric fertilizer, mineral processing and formation radioactive waste landfill, improper waste storage practices and uranium tailings are the main anthropogenic sources of uranium entering the environment. All these human activities resulted in soil contamination with uranium, ie. "Technologically-Enhanced Naturally Occurring Radioactive Material." - TENORM.

Important sources of uranium in serbian area are certain technological processes of production, such as production and combustion of coal in vicinity of power plants, the production of phosphoric acid, phosphate fertilizers, phosphogypsum and other.

So,near the thermal power plant "Kolubara" and "Nikola Tesla", strength of the equivalent dose is in the range from 1.42 to 4.87 nSv / h. These values are 3 to 4% above the natural level of radiation, but are 3-4 times more than the highest level of nuclear power in normal operation and in the immediate vicinity [1].

Production and use of phosphate fertilizers is another important source of uranium in our environment.

The concentration of uranium in phosphate ore is 12 to 180 Bq/kg. In Serbia are imported annually about 1,000,000 tons of phosphorite for production of mineral fertilizers. The average concentration of uranium in phosphorite imported was 150 Bq / kg. This mean that annually imported about 150 tons of uranium or 50 TBq of radioactivity, which ere applied to Serbian agricultural solis [2].

Waste rock dumps and uranium mines only in southeast of Serbia in Gabrovnica- Kalna, who stopped mining ore and uranium flotation process forty years ago, is one of the sources of uranium mines in the surrounding area. Barren soil contained uranium in range from 15,33 mg/kg to 17 mg/kg, which today cover an area of about 0.1 km2. (Stojanović and Milojković, 2011) [1].

These data indicate that the sources of uranium in Serbia result of natural geological and geochemical origin of sediments, rocks and soils (NORM) and present "background of natural ionizing level".

Technological processes in power plants and production of phosphate fertilizers and their use has contributed to the increased the concentration of uranium in certain areas and present the main form of TENORM. According to some estimates the "natural level of ionizing radiation", in Serbia, has increased about 30 times in the last 40 years [2].

Finally, during the NATO aggressions in Yugoslavia were bombing 112 sites in Kosovo and Metohija and 12 locations in southern Serbia with depleted uranium (DU) ammunition. On this occasion around 10 tonnes of DU was introduced into environment.

The degree of contamination ranges from the bottom limit of 200 Bq/kg to 235,000 Bq/kg in sample of soil, mainly agricultural land, or 1 000 times above the naturals level. In wars of the past 20 year (1991 Gulf War, the Bosnia and Serbia war, the 2003 invasion of Iraq) approximately 1.4 million DU missiles were used. During Gulf War I (1990-1991), approximately 320 tonnes (equivalent to over 1 million 30-mm rounds) of DU munitions were used by the US forces, and approximately 1 ton of DU was fired from UK tanks.

During the Bosnia-Herzegovina conflict (1994-1995), approximately 3 tonnes of DU was fired in NATO airstrikes, and about 10 tonnes of DU was fired during the 1999 Kosovo conflict. During the 2003 Iraq War, approximately 2 tonnes of DU was fired by the UK MOD, the amount of DU fired by USA forces has not yet been disclosed, but speculative figures range between 170 and 1700 tonnes [3,4].

Today, unfortunately, in Serbia encounter with "invisible threat" use of depleted uranium ammunition, with highly radioactive and chemotoxic effect on human health.

Hybrid, combined, remediation technology for cleanup uranium contaminated media, with synergistic effects are increasingly being used for environmental and economic efficiency. Integrated management of soils contaminated with uranium, based on results obtained in Institute for nuclear and other mineral raw materials in Belgrade. Conceptual approach is a synergy of physical, chemical and biological remediation processes and techniques. In situ treatment includes a combination phytoextraction and phytostabilisation with uranium hyperaccumulator plants with application of uranium immobilization materials, based on Serbian (domestic) aluminosilicate minerals. Such a treatment would provide a prevention of inclusion of uranium in the food chain and protection of the population from ionizing radiation.

The objective of any remedial action is to reduce the risks to human health and the environment to acceptable levels by removing or reducing the source of contamination or by preventing exposure to it. Various strategies have been proposed for the remediation of contaminated environments in order to reduce the detrimental chemical and biological technologies. Environmental uranium contamination based on human activity is a serious problem worldwide [5].

Uranium is one of the radionuclide whose mobility in soils strongly varies depending on soil type and physico-chemical properties. Distribution of uranium in the lithosphere and hydrosphere is performed in conditions of complex chemical and physical-chemical natural processes, including mechanisms of degradation of minerals that contain uranium. Solubility of uranium in the soil primarily depends on the environmental pH, redox potential, soil structure and mineral composition of the solid phase, concentration of inorganic compounds, the quantity and type of organic compounds in soil and soil solution, soil temperature, pressure, moisture content and microbial activities [6,7,8]. Sorption of U(VI) onto soil particles is higher at lower pH values in soils and decreases strongly with increasing pH. The reduction of U(VI) to U(IV) by abiotic and biotic processes, as well as its re-oxidation has received considerable attention because the oxidation state of uranium has a significant effect on its mobility in the natural environment [9].

The cycle of mobilization of uranium in nature begins with U(IV) oxidation but the process of contamination of uranium in nature stops, when U(VI) is reduced or immobilized. However, with changing conditions in nature, U(IV) uranium can oxidize to U(VI), and so the cycle will start again.

Immobilization of uranium as precipitation from solution is the only way for nature to protect from the spread of uranium and its radioactive products. Fixation of uranium can be described by two main mechanisms:

- *precipitation (oxido-reduction), and*
- *adsorption.*

Precipitation process may begin in the form of uranium, uraninite, autunite, and uranium phosphite $[U(PO_3)_4]$ low solubility, to $Kp=10^{-49}$ as a basis of their stability in the long geological period under very different conditions, important from the point of view of environmental protection and production of healthy and safe food [2].

METHODS AND TECHNIQUES FOR URANIUM REMOVAL

Remediation technologies for treatment of uranium contaminated soils and groundwater could be applied as either ex situ or in situ techniques. According to Gavrilescu et al, [7] can be classified methods and techniques for uranium removal as: Natural attenuation, Physical processes, Chemical methods, Biological methods and Electrokinetic methods. These techniques can be applied individually or in combination (hybridization) and they are presented on Figure 2.

Each one of the above fundamental technical choices will direct decision makers to substantially different paths with regard to their subsequent choices, actions and potential results, making available significantly different technological options for application, within a remediation program, which involves multidisciplinary environmental research on characterization, monitoring, modeling and technologies for remediation.

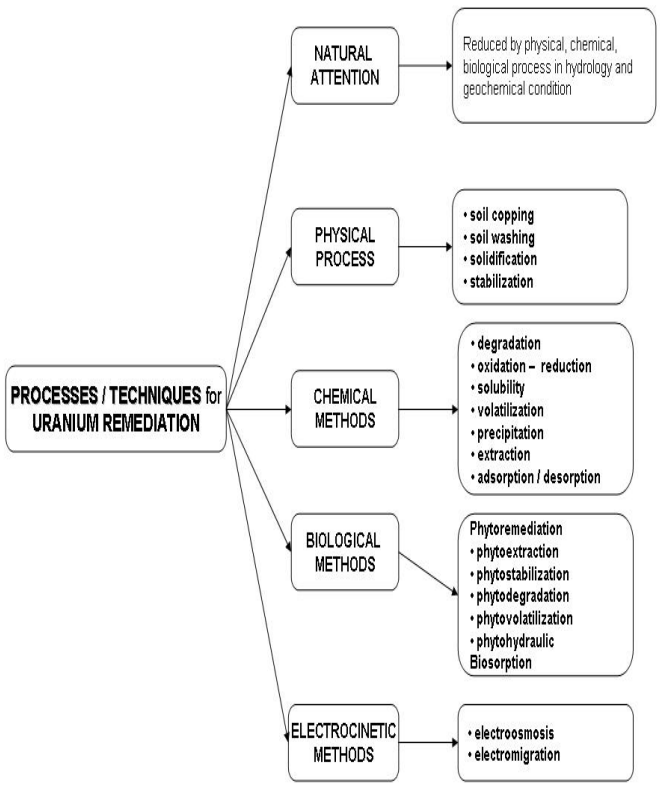

Figure 2. Processes and techniques for uranium removal

Each one of the above fundamental technical choices will direct decision makers to substantially different paths with regard to their subsequent choices, actions and potential results, making available significantly different technological options for application, within a remediation program, which involves multidisciplinary environmental research on characterization, monitoring, modeling and technologies for remediation

Biological method

In situ remediation techniques are more suitable for radioactive contamination due to reduced exposure of workers during the construction or transportation. Among the remediation techniques currently used, soil excavation is the most common treatment for radioactively contaminated soils as well as encapsulation size separation, soil washing, electrokinetics and ion exchange [6].

However, these in situ techniques are expensive compare to phytoremediation techniques.

Phytoremediationinvolves the use of plants to extract, sequester and/or detoxify the pollutants present in soil, water and air. This technique may be particularly useful for remediation of a wide variety of contaminated surfaces (usually 15-30 cm deep), including soil, water or wetland systems.

Plant-assisted remediation of soil can generally occur through one or more of the following mechanisms:

phytostabilization, phytodegradation / phytotransformation, phytovolatilization, rhisodegradation, phytohydraulics, phytoextraction.

Phytoremediation offers advetntages such as: cheap and simple option, better metal recycling, better public acceptance and less destruction to remediation sites. Phytoextraction efficiency is determined by the metal availability, which is influenced by pH, redox potential and metal complexation.

The major disadvantage of the technique is the time of requirement - from 18 to 60 months or even decades Phytoextraction, a type of phytoremediation, use of metal-accumulating plants (hyperaccumulators) that can transport metals from the soil to the roots and and concentrate them in above-ground plant tissue - shoots [9, 10,11]. Hyperaccumulators plants are those plants that adopt the pollutants from the soil at a much higher rate than other plants (100 to 1000 times). According to the PHYTOREM data base sunflower is recognized as hyperaccumulator of uranium. PHYTOREM was developed by Environment of Canada and this database consist of 775 plants with capabilities to accumulate or hyperaccumulate one or several of 19 key metallic elements. Species were considered as hyperaccumulators if they took up greater than 1000 mg/kg dry weight of most metals. Plants hyperaccumulators like sunflower had content of uranium more than 15000 mg kg^{-1} dry weight [12]. There are two general approaches to phytoextraction:

- *continuous, and*
- *chemically enhanced phytoextraction.*

The first approach uses naturally hyperaccumulating plants with the ability to accumulate an exceptionally high metal content in the shoots. Another method is the application of synthetic and nature organic agents in order to improve the mobilization of uranium and increase efficiency of phytoextraction. A key to the success of U phytoextraction is to increase soil U availability to plants [13].

In literature there have been numerous reports about amendments in phytoremediation compaunds that increase the uptake of uranium by varius plants. Addition of chelates increases the mobility of metals in the soil and form complexes with metals reducing the positive charges and thus affects the availability of metal to plants. Amendments could be organic compounds: synthetic chelating agents (ethylenediaminetetraacetic acid (EDTA), N-hydroxyethyl-ethylenediamine-N,N',N'-triacetic acid (HEDTA), diethylenetrinitrilopentacetic acid (DTPA)), natural fulvic acid, humic acid and more natural low molecular weight organic acids (citric, malic, oxalic, and acetic acid). The most frequently used is EDTA, which has been reported as more effective than other synthetic chelators for several heavy metals [13].

Phisical and chemical method

During the selection of remediation technologies one of the key factors is the optimal choice of immobilization materials, based on efficiency and the price. Therefore, there is a need for application of alumosilicate minerals as sequestering agents (apatite, zeolite, clay, diatomite,bentonite,etc.), that will enable hydrological control and in situ, long term, immobilization (solidification/stabilisation) of uranium.

Mechanisms of action these materials are different and depend on their type and characteristics as well as and chemical and physical-chemical properties of contaminated soils. The most common mechanisms are adsorption, exchange, oxidation-reduction, or precipitation.

Addition of chelating agents in order to enhance phytoextraction may promote leaching of the pollutants (uranium) into groundwater. Therefore, there is a need for application of properly selected sequestering agents that will enable hydrological control and immobilization (solidification/ stabilisation) and transformation of excess uranium, which plant didn't accept. Furthermore, sequestering agents can be used as ground cover in perennial phytoremediation, for adsorption of uranium, which can leach from fallen leaves in autumn (Figure 2).

Stojanović et al., [2,14], conclude that setting time for uranium ions follows the rule:

organomodif. zeolites (modified with quaternary ammonium ions)> phosphate concentrate (34.95 P_2O_5%) > organomodif. bentonite > diatomite > mechanochemically activated apatite > natural bentonite > natural zeolite > natural phosphate (14.43% P_2O_5).

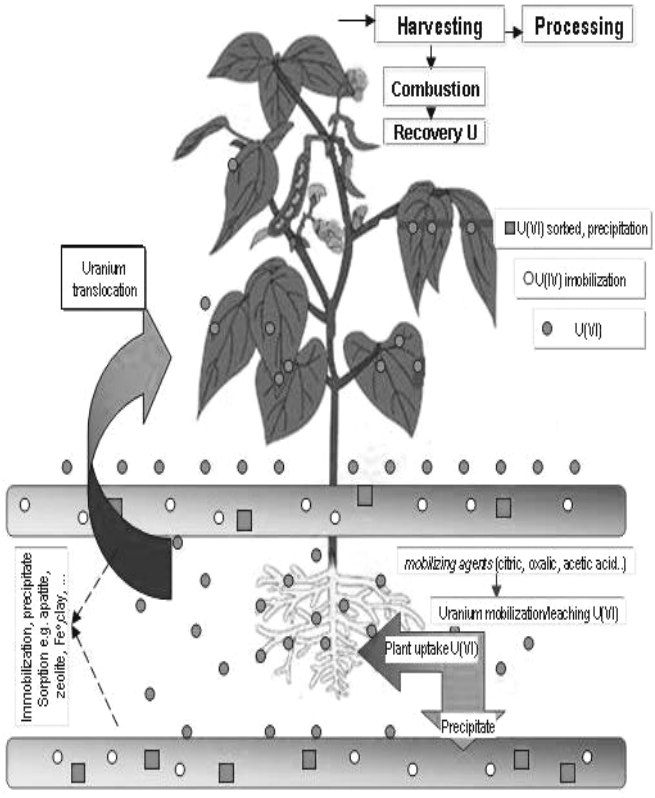

Figure 2. Hybrid technology for remediation of uranium polluted soils

Application of fast - acting sequestering agents (diatomite, organomodif. zeolite and bentonite) with slow - acting adsorbent (natural phosphate), achieves a synergistic effect of mixtures of reactive materials like a permanent solution for the "in situ" stabilization of uranium ions in the remediation of soil contaminated by uranium.

Mixture of apatite and organomodified zeolite confirmed the synergism of action of these materials which is reflected in the rapid binding of uranium with organomodified zeolite and the formation of stable phase uranium-phosphate-autunite. Application of this mixture eliminates the risk of desorption of organomodified zeolite due to changes in soil conditions. For the remediation of large areas of contaminated soil with a lower level of radionuclides application of natural apatite is justified. If the economic effect is not important, natural apatite reactivity can be increased mechanochemically with vibratory mill or applying the concentrate with high content of P_2O_5 - 34.95% [15].

Modified zeolite with NH_4^+ ions, increases the solubility of phosphate rock (PR) through the exchange of cations Ca^{2+}, can be described by the following equation(1):

$$PR + NH_4^+\text{- zeolite} \leftrightarrows Ca^{2+}\text{- zeolite} + NH_4^+ + PO_4^{3-} \quad (1)$$

To extend the possibility of their use on different soil types, it is necessary to design a functional material which should contribute to greater phospho immobilization in wide range of soil pH [16].

Preliminary results showed that the addition of modified zeolite (with 2M ammonium sulphate solution) increase PR dissolution due to removal of Ca^{2+} by zeolite through cation exchange. In time period of 24 h it increased the PR phosphate rock dissolution from 0.406 mg P/dm^3 to 3.621 mg P/dm^3 which was confirmed by an increase in pH value and decrease in concentration of Ca^{2+} ions. Such hybrid materials can be applied for stabilization of uranium contaminated soils and as natural phosphate fertilizers.

CONCLUSIONS

Remediation of soil contaminated with uranium requires a holistic approach including the use of secure "environmental friendly" materials that are cheap, easily applicable and available locally. The results confirm the applicability of the studied natural and modified aluminosilicate materials (zeolite, apatite, bentonite and diatomite) individually and in mixture.

The use of adsorbents with faster and stable action, together with the materials with slower acting, provide synergistic effect of reactive materials mixtures for in situ stabilization of uranium ions. Hybrid technology represents a permanent solution and means integrated management strategy for contaminated site which includes:

- *proper selection of plants (hyperaccumulators uranium),*
- *improving mobility of uranium with amendments (organic agents), and*
- *application sequestering agents for immobilization and transformation of excess uranium, which plant didn't accept.*

These technologies combine: chemical, physical, and/or other biological processes.

Acknowledgements

The authors are grateful to Serbian Ministry of Education and Science which support this research through its Project N° TR 31003 and TR34013

REFERENCES

[1.] *Djuric G., Popovlc Lj.D.:Uranium in the environment- "Zero state" in Serbia, Chemical Industry 55 (7-8), 289-294, 2001.*

[2.] *Stojanović M., Milojković J.: Phytoremediation of Uranium Contaminated Soils, Handbook of Phytoremediation Ed.: Ivan Golubev, Nova Science Publishers Inc., New York, United States of America, 93-136., 2011.*

[3.] *Stojanović M., Milojković J., Lopiči Z., Mihajlović M., Rajković M., Vitorović G.: Anthropogenic sources of uranium in serbia-risk assessment on environment and human health. In: Uranium: Characteristics, Occurrence and Human Exposure , Ed: Alik Ya. Vasiliev and Mikhail Sidorov, Nova Science Publishers Inc., New York, United States of America, ISBN: 978-1-62081-207-5, 2012.*

[4.] *UNEP, (2007): Technical report on capacity-building for the assessment of depleted uranium in Iraq. Switzerland: United Nations Environmental Program; 2007.*

[5.] *Stojanović, M., Babić, M., Stevanović, D., Martinović, Lj.: Effect of long-term application of phosporus fertilizers on uranium contaminated Serbian soils in: Radionuclide contamination of Serbian soil and remediation possibility, 67-117, ITNMS Belgrade, 2006.*

[6.] *Ebbs, S.D., Brady, J.D., Kochian V.L.: Role of uranium speciation in the uptake and translocation of uranium by plant, J. Exp.Bot. 49, 324, 1183-1190, 1998.*

[7.] *Gavrilescu, M., Pavel, L. V., Cretescu, I.: Characterization and remediation of soils contaminated with uranium, Journal of Hazardous Materials, 163, 475-510, 2009.*

[8.] *Duquène, L., Vandenhove, H., Tack, F., Van der Avoort, E, Phytoavailability of uranium: influence of plant species and soil characteristics, in: Uranium in the Environment. Mining Impact and Consequences, 469-476, Netherlands Springer Verlag -Berlin Heidelberg, 2006.*

[9.] *Evans K.G.: Methods for assessing mine site rehabilitation design for erosion impact. Aust J Soil Res 38, 231-248, 2000.*

[10.] *Ebbs, S.D. Brady, D.J. Kochian L.V. : Role of U speciation in the uptake and the translocation of uranium by plants, Journal of Experimental Botany, 49,1183-1190,1998.*

[11.] *AbdEl-Sabour, M.F.: Remediation and bioremediation of uranium contaminated soils, Electronic Journal of Environmental, Agricultural and Food Chemistry, 6(5), 2009-2023, 2007.*

[12.] *McIntyre, T. Phytoremediation of Heavy Metals from Soils In: Advances in Biochemical Engineering/Biotechnology, 78, 97-123, New York: Springer-Verlag Berlin Heidelberg, 2003.*

[13.] *Leštan, D., Enhanced heavy metal phytoextraction, In: Phytoremediation Rhizoremediation, 115 - 132, Springer the Netherlands, 2006.*

[14.] *Stojanović M., Milojković J., Grubišić M.: Application alumosilicate minerals for remediation of uranium contaminated land, I međunarodni kongres „Inženjerstvo, materijali i menadžment u procesnoj industriji“, Jahorina, Republika Srpska, 523-526, 2009.*

[15.] *Stojanović, M., Grubišić, M., Stevanović, D., Milojković, J. and Ileš, D.: Remediation of the Serbian soils contaminated by radionuclides in the function of sustainable development, Chemical Industry &Chemical Engineering Quarterly, 14(4) , 265-267,2008.*

[16.] *Stojanović M., Milojković J., Lopičić Z., Mihajlović M., Radulović D.:In situ immobilisation of uranium using alumosilicate minerals as sequestering agents, The 43rd international october conference on mining and metallurgy, Oktobar, 12-15, Kladovo, Srbija, 246-249, 2011.*

ACTA TECHNICA CORVINIENSIS – Bulletin of Engineering

ISSN: 2067-3809 [CD-Rom, online]

ACTA TECHNICA CORVINIENSIS - BULLETIN of ENGINEERING

ISSN: 2067-3809 [CD-Rom, online]

ACTA TECHNICA CORVINIENSIS - BULLETIN of ENGINEERING

ISSN: 2067-3809 [CD-Rom, online]

copyright © UNIVERSITY POLITEHNICA TIMISOARA,
FACULTY OF ENGINEERING HUNEDOARA,
5, REVOLUTIEI, 331128, HUNEDOARA, ROMANIA
http://acta.fih.upt.ro

ACTA TECHNICA CORVINIENSIS – Bulletin of Engineering
Tome VI (Year 2013) – FASCICULE 3 [July–September]
ISSN 2067–3809

[1.] Mamun Bin Ibne REAZ, [2.] Mohd. MARUFUZZAMAN

PATTERN MATCHING AND REINFORCEMENT LEARNING TO PREDICT THE USER NEXT ACTION OF SMART HOME DEVICE USAGE

[1-2.] DEPARTMENT OF ELECTRICAL, ELECTRONIC AND SYSTEMS ENGINEERING, UNIVERSITI KEBANGSAAN MALAYSIA, 43600, UKM, BANGI, SELANGOR, MALAYSIA

ABSTRACT: Future Smart-Home device usage prediction is a very important module in artificial intelligence. The technique involves analyzing the user performed actions history and apply mathematical methods to predict the most feasible next user action. This paper presents a new algorithm of user action prediction based on pattern matching and reinforcement learning techniques. Synthetic data has been used to test the algorithm and the result shows that the accuracy of the proposed algorithm is 87%, which is better than ONSI, SHIP and IPAM algorithms from other researchers.
KEYWORDS: Smart home, artificial intelligence, pattern matching, reinforcement learning, Markov Model

INTRODUCTION

Smart home system is an intelligent system that needs to adapt to the inhabitant's lifestyle, predict their future actions and minimize the user device interaction. Such requirements will never be achieved without proper analysis of inhabitant's device interaction history for each particular state of the home environment. The basic idea behind prediction is given a sequence of user device interaction events, how can the next user action be predicted [1].

In the previous year's many researchers developed techniques for predicting user actions. Some of these methods were used for intelligent Human Computer Interaction (HMI) [2]; others were used for smart-home environment [3, 4, 5]. Although the domain were different prediction techniques, the idea behind the techniques was the same and it is possible to apply a method of a particular domain to another by modifying the representation of the environment and action sequence.

Some of the techniques that were previously used has employed Markov models to optimally predict the next user action in any stochastic sequence, one such example of these algorithms is Smart Home Inhabitant Prediction (SHIP) [6,7,8]. SHIP can predict the user future actions but only achieve 60% prediction accuracy which is undesirable for sensitive application such as Smart home. On the other hand, some techniques have simply used sequence matching to predict the next user action like Incremental Probabilistic Action Modeling (IPAM) and On-line implicit State Identification (ONSI) [2]. While IPAM performs better than SHIP, it chooses pairs of actions occurring in sequence as a pattern and summarizes them by increasing the probability of those that occur and decreasing the probabilities of all others. IPAM make an implicit Markov assumption, namely the last action together with the current summary provided by the probability estimation, which contain enough information to predict the next state. Looking at real user interaction traces, it has been found that often users enter modes that can be easily identified by examining the behavioral patterns they engage in, but these patterns span more than two actions in a row. While the techniques that is currently being used passively predicts the user actions where they do not take into consideration the user most preferred action for a particular environment state. ONSI solves IPAM problem by using varying pattern matching length however it tend to ignore the adaptation to the user preferred actions and the relation between the actions and the environment state.

Inspired by behaviorist psychology, reinforcement learning is an area of machine learning in computer science, concerned with how an agent ought to take actions in an environment so as to maximize some notion of cumulative reward. The reinforcement learning algorithms do not need the knowledge of the Markov decision process (MDP). Reinforcement learning differs from standard supervised learning in that correct input/output pairs are never presented, nor sub-optimal actions explicitly corrected. A reinforcement learning agent interacts with its environment in discrete time steps. At each time t, the agent receives an observation o_t, which typically includes the reward r_t. It then chooses an action a_t from the set of actions available, which is subsequently sent to the environment. The environment moves to a new state s_{t+1} and the reward r_{t+1} associated with the transition (s_t, a_t, s_{t+1})

is determined. The goal of a reinforcement learning agent is to collect as much reward as possible. The agent can choose any action as a function of the history and it can even randomize its action selection [9-13].

In computer science, pattern matching is the act of checking some sequence of tokens for the presence of the constituents of some pattern. In contrast to pattern recognition, the match usually has to be exact. The patterns generally have the form of either sequences or tree structures. Uses of pattern matching include outputting the locations (if any) of a pattern within a token sequence, to output some component of the matched pattern, and to substitute the matching pattern with some other token sequence (I.e., search and replace). Graph rewriting languages rely on pattern matching for the fundamental way a program evaluates into a result [14-15].

This research proposed a novel technique by combining the pattern matching and reinforcement learning techniques to predict the user next action, which was never been thought of using earlier. By applying reinforcement learning the intelligent home system can receive positive reward for each action that is correctly predicted, on the other hand negative reward is given for each wrong action. By using this method the system can adapt the user ideal actions. On the other hand pattern matching will be used to match the most recent user event sequence with the history of the recorded sequences, by combining the results obtained from both methods the algorithm should have sufficient information to calculate the probability of the next user action thus the performance improvement should be significant.

DESIGN METHODOLOGY

The goal of the proposed algorithm is to predict the user future actions and to base the prediction decision on the user's preferences. The first thing that has to be taken into consideration in designing any decision algorithm is how the state of the environment will be represented. The algorithm was designed with the aim to employ the algorithm for a smart-home system, therefore the environment representation is based on smart-home environment.

The environment of the home can include massive amount of information such as room temperature, time (time of the day and the date of the month), devices states, user location and many other parameters that can be sensed by the inhabitant. For the purpose of simplification the explanation will take into consideration the time and the devices state as the state of the environment, and the action performed on these devices will be simply a device turning switching On or OFF actions.

Graph theory will be used to visualize the representation of the environment states and the actions [16]. According to graph theory, a directed graph G is an ordered pair of nodes N and vertices or arrows V as expressed by $G := (N, V)$.

According to this representation each state will be represented as a node in the graph and the action that is performed in that particular state will yield an edge that will produce another state in the environment as shown in Figure 1.

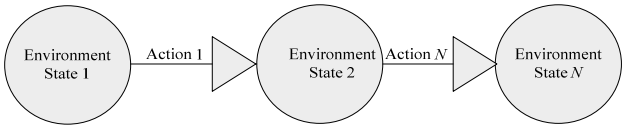

Figure 1. Environment state and action representation using graph theory

It is worth mentioning that although the representation of the environment state is simplified it can be easily extended to include more information. But it must be taken into consideration that by including more environment variables will require more storage and processing time however prediction accuracy will be improved since the inhabitant interaction history will be significantly more comprehensive.

ALGORITHM STRUCTURE

After illustrating how the environment state and the actions will be represented to clarify the internal construction of the algorithm. The algorithm has two main components and they are:

- *The reinforcement learning component.*
- *The pattern matching component.*

The Reinforcement Learning Component

The reinforcement learning component is modeled using Q-learning algorithm. Q-learning algorithm is a recent form of reinforcement learning technique that can be implemented to support online decision making and does not need a model of the environment, which makes it a great choice for Smart home system because Smart home system is a real-time application.

Q-Learning is a reinforcement learning technique that works by learning an action-value function that gives the expected utility of taking a given action in a given state. Given the environment devices states as [S], and the device actions that can be taken on a given environment state as [A], then Q value array of reinforcement learning can be formed as shown in Equation 1.

$$Q = S \times A \qquad (1)$$

According to Q-Learning algorithm the Q value array is used to store the rewards the agent has received by performing a particular action at a given environment state. Each time the agent makes a correct decision, the agent is given a positive reward or a negative reward. The reward is calculated based on the user feedback to the agents performed action, which can be sensed by the system through monitoring the devices state constantly. The Q value function will be calculated as shown in Equation 2.

$$Q^*(x,a) = (1-\alpha)Q^*(x,a) + \alpha(r + \gamma V^*(y)) \qquad (2)$$

Where Q is the Q-learning value function, x is the environment states, a is the action that can be taken,* α *is the learning rate,* γ *is the value of future reinforcement, r is the immediate reward, y is the next state resulting from taking action in state x and V* is the future Q-learning value function.*

The uniqueness is that Q-learning does not specify which action to be taken, it also allow us to perform experimental trials while preserving the current optimal state. Furthermore, since this function is

updated according to the ostensibly optimal choice of action at the following state, it does not matter what action is actually followed at that state. For this reason, the estimated returns in Q-learning are not contaminated by "experimental" actions so Q-learning is not experimentation-sensitive [17].

The Pattern Matching Component

The pattern matching of the component of the algorithm is inspired by method used in ONSI algorithm [2]. In ONSI algorithm, a pattern matching is extracted from the user interaction history and summary of those pattern is formed, then those pattern summaries is ranked accordingly and the prediction is made based on the ranking. The algorithm presented in this paper follows the same approach used by ONSI for pattern matching. The algorithm maintains two main directed graphs data structure, multiple graphs of device usage history sequence and a graph of the most recent device usage sequence. The history sequence is an ordered set of device usage history that has occurred at a particular environment state. The history sequence is used to train the algorithm. During the training state of the algorithm, the Q value array of the reinforcement learning algorithm is initialized based on the user selected action in the history. This will make the algorithm learn the optimal user actions for a given state.

The other graph of the algorithm is the recent device usage patterns that are supposed to be sensed by the smart-home system. Each graph will represent the device usage for one particular day. Therefore, the recent device usage graph will store the usage patterns for the current day that the smart-home system is running at.

The pattern matching operation starts from the most recent state recorded in the recent graph and going backward to match with each history graph. This operation will continue until the history graphs are completely searched for pattern matching. After the last iteration of this process is reached the longest pattern matching is calculated. This operation can be seen in Figure 2. As shown in Figure 2, the yellow nodes in the graph represent the pattern matched in the history graphs based on the recent graph starting at node with state S4. The pattern match will be taken into account only if the successor state, the predecessor state and the action between them is similar to the most recent graph states actions pairs.

The pseudo code of the algorithm is shown in the following steps:

i. Let α is the threshold value $0 \le \alpha \le 1$, $f(s,a)$ is the action under consideration under the latest current state in the recent graph of event sequence.
ii. Calculate the longest pattern match starting from the current state in the recent graph of event sequence and store it in variable L.
iii. Calculate the Q-value function for the current action under consideration based on the previous history of events using and store it in variable R.
iv. $h(s,a)$ is the total number of occurrences of action a under the current state s and $\sum_i h(s,a_i)$ is the calculated total number of occurrences of other actions a_i at the same state s
v. Calculate the probability for the current action a under consideration using the formula

$$f(s,a) = (1-\alpha)L + \alpha\left\{\frac{h(s,a)}{\sum_i h(s,a_i)} + R\right\} \qquad (3)$$

vi. Repeat steps 2 to 5 for the subsequent actions for the same state s and select the action with the highest ranking.
vii. After all the actions have been taken under consideration receive feedback from the home inhabitant. If the action was satisfying give the action a positive reward otherwise give the action a negative reward while taken the user chosen action under consideration. Calculate the Q-value for the selected action by the algorithm using Q-learning equation (2).

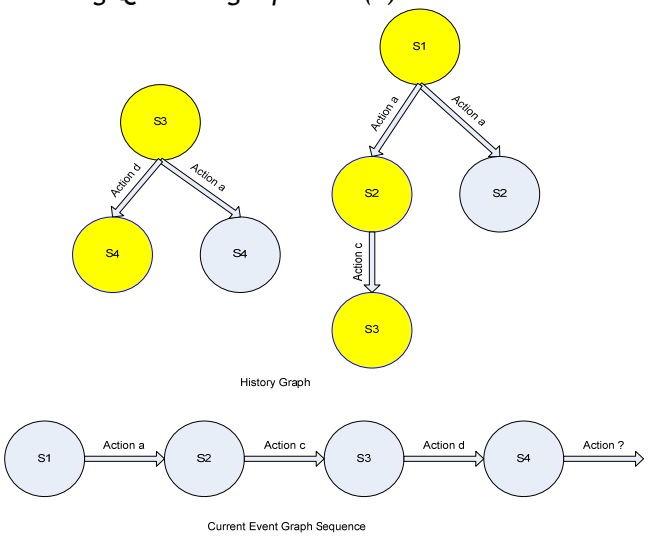

Figure 2. Illustrating pattern matching operation

TESTING RESULTS AND COMPARISON

To test the algorithm, the JAVA programming language is used to implement the testing module for the algorithm. The data used for testing the algorithm has been generated synthetically to simulate device usage patterns of home inhabitant. The data was generated with 1 months usage of 5 devices. The total data volume was 4800 with random actions. The data then has been formulated and stored in a database file then fed into the testing module to train the algorithm and the Q-learning module. After the training phase pattern, testing is performed with carefully analyzing the result and the synthetic generated patterns. In the testing it is assumed that the home consist of five devices and the actions that can be taken on these devices is simply device (On, Off) actions. Sample data format is shown in Table 1.

Table 1. Sample synthetic data used to train the multi-agent system

Date and Time	Action	Device	Location
2011-03-03 / 09:21	On	Lamp1	Living Room
2011-03-03 / 10:26	Off	Fan1	Bedroom
2011-03-03 / 10:29	On	Tv1	Living Room
2011-03-03 / 18:21	Off	Lamp2	Living Room
2011-03-03 / 20:22	Off	Tv2	Bedroom

Random trials have been performed to set the most suitable threshold value a. The optimal result was found while the threshold value was set to 6.0. Figure3 shows the results together with the comparison of results from other researchers [2, 18].

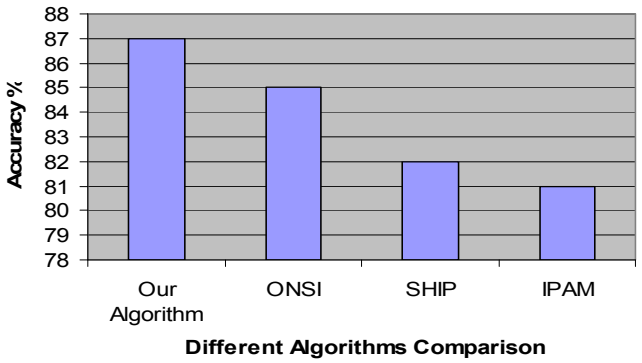

Figure 3. Result comparison with different prediction algorithms

The formula used to rank the accuracy of the algorithms is shown below:

$$f(h) = \frac{i}{q} \qquad (4)$$

where i is the number of accurate predictions and q is the number of input data that is fed to the algorithm.

Using Equation 4, the result shows that the accuracy of the proposed algorithm is 87%, where the accuracy of ONSI algorithm is 85%, accuracy of SHIP algorithm is 82% and the accuracy of IPAM algorithm is 81%, which is graphically represented in Figure 3. Therefore, by combining the pattern matching and reinforcement learning techniques in predicting the user next action of smart home devices clearly shows that it gives better accuracy than others.

CONCLUSIONS

This paper has presented a novel technique of user action prediction for smart home system. The algorithm introduces a new technique of adapting the user proffered actions using a combination of pattern matching and reinforcement learning. The result shows that the algorithm performs better than ONSI, SHIP and IPAM, which validate the supremacy of the proposed technique compare to others.

REFERENCES

[1] *ALAM, M.R., REAZ, M.B.I., ALI, M.A.M., SAMAD, S.A., HASHIM, F.H., HAMZAH, M.K. Human activity classification for smart home: A multiagent approach. In IEEE Symposium on Industrial Electronics & Applications (ISIEA), Penang (Malaysia), 2010, p. 511 - 514.*

[2] *GORNIAK, P., POOLE, D. Predicting future user actions by observing unmodified applications. In Proceedings of the Seventeenth National Conference on Artificial Intelligence, Cambridge, MA, 2000, p. 217-222.*

[3] *EDWIN, O.H., COOK, D.J. Improving home automation by discovering regularly occurring device usage patterns. In Third IEEE International Conference on Data Mining. Washington DC (USA), 2003, p. 537- 540.*

[4] *RASHIDI, P., COOK, D.J., HOLDER, L.B., SCHMITTER-EDGECOMBE, M. Discovering activities to recognize and track in a smart environment. IEEE Transactions on Knowledge and Data Engineering, 2011, vol. 23, no. 4, p. 527 - 539.*

[5] *WU, C. L., FU, L.C. Design and realization of a framework for human-system interaction in smart homes. IEEE Transactions on Systems, Man and Cybernetics, Part A: Systems and Humans, 2011, vol. PP, no. 99, p. 1-17.*

[6] *RAO, S.P., COOK D.J. Identifying tasks and predicting action in smart homes using unlabeled data. International Journal on Artificial Intelligence Tools, 2004, vol. 13, no. 1, p. 81-100.*

[7] *VINTAN, L., GELLERT, A., PETZOLD, J., UNGERER, T. Person movement prediction using neural networks. In Proceedings of the KI2004 International Workshop on Modeling and Retrieval of Context (MRC 2004). Ulm (Germany), 2004, vol. 114, p. 618-623.*

[8] *KANG, W., SHINE, D., SHIN, D. Prediction of state of user's behavior using Hidden Markov Model in ubiquitous home network. In International Conference on Industrial Engineering and Engineering Management (IEEM), Singapore, 2010, P. 1752 - 1756.*

[9] *KAELBLING L.P., MICHAEL L.L., ANDREW W.M. Reinforcement Learning: A Survey. Journal of Artificial Intelligence Research, 1996, vol. 4, p. 237-285.*

[10] *SUTTON R.S. Learning to predict by the method of temporal differences. Machine Learning, 1988, vol. 3, p. 9-44.*

[11] *BUSONIU L., ROBERT B., BART D.S., DAMIEN E. Reinforcement Learning and Dynamic Programming using Function Approximators. Taylor & Francis, CRC Press, 2010.*

[12] *SUTTON R.S., BARTO A.G. Reinforcement Learning: An Introduction. Cambridge: MIT Press, 1998.*

[13] *ZHANG Z.C., HU K.S., HUANG H.Y., LI S., ZHAO S.Y. (2010). A multi-step reinforcement learning algorithm. Applied Mechanics and Materials, 2010, p. 3611-3615.*

[14] *TROCHIM W. M. K. Pattern Matching, Validity, and Conceptualization in Program Evaluation. Evaluation Review, 1985, vol. 9, p. 575-604.*

[15] *LIN J. W. (2011). Neural network model and geographic grouping for risk assessment of debris flow. International Journal of the Physical Sciences, 2011, vol. 6, No. 6, p. 1374-1378.*

[16] *DIESTEL, R. Graph Theory. Springer: 2005.*

[17] *SUTTON, R.S., BARTO. A.G. Reinforcement Learning: An Introduction. Cambridge: MIT Press, 1998.*

[18] *DAS, S.K., COOK, D.J., BATTACHARYA, A., HEIERMAN, E.O., TZE-YUN, L. The role of prediction algorithms in the Mavhome smarthome project. IEEE Wireless Communications, 2002, vol. 9, no. 6, p. 77- 84, December 2002.*

ACTA TECHNICA CORVINIENSIS - Bulletin of Engineering

ISSN: 2067-3809 [CD-Rom, online]

ACTA TECHNICA CORVINIENSIS – Bulletin of Engineering
Tome VI (Year 2013) – FASCICULE 3 [July–September]
ISSN 2067–3809

[1.] Michal DÚBRAVČÍK

COMPOSITE MATERIALS – THEIR POTENTIALITIES AND APPLICATIONS IN AUTOMOTIVE INDUSTRY

[1.] TECHNICAL UNIVERSITY OF KOSICE, DEPARTMENT OF MATERIALS AND TECHNOLOGIES, MASIARSKA 74, 04001 KOSICE, SLOVAKIA

ABSTRACT: Modern car design and production trends are demanding continually decreasing of car weight. The decreasing of weight is strong connected with fuel consumption. This connection put pressure on the designers to apply unconventional materials in the car construction. Simultaneously the safety demands are increasing. One from many options to synchronize these requirements is an application of composite materials. Their properties are fated to using in machine industry. Submitted paper brings closer an example of composite materials using for chosen car component weight decreasing.
KEYWORDS: Composite materials, automotive industry, applications, testing

INTRODUCTION

Decreasing of car weight together with increasing of car safety is a big challenge in the car construction processes. One from many options is to use and apply the composite materials. Using of these materials for example in F1 constructions suggests the right way. Composite materials wide varieties of usage in combination with their universal utilization are the material engineering future. In our project, we decided to focus on composite materials based on resin and carbon fibres.

Carbon fibres are characterized via high toughness and low weight. In connection with resin, it can be made tough and light material, that can be shaped (in the production process) into required shapes and structures (Figure 1). Production technologies of these composites allow us to produce practically any product. Disadvantage of carbon composites is their predisposition on fragility. After material break, the product is no longer functional and it became corrupt. It is possible to eliminate even these negative characteristics, by addition of another material with proper properties like aramid fibres etc.

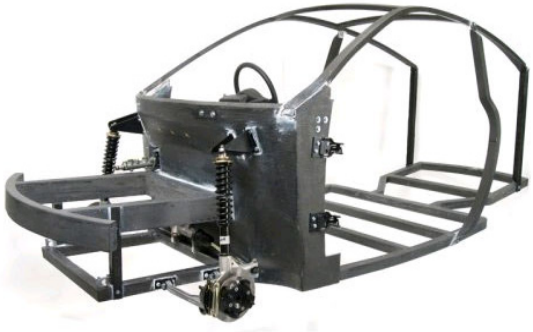

Figure 1: Axon carbon fibre frame [1]

Application of composites in serial production is currently financially no bearable a so it isn't much exploited yet. Though, the unstoppable technologies development gets good assumption for progressive introduction of composites into the conventional cars. Progressive substitution of individual components with composites, warranting the required component parameters and also the safety requirements, is one from many options by which one can the automotive industry with increasing requirements set out.

We tried to compare and test a possible substitution of classic component with composite component in our project.

APPLICATION OF COMPOSITE MATERIALS - Component selection

During the preparation phases of the experiment it was required to define suitable car component. It's to be a component witch could be real replaced by composite component and there should be possibility to test and compare the new component with original.

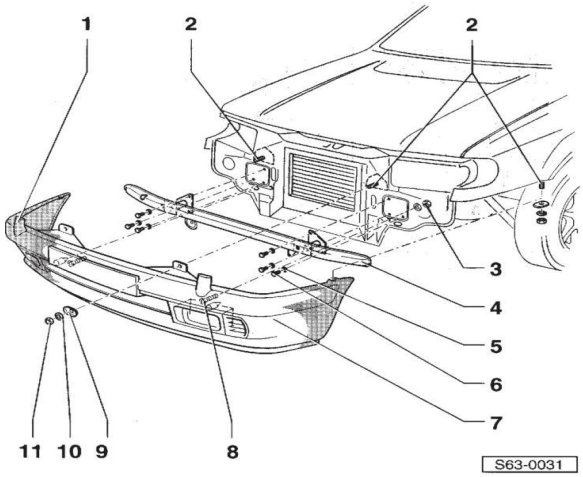

Figure 2: Front bumper reinforcement - position 4

For the proper component was chosen the front bumper reinforcement of Skoda Felicia (Figure 2). As

this component isn't visible from outside of the car, it allows us to focus on the function side of component. This fact allows us simplification and accelerating of composite component production.
Decomposition of the component showed us some problematic parts those must be solved. It bargains about the drawbar hook attachment and the horn attachment. These parts should be relocated to the main car body. They functionality doesn't have any effect on the bumper reinforcement and so they are irrelevant for our project.
Final component was simplified. CAD model of chosen component can be seen on Figure 3.

Figure 3: CAD model of bumper reinforcement

Mould production

Introductory step for component production is mould production. It's highly necessary to prepare the original component surface for mould production. These preparations have determining effect for resultant mould parameters and that's why it's so necessary to put adequate care.
Single mould production begins with precise surface separation of the original component. For the first layer we have used gentle glass fibre (220g/m^2) for high surface quality of the mould. Another four layers are from rough glass fibre mat (450g/m^2). This mat gives required weight and toughness to the mould. After this manner produced mould (Figure4), it's separated from the original component and it edges and surfaces are mechanically adjusted (Figure5).

Figure 4: Mould production

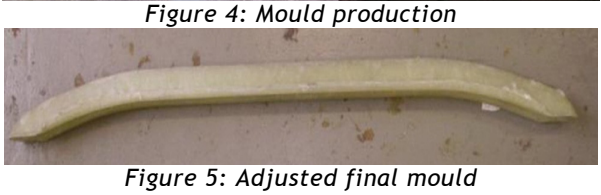

Figure 5: Adjusted final mould

Despite modifications of the original component surface, isn't the mould surface totally smooth. This can cause a surface defectiveness of the produced component. Therefore it's necessary to modify the mould surface before another usage. This phase is even more necessary for production of high quality surface products. Mould modified like this is prepared for another usage.

Component production

We elected following material composition for final component production (Table 1):

Table 1: Material composition

Layer	Fibre orientation	Material
1.	90°	Carbon 160g/m^2
2.	45°	Carbon 160g/m^2
3.	90°	Carbon 160g/m^2
4.	45°	Glass-fiber 450g/m^2
5.	90°	Carbon 160g/m^2
6.	90°	Kevlar-Carbon 165g/m^2

We have selected vacuum technology for composite component production and applied resin and fibres into the mould by help of conventional methods in the order of Table 1 (Figure 6).

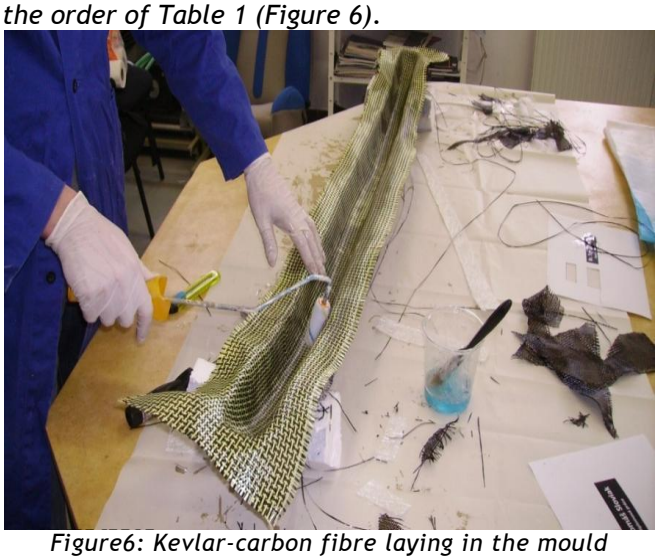

Figure6: Kevlar-carbon fibre laying in the mould

Prepared and saturated fibres have been placed into vacuum and they got hardened (Figure 7). After the material hardened, the work layers were getting off. The surface of one side was adjusted for deformation elements connection and the other side for better look.

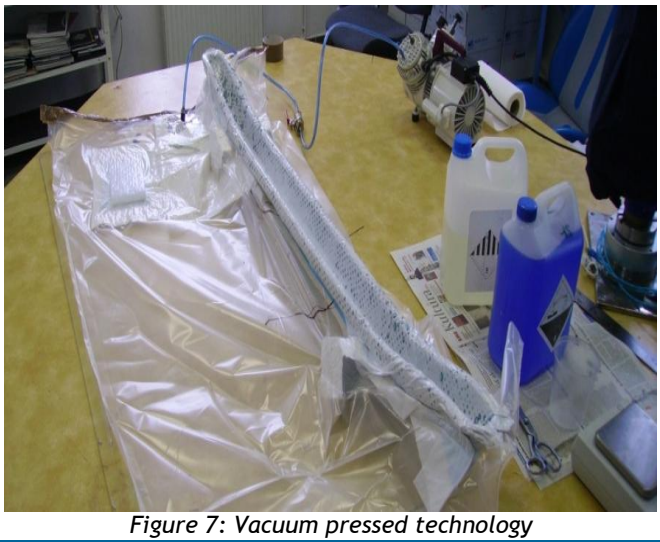

Figure 7: Vacuum pressed technology

Deformation elements production

Deformation elements are consisted of:

- plate - this part made the connection surface for bumper reinforcement connection to car body
- tube - main deformation element (Figure 8)

Single parts were made separately and thereafter they were connected in one piece (Figure 9). The complete units were mounted to the bumper reinforcement (Figure 10).

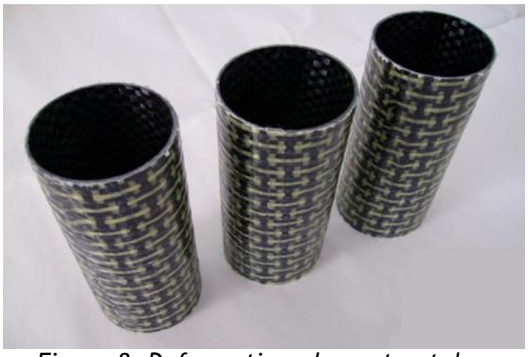

Figure 8: Deformation elements - tubes

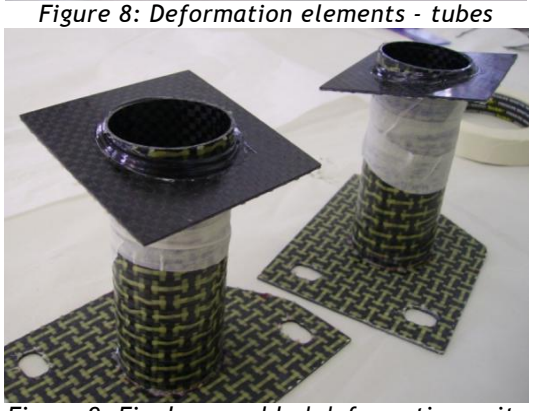

Figure 9: Final, assembled deformation units

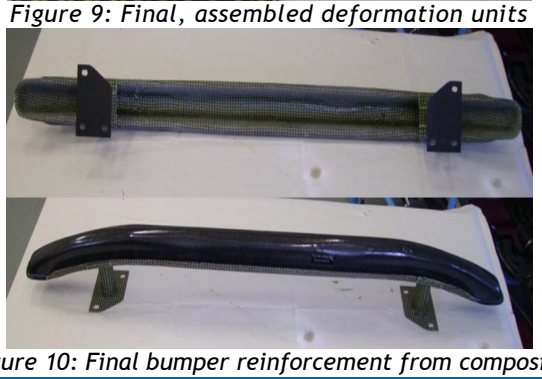

Figure 10: Final bumper reinforcement from composite

TESTING

Two testing methods were for testing chosen:

- material tension test
- deformation element pressure test

Composite material tension test

Composite material tension test was realised by static tension test. Test principle is to charge the specified testing sample till its breaking. There were four samples with specific dimensions - 250 x 25 mm and 1.4 mm thickness (Figure 11).

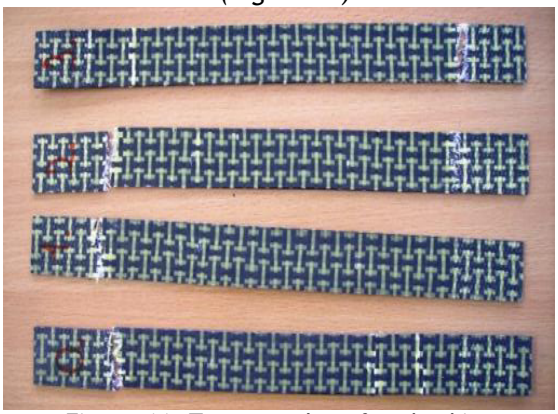

Figure 11: Test samples after braking

From the next table results, that the general measured strength of used composite material, which was averaged from the results of the 4 samples, is 387 MPa.

Table 2. Composite material tension test results

Sample	0	1	2	3	Averaged result
Volume of the limit strength F_m (N)	14904	11865	13833	15694	14074
Extension after breaking ΔL_c (mm)	1.02	4.73	1.79	2.77	2.58
Strength R_m (MPa)	442	321	370	414	387

Deformation element pressure test

Deformation element is the main reinforcement part, which is deforming yourself during crash. This deformation absorbs most of crash energy. This was main reason to make s test. The test was made by hydraulic test machine ZD40, which can forces 400kN or 40 tons. The test machine counteracted the test fair sample of deformation element, and the process was graphical recorded (Figure 12).

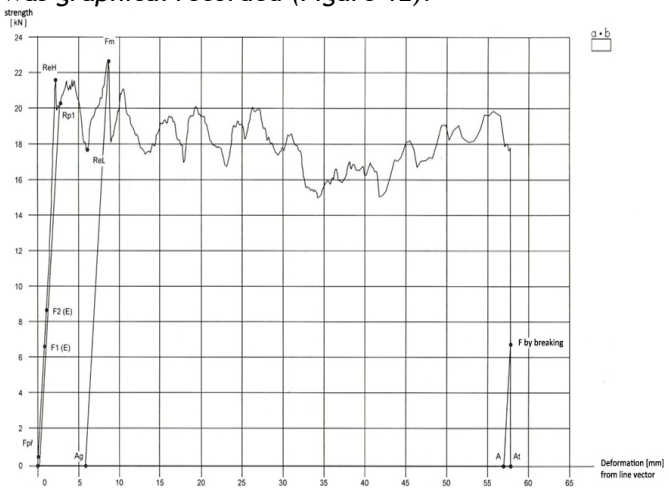

Figure 12: Deformation graph

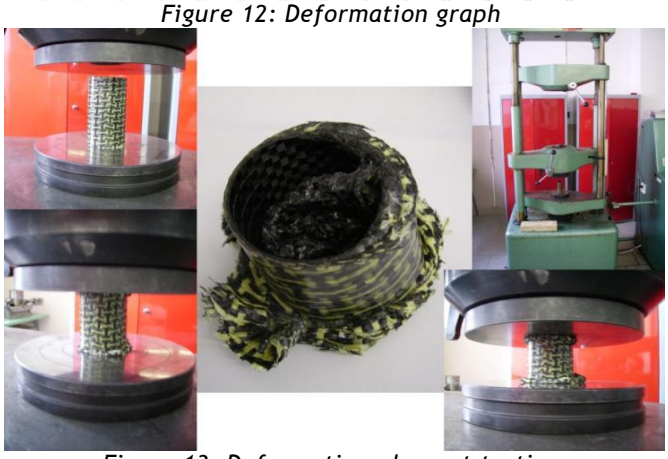

Figure 13: Deformation element testing

As you can see in table Table 3, the sample was deformed/compressed about 58 mm with average loading of 1818 kg, whereby the maximum loading reached 2270 kg.

Table 3. Deformation element test results

Sample length (mm)	100
Sample diameter (mm)	45
Compression (mm)	58
Max. loading strength (N)	22700
Max. loading (kg)	2270
Average loading strength (N)	18184
Average loading (kg)	1818

CONCLUSIONS

As shown in Table 4, measured mechanical parameters values of composite are comparable with metal reinforcement. The most important results and comparing with original component are shown in the next table.

Table 4: 1Final results

	Composite reinforcement	Metal reinforcement
Weight (g)	650	3700
Pull strength (MPa)	387	380
Maximum def. element loading (kg)	2270	-

Primary result indicator of our project is component weight decreasing with maintenance of mechanical properties. To show this property was out goal. The composite component weight is about 3050g lower as the metals.

Usage of composites in the car production gives us a very good option to decrease the car weight. Though not every component can be substituted, it can decrease the car weight up to dozens of kilos. This is the way we should go on for decreasing the fuel consumption. This way is also important for electric cars those need to be light for increasing of the endurance distance.

REFERENCES

[1.] available on network: http://www.carbonfibergear.com/wp-content/uploads/2008/07/axon-carbon-fiber-frame.jpg

[2.] ŠTEFÁNIK, Pavol: Ľahkékonštrukčnémateriálynabázepolymérnych a kovových kompozitov. Moderníľahkékonštrukčnémateriály. [online]. Aktualizované 11-07-2006 [cit 2012-04-02]. Dostupnénainternete: < http://www.matdesign.sav.sk/data/long_files/kompozity.pdf>.

[3.] DÚBRAVČÍK, Michal: Substitúciakovovýchautomobilovýchkomponentov kompozitnými. In: Transfer inovácií, roč.2011, č.19, s. 220-222

[4.] KLEISNER, Václav - ZEMČÍK, Robert: Applied and Computational Mechanics: Analysis of composite car bumper reinforcement. [online] 2009. Plzeň: ZápadočeskáUniverzita v Plzni, Fakultaaplikovaných vied. [cit 2012-04-20]. Dostupné na internete: < http://www.kme.zcu.cz/acm/index.php/acm/article/viewFile/92/24>

[5.] SLOVIAK, Bc. Tomáš: Substitúciakonvenčnýchmateriálovautomobilovýchkomponentov. Diploma work. Košice: Technickáuniverzita v Košiciach, Strojnickafakulta, 2012. 75 s.

ACKNOWLEDGMENT

This contribution is the result of the project implementation: Centre for research of control of technical, environmental and human risks for permanent development of production and products in mechanical engineering (ITMS: 26220120060) supported by the Research & Development Operational Programme funded by the ERDF.

ISSN: 2067-3809 [CD-Rom, online]

ACTA TECHNICA CORVINIENSIS – Bulletin of Engineering
Tome VI (Year 2013) – FASCICULE 3 [July–September]
ISSN 2067–3809

[1.] R.N. BARIK

RADIATION EFFECT AND MHD FLOW ON MOVING VERTICAL POROUS PLATE WITH VARIABLE TEMPERATURE

[1.] DEPARTMENT OF MATHEMATICS, TRIDENT ACADEMY OF TECHNOLOGY, INFOCITY, BHUBANESWAR-751024, ODISHA, INDIA

ABSTRACT: An attempt is made to study the combined effects of magnetohydrodynamics (MHD) and thermal radiations on unsteady flow of an electrically conducting fluid past an impulsively started infinite vertical porous plate with variable temperature is investigated. A magnetic field of uniform strength is applied along an axis perpendicular to the plate. The plate temperature is raised linearly with time. An exact solution is obtained by Laplace transformation technique. The dependence of the amplitude and skin-friction on various parameters is discussed in detail with the help of graphs.
KEYWORDS: MHD/thermal radiations/porous plate/ variable temperature

INTRODUCTION

Study of MHD flow with heat and mass transfer play an important role in various industrial applications. Some important applications are cooling of nuclear reactors, liquid metals fluid, power generation system and aero dynamics. It is of importance in connection with many engineering problems, such as sustained plasma confinement for controlled thermo nuclear fusion and electromagnetic casting of metals.MHD finds applications in electromagnetic pumps, crystals growing, MHD couples and bearing, plasma jets and chemical synthesis. Radiative heat and mass transfer play an important role in manufacturing industries for the design reliable equipment. Nuclear power plants, gas turbines and various propulsion devices for aircraft, missiles, satellites and space vehicles are examples of such engineering applications.

Hydromagnetic incompressible viscous flow has many important engineering applications such as magnetohydrodynamic power generators and the cooling of reactors also its applications to problems in geophysics, astrophysics etc. On the other hand, the study of heat generation or absorption in moving fluids is important in problems dealing with chemical reactions dissociating fluids. Since some fluids can emit or absorb thermal radiation, it is of interest to study the effects of magnetic field on the temperature distribution and heat transfer when the fluid is not only an electrical conductor but also when it is capable of emitting and absorbing radiation, Hence, heat transfer by thermal radiation is becoming of greater importance in space applications and higher operating temperatures.

The non-linearity of the Navier-Stokes equations presents mathematical difficulties in obtaining the exact solution. One of the exact solutions of the Navier-Stokes equations of the flow due to an impulsively started infinite flat plate was first studied by Stokes [1]. Georgrantopoulous [2] has discussed the free convection effects of the oscillating flow in the Stokes problem past an infinite vertical porous plate with constant suction. Kafousias et.al [3] has extended the above problem in the presence of a transverse magnetic field without taking into account the induced magnetic field.

A number of researchers have made contributions in solving the problems of free-convection flows under various boundary conditions. Notably among them are Singh [4], Muthucumaraswamy and Kulandaivel [5], Singh and Garg [6]. Very recently Singh and Garg [7] have analyzed the Hall current effects on free convection flow past an accelerated porous plate in a rotating system with Heat source/sink by Laplace transformation technique. The current interests in the study of magnetohydynamic (MHD) of relating fluid has been motivated by several important problems such as maintenance and secular variations of earth's magnetic field, the internal rotation rate of sun, the structure of rotating magnetic stars, the planetary and solar dynamo problems and centrifugal machines etc. On the other hand, in view of the increasing technical applications using magnetohydrodynamic (MHD) effect, it is desirable to extend many of the available hydrodynamic solution to include the effects of magnetic field for those cases where the viscous fluid is electrically conducting. The effect of a transverse magnetic field on free convective flows of an electrically conducting viscous fluid, has been discussed in recent and past years by several authors, notably by Gupta [8], Soundalgekar [9], Mishra and Mudili [10], Mahendra Mohan [11], Sarojamma and Krishna [12] and Singh and Garg [13] and Garg et al [14]. Such type of flows has wide range of applications in aeronautics, fluid fuel nuclear reactors and chemical engineering. The

various applications of MHD flows in technological fields have been complied by Moreau [15]. Recently, Ramana Reddy et al. [16] have studied the mass transfer and radiation effects of unsteady MHD free convective fluid flow embedded in porous medium with heat generation/absorption. Radiation effects on MHD free convection flow over a vertical plate with heat and mass flux was studied by Sivaiah et al. [17]. Recently, radiation and mass transfer effects on MHD free convection flow through porous medium past an exponentially accelerated vertical plate with variable temperature has been studied by Pattnaik et al. [18]. Reddy et al. [19] have studied the radiation and chemical reaction effects on MHD heat and mass transfer flow inclined porous heated plate.

The purpose of the present investigation is to study the effects of magnetic field on unsteady free convective moving vertical porous plate in the presence of variable temperature and thermal radiations. The effects of different pertinent physical parameters on the velocity, temperature and skin-friction are presented graphically.

MATHEMATICAL ANALYSIS

Consider an unsteady, free convective flow of an in compressible, electrically conducting, viscous fluid past an impulsively started infinite insulated vertical porous plate with variable temperature. Let us introduce a co-ordinate system with plate lying vertically on x'y' plane such that x-axis is oriented in the direction of buoyancy force and the z-axis is perpendicular to the plane of the plate. A uniform magnetic field $\vec{H}$ is acting transverse to the plate in the presence of thermal radiations. Initially, the plate and the fluid were at rest and temperatures of both are also same. At time t' > 0, the plate is given impulsive motion in the vertical direction against gravitational field with constant velocity u'_0, the plate temperature is raised linearly with time. Since the plate occupying the plane z' = 0 is of infinite extent, all the physical quantities depend only on z' and t'. The equation of continuity $\nabla.\vec{V}=0$ gives on integration w' = -w_0, where $\vec{V}\equiv$(u', v', w'). The constant w_0 > 0 represents the suction velocity at the plate. Using the relation $\nabla.\vec{H}=0$ for the magnetic field $\vec{H}\equiv(H'_x,H'_y,H'_z)$, we obtain $H'_z = H_0$ everywhere in the fluid (H_0 is a constant). In addition, thermal radiation term is added in the energy equation.

The fluid considered here is a gray, absorbing-emitting radiation but a non-scattering medium. Then by usual Boussinesqs' approximations, the governing equations to the problem are obtained as

$$u'_{t'} - w_0 u'_{z'} = g\beta(\theta'-\theta'_\infty)+\nu\ u'_{z'z'} - \frac{\sigma\ \mu_e^2 H_0^2}{\rho}u' \quad (1)$$

$$v'_{t'} - w_0 v'_{z'} = \nu v'_{z'z'} - \frac{\sigma\mu_e^2 H_0^2}{\rho}v' \quad (2)$$

$$\rho c_p(\theta'_{t'} - w_0\theta'_{z'}) = k\theta'_{z'z'} - q'_{z'}, \quad (3)$$

The initial boundary conditions of the problem are

$$u'=v'=0,\quad \theta'=\theta'_\infty \quad for\ all\ z'\ at\ t'\le 0\ ,$$

$$u'=u'_0\ ,\quad v'=0,\quad \theta'=\theta'_\infty+(\theta'_{w'}-\theta'_\infty)\quad ct'$$

at z' = 0 for t' > 0, $u'=0$, $v'=0$, $\theta'=\theta'_\infty$

as $z'\to\infty$ for t'> 0. (4)

where g, the acceleration due to gravity; β, the coefficient of volume expansion of the fluid; ν, the kinematic viscosity; ρ, the density; θ' the fluid temperature inside the thermal boundary layer; θ'_∞, fluid temperature away from the porous wall; k, the thermal conductivity, c_p the specific heat of the fluid under constant pressure and $c = \frac{u'^2_0}{\nu}$.

The local radiant for the case of an optically thin gray gas is expressed by

$$q'_{z'} = -4a^*\sigma^*(\theta'^4_\infty - \theta'^4). \quad (5)$$

where a^* is the absorption coefficient and σ^* is the Stefan-Boltzmann constant.

We assume that the temperature differences within the flow are sufficiently small such that θ'^4 may be expressed as a linear function of the temperature. This is accomplished by expanding θ'^4 in a Taylor series about θ'_∞ and neglecting higher order terms, thus

$$\theta'^4 \cong 4\theta'^3_\infty\theta' - 3\theta'^4_\infty. \quad (6)$$

By using equations (5) and (6), equation (3) reduces to

$$\rho c_p(\theta'_{t'} - w_0\theta'_{z'}) = k\ \ \theta'_{z'z'} + 16a^*\sigma^*\theta'^3_\infty(\theta'_\infty - \theta') \quad (7)$$

On introducing the following non-dimensional quantities

$$\left.\begin{aligned} u &= \frac{u'}{u'_0},\quad t = \frac{t'u'^2_0}{\nu},\quad v = \frac{v'}{u'_0},\\ z &= \frac{z'u'^2_0}{\nu},\quad \theta = \frac{\theta'-\theta'_\infty}{\theta'_w-\theta'_\infty},\quad w = \frac{w_0}{u'_0},\\ Gr &= \frac{\nu\ g\beta(\theta'_w-\theta'_\infty)}{u'^3_0},\quad M = \frac{\sigma\mu_e^2H_0^2\nu}{u'^2_0\rho},\\ R &= \frac{16a^*\nu^2\sigma^*\theta'^3_\infty}{k\ u'^2_0},\qquad \Pr = \frac{\rho\nu\ c_p}{k}, \end{aligned}\right\} \quad (8)$$

into equations (1), (2) and (7), we get,

$$u_t - wu_z = Gr\theta + u_{zz} + M\,u, \quad (9)$$

$$v_t - wu_z = v_{zz} - M\,v, \quad (10)$$

$$Pr(\theta_t - w\theta_z) = \theta_{zz} - R\theta, \quad (11)$$

where Gr = Thermal Grashof number, M = Hartmann number , Pr = Prandtl number,

R = Radiation parameter.

The transformed boundary conditions

$$\left.\begin{aligned} &u=0, v=0, \theta=0, \quad for\ all\ z,\ at\ t\le 0\\ &u=1, v=0, \theta=t, \quad at\ z=0,\ for\ t>0,\\ &u\to 0,\ v\to 0,\ \theta\to 0 \qquad as\ z\to\infty,\ for\ t>0. \end{aligned}\right\} \quad (12)$$

The equations (9)-(11) subject to the boundary conditions (12) describe the hydromagnetic free-convection flow past the moving porous plate.

Introducing the complex velocity F = u + iv, we find that equations (9) and (10) can be combined into a single equation of the form

$$F_t - wF_z = Gr\,\theta + F_{zz} - MF. \quad (13)$$

The corresponding transformed boundary conditions in the complex notations are given as

$$F = 0,\ \theta = 0 \ \text{for all } z,\ \text{at } t \le 0,$$
$$F = 1,\ \theta = t \quad \text{at } z=0,\ \text{for } t>0, \quad (14)$$
$$F \to 0,\quad \theta \to 0 \quad \text{as } z \to \infty,\ \text{for } t > 0.$$

In order to find the solution of equation (13), we take Pr = 1. This is possible assumption since the Prandtl number is a measure of relative importance of viscosity and heat conductivity in the fluid. For most gases the Prandtl number is of unit order, so that the velocity and the thermal boundary layer will be of the same order of thickness (cf. Houghton and Boswell [20]). By using the Laplace transformation technique solutions of equations (11) and (13) subject to the boundary conditions (14) are derived as:

$$F = A_1 A_3 (\eta_1 \exp X_1\, erfc\,\eta - \eta_2 \exp X_2\, erfc\,\eta_2) - A_2 A_3 (\eta_3 \exp X_3\, erfc\,\eta_3 - \eta_4 \exp X_4 erfc\,\eta_4) + \frac{1}{2}(\exp X_1\, erfc\,\eta_1 + \exp X_2\, erfc\,\eta_2), \quad (15)$$

$$\theta = A_4\{\eta_5 \exp X_5 \quad ecfc\eta_5 - \eta_6 \exp X_6 \quad erfc\eta_6\} \quad (16)$$

Using equation (15), we get the following expression for the skin friction components τ_x and τ_y as:

$$\tau_x + i\tau_y = -\left.\frac{dF}{dz}\right|_{z=0} = A_3 \left[\begin{array}{l} A_5 \quad erf \quad X_7 + \\ \left(\frac{t}{\pi}\right)^{1/2} \left\{ \begin{array}{l} \exp(-X_7^2) \\ -\exp(-X_8^2) \end{array} \right\} - \\ A_6 \quad erf \quad X_8 \end{array} \right]$$

$$+ b_1 erf X_7 + \frac{w}{2} + \frac{1}{\sqrt{\pi t}} \exp(-X_7^2) \quad (17)$$

where all A_i's, X_i's and η_i's are given in the appendix.

In equations (15)-(17), the argument of the complementary error function and error function is complex. Hence in order to obtain the x- and y-components of velocity, temperature and skin-friction, it is necessary to introduce some properties of the error function with complex arguments due to Abramowitz and Stegun [21]: i.e.

$$erf(c+id) = erf\ c + \frac{\exp(-c^2)}{2\pi c} \left\{ \begin{array}{l} 1-\cos(2cd) \\ +i\sin(2cd) \end{array} \right\}$$
$$+ \frac{2\exp(-c^2)}{\pi} \sum_{n=1}^{\infty} \frac{\exp(-n^2/4)}{n^2+4c^2} \{ f_n(c,\ d) + i g_n(c,\ d) \} \quad (18)$$

where:

$$f_n(c, d) = 2c - 2c\cosh(nd)\cos(2cd) + n\sinh(nd)\sin(2cd), \quad (19)$$

$$g_n(c, d) = 2c\cosh(nd)\sin(2cd) + n\sinh(nd)\cos(2cd), \quad (20)$$

and $|\in(c, d)| \cong 10^{-16}\,\mathrm{erf}(c, id)$.

RESULTS AND DISCUSSION

The expressions for velocity, temperature and the skin friction τ are calculated numerically for different values of suction parameter w, Hartmann number M, Grashof number Gr, Radiation parameter R and time t. The resultant velocity profiles are shown graphically in Figure-1. It is observed that the amplitude F of the velocity decreases with the increase of Grashof number Gr and suction parameter w. The velocity F increases with the increase of Hartmann number H and time t. But no alteration in the velocity is found with the increase of Radiation parameter R. The temperature profiles are presented in Figure-2. This figure clearly shows that the temperature decreases with the increase of suction parameter w,

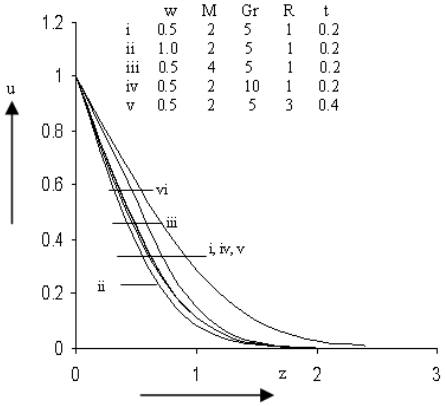

Figure 1. Velocity profiles

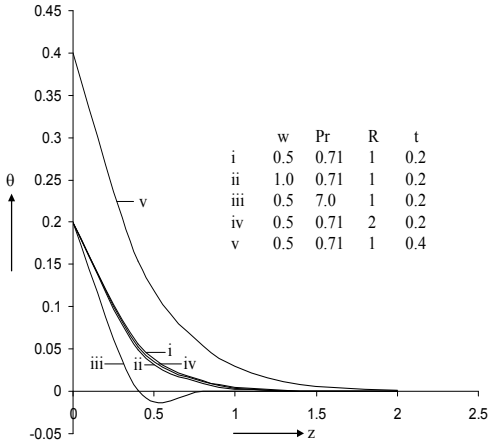

Figure 2. Temperature profiles

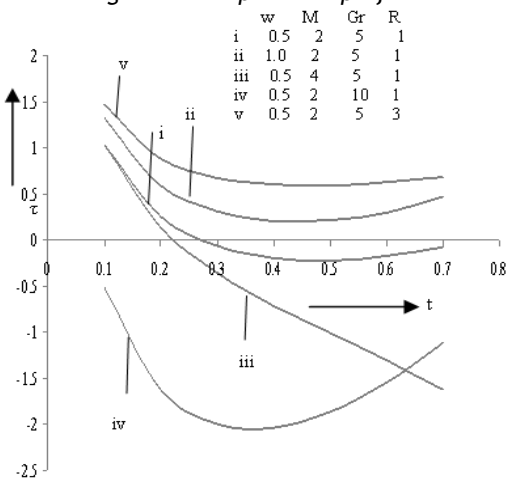

Figure 3. Variations of skin-friction

Prandtl number Pr and Radiation parameter R. But increase with the time t only. Figure-3 shows the variation of the skin-friction with various values of different parameters. This figure clearly depicts that the skin friction τ increases with the increase of suction parameter w,

Radiation parameter R. But τ decreases with the increase of Hartmann number M and Grashof number Gr.

Appendix

$$b_1 = \left(\frac{w^2}{4} - M\right)^{\frac{1}{2}},\ b_2 = \left(\frac{w^2}{4} + R\right)^{\frac{1}{2}},\ b_3 = \left(R + \frac{w^2\,Pr^2}{4}\right)^{\frac{1}{2}}$$

$$\eta_1,\eta_2=\frac{z\pm 2b_1t}{2t^{\frac{1}{2}}},\ \eta_3,\eta_4=\frac{z\pm 2b_2t}{2t^{\frac{1}{2}}},\eta_5,\eta_6=\frac{z\,Pr\pm 2b_3t}{2t^{\frac{1}{2}}\,Pr^{\frac{1}{2}}}$$

$$A_1=\frac{t^{\frac{1}{2}}}{2b_1},\quad A_2=\frac{t^{\frac{1}{2}}}{2b_2},\quad A_3=-\frac{Gr}{M+R},\quad A_4=\frac{t^{\frac{1}{2}}}{2b_3},$$

$$A_5=tb^{\frac{1}{2}}+\frac{1}{2b_1},\ A_6=tb_2+\frac{1}{2b_2},$$

$$X_1=\left(b_1-\frac{w}{2}\right)z,\ X_2=-\left(b_1+\frac{w}{2}\right)z,\ X_3=\left(b_2-\frac{w}{2}\right)z,$$

$$X_4=-\left(b_2+\frac{w}{2}\right)z,\ X_5=\left(b_3-\frac{w\,Pr}{2}\right)z,$$

$$X_6=-\left(b_3+\frac{w\,Pr}{2}\right)z,\ X_7=b_1t^{\frac{1}{2}},X_8=b_2t^{\frac{1}{2}}$$

CONCLUSIONS

(i) The amplitude of the velocity field decreases with the increase of Grashof number and suction parameter but the reverse effect is observed in case of Hartmann number and time span.

(ii) The radiation parameter has no significant effect on velocity field.

(iii) The temperature field decreases with the increase of either suction parameter or Prandtl number or radiation parameter but the reverse effect is observed in case of time span.

(iv) The skin friction co-efficient increases with the increase of either suction parameter or radiation parameter whereas the opposite effect is marked in case of Hartmann number and Grashof number.

REFERENCES

[1.] Stokes GG. On the effect of the internal friction of fluids on the motion of pendulums, Camb. Phil. Trans. 1851; ix: 8.

[2.] Georgantopoulous, G.A. Effects of free-convection on the hydromagnetic accelerated flow past a vertical porous limiting surface. Astrophysics and Space Science 1979; 65: 433-441.

[3.] Kafousias NG, Massalas CV, Raptis AA, Tzivanidis GL, Georgantopoulous GA & Goudas GL. Free convection effects on the hydromagnetic oscillatory flow in the Stokes problrem past an infinite porous vertical limiting surface with constant suction-1. Astrophys. Space Sci 1980; 86: 99-110.

[4.] Singh Ajay Kumar. Hydromagnetic mixed monvection flow and heat transfer with periodic suction velocity, permeability and heat sink. J Energy Heat and Mass Transfer, 2008; 30: 21-43.

[5.] Muthucumaraswamy R & Kulandaivel T. Radiation effects on moving vertical plate with variable temperature and uniform mass diffusion. J Energy Heat and Mass Transfer, 2008; 30: 79-88.

[6.] Singh KD & Garg BP. Exact solution of an oscillatory free-convective MHD flow in a rotating porous channel with radiative heat. Proc Nat Acad Sci 2010; 80 A: 81-89.

[7.] Singh KD & Garg BP. Effects of Hall current on free-convective flow past an accelerated vertical porous plate in a rotating system with heat source/sink, J Raj Acad Phy Sci 2009; 8(2): 191-202.

[8.] Gupta AS. Combined free and forced convection effects on the magnetohydrodynamic Flow through a Channel". ZAMP 1969; 20: 506-513.

[9.] Soundalgekar VM. Free convection effects on steady MHD flow past a vertical porous plate. J. Fluid Mechanics 1974; 66: 541-551.

[10.] Mishra SP & Mudili JC. Combined free and forced convection effects on the magneto-hydrodynamic flow through a porous channel. Proc. Ind. Acad. Sci, 1976; 84-A: 257-272.

[11.] Mahendra Mohan. Combined effects of free and forced convection on magnetohydrodynamic flow in a rotating channel. Proc. Indian Acad. Sci. 1977; 84: 383-401.

[12.] Sarojamma G & Krishna DV. Transient hydromagnetic convective flow in a rotating channel with porous boundaries. Acta Mech. 1981; 40: 277-288.

[13.] Singh KD & Garg BP. Radiation effects on unsteady MHD free convective flow through porous medium past a vertical porous plate. Proc. Indian Natn. Sci. Acad. 2009; 75(1): 41-48.

[14.] Garg BP, Singh KD & Pathak Reena. An analysis of radiative, free-convective and mass transfer flow past an accelerated vertical plate in the presence of transverse magnetic field. J. Rajasthan Acad. Phy. Sci. 2011; 10(1): 1-10.

[15.] Moreau R. Magnetohydrodynamics. Kluwer Academic Publishers, Dordrecht, 1990.

[16.] Ramana Reddy, G.V., Ramana Murthy, Ch. V. and Bhaskar Reddy, N., Mass transfer and radiation effects of unsteady MHD free convective fluid flow embedded in porous medium with heat generation/absorption, Journal of Applied Mathematics and Fluid Mechanics, vol.2, No.1, pp. 85—98 (2010).

[17.] Sivaiah, M., Nagarajan, A.S. and Reddy, P.S., Radiation effects on MHD free convection flow over a vertical plate with heat and mass flux, Emirates Journal for Engg. Research, vol.15 (1), pp. 35-40 (2010).

[18.] Pattnaik, J.R., Dash, G.C. and Singh, S., Radiation and mass transfer effects on MHD free convection flow through porous medium past an exponentially accelerated vertical plate with variable temperature, Annals of Faculty Engineering Hunedoara - International Journal Engineering, Tome X. Fascicule 3. ISSN 1584-2673. Pp. 175-182 (2012).

[19.] Reddy, S., Reddy, G.V.R. and Reddy, K.J., the radiation and chemical reaction effects on MHD heat and mass transfer flow inclined porous heated plate, Asian Journal of Current Engineering and Maths 1:3, pp. 115-119 (2012).

[20.] Houghton EL & Boswell RP. Further aerodynamics for engineering students, Edward Arnold Ltd. 1969; 252.

[21.] Abramowitz BM & Stegun IA. Handbook of mathematical functions with formulas, graphs and mathematical tables. U.S. Govt. Printing Office, Washington D.C., USA. 1964.

ACTA TECHNICA CORVINIENSIS – Bulletin of Engineering
Tome VI (Year 2013) – FASCICULE 3 [July–September]
ISSN 2067–3809

[1.] Fathollah OMMI, [2.] Ehsan MOVAHEDNEJAD, [3.] Kouros NEKOFAR

EXPERIMENTAL INVESTIGATION OF FUEL INJECTION AND FUEL TRANSPORT INTO THE CYLINDER IN A PORT-INJECTED SI ENGINE (XU7JP-L3)

[1.] TARBIAT MODARES UNIVERSITY, TEHRAN, IRAN
[2.] ISLAMIC AZAD UNIVERSITY OF JOLFA, JOLFA, IRAN
[3.] ISLAMIC AZAD UNIVERSITY OF CHALOOS, CHALOOS, IRAN

ABSTRACT: Liquid fuel inflow into the cylinder is considered to be an important source of exhaust hydrocarbon (HC) emissions from automotive spark ignition engines. These liquid-fuel caused emissions are increased significantly during the start up and subsequent warm-up period. The two phase fuel/air flow through an internal combustion engine inlet valve has been studied experimentally in a specially designed rig. The separated flow associated with fuel films on the inlet port and droplets on the valve stem can readily be seen. This study analyzes the influence of several engine and injection design variables on the fuel entrainment and in cylinder liquid fuel behavior. The effect of the following parameters on the characteristics of the fuel droplets entering the cylinder was studied: spray geometry, spray targeting, flow velocity and intake valve lift. The present study shows substantial dependence of in cylinder liquid fuel characteristics on the above parameters. It is shown that the droplet size distribution, the amount of liquid fuel, and the spatial distribution of droplet characteristics around the intake valve circumference were affected to different degrees. The observed trends in the droplet characteristics are explained in terms of changes in the previously identified mechanisms. The observed differences in in-cylinder liquid fuel behavior are significant enough to be reflected in engine out emissions behavior.
KEYWORDS: Injectors, inlet port, spraying, lift

INTRODUCTION

Today the high volume of fuel consumption in addition of using so much energy and so expensive costs that puts on the shoulder of humans, in regards of air pollution and environmental dangers that exists for the citizens of a community, it has been under attention, so scientists are trying to find a way to reduce fuel consumption and optimize its combustion.

Therefore, many efforts have been done that the great deals of these efforts are about the fueling process in automotive engines and propulsions. Also the use of injector for the disperse of fuel and creation of full combustion was the result of such efforts and it led to the reduction of fuel consumption and lesser pollution and better combustion are the result of this significant change in the engine industry and propulsion.

The formation of a fuel mixture and air reasonably and the procedure of fuel entry into cylinder in the spark ignition engines was one of the important factors in getting ideal efficiency with the level of low pollutants and it can occur when the fuel droplets with diameters less evenly with the lowest concentration in the port enter into the cylinder.

Lefebvre has studied the liquid film thickness on the air jet in 1980and found that the droplet size is dependent on the film thickness and also concluded that the fluid velocity, air velocity and mass flow rate of liquid and air are dominant on the thickness of the liquid fuel [1].

Lawta has measured the rate of transient torque and ratio of air to the transient fuel for an engine in two states of the injector in 1987 and found that by changing the injector's position in the cylinder, the surface of the wetting wall will significantly changed. Also the ratio of air to fuel and momentum will be changed too.

Mayer considered the effects of fuel characteristics and engine design parameters on the analysis of the fuel transfer in 1999; the results measure the amount of pollutants changes of parameters output of the fuel [3]. Ohyama used the process of fuel mixture combination and the level of liquid fuel film for the purpose of assessing the quality of creation and preparation of the mixture in 1996 [4].

Behnia investigated the effect of the location of the fuel injector to the cylinder and the result of study was the formation quality of the mixture in the cylinder and measuring the fuel films and droplet size on entry to the cylinder in 2001 [5]. Curtis observed the phenomenon of film failure by applying the symmetric steady flow with a single cylinder engine. Repeated research work developed by Curtis.

In 2002 concluded that how the valve changes and port geometry affected better than fuel properties on atomization fuel film [6].
In order to develop and optimize the fuel system in injector engine with multi-point dispersion (Chen), a one-dimensional transient model was developed from a multi phase flow in an intake manifold and the formation process of air-fuel was investigated along the input port [7]. Milton and Elerman experimentally investigated two-phase flow of air and fuel in an internal combustion engine in different places of high-dispersion, different nesses of valves and velocity of flow and showed the effects of these parameters on entry and re-fuel atomization [8].
In this paper, a model of a glass from a series of entry port and the cylinder head of an engine (engine of Samand) is made and an auxiliary facility for modeling the performance of engine is fitted in the suction cycle. Using the made sets, different behavior of air and fuel engine performance is studied and analyzed; all models has been achieved for sucking cycle in steady state. Finally, the test conditions are consistent with the predicted function of air flow rate corresponding period RPM 2600 and 6000 and in every cases mentioned, movement quality of the film and droplets of fuel is investigated into the inlet port and its entry to the cylinder. In addition, the influence of injection parameters such as target location, flow rate and valve opening is determined.

ASSUMPTIONS

The study hypothesis is as follows:

A - The behavior of water and mixing with air is very similar to the behavior of fuel in actual condition.
B - The made model is geometrically similar to the true model.
C - The conditions of the experimental model are close to the actual model.

PREPARING THE TEST SET

The built motor is based on Motor XU7JP-L3 (Peugeot 405 and Samand engine) and the engine's information is used for its preparation. A cylinder from the mentioned four-cylinder engine includes the port - the cylinder head, cylinder and ... which is made of transparent glass compromises of glass and Plexy Glass. Meanwhile, the fuel rails and its accessories are made of aluminum.

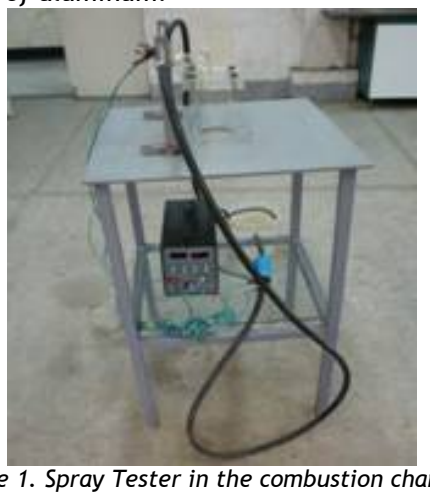

Figure 1. Spray Tester in the combustion chamber

Figure 1 shows the spray test components as follow:

A - A set of a single-cylinder glass engine of the type MPFI includes: Cylinder head, cylinder, port
B - A set of fuel rails: To supply fuel and necessary pressure for fuel into injector includes: aluminum fuel rails, injector, regulator, injector pump of the feeding source, interface pipes.
C - Collect water: used to gather fluid sprayed into the cylinder and prevent fluid contact with internal components of the machine table.

Cylinder Head

The cylinder head used in the research motor is made of Plexy Glass. First, the cylinder head should be provided as map and all parts are made of the entire lathe and milling operations. The actual dimensions of the cylinder head are presented in Figure 2.

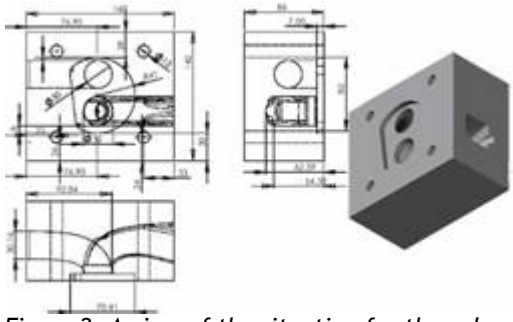

Figure 2. A view of the situation for the valves and ports in cylinder head

Injector

The sprayed injector has multiple flows; as Figure 4 showed opening the ball-valve caused the mainstream fuel flow passed from the primary nozzle and contacted to the center of a plate with three holes around itself and then is divided into three distinct jets.
Cross-section of a sprayed cone yield by jets away from the nozzle has the conical shape.
A view of spray with three non-uniform jets is shown in Figure 4.

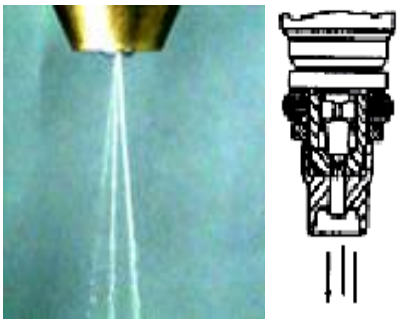

Figure 3. A) The geometry of the spray nozzle (left) B) A view of the spray pattern of spray [9]

Injector is capable of moving in three directions into front, back, up and down and moves around, with 3 degrees of freedom; How to get the pump and the fuel rail and engine power are shown in Figure 1.
The Flow bench is used in order to simulate the air flow into the cylinder during the suction cycle (Figure 4). Using this device, air flow with a distinct and adjusted flow is sucked by the fan from the end of the cylinder. Because the flow of water is not penetrating into the fan and the flow table elements, collector water is used for that as Figure 5 shown. In the collector that put on the flow bench

and cylinder, the aluminum sheets of 0.5 mm is used and when suction, the dye-water and material mixture is collected in the bowl and does not achieved the sucking air.

Figure 4. A view of flow bench [10]

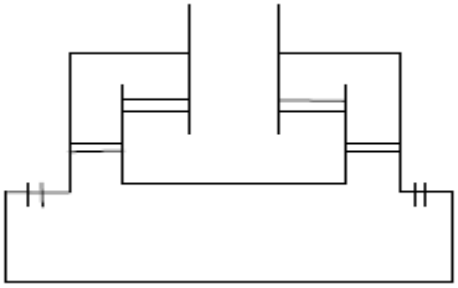

Figure 5. A schematic of absorptive system of water

THE PROCEDURE OF TESTS

The dye-water and material mixture of Proidin Aidin that is used in medicine for disinfecting wounds, is applied for doing test. Proidin Aidin is a colored material that completely dissolved in water and will not leave any sediment that causes clogging the pump and injector; because the used injector is very sensitive and reacted across the smallest sediment and not to show the spraying operations and it become inactive.

MECHANISM OF FUEL ENTRY INTO THE CYLINDER

As pointed out, the made series for the purpose of test of fuel injection is designed during the intake cycle. In this cycle, by moving piston downward, and opening the air valve, the air flows into the cylinder with high-speed. This is the mechanism for transfer of fuel to the cylinder that first the fuel flow is transferred with suitable pressure behind the injector and by opening the injector; the fuel is converted as liquid jet that is a mixture of liquid droplets and fuel film.

After fuel injection into the port, as for their size and speed, some of the fuel particles are divided to the smaller droplets by the effect of drag force or pressure fall that is in port and then evaporated and other fuel particles contacted to the walls of the port and the valve's seat and calf and the film formed the liquid fuel on the wall of the port that its control has an important role in improving atomization and complete combustion.

Flowing the air into the cylinder port, the remained fuel film under the influence of shear stress and gravity began to move towards the regions near the inlet valve, because the higher fuel shall be deposited in the port walls or valves, so it is under study and research and also transferring and fuel atomization have been studied again. In continue, opening the air valve, a percentage of the atomized fuel hovering is evaporated and then entered the cylinder with the flow of air. Despite the presence of air flow through, some of the fuel films that is near the fuel valve is still not atomized and not entered the cylinder through but it moved into the cylinder as the liquid fuel film. After entering the fuel into the cylinder head as the port shape, a vortex of air and fuel mixture is composed in the cylinder head that the shape and thickness and the vortex intensity are varied depending uplifts the valve and the flow rate. Mixture of air and fuel film move on the surface of the upper cylinder clockwise and contact to the bezel area 1 (Figure 6) and form a small vortex of fuel film in area 4. Finally the fuel film shown in Figure 7 entered the cylinder in front port (area 4).

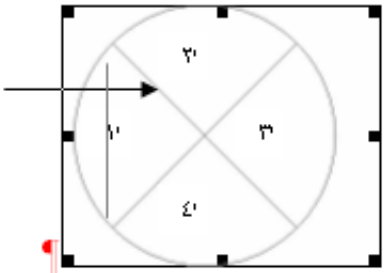

Figure 6. Viewing areas divided by cylinder head

EVALUATING THE EFFECTS OF THE INJECTOR

This case is studied the spray mode in FRONT, CENTER, BACK of the valve and also the valve low uplift and low speed motor. As seen in Figure 7, the fuel goes behind the valve in the spray back of the valve and more fuel goes out of the area and the amount of fuel is collected below the bezel. In the case shown in Figure 8, gathering the fuel film on the bezel is much lesser in spray mode in CENTER & FRONT of the valve.

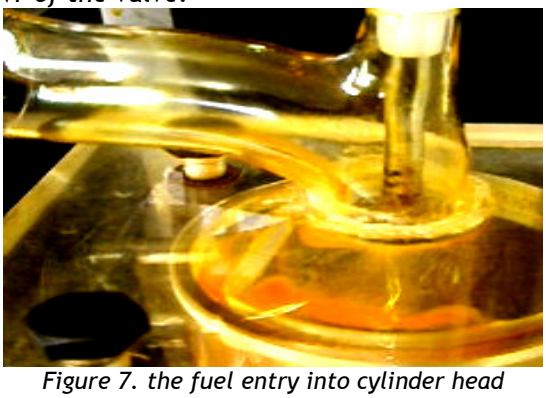

Figure 7. the fuel entry into cylinder head in spray mode behind valve (low lift)

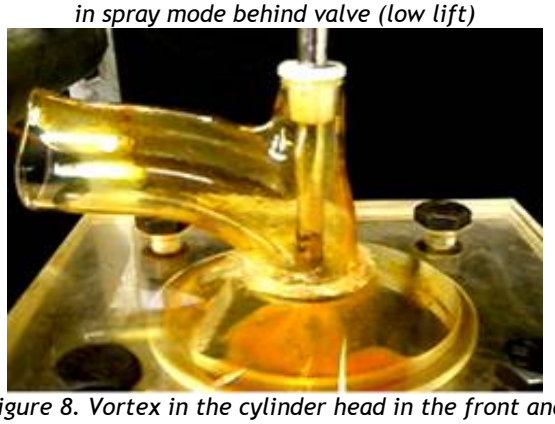

Figure 8. Vortex in the cylinder head in the front and center of the valve in spray mode (low lift)

Since the amount of fuel is collected below the bezel in area 1, the Vortex formation is varied at spray mode behind the valve with the spray mode front the valve. Also in the spray mode center the valve due to air flow, some of the jet fuel is diverted to the front of the valve. In the spray mode in front and center of the valve, a powerful vortex of fuel is formed in the cylinder head.

In spray mode behind the valve, the fuel film hits to the bezel after it leaves the valve (rear area 4 and 1) and some of them is collected below the bezel in area 1 and then returns. But front and center spray valve, the fuel film hits to the bezel in area 1 after removal of the front valve in area 3 and then returns and it flows into the cylinder from there. A few fuel is gather in the bezel, it can to be said that the difference of removal of fuel film in modes 1 and 2 is due to the collision of the jet to the front valve in one case, and back to the valve in another case. Also the thickness of fuel film on the port at the front spray is more than fuel injection in center and back valve.

Also the speed and openness of the valve are the same on the cylinder head in three modes, because the air rotation is also the same. In spray mode back of the valve, due to lack of fuel vortex in the cylinder head, the rate of diffusion of fuel film in the cylinder might be differed with two other modes; As seen in Figure 9, diffusion of fuel film into the cylinder is higher than the other two modes and also we can observe an uniform state in the cylinder than the diffusion of fuel film.

Figure 9. Fuel film diffusion into the cylinder at the back valve in spray mode

But according to Figure 8, as previously mentioned, because the vortex on the cylinder head has more focus in center and front spray valve, the fuel flows into the cylinder as the vortex is formed there and it cannot enter the cylinder evenly. The fuel film thickness in the cylinder is more than the spray mode in back.

Evaluating the uplift of valve

The effect of the inlet valve opening at low engine speed is investigated in this part. First, the excessive uplift of the valve and the spray in front of the valve should be investigated.

As shown in Figure 11, the jet fuel is more deviated due to the excessive uplift of the valve and the air flow passage of the valve, and then the collision of the fuel jet is done in the larger region. This area has been increased due to dispersion of fuel jet; as a result the fuel film thickness is less than the low lift mode. It should be noted that increasing the collision of the jet fuel may be increased the wetted surface portions; however, the evaporation rate is also increased there. In this case, the fuel jet is seen on the port as the fuel film; and there is less fuel film droplets.

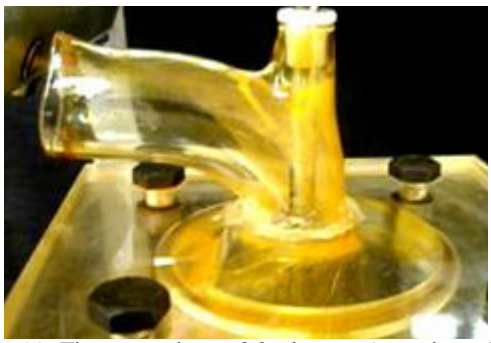

Figure 11. The procedure of fuel entry into the cylinder head at high-lift

According to Figure 11, the fuel exits from the front of the port and it falls in the cylinder head but it cannot gather into the cylinder due to the excessive openness and high speed flow after exiting the valve and the horseshoe vortex do not formed as the low lift mode (Figure 8), and fuel falls speedily into the cylinder (walls, etc.) and due to lack of fuel in the cylinder head, the fuel film thickness is less than the low lift mode in the cylinder head.

After leaving the port on the cylinder head, the fuel hits to the bezel in back of the port as the fuel film and then returns and flows into the cylinder; but returning the fuel from back of the bezel is higher than the low lift is (due to the high velocity air flow). Due to high openness of the valve, the fuel flows into the cylinder more than the low lift mode. Immediately, after leaving the port, the fuel flows directly into the cylinder without any contact with the cylinder head. Also, due to the high speed flow, the diffusion of fuel in the cylinder is more than the low lift mode as it can be seen in Figure 12. Most films in areas 4 and 3 and lowest fuel film below areas 1 and 2 for the cylinder head are visible.

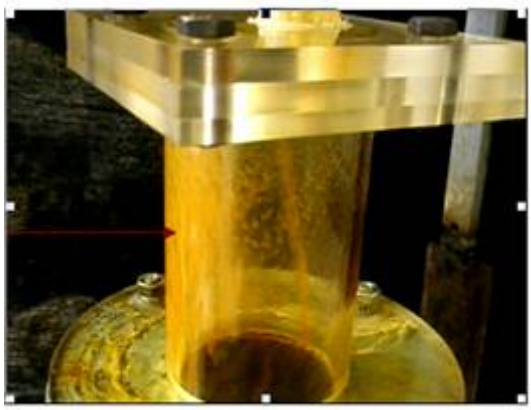

Figure 12. Fuel film diffusion into the cylinder at high-lift

EVALUATING THE EFFECTS OF FLOW RATE - Evaluating the high speed of engine at low uplift valve

The low uplift of the valve (1 mm) and high speed engine (6000 rpm) is investigated in this part.

It is observed that due to the high speed air flow, about 90% fuel film hits into the front of the valve, it means this mode is the same as if we target the

center of the valve so out target will be mistake by increasing the air flow velocity and the fuel jet is deviated from its way and then hits on the front of the valve.

Meanwhile, the fuel film thickness is low on the surface (front surface) because there is a high flow rate (Figure 13). The fuel film exits from the front of the valve (part 3) and returns to the back by contacting the bezel in area 1 and formed the horseshoe vortex. It should be noted that according to Figure 13, due to the high air flow, the horseshoe vortex is larger and more elongated and high levels of turbulence in the cylinder head is seen more than before and also retuning the bezel is higher than in area 1 (distance of collision to the bezel and return to the fall). Fuel film thickness is high at the cylinder head as mentioned previously, it causes the low valve openness which the fuel film flows to the upper cylinder head before hitting the cylinder's wall; as a result the film thickness can appear high in the cylinder head.

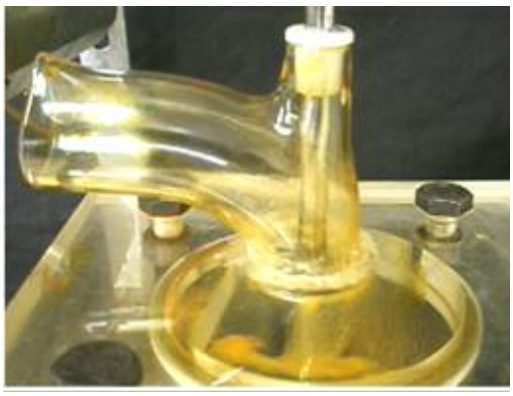

Figure 13. The procedure of fuel entry into the cylinder head at the back valve in spray mode

The fuel falls into the cylinder from area 4 by forming the horseshoe vortex. As shown in figure 14, the fuel film is spread in other parts due to the high speed air flow; and the film's diffusion is observed in regions 2 and 3 and 4 and there is only less fuel film in area 1; and less fuel film is also seen into the cylinder as droplets of different sizes due to the high velocity air flow. There is far too much spin inside the cylinder and generally the spread rate is varied in various parts of the cylinder (Figure 14).

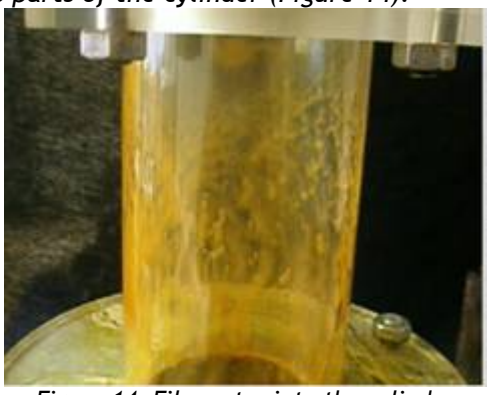

Figure 14: Film entry into the cylinder at high speed

Evaluating the high-speed engine at high uplift valve

The high engine rpm that increases the air flow velocity has a similar effect by increasing the valve opening. In both cases, the inlet air to the cylinder increases by the momentum conditions. In this part, the engine speed increased along with lift (uplift valve) and it investigated the high velocity flow effects associated with the uplift valve.

As seen in Figure 11, increasing the openness of valve causes the fuel jet more deviation and almost the entire surface of the port is covered by the fuel. In this part, the high velocity flow in one hand and high openness of the valve on the other hand may deviated the fuel jet more and also the fuel's diffusion will increase by both mentioned elements and covered the entire surface of the port, so the fuel film thickness seems less likely in the port's surface than the low openness mode by the effect of diffusion and high surface area.

The fuel film returns after collision to the bezel in area 1 and a strong vertex is seen in area 4 where the fuel flows into the cylinder. When more valve lift, the fuel film becomes colorless and pale, because of high velocity flow for the fuel film and low thickness of the film after leaving the valve in the area 3.

In these conditions, the intensity of swirl flow rate will increase the rotating of fuel film on the walls of cylinder as shown in figure 15. (Compare with Figure 14) On the other hand, high air rate will increase the homogeneity of the inlet fuel into the cylinder, so the fuel film thickness is lesser in the cylinder.

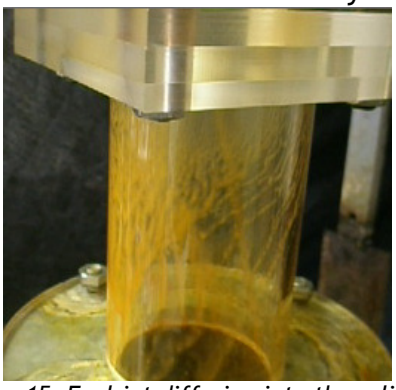

Figure 15. Fuel jet diffusion into the cylinder at high lift and speed

When the engine speed or uplift valve is high in the spray mode back of the valve, the fuel jet is deviated due to high velocity air flow and then hits on the center and back of the valve; and no spray in the back.

CONCLUSIONS

In the engines that the fuel is sprayed on the entry port, the spray features are less important than the air flow and the port geometry and cylinder head, and the advantage and the effect of some parameters such as speed, the level of flow rotation overcomes more than the spray parameters. It is more important at high speed engines, so the spray characteristics are affected by the air flow. The flow rate will be affected by jet's deviation, diffusion of fuel injection and precision targeting, fuel film formation in the port, cylinder head, cylinder, air flow rotation in the port, cylinder head, cylinder, homogeneous fuel into the cylinder. So that the high velocity flow will increase the deviation of jet fuel and diffusion of fuel injection, as a result there is less accurate targeting; and the more fuel film is formed on the port's walls. Also the rotation of air

flow rate and its distortion is more important. On the other hand, the high speed air will increase the homogeneity of the fuel entry into the cylinder, and then the fuel film is less formed in cylinder.
Changing the spray targeting has not any effect in the deviation of jet, fuel injection's diffusion and the accuracy targeting. But it is effective in forming the fuel film in the port and cylinder and homogeneity of the fuel when entering the cylinder. The high openness of the valve will increase the deviation of fuel jet and therefore the diffusion of fuel injection or fuel film in the port. Also, the intensity of flow rotation and homogeneity of the fuel will increase into the cylinder but reduce the accuracy targeting. No gathering fuel in the port and cylinder head at the high speed flow along with uplift valve because the fuel film thickness is much smaller than in the port and cylinder head.

REFERENCES

[1.] *Lefebvre A.H., " Atomization and Sprays" Hemisphere Publishing Corp., pp 309-369, 1989.*

[2.] *Zahao Y.H., Hou M.H. & Chin J.S. ''Drop Size Distribution from Swirl & Air-blast Atomizer'', Atomization and Spray Technology, pp. 3-15, 1986.*

[3.] *Meyer R.," Liquid Fuel Transport into the Cylinder in Port Injected SI Engines", PhD Thesis, Massachusetts, M.I.T University, 1998.*

[4.] *Ohyama Y., "The Effects of Fuel Injection System in Spark Ignition Engine on Exhaust Emissions and Fuel Economy", ATA Technical Paper, NO. 95A6022, 1995.*

[5.] *Behnia, M., Milton, B.E. "Fundamentals of the Fuel Film Formation and Motion in SI Engine Induction Systems", School of Mechanical and Manufacturing Engineering, The University of New South Wales, Sydney, NSW 2052, Australia.*

[6.] *Curtis E. W. and Aquino Ch. F.,'A New port And Cylinder Wall Wetting Model to Predict Transient Air/Fuel Excursion in a port Fuel Injected Engine ", SAE Paper No.961186, 1996.*

[7.] *Chen G.," Study of Fuel-Air Mixture Formation in Port-Injected Gasoline Engine", Ph.D. Dissertation University of Illinois, Chicago, 1995.*

[8.] *Milton, M.E., Behnia M., Ellerman D.M., "Fuel Deposition and Re-Atomization ", School of Mechanical and Manufacturing Engineering, university of NSW, Australia.*

ACTA TECHNICA CORVINIENSIS - Bulletin of Engineering

ISSN: 2067-3809 [CD-Rom, online]

ACTA TECHNICA CORVINIENSIS – Bulletin of Engineering
Tome VI (Year 2013) – FASCICULE 3 [July–September]
ISSN 2067–3809

[1.] Nicolae BURNETE, [2.] Dan MOLDOVANU, [3.] Doru BALDEAN

STUDIES AND RESEARCHES REGARDING THE INFLUENCE OF LUBRICATING OIL TEMPERATURE ON DIESEL ENGINES

[1.] TECHNICAL UNIVERSITY, CLUJ-NAPOCA, ROMANIA

ABSTRACT: The thermal regime has an important role on the wear of the engine and it affects the good functioning (also influencing the functioning parameters). The lubrication system of the internal combustion engine has the important role of ensuring an oil film between the moving surfaces. This paper highlights the effect that the engine lubricating oil temperature has on a diesel single cylinder research engine, on some important parameters of the engine (fuel consumption, power and torque). Experimental investigations were conducted in TestEcoCel Laboratory, Technical University of Cluj-Napoca.
KEYWORDS: lubricant oil, fuel, power, torque

INTRODUCTION

The functioning cycle of an internal combustion engine is characterized by: speed, load and the thermal regime.

The thermal regime has an important role on the wear of the engine and it affects the good functioning (also influencing the functioning parameters). It is a known fact that the friction between the moving parts (for example the piston-piston rings-cylinder, connecting rod-crankshaft) is reduced with the lowering (within some limits) of the viscosity of the oil from within the lubrication system.

A high viscosity of the oil can cause some power losses - loses that determine the rise of the fuel consumption and a low viscosity adversely affects the component parts wear, so it also affects the durability of the engine. The lubrication system of the internal combustion engine has the important role of ensuring an oil film between the moving surfaces.

EXPERIMENTAL RESEARCH

The determination of the lubricant oil temperature influence on the diesel engine performance was made in the TestEcoCel Laboratory, a high performance laboratory that is specialized in testing, research and certification of internal combustion engine that work with different fuels (Figure 1.)

The used test-bed consists of a single cylinder research engine that is equipped with an endoscopic camera for observing the phenomena that occur inside the combustion chamber, an active dynamometer used to rotate the engine up to speed, but also used to simulate the load of the road (loading the engine with a torque), a conditioning system for the cooling liquid and for the lubricating oil, a ventilation system used to condition the temperature of the air inside the test cell, a gas analysis system capable of measuring the pollutants in the exhaust gas; and all the systems are controlled by an automation system.

Figure 1. TestEcoCel Laboratory

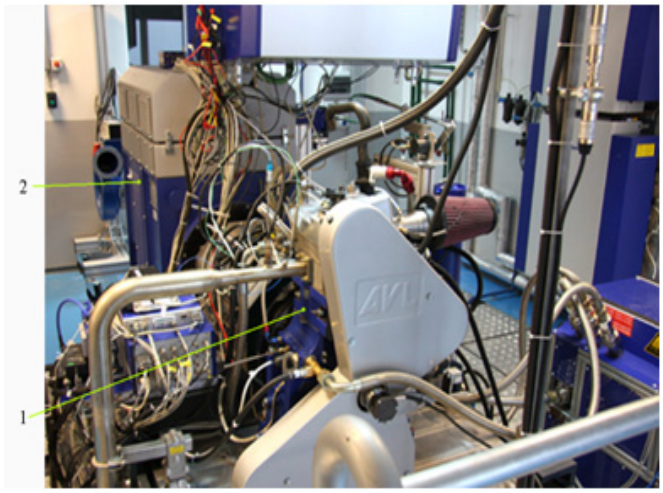

Figure 2. The test bed
1 - Single cylinder engine; 2- dynamometer

The tests were made at different temperatures of the lubricating oil, at constant speed, in order to exclude the influence of other factors that cannot be appreciated objectively.
Although the laboratory allows the use of different fuels, for this study, the only fuel that was used is classic: Diesel.

RESULTS

The measurements were made following some predefined steps, and materialized by getting a large number of results, some of which are presented in Table 1.

Table 1. Measurement results for the speed of 1000 rot/min

Lubricant oil temperature [°C]	Power [kW]	Torque [Nm]	Fuel consumption [kg/h]
30	1.55	15.9	0.75
35	1.76	18.0	0.70
40	1.85	18.7	0.66
45	1.96	19.1	0.64
50	2.05	19.4	0.60
55	2.13	20.3	0.58
60	2.21	21.2	0.55
65	2.35	22.6	0.53

The results from the measurements for the fuel consumption, power and torque, for the case where the speed was 1000 rot/min are transposed in figures 3, 4 and 5.

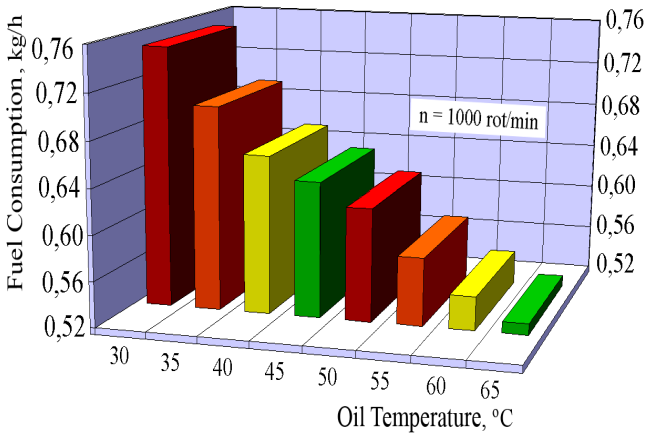

Figure 3. Fuel consumption variation depending on the lubricating oil temperature

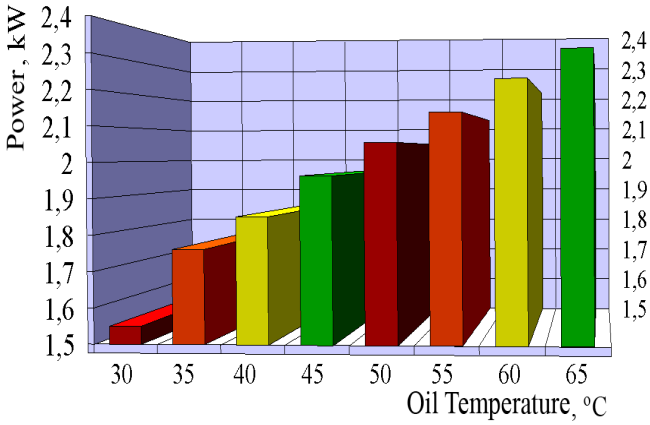

Figure 4. Power variation depending on the lubricating oil temperature

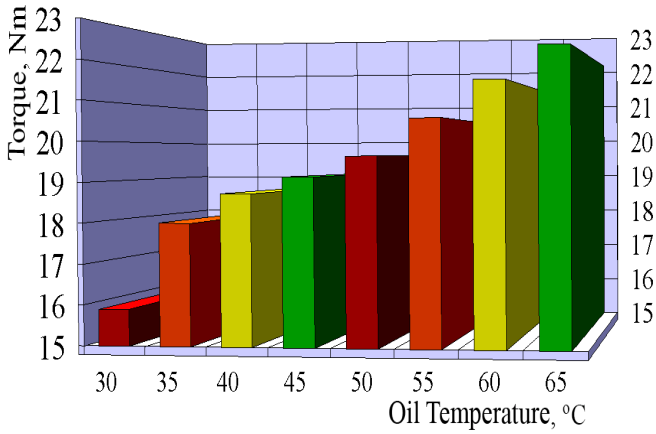

Figure 5. Engine torque variation depending on the lubricating oil temperature

In figure 6 the variation of the fuel consumption is presented, for the same engine, but for the speed of 2000 rot/min, and in figure 7 the specific fuel consumption is presented.
Effective power and torque variation depending on engine speed, for different temperatures of the lubricating oil are presented in figures 8 and 9.

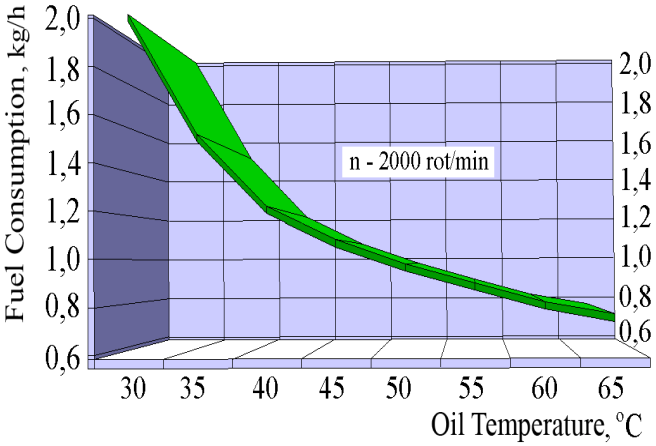

Figure 6. Fuel Consumption variation depending on the lubricating oil temperature, for the speed of 2000 rot/min

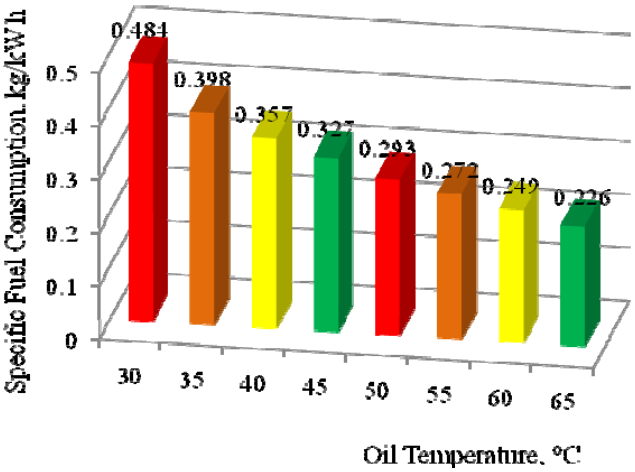

Figure 7. Specific Fuel Consumption variation depending on the lubricating oil temperature, for the speed of 2000 rot/min

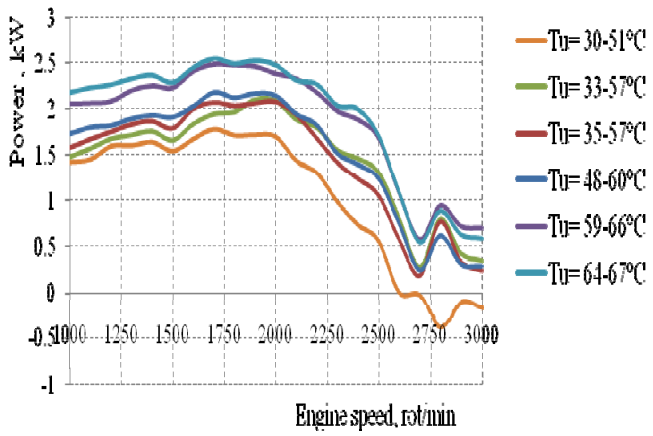

Figure 8. Engine power variation depending on the lubricating oil temperature,

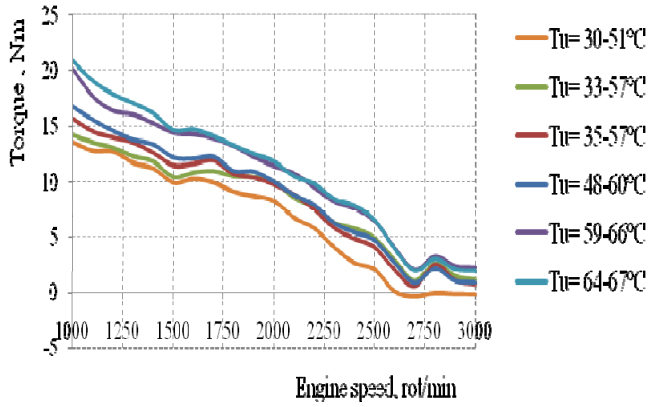

Figure 9. Engine torque variation depending on the lubricating oil temperature

CONCLUSIONS

The temperature inside the combustion chamber (determined also by the temperature of the lubricating oil) is the one that significantly influences the ignition delay. But the ignition delay (during which the fuel suffers important physical and chemical transformations), is a decisive factor when starting the engine, and also influence the functional parameters, the quietness and the durability of the engine.

From the present results, the conclusions are that the lubricating oil temperature (which causes its viscosity reduction) reduces fuel consumption and improves power and torque performance resulting explained by reducing friction between parts in relative motion (both from lubrication oil viscosity reduction and because at higher temperatures the clearance between the moving parts is smaller).

From figure 8, it can be seen that for a variation of the oil temperature from 30 to 51°C, at engine speeds of over 2600 rot/min, the effective power of the engine has negative values, which indicates that the engine is no longer rotating the dynamometer, but the dynamometer rotates the engine, which is allowed due to the measurement control method (the used method was speed/alpha, meaning that the speed is controlled by the dynamometer and for the engine, throttle position is controlled, in this case of measurements, it was 50%)

REFERENCES

[1.] *Bățaga, N., Burnete, N., Căzilă, A., Motoare cu ardere internă, Editura Didactică și Pedagogică, București, 1995, ISBN 973-30-4922-0.*

[2.] *Bățaga, N., Burnete, N., Motoare cu ardere internă, Vol. I și II, Litografia UTC-N, Cluj-Napoca, 1995.*

[3.] *Burnete, N., ș.a., Construcția și calculul motoarelor cu ardere internă (Mecanismul motor), Editura Todesco, Cluj-Napoca, 2001, ISBN 973-8198-17-8.*

[4.] *Burnete, N., Naghiu A., Rus I., ș.a., Motoare Diesel și Biocombustibili pentru transportul urban, Editura Mediamira, Cluj-Napoca, 2008, ISBN 978-973-713-217-8*

ACTA TECHNICA CORVINIENSIS – Bulletin of Engineering

ISSN: 2067-3809 [CD-Rom, online]

ACTA TECHNICA CORVINIENSIS - BULLETIN of ENGINEERING

ISSN: 2067-3809 [CD-Rom, online]

ACTA TECHNICA CORVINIENSIS - BULLETIN of ENGINEERING

ISSN: 2067-3809 [CD-Rom, online]

copyright © UNIVERSITY POLITEHNICA TIMISOARA,
FACULTY OF ENGINEERING HUNEDOARA,
5, REVOLUTIEI, 331128, HUNEDOARA, ROMANIA
http://acta.fih.upt.ro

ACTA TECHNICA CORVINIENSIS – Bulletin of Engineering
Tome VI (Year 2013) – FASCICULE 3 [July–September]
ISSN 2067–3809

[1.] Sorin RAȚIU, [2.] Corneliu BIRTOK-BĂNEASĂ, [3.] Vasile ALEXA

DYNAMIC AIR TRANSFER DEVICE FOR INTERNAL COMBUSTION ENGINES

[1, 3.] "POLITEHNICA" UNIVERSITY OF TIMISOARA, ROMANIA, ENGINEERING FACULTY OF HUNEDOARA, ROMANIA
[2.] CORNELIU GROUP: www.corneliugroup.ro

ABSTRACT: The paper presents an experimental study conducted with the support of the Laboratory of Internal Combustion Engines belonging to the Road Motor Vehicles specialization within "Politehnica" University of Timisoara, Engineering Faculty of Hunedoara. The purpose of this experiment is to test concepts of some devices conceived and made by the authors, awarded at numerous invention rooms, both inside the country and abroad. By the interposition of these devices on the intake route of internal combustion engines it is aimed to optimize the air intake process into the engine cylinders by two methods: 1 - increasing air pressure into cylinders by reducing pressure losses due to the air filter, and 2 - increasing the amount of air let into the cylinders by increasing its density due to lowering the temperature of the intake route. The experimental measurements have been made on different vehicles running in real traffic conditions, and on a stand holding a spark engine - and its afferent apparatuses - conceived by the authors. The experimental results have been processed and compared with the ones obtained during the operation without these devices.
KEYWORDS: Dynamic air transfer, pressure losses, internal combustion engine

INTRODUCTION

The piston internal combustion engine is a thermal engine that converts the chemical energy of the engine fluid fuel into mechanical energy. Engine fluid developments are achieved by means of a piston. The alternative movement of the piston inside a cylinder becomes rotating movement due to the crank gear.

For an internal combustion engine, the gas changing process encloses the intake and exhaust, which condition each other. The intake process is the process during which fresh fluid (air) enters the engine cylinders. The intake (or filling) determines the amount of fresh fluid retained in the cylinder after closing the last filling body and thus the mechanical energy developed during relaxation. The exhaust determines the purification degree of the cylinder with a view to a subsequent fill. In other words, the bigger the amount of fresh fluid (respectively air) retained into the engine cylinders, the higher the engine performance. The large amount of air in the engine cylinders means high pressure and low temperature on the inlet. This is the origin of the idea for this study which seeks ways to maximize, as much as possible, the amount of air introduced into the engine cylinders (by increasing pressure and decreasing temperature into cylinders), during an operating cycle, the costs for this goal being minimal. Cylinder filling can be normal or forced (supercharging). Normal filling, or normal inlet, typical of only 4-stroke engines, is achieved due to the piston's movement in the cylinder, in the sense of volume increase. Volume growth is recorded in the intake stroke, the fresh fluid with atmospheric pressure on the inlet.

Forced filling is achieved when the inlet pressure is greater than atmospheric pressure, indispensable in the 2-stroke engine without gas exchange bound drives. Forced filling can be achieved by supercharging when special equipment prepares the fresh fluid to enter the engine inlet at a pressure greater than the atmospheric one.

The cylinder filling process is strongly influenced by gas-dynamic losses on the engine intake route. There are two kinds of losses:

- Thermal losses due to heating the fluid through the inlet route walls, thus the final temperature being $T + \Delta T$, the temperature increase resulting in diminishing density and hence the filling penalty.
- Pressure losses caused by the existence of hydraulic resistances on the intake route and fluid friction with the pipe walls. These can be quantified according to the well-known formula (1):

$$\Delta p = \xi \cdot \rho \cdot \frac{w^2}{2} \qquad (1)$$

where ξ is the pressure loss coefficient, w is the flow speed of the fresh fluid and ρ is its density.

Due to these losses, the amount of fresh charge retained in the engine cylinders, while providing

information on the filling conditions, cannot serve as a comparison standard for different engines, but only for the same engine (the size of the losses mentioned above differs from one engine to another). This is why we introduce the notion of filling degree, or filling coefficient, or filling efficiency as a criterion for assessing filling perfection [1]:

$$\eta_v = \frac{C}{C_0} \qquad (2)$$

where C is the amount of fresh fluid actually retained in the cylinder, and C_0 is the amount of fresh fluid that could be retained in the cylinder, under the state conditions of the engine inlet, i.e. without taking into account the losses mentioned above.

Proper filtering of the air that enters the internal combustion engine cylinder is essential to extend its operation. Preventing the intake of various impurities along with atmosphere air significantly reduces the wear and tear of engine parts in relative movement.

Unfortunately, besides the function of filtering air drawn from the atmosphere, the air filter - as a distinct part in engine composition - is a significant gas-dynamic resistance interposed on the suction route. If it is not cleaned regularly and the vehicle is driven frequently in dusty areas, the suction pressure p_a is reduced consistently and the filling efficiency η_v suffers penalties [1].

DYNAMIC AIR TRANSFER DEVICE (DATD) [2,5]

During operation of internal combustion engines fitted on motor vehicles in summer, there can be noted two shortcomings of the air filters, leading to their poor performance:

- *insufficient air suction effect due to their installation in the engine compartment, area where the airflow is turbulent, the airflow around the filter not being laminar but turbulent, and the volumetric efficiency suffering penalties;*
- *increase in the absorbed air temperature due to their installation in the engine compartment, area which is subject to thermal radiation (of the cooling radiator and exhaust manifold). The overheating of the fresh fluid increases engine temperature, the appearance of detonation combustion and engine power reduction.*

Figure 1 presents the most disadvantageous fitting solutions in terms of exposure to thermal radiation and eddy currents.

It was tried to use a separator compartment for the air filter (Figure 2). But the separator compartment does not provide ideal insulation against the engine compartment, allowing thermal radiation to enter the air filter. Due to its design, turbulent air currents are created inside the separator compartment.

Moreover, the extension of the intake route outside the engine compartment is also practised. The example is given by mounting the air filter in the front bumper of a Honda Civic R Type. At the same time, the incorporation of the air filter in aluminum or carbon cage is also practised.

By using the above solutions, the disadvantages mentioned are partially eliminated, but there is significant pressure loss due to extension of the intake route and existence of casting. Suction pressure is reduced consistently.

On average, the intake route distances increase by over 500 mm, leading to increased drag created by additional friction arising from contact with the intake route wall.

a.

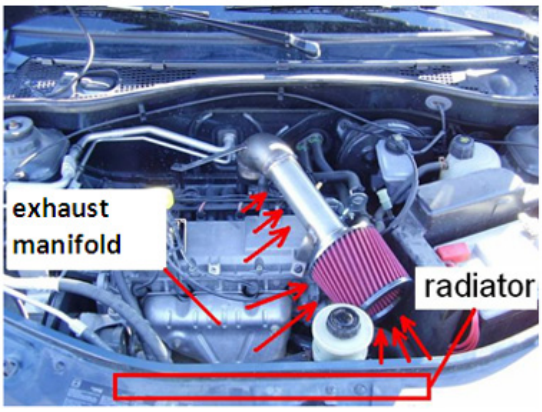

b.

Figure 1. Assemblies that lead to direct exposure of the filters

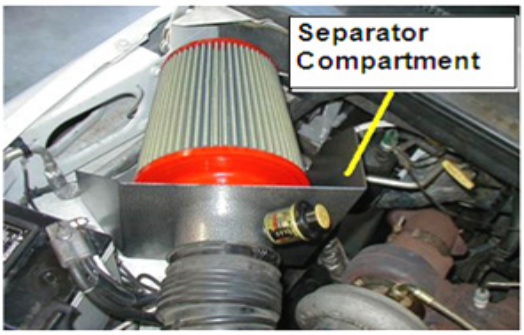

a.

b.

Figure 2. Installing filters in separator compartments

Considering the above drawbacks, an efficient intake device was designed for internal combustion engines, called dynamic air transfer device (DATD) (Figure 3). It helps improve air circulation to the filter air through the engine compartment.

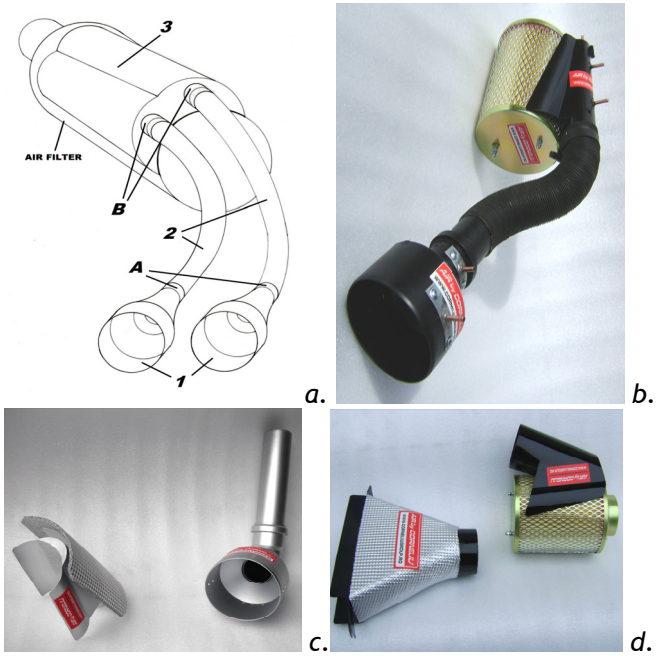

a. b. c. d.

Figure 3. Dynamic air transfer device (DATD)
a - design scheme: 1 - external collector diffuser, 2 - pipe connection, 3 - axial external collector, A, B - connecting surfaces; b - real overview; c - axial external collector and external collector diffuser - overview; d - different types of axial external collector and external collector diffuser.

The novelty consists in mounting external collector diffusers longitudinally with the vehicle axis, in the front area (in front of the radiator area or in the front bumper). They drive the air trapped outside the engine compartment, through the pipe connection, to the axial external collector, where the transfer to the air filter takes place.
The dynamic air transfer device consists of:

1. *External collector diffusers (one or more), whose role is to capture and accelerate air velocity (Figure 4).*
2. *Pipe connection, which connect the external collector diffusers and axial external collector (Figure 5).*
3. *The axial external collector (mono or bi-route), Figure 6, is mounted on the super absorbing air filter oriented to the high heat radiation areas (exhaust manifold, radiator, engine). It takes at least 30% of the lateral filter area, being at a well-determined distance away from the filter (between 3 and 8 mm). Its role is to transfer the air flow in the filter, flow divided into two components: one that actually enters the filter, the actual flow being admitted into the engine cylinders and one that surrounds the lateral surface of the filter, leading to keeping a relatively low filter temperature.*

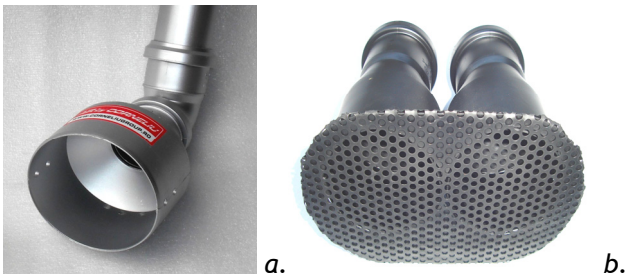

a. b.

Figure 4. External collector diffusers - physical models

Figure 5. Pipe connection

a. b.

Figure 6. Axial external collector
a - mono-route, b - bi-route

While driving the vehicle, the air is taken over by the external collector diffusers which enhance its speed, concentrate and convey it through the pipe connection to the axial external collector that transfers it to the super absorbing air filter.
The air stream transferred (brought) from outside the engine compartment has laminar focused flow. Speed increases (task performed by the external collector diffusers), and at the same time the air flow temperature decreases significantly. Because of its design geometry, the axial external sensor ensures good transfer and dispersion of the air on the side area of the super absorbing air filter. The amount of transferred air increases proportionally with the speed of the vehicle.

a.

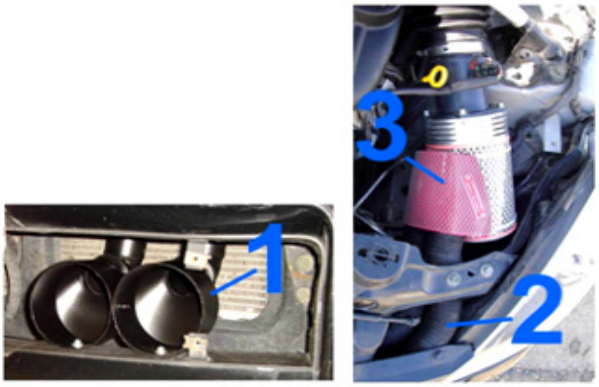

b.

Figure 7. a - DATD mounted on the engine; b - component parts: 1 - external collector diffusers, 2 - pipe connection, 3 - bi-route axial external collector

Advantages of DATD:

- *the air transfer to the filter has laminar focused flow;*
- *the low air temperature provides improved filling efficiency;*
- *a slight boost is created increasing proportionally with the speed of the vehicle;*
- *the combustion process is improved;*
- *the tendency is toward dynamic inlet;*
- *it allows shortening the distance between the filter and the intake manifold.*

Depending on engine capacity, one should use one or two external collector diffusers and an axial external collector in one or two transfer routes with varying sizes.

Experimented DATD:

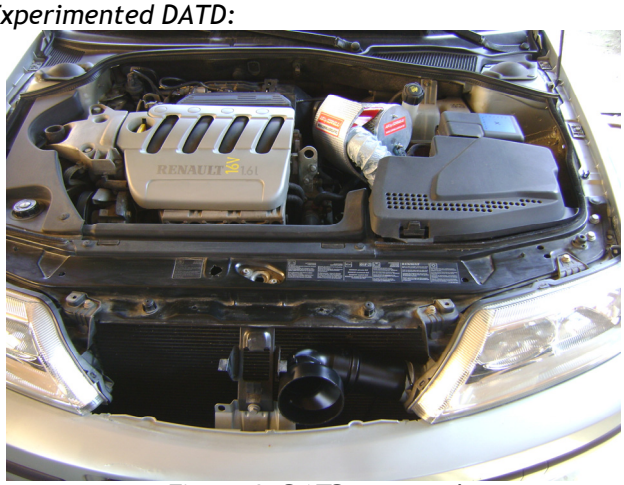

Figure 8. DATD mounted on Renault LAGUNA 1.6 16V

Figure 9. DATD mounted on WV Golf 5, 1.4 16v

Figure 10. DATD, bi-route mounted on Honda Civic, 1.6

Figure 11. DATD, mounted on Renault Megane Coupe

Differential pressure measurements were made both in the presence of the axial external collector of the DATD, and in its absence, in the suction area of the air filter, on different speed ranges. Data were taken while driving in real traffic at different speeds of the vehicle.

For measurements in the transfer area of the axial external collector - air filter, the pressure intake port was oriented axially to the airflow direction.

For measurements without DATD, in the suction area of the air filter, the pressure intake port is directed axially to the air absorption direction.

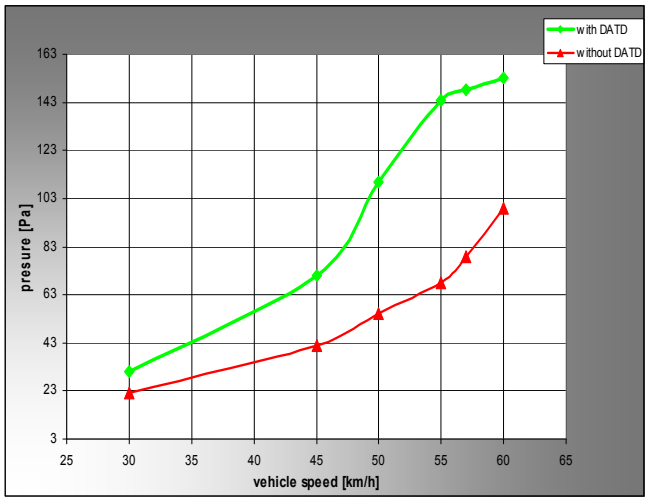

Figure 12. Comparative graph of the relative air pressure fields in the suction area of the air filter, in the presence and respectively absence of DATD

One can notice a higher air capture and transfer effect obtained by DATD, in comparison with the simple absorption of the super absorbing air filter. This effect is accentuated by higher values of the relative air pressure in the capture area obtained by DATD, in comparison with the relative pressure values in the absorption area of the air filter in the absence of DATD. This is particularly beneficial, especially for non-supercharged engine intake (normal inlet), the amount of air admitted into the engine cylinders being directly proportional to the intake pressure.

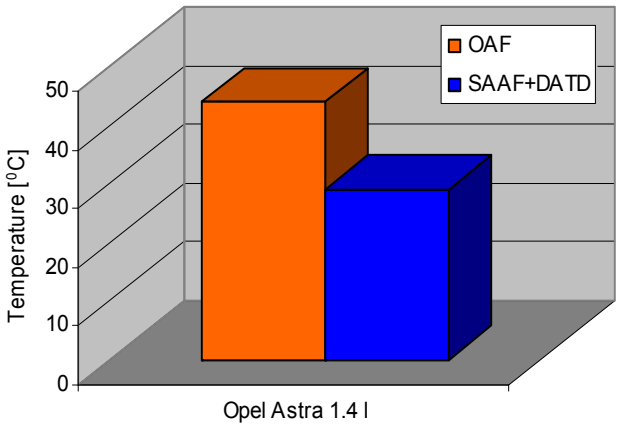

Figure 13. Temperatures of the outer surfaces of the OAF and SAAF+DATD for Opel Astra 1.4i

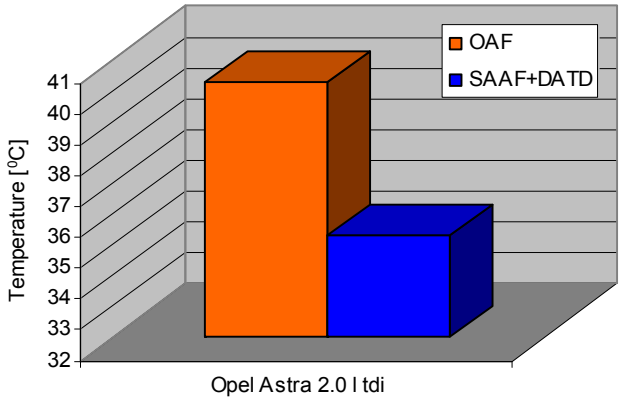

Figure 14. Temperatures of the outer surfaces of the OAF and SAAF+DATD for Opela Astra 2.0tdi

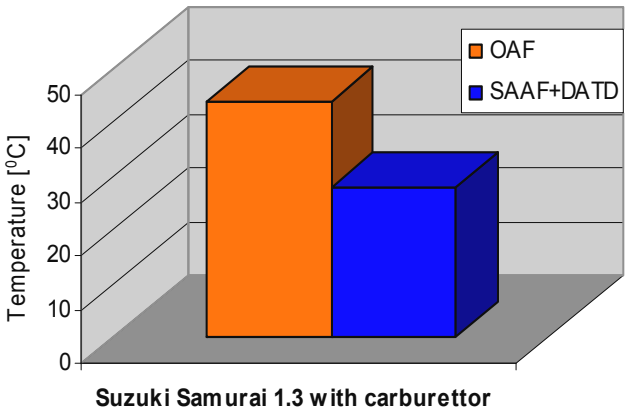

Figure 15. Temperatures of the outer surfaces of the OAF and SAAF+DATD for Suzuki Samurai

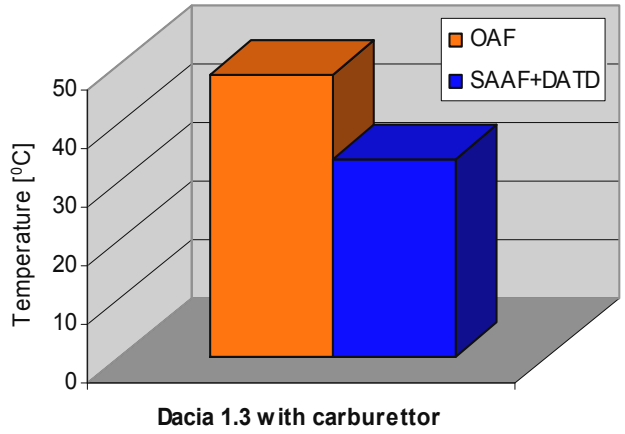

Figure 16.Temperatures of the outer surfaces of the OAF and SAAF+DATD for Dacia 1.3

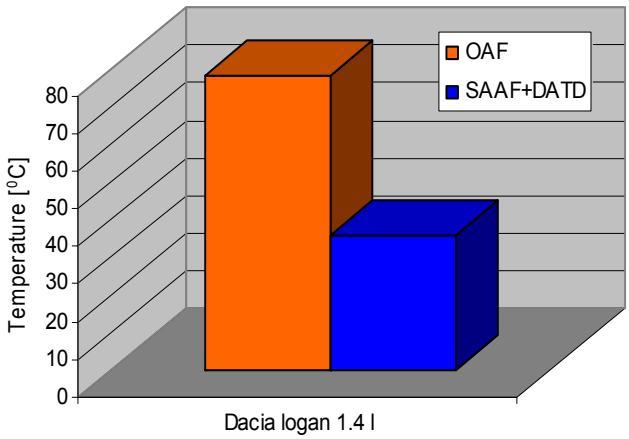

Figure 17. Temperatures of the outer surfaces of the OAF and SAAF+DATD for Dacia Logan 1.4i

Here are some comparative measurements of the temperatures of the outer surfaces of the original classic air filter (OAF) and super absorbing air filters with DATD (SAAF+DATD) in real traffic conditions.

CONCLUSIONS

From the graphs above it can be seen that the temperatures of the outer surfaces of the super absorbing filters, in combination with the dynamic air transfer device (SAAF+DATD), are much lower than the ones corresponding to the outer surfaces of the original air filters (OAF). Consequently, the use of super absorbing air filters together with DATD leads to less acute air heating on the intake route and therefore improvement of the filling coefficient.

REFERENCES

[1.] Rațiu S, Mihon L (2008) Internal Combustion Engines for Motor Vehicles - Processes and Features, MIRTON Publishing House, Timișoara, pp. 44-47;
[2.] Birtok-Băneasă C, Rațiu S (2011) Air Intake of Internal Combustion Engines - Super Absorbing Filters - Dynamic Transfer Devices, POLITEHNICA Publishing House, Timișoara, pp. 15-90;
[3.] Rațiu S (2009) Internal Combustion Engines for Motor Vehicles - Processes and Features - Laboratory Experiments, MIRTON Publishing House, Timișoara, pp. 40-42;
[4.] Rațiu S, Birtok-Băneasă C, Alic C, Mihon L (2009) New concepts in modeling air filters for internal combustion engines, 20th International DAAAM SYMPOSIUM "Intelligent Manufacturing & Automation: Theory, Practice & Education", Vienna, Austria, ISSN 1726-9679
[5.] www.corneliugroup.ro

ISSN: 2067-3809 [CD-Rom, online]

ACTA TECHNICA CORVINIENSIS – Bulletin of Engineering
Tome VI (Year 2013) – FASCICULE 3 [July–September]
ISSN 2067–3809

[1,2.] Joachim STRITTMATTER, [1.] Paul GÜMPEL, [3.] Anghel CHIRU, [1,3.] Viorel GHEORGHITA

ELECTRICAL ACTIVATION OF THE SHAPE MEMORY EFFECT FOR NiTi WIRES

[1.] UNIVERSITY OF APPLIED SCIENCES KONSTANZ, GERMANY
[2.] WITG INSTITUT FÜR WERKSTOFFSYSTEMTECHNIK THURGAU AN DER HOCHSCHULE KONSTANZ,GERMANY
[3.] UNIVERSITY „TRANSILVANIA“ FROM BRASOV, ROMANIA

ABSTRACT: The basis of shape memory alloys is the martensite - austenite transformation. For this transformation of the lattice structure the temperature change is one of the driving forces. In most cases electrical or thermal energy is used to activate the memory effect. In this paper, the tests and results regarding the required electrical energy to activate the memory effect will be described. If the shape memory wires work like actuators in automotive industry it is important to find the best values for the current intensity and the electrical tension. One of the questions of this investigation is to find the electrical value when the contraction and mechanical stress is constant. The defined goal is to obtain in less than one second 4-4,5% contraction at different stresses between 100-450 N/mm² and to analyze the electrical behavior of the samples. A great focus was given to the electrical connection to realize the activation of the actuator wires. Different parallel and serial connections were investigated and the advantages and disadvantages of each installation will be presented in this paper. The final goal of this research is to find a matrix where it will be possible to choose the wire and the mechanical load and to read out the values for the electrical tension and the current intensity.
KEYWORDS: NiTi wires, shape memory alloy, electrical energy

INTRODUCTION

Shape memory alloys (SMA, smart metal, memory metal, memory alloy, muscle wire, smart alloy) are alloys that "remember" their original, cold-forged shape by returning to the pre-deformed shape by heating. This material is a lightweight, solid-state alternative to conventional actuators such as hydraulic, pneumatic, and motor-based systems. Shape memory alloys are finding applications in industries including medical and aerospace [1].

In automotive industry they can replace electrical, thermal, hydraulic, magnetic actuators from different systems, like safety systems, clutch drive, folding and setting mirror, and others by showing additional advantages.

Today the following alloys are used in engineering: Nickel-Titanium (NiTi), Copper-Zinc-Aluminium (CuZnAl), Copper-Aluminium-Nickel (CuAlNi) and iron based alloys [3].

The difference between the heating transition and the cooling transition gives rise to hysteresis where some of the mechanical energy is lost in the process.

The one way shape memory effect takes place when a shape memory alloy is in its cold state (below A_s): the metal can be bent or stretched and will hold those shapes until heated above the transition temperature. Upon heating, the lattice changes to its original lattice structure and therefore to its original shape. When the metal is cooled again it will remain in this "hot" shape, until it is deformed again. Deformation in this case can be up to 8%.

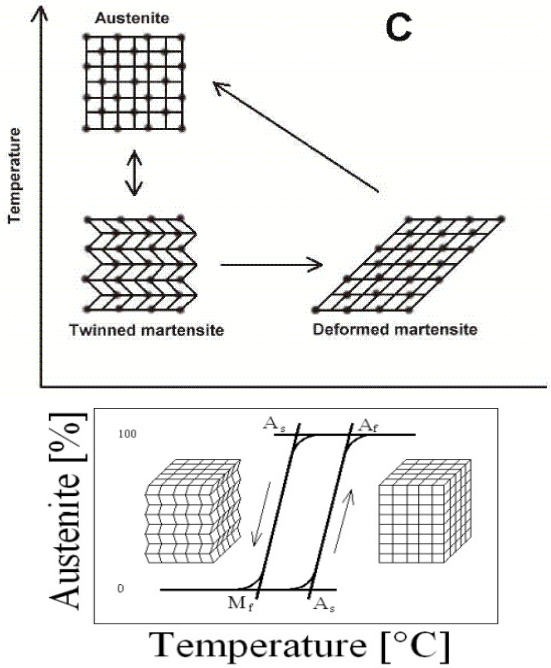

Figure 1.Martensitic transformation and shape memory effect [1],[3]

The difference between the heating transition and the cooling transition gives rise to hysteresis where some of the mechanical energy is lost in the process.

One way shape memory effect takes place when a shape memory alloy is in its cold state (below A_s): the metal can be bent or stretched and will hold those shapes until heated above the transition temperature. Upon heating, the lattice changes to its original lattice structure and therefore to its original shape. When the metal is cooled again it will remain in this "hot" shape, until it is deformed again. Deformation in this case can be up to 8%.

During the two way shape memory effect the material remembers two different shapes: one at low temperature, and one at the high-temperature. This can also be obtained without the application of an external force (intrinsic two-way effect). The reason that the material behaves so differently in these situations is due to a special thermo-mechanical training process [3].

The pseudo-elastic propriety occurs in the austenitic temperature. For example, the frames of some eyeglasses are made of shape memory alloy as they can undergo large deformations in their high-temperature state and then instantly revert back to their original shape when the stress is removed. This is the result of pseudo-elasticity; the martensitic phase is generated by stressing the metal in the austenitic state and this martensitic phase is capable of large strains. With the removal of the load, the martensitic phase transforms back into the austenite phase and resumes its original shape. The shape memory effect can be activated by changing the thermal or electrical energy [2], [5] and in the case of pseudo-elasticity by changing the applied stress upon the material.

This paper presents the results regarding electrical activation of the shape memory effect in NiTi wires at different loads. The goal of the test is to obtain at least 4.5% contraction in less than 1s.

METHODOLOGIES AND DEVICES USED IN RESEARCH

There are numerous available methodologies for testing the shape memory alloy wires. Because they will be activated by using the electrical energy in this subchapter an electrical circuit is presented where the sample is like a variable resistance. This method (that is not standardized) presents a sample of Ni-Ti alloy that is fixed with one side in a frame. At the other side free in the air (fig. 2) will be attached the mechanical load (weight) that causes the stress upon the sample. The sample is "electrically" heated by Joule effect and cooled by convection at room temperature.

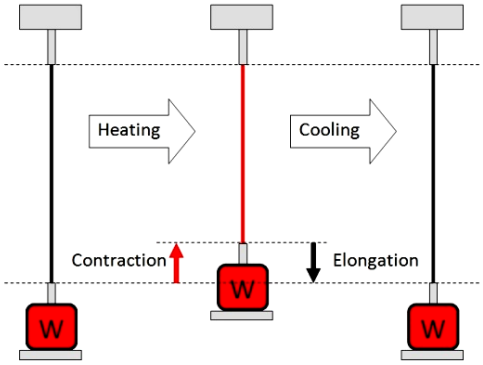

Figure 2. Model of the test

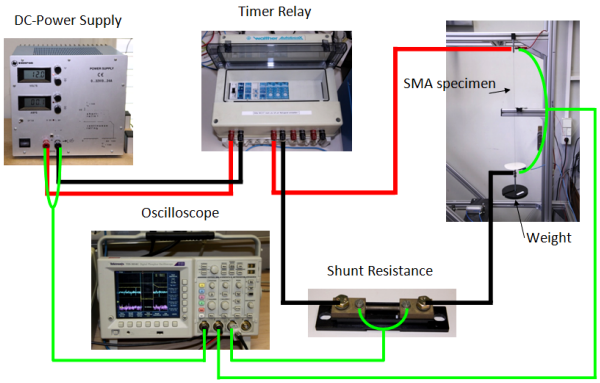

Figure 3. Electrical circuit of the test

This testing method uses a wire which was loaded with a weight at the end in vertical axis. The weight is calculated for each sample to get values very close to the presented stresses in the table 1. The ends of the wire are connected with the power supply. Between power supply and positive pole from the sample it is a timer delay used, where the activation time can be adjusted. For the minus line of the electrical energy is inserted a shunt resistance. The value of the resistance is constant and in that way it can be calculated the current intensity, if the electrical tension is measured.

During the heating process the lattice is changed from the martensite to austenite causing a rapid contraction an up moving of the weight (see fig 2). Afterwards the NiTi wire is cooled down to room temperature in the unmoved air. In this period the lattice of the sample will change again into the martensitic form.

During the test the electrical tension at the power supply, sample and shunt resistance are recorded.

ELECTRICAL ACTIVATION OF NiTi WIRES

The goal of this experiment is to identify the electrical energy to activate the actuator wires with different diameters(0.5, 0.4, 0.3, 0.2 and 0.1 mm) at different mechanical stresses (100, 150, 200, 250, 300, 350 and 400N/mm^2).The length of each sample is 500mm and the activation time is 1s. These values were determined, because it is planned to use SMA wires in applications for passengers' cars, in comfort and safety areas. The electrical energy was scanned until the contraction is higher than 4%.

Table 1. Mechanical stress for the specimen

Diameter	Constant stress (N/mm^2)						
	100	150	200	250	300	350	400
0.1							
0.2							
0.3							
0.4							
0.5							

gray box = the specimens was tested, write box = the specimens was not tested

After the first tests the Kirchhoff theory could not be confirmed. To prove the theory the shunt resistance was removed. First graphic without the Shunt resistance is presented in the next figure.

In the fig. 4 the blue line represents the electrical tension measured at the power supply and the green one is the value of the electrical tension measured at the sample. At the graphic are defined: 1 - value of the tension at power supply, 2 - value of the tension

at sample, 3- value of the tension at power supply when the sample is activated, 4- value of the tension at the sample when it is activated and 5 - activation time.

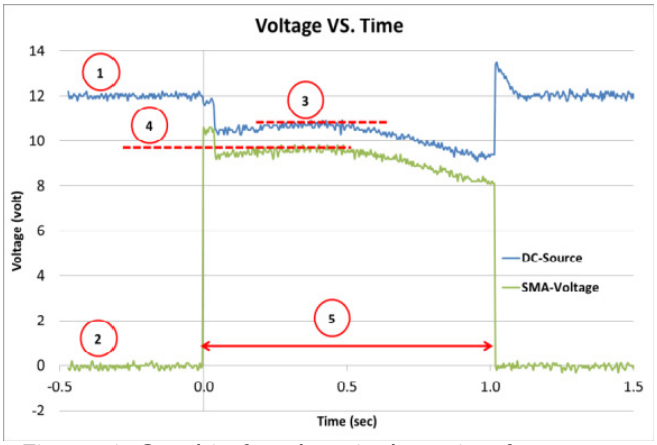

Figure 4. Graphic for electrical tension from power supply (blue line) and sample (green line)

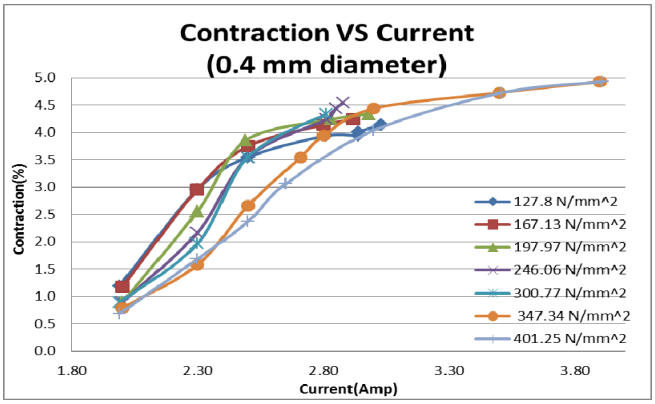

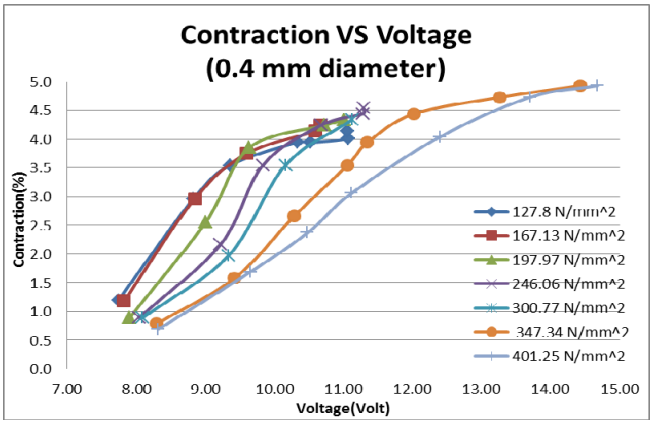

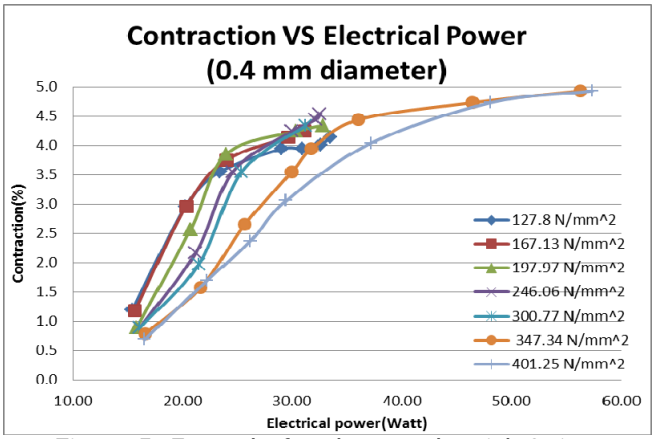

Figure 5. Example for the sample with 0,4mm diameter and length 500 mm

In this case the characteristic curve from sample should be "negative" compared to the characteristic curve from the power supply. In the graphic can be observed a difference between curve 3 and 4 when the sample is activated. The reason for this difference is the internal resistance from the timer delay. In this case the registered value which will be recorded is the value from the sample (green curve).

According to this method samples presented in the beginning of the chapter were tested. Each sample produced at least seven graphics, but in this paper only the final results will be presented, exemplarily for the samples with 0.4 mm diameter (fig. 5).

The contraction and current graphs for sample with 0.4 mm diameter show an increasing of contraction until more or less 4.5% with the range of current about 2.8-3.8A. If the reference is the graph voltage vs. contraction it can be observed that for 4.5% at different loads an electrical tension of at least 11 till 14.8 Vis necessary.

It can also be observed that the sample needs more current to achieve higher stresses.

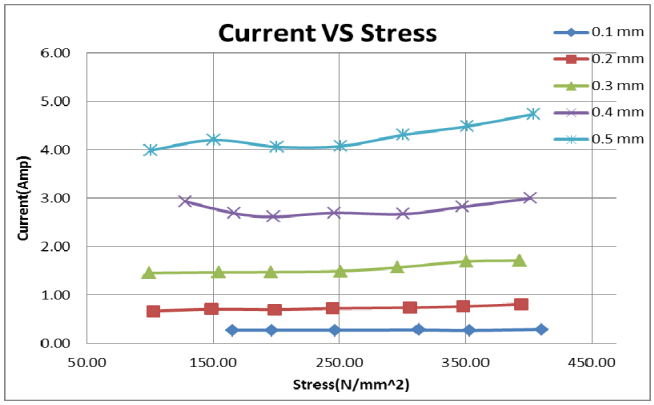

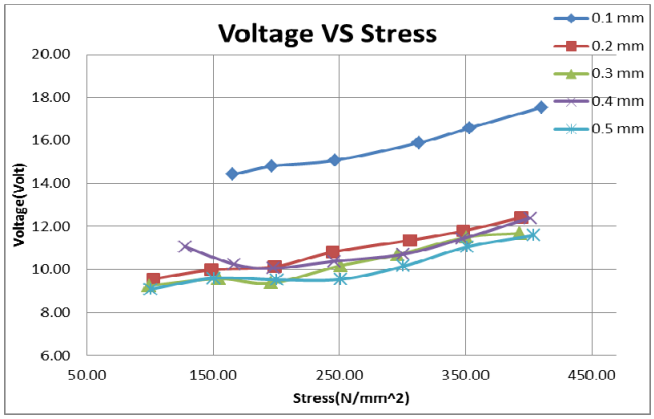

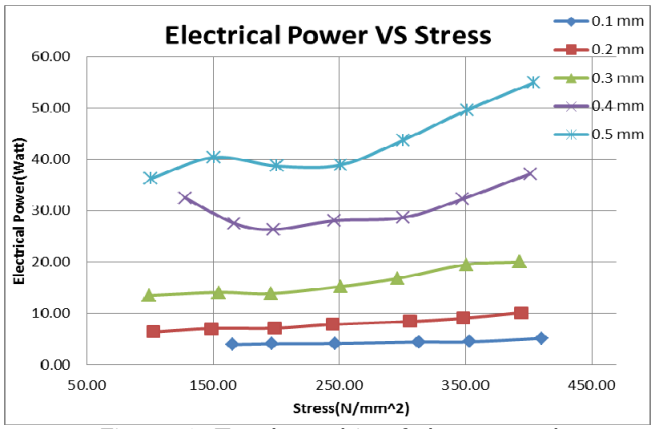

Figure 6. Total graphic of the research

In figure 6 is presented the total graphic of the research for 4%. An important fact of the research is the point when the samples reach 4% contraction. In this figure, the characteristic curves show that the current values slightly increase when the stress values are higher. It can also be observed that the current levels are higher when the diameters are bigger. It can be concluded that when the diameter is bigger and the mechanical stress increases is necessary to insert a bigger electrical energy quantity. By means of this total graphic the necessary quantity of electrical energy can be read out for any application according to the assumed conditions.

If the desired mechanical stress, for another application is higher than the mechanical stress which was tested in this work, the required condition possibly can be achieved by using several wires in parallel. When the wires are used in parallel the current intensity is growing up. Using several NiTi wires in serial connection the electrical tension is growing up. A special research work concerning the different electrical connections has been carried out and published [6].

The behavior of the sample is like an electrical resistance and the results can be calculated when the input values contraction, mechanical tension, diameter and length of the wire are known.

CONCLUSIONS

After this research it can be concluded that the results can be very useful for the actuator industry when shape memory activator wires are applied in different fields. For example these alloys are able to replace hydraulic, mechanical, electromechanically and pneumatic actuators from the automotive industry. For this it is necessary to know from the beginning what are the requirements for the new system in order to replace another one. This paper gives some answers for NiTi wires used in automotive industry and also other actuator fields.

One of our concrete applications of these alloys is to replace the clamping system from steering column [7] through a new system using NiTi wires. In this sense further developments are going to be undertaken in order to use the wires in future safety systems.

REFERENCES

[1.] Gümpel, P. and 5 Co-authors, Formgedächtnislegierungen, Expert Verlag, Renningen, 146, 2004

[2.] Frémond, M., Phase Change in Mechanics, Springer Berlin Heidelberg, 2012

[3.] Hornbogen, E., Shape Memory Alloys-Advanced Structural and Functional Materials, Koln, Germany, 1991

[4.] Hornbogen, E., Review Thermo-mechanical fatigue of shape memory alloys, Journal of Material Science, 32, 385-399, 2004

[5.] Jinlian, H., Yong, Z., Huahua, H., Jing L., Recent advances in shape-memory polymers: Structure, mechanism, functionality, modeling and applications, Progress in Polymer Science, 44, 2012

[6.] Strittmatter J., Gheorghita V., Guempel P., Shape memory wires with activation times less than one second, Proceedings of the XXVI. microCAD International Scientific Conference, University of Miskolc, Hungary, 29-30 March 2012, 6 pages on CD, ISBN: 978-963-661-773-8

[7.] Gheorghita V., Gümpel P., Heitz T., Senn M., Strittmatter J., Shape memory alloys open new possibilities in automotive safety systems, Proceedings of EAEC 2011, the 13th European Automotive Congress, Valencia, 13-16 June 2011, 7 pages on USB-Card, available on CD-ROM, publisher STA, ISBN 978-84-615-1794-7

ACTA TECHNICA CORVINIENSIS - Bulletin of Engineering

ISSN: 2067-3809 [CD-Rom, online]

ACTA TECHNICA CORVINIENSIS – Bulletin of Engineering
Tome VI (Year 2013) – FASCICULE 3 [July–September]
ISSN 2067–3809

[1.] Ioan HITICAS, [2.] Liviu MIHON, [3.] Emanuel RESIGA, [4.] Walter SWOBODA

GAS EMISSION OF A SPARK IGNITION ENGINE WITH PROGRAMMABLE ECU

[1.] "POLITEHNICA" UNIVERSITY, TIMIȘOARA, ROMANIA

ABSTRACT: The evolution of engine performances of our today vehicles involves some "prices" from us, as drivers, also as car manufacturers. Between power and engine gasses evolution must be "an agreement": if we would like to have low gas emission for our engines, do not expect to achieved top of vehicles performances; also, if we would like to achieve high performances with our cars, we must know that is possible, but the evolution of exhaust species won't be all the time in normal values. Below we present the evolution of exhaust species, CO, CO_2, O_2, HC and NO_x for our tested vehicle, namely Renault 5, car equipped with a programmable ECU, which was installed with the purpose to obtain higher curves of power and torque. The question was concerning the exhaust species. The article offer, to the engineering of the fields, the conclusion of our team, after theoretical and experimental research: the engines equipped with programmable ECU's can offer very good performances, but the gas emissions are not always in normal values. The main factor is the traction of the vehicle and the drivers.
KEYWORDS: spark ignition engine, programmable ECU, gas emission, performances

INTRODUCTION

Safety, power and low emission are the request from our vehicles. The differences between vehicles are made by the car project, which will take into consideration the drivers demands. As the industry and technology start to go on with very big steps, almost all this demands can be achieved.

Our team prepared a vehicle to offer more power, namely Renault 5, car designated for racing. It was a spark ignition engine, turbocharged. We decided to mounted on stand alone ECU, prepared to adjust the sensors limits in order to major the values from the power curves, namely a programmable ECU.

This ECU is one of the on-board ECU, connected with the ECU of the engine and which can be commanded from a little board [1], mounted inside the engine, like on the image.

Figure 1. Commands board for programmable ECU, inside the vehicle

The logical scheme for position of the programmable ECU is presented below. The advantage offered by this system is by controlling the limits of the sensors involved in spark ignition engine evolution and in performances evolution [8], [9]. The main two elements needed by the engine to work very well is air and fuel, but this mixture, as it is well known, must achieve some proprieties, like a specific temperature, a specific pressure, and so all the parameters involved in burning process can proved the energy need by the engine to run properly.

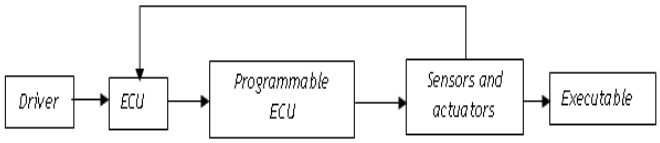

Figure 2. Block scheme for programmable ECU position

Some of the sensors involved in ECU programming are rpm sensor, lambda sensor, EGT sensor, manifold absolute temperature sensor (MAT), manifold absolute pressure sensor [2], [3], [4].

Our question was about the exhaust. How the exhaust species are after this new system was mounted on the engine? Do are better or not?

TECHNICAL DATA

One of the most important sensor was oxygen sensor, lambda. Lambda value is a ratio between two parameters, namely AFR and AFR_{stoech}.

$$\lambda = AFR / AFR_{stoech} \qquad (1)$$

where AFR is Air Fuel Ratio.

The AFR values can varies from maximum to minimum with consequences for burned mixture inside the combustion chamber [5], [6], [7] and also in exhaust.

As it is know from scientific literature AFR is:

$$AFR = m_{air} / m_{fuel} \qquad (2)$$

where: m_{air} - the amount of air needed for mixture
m_{fuel} - the amount of fuel needed for combustion mixture
Equivalence between AFR and excess air ratio λ can be done using the table below:

Table 1. Lambda to AFR conversion

Lambda	AFR	Lambda	AFR	Lambda	AFR
0.6	8.82	0.81	11.9	1.02	15
0.61	8.97	0.82	12.1	1.03	15.1
0.62	9.11	0.83	12.2	1.04	15.3
0.63	9.26	0.84	12.4	1.05	15.4
0.64	9.41	0.85	12.5	1.06	15.6
0.65	9.56	0.86	12.6	1.07	15.7
0.66	9.7	0.87	12.8	1.08	15.9
0.67	9.85	0.88	12.9	1.09	16
0.68	10	0.89	13.1	1.1	16.2
0.69	10.1	0.9	13.2	1.11	16.3
0.7	10.3	0.91	13.4	1.12	16.5
0.71	10.4	0.92	13.5	1.13	16.6
0.72	10.6	0.93	13.7	1.14	16.8
0.73	10.7	0.94	13.8	1.15	16.9
0.74	10.9	0.95	14	1.16	17.1
0.75	11	0.96	14.1	1.17	17.2
0.76	11.2	0.97	14.3	1.18	17.4
0.77	11.3	0.98	14.4	1.19	17.5
0.78	11.5	0.99	14.6	1.2	17.6
0.79	11.6	1.00	14.7		
0.8	11.8	1.01	14.9		

Technical data from the tested vehicle are:

- *year of manufacture 1989;*
- *turbocharged;*
- *displacement of 1721 cc;*
- *power 89.5 kW at 5400 rpm;*
- *torque 175 Nm at 3300 rpm;*
- *Compression ratio being 8.1: 1.*

Therefore, if we can get closer to the values for λ on 11.5-12.00 using a programmable engine control unit, it means that we will have an increased performance of the car.

EXPERIMENTAL RESEARCH

For determining the exhaust species and them evolution during the measurements, we mounted the vehicle on the test bench, MAHA LPS 3000. The vehicle was fixed on the roller; air fan was also connected - for air resistance and for simulating the real situation from the road - and the probe was mounted on the tailpipe.

Figure 2. Tested vehicle on Dyno

The equipment for measuring the emission of the exhaust species allows us to monitor all the species on the same window, very helpful for experimental research. The engine speed also can be monitored on the same window. A very important element was the lambda coefficient [10], [11], which allows following the quality of the combustion mixture, around the stoechiometric values.

Figure 3. MAHA MET 6.1 exhausts analyser

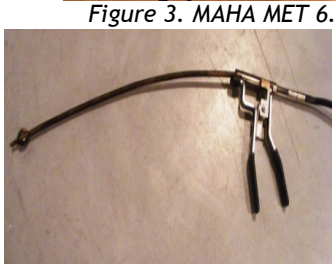

Figure 4. Exhaust gas prove

Figure 5. Clamp for RPM detection

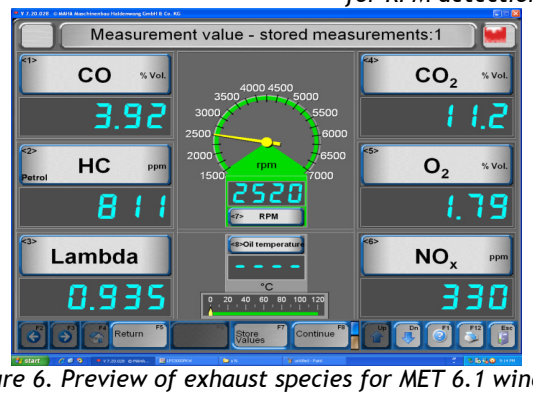

Figure 6. Preview of exhaust species for MET 6.1 window

Exhaust species measured with Maha analyser, MET 6.1, were recorded using dedicated software, namely Eurosystem, than were stored in tables. To monitor the evolution of all exhaust species [12], we run on Dyno with different loads, starting from 0 N and finishing with a load by 2000 N. On this paper we will present two cases, namely for load by 200 N and 2000 N.

Table 2. Exhaust values for 200N load

n [rot/min]	CO	CO_2	O_2	HC	NOx	Lambda
1480	4.65	10.1	2.08	453	168	0.936
1940	4.72	10.4	1.94	413	293	0.931
2020	4.21	10.6	1.84	523	309	0.933
2520	3.92	11.2	1.79	811	330	0.935
3080	0.94	13.8	1.23	169	481	1.024

Table 3. Exhaust values for 2000N load

n [rot/min]	CO	CO2	O2	HC	NOx	Lambda
1600	3.25	11.8	2.3	404	213	0.993
2050	2.56	12.4	2.04	492	301	0.999
2920	1.05	13.1	2.16	168	707	1.068
3120	2.01	12.9	1.74	198	639	1.015
4040	0.9	13.6	1.15	126	927	1.025

Exhaust species for tested vehicle running on 200 N loads:

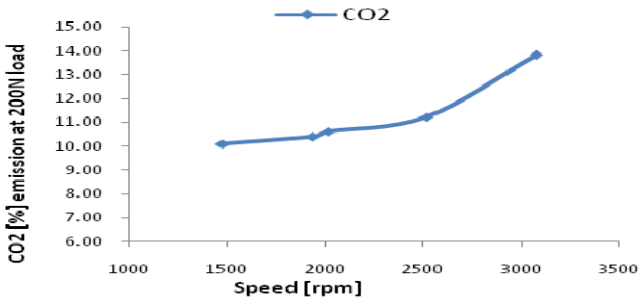

Figure 7. CO_2 [%] emission according with engine speed

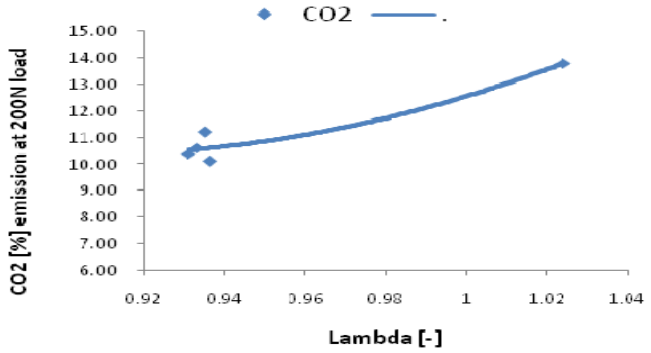

Figure 8. CO_2 [%] emission according with lambda

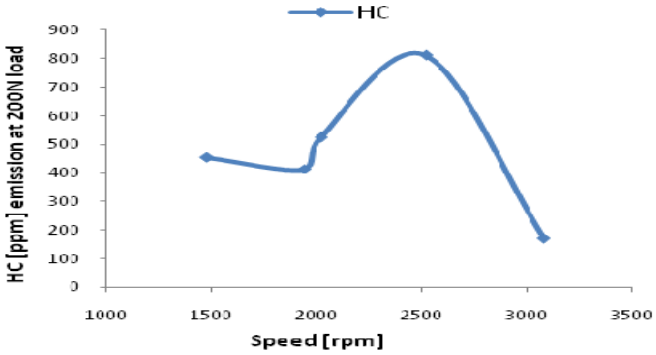

Figure 9. HC [ppm] emission according with engine speed

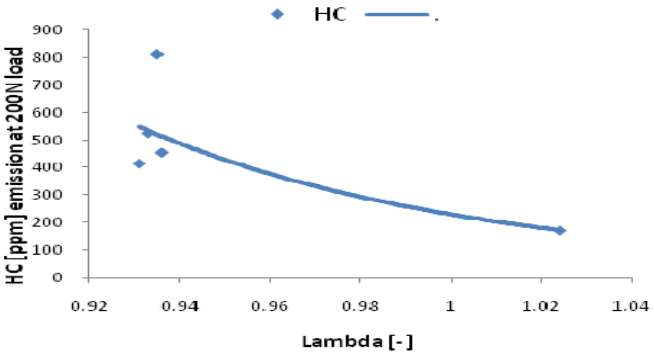

Figure 10 HC [ppm] emission according with lambda

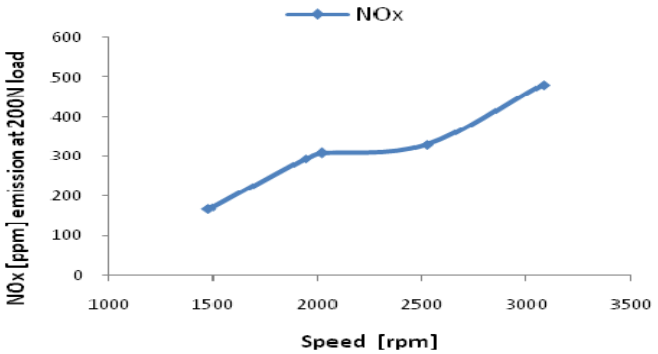

Figure 11. NOx [ppm] emission according with engine speed

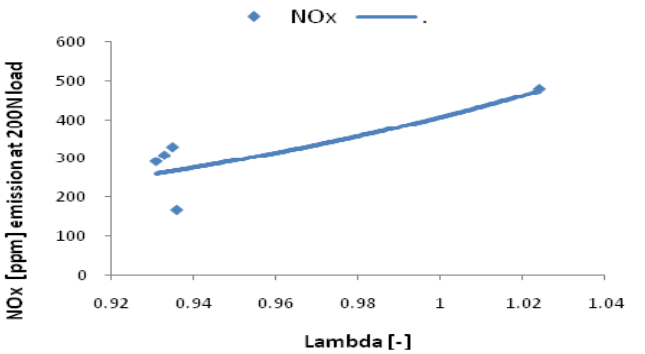

Figure 12. NOx [ppm] emission according with lambda

Exhaust species for tested vehicle running on 2000 N loads:

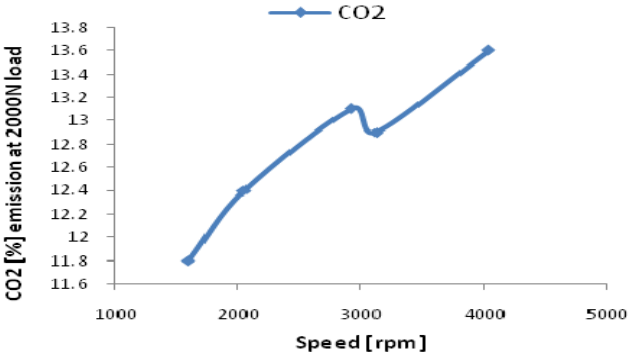

Figure 13. CO_2 [%] emission according with engine speed

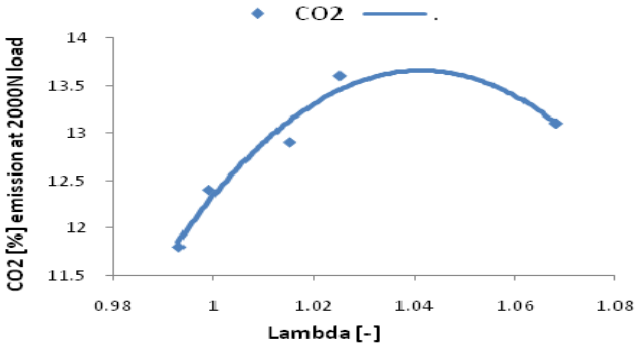

Figure 14. CO_2 [%] emission according with lambda

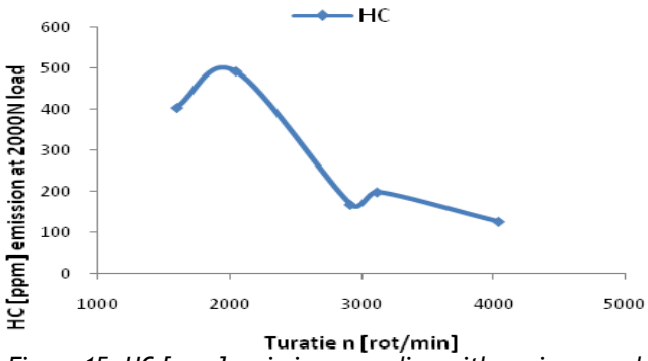

Figure 15. HC [ppm] emission according with engine speed

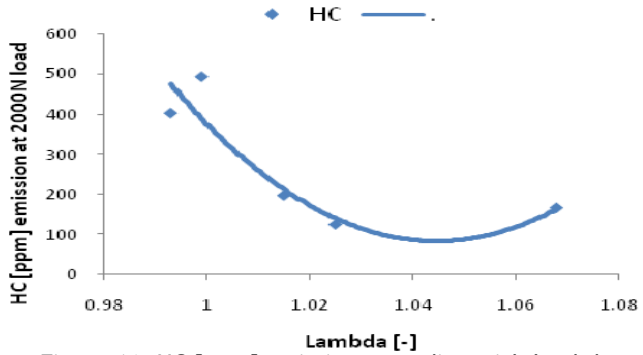

Figure 16. HC [ppm] emission according with lambda

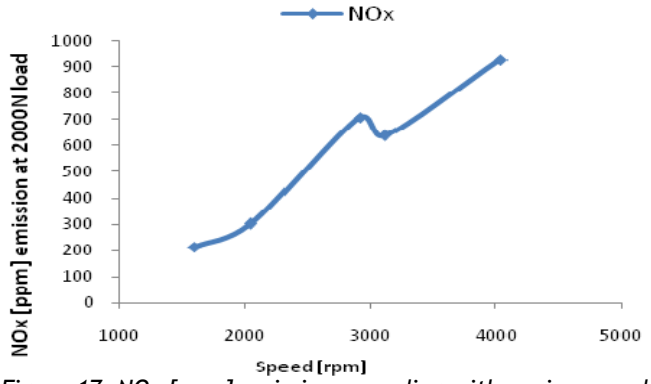

Figure 17. NOx [ppm] emission according with engine speed

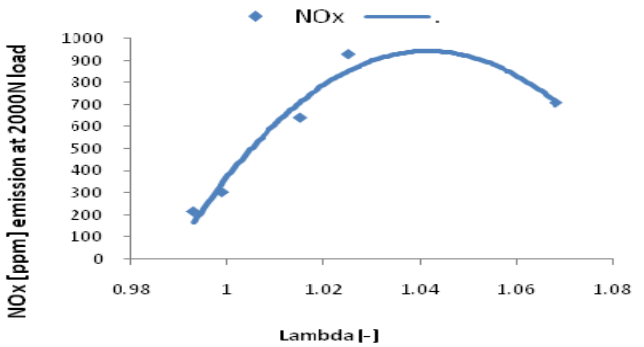

Figure 18. NOx [ppm] emission according with lambda

CONCLUSIONS

The comparison between these two cases, namely 200 N loads and 2000 N load for tested vehicle, completed with programmable ECU, make us to affirm the following conclusion:

- *The engine behaviour was very good, especially because the vehicle was running on vehicle competition and there were no technical or software problems.*
- *The engine power curves presented high vales after the programmable ECU was mounted on the vehicle, also the AFR and lambda values achieved very good vales (lambda values at the top for this adjustments was 0.75, which means an AFR by 11.00).*
- *The exhaust species presented interesting values for both situation, and 200 N and 2000 N. The evolution of all the exhaust species presented ascending curves, on evolution, namely, for CO_2, and for NOx; for HC values, the curves present decreasing values, which is very good.*

For future research, concerning the performances of the engine by programmable ECU is to obtain values for AFR between 12.50÷13.97, and for exhaust emission, situation very comfortable watching the fuel consumption and the behaviour of the engine. Also, future research concerning the programmable ECU is to use an alternative fuel, as isobutene, which takes into account the real problem about concentration of CO_2 from the atmosphere, concerning the apertures for the renewable energy from today.

Acknowledgment

This work was partially supported by the strategic grant POSDRU/88/1.5/S/50783, Project ID 50783 (2009) co-financed by the European Social Fund - Investing in People, within the sectorial Operational Programme Human Resources Development 2007-2013. This work was partially supported by the strategic grant POSDRU/21/1.5/G/13798, inside POSDRU Romania 2007-2013, co-financed by the European Social Fund - Investing in People.

REFERENCES

[1.] *B. Bowling, and A. Grippo, "Building a Fuel-Injection ECU", Circuit Cellar Ink 138, USA, January 2002.*

[2.] *N. N. Hassan and all, "Micro-Controller Based on-board diagnostic (OBD) system for non-OBD vehicles", IEEE Computer Modeling and Simulation (UKSim), Cambridge, April 2011.*

[3.] *S. Chuck, A. Dave, "Specialized I/O and High-Speed CPU Yields Efficient Microcontroller for Automotive Applications", IEEE Industrial Electronics Society, April 2007.*

[4.] *M. Dickinson, "Introduction to Control Engineering", Elektor Verlag, Germany, March 2011.*

[5.] *G.P.Blair, "Design and Simulation of Four-Stroke Engines", SAE International, USA, 1999.*

[6.] *B. Koerner, J. Klopatek, "Anthropogenic and natural CO_2 emission sources in an arid urban environment", Elsevier, Environmental Pollution 116 (2002) S45-S51.*

[7.] *T. J. Wallington, J.L. Sullivan, M.D. Hurley, Emissions of CO_2, CO, NOx, HC, PM, HFC-134a, N_2 O and CH4 from the global light duty vehicle fleet, Meteorologische Zeitschrift, Vol. 17, No. 2, 109-116 (April 2008).*

[8.] *Hiticas, D. Marin, L. Mihon, "Experimental research concerning the pollution of an internal combustion engine with injection of gasoline, in conditions of changing the fuel", IN-TECH, Croatia, Proceedings, pp. 239-243, ISBN 978-953-6326-77-8, 2012.*

[9.] *Hiticaș, et all, "Parameters Control of a Spark Ignition Engine through Programmable ECU for Specific Regimes", SACI 2012, IEEE Proceedings, pp.399-404. 2012.*

[10.] *UNFCCC / CCNUCC Report, "Tool to calculate project or leakage CO_2 emissions from fossil fuel combustion", Methodological tool, 2008.*

[11.] *International Energy Agency, CO_2 emission from fuel combustion, Highlight, 2011.*

[12.] *M. Crass, "Reducing CO_2 emissions from urban travel: local policies and national plans, OECD International Conference, Competitive Cities and Climate Change, Milan, Italy, Proceedings, 2008*

ACTA TECHNICA CORVINIENSIS – Bulletin of Engineering

ISSN: 2067-3809 [CD-Rom, online]

ACTA TECHNICA CORVINIENSIS – Bulletin of Engineering
Tome VI (Year 2013) – FASCICULE 3 [July–September]
ISSN 2067–3809

[1.] Camelia PINCA-BRETOTEAN, [2.] Lucia VÎLCEANU

EXPERIMENTAL INVESTIGATIONS FOR MODELLING THE THERMAL FATIGUE PHENOMENON IN MACHINES PARTS OF AUTOMOTIVE ENGINES

[1-2.] "POLITEHNICA" UNIVERSITY OF TIMISOARA, ENGINEERING FACULTY OF HUNEDOARA, ROMANIA

ABSTRACT: The purpose of this paper is to present some experimental investigations for validate an experimental plant designed and built for study the thermal fatigue phenomenon that occurs in machines parts of internal combustion engines. Our study based under the concepts and methods used for thermal fatigue modeling under laboratory conditions presented in literature. To determine the thermal fatigue phenomenon we should know how resisting are these machine parts for being able to determine their estimated operation time by the number of operating cycles until the first cracks occur on their surface. Thermal fatigue study under laboratory conditions lead to the thermal fatigue resistance limits for different machine parts in the composition of internal combustion engines, specific to avoid cracking of the engine by optimizing the thermal regime and proposals for new materials with high resistance to thermal fatigue. The paper present the original measurement method developed by autors under an original experimental plant. This equipment allows modeling thermal fatigue of machines parts of internal combustion engines and it is property of the laboratory of "Industrial Mechanical Equipments" of the Faculty of Engineering of Hunedoara, University "Politehnica" from Timisoara, which is the subject of a patent registered at OSIM A/00439 number of 17.06.2010, published in bopi_inv_12_2011.
KEYWORDS: thermal fatigue, field, cycles, variations, model, temperature

INTRODUCTION

Fixed and mobile machine parts composing vehicle motor participate in the working cycle which is characterized by variations of temperature. They take a significant part of the heat developed inside the combustion chamber and transfer it to the cooler liquid. Thus, in certain areas of machine parts are created variable temperature fields. These temperature fields generate the occurrence of cyclic thermal stresses. The thermal stress values can be higher than the mechanical ones, and can lead to cracks on the surface and in the surface layer of the parts, specific to the thermal fatigue cracking phenomenon. This phenomenon is especially pronounced to the engines operating in very different thermal regimes, and where the part lifetime is higher. Heat load of combustion chamber generated thermal stresses which are the main factor limiting the performance and durability of internal combustuion engines, [1], [9].

Heating up and cooling cycles of the component parts of internal combustion engines can have different character. It is assumed [3] that heat strokes caused by high heating velocity are more damgerous than those that are caused by sudden cooling, which can be explained by lower durability of materials in high temperatures. For exemple, the piston heats up from an ambient temperature to working temperature in the time ranging from several dozen seconds to a few minutes, while the process of estabishing the average fild temperatures during engine transition between different load stages taken even less time, [3], [7], [10]. An average temperature fluctuation range depends on how and where the engine is used, [1], [3]. Frequent load changes are unavoidable in engines used to propel cars in city traffic, while long-distance truck, railway, naval and stationary engines have more stable work conditions, [3]. On the other hand, temperature variation field can cause cracking and leaking that disturbus or even makes engine operation impossible, [1]. Knowing the negative effects of the destruction of machine parts of internal combustion engines, in order to mitigate the causes of destruction by cracking of those parts we should make some thorough research, both theoretical and experimental.

Nowdays it is possible to calculate precisely the temperature distribution and internal stresses distribution in the fixe and mobile parts of the internal combustion engines by means of computer simulation. This can be done only if the boundary conditions are correcyly estimated by measuring the temperature of real objects of similar geometry and working in similar conditions. Such measurements are difficult to take considering significant the working cycle of the internal combustion engines, which

generated cyclic variation in temperature with a speed of the order of seconds or even tenths of seconds, [3],[5].

The concept of thermal fatigue which is generated by variation temperature field is the subject of numerous studies, specific to various fields. In case of internal combustion engines, this phenomenon is mentioned in several works [1], [4], [5], [6], [7], [8], [10].

The basic criterion to characterize material behavior during variable cyclical thermal stress is the resistance to thermal fatigue [1], [3], [4]. This is determined and expressed by the number of thermal cycles suffered by a machine part until its surface cracks, [8].

Multitude of factors influencing the damage by thermal fatigue makes it impossible to develop a methodology to provide universal results consistent with the specific phenomenon actually performed. Actual heat strain can not be modeled in laboratory always, [1].

Some cycles require two separate programs application and synchronized modeling, one for temperature and one for deformation, [2].

The literature has not mentioned an indicator for estimating thermal fatigue resistance of materials that is applicable under conditions of temperature, both stationary and transient [1], [2], [6]. It is however known that thermal stress generated by variable temperature fields is proportional to the thermal gradient "Δt", decreasing along with increasing thermal conductivity 'λ', [1], [8].

For evaluation of thermal fatigue resistance of materials we must take into account the following factors [1], [8]: the number of cycles of temperature variation until noticeable cracks on the surface of the sample occur; the number of temperature variation cycles until it is destroyed and crack intensity.

Whatever test methods/testing, thermal fatigue phenomena research solves two problems, [1], [8]:

- *obtaining comparative data on thermal fatigue resistance in a group of materials with application to particular conditions of operation and exploitation;*
- *collecting and processing experimental data through quantifying the quantitative evaluation of resistance to thermal fatigue to enable and ensure performance.*

In the study of thermal fatigue, the determining factor is not the time nor the range in which requests are variable, but the number of load cycles until the fatigue cracking [1], [3]. Regarding the level of thermal stress, it will depend on: thermal parameters; physic-mechanical properties of materials and the change rate during temperature oscillations; and the appearance of stress state, geometry and constructive parameters of the item, [7]. For a part machine subjected to the stress caused by cyclic thermal fatigue, damage is always dictated by thermal values higher than mechanical ones, [7].

Based on these criteria, concepts and methods of the phenomenon of thermal fatigue treated in the literature, we designed and built up an experimental system for studying this phenomenon in case of fixed and mobile machine parts of internal combustion engines. Designing and building an experimental facility allows us to study thermal fatigue resistance of main machine parts of vehicle engines. The experimental plant is the subject of a patent registered at OSIM A/00439 number of 17.06.2010, published in bopi_inv_12_2011.

The equipment allows modeling thermal fatigue of internal combustion engines and is property of the laboratory of "Industrial Mechanical Equipments" of the Faculty of Engineering of Hunedoara, University "Politehnica" from Timisoara.

THE EQUIPMENT USED AND THE CONDUCT OF THE RESEARCH

According to literature studies, qualitative method was chosen for laboratory modeling of thermal fatigue while testing, and thermal cycling was used to shape up the corrected Mason model and the corresponding hysteresis loop [2], [8]. In modeling real thermal cycles, the samples used are heated in a semicircle furnace with electric resistors and cooled off in different environments, such as air, water or ice. Based on these principles we designed an experimental facility for laboratory research of thermal fatigue which is presented in fig.1a,b, [8].

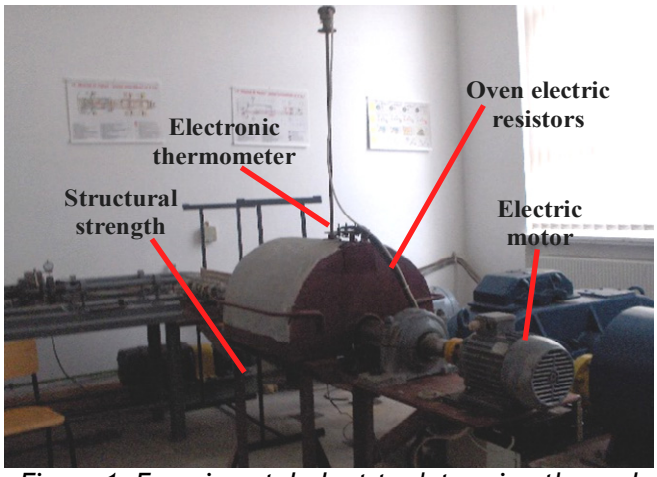

Figure 1. Experimental plant to determine thermal fatigue resistance with sample heating furnace

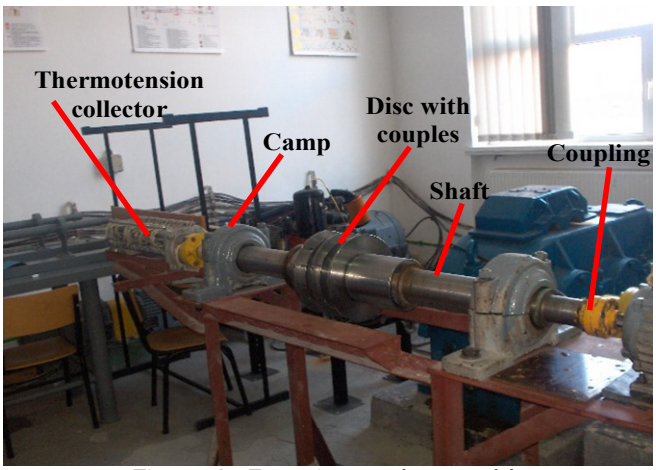

Figure 2. Experimental ensemble without sample heating furnace

The constructive scheme of the installation to determine thermal fatigue resistance is shown in figure 3, where an electric motor 1 controlled by a static frequency converter 2 which drives the main

shaft 3 is assembled and mounted on the metal frame 4. Overlapping the samples mounted on the main shaft 5 there is a semicircular furnace 5 who is ordered to perform sample heating. At the end of the main shaft, as opposed to drive electric engine, there is the thermo-tension collector 6 which takes the electric signals from thermocouples whose wires are connected to the contact brushes rings.

Disk supports are mounted on the main shaft - intermediate 7 and sideward 8, with screwed samples mounted on the generators 10. Support disks are mounted according to the length amongst samples and to the intermediate bushes 11 and end bushes 12; system hardening is achieved by means of interior screws 13 and pressure collar 14.

Thermocouples are mounted placed on two opposite samples 15, with corresponding response inertia corresponding to operating cycle of the machine parts that were subject to thermal fatigue.

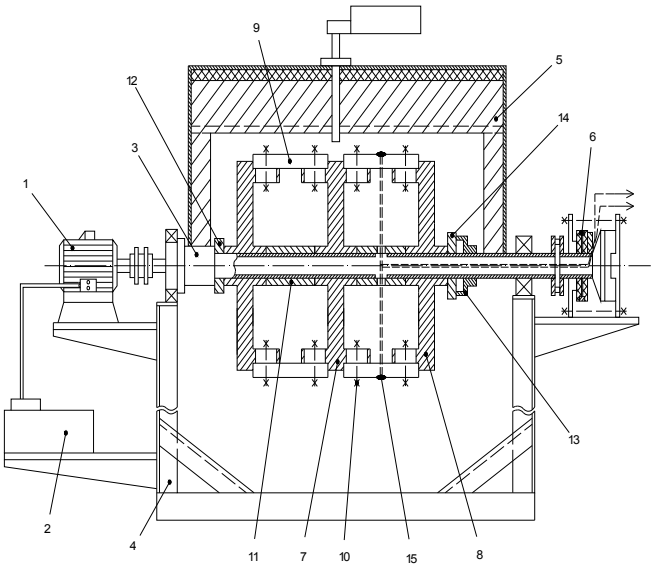

Figure 3. Constructive scheme of experimental installation for determining thermal fatigue resistance of machine parts from internal combustion engines

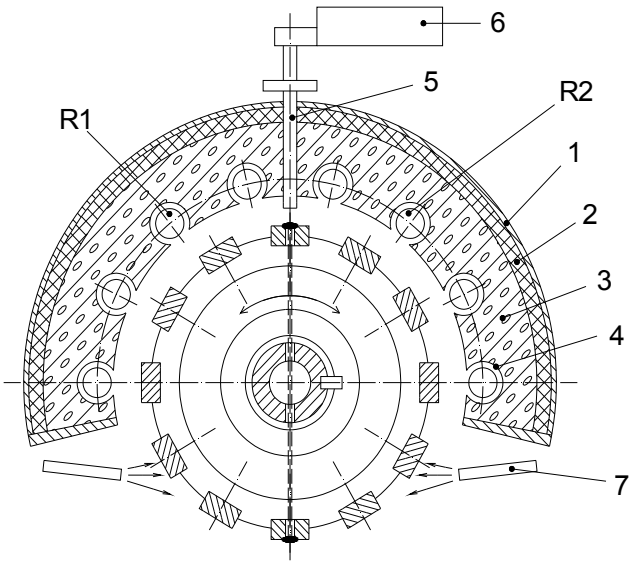

Figure 4. Cross-section of the plant laboratory experimental study of thermal fatigue

Figure 4 describe a section through the electric furnace for heating testing samples. The furnace is composed of a metal housing 1, lined with a heat insulating material 2, and the furnace is poured thermo steady concrete 3, with inner heat stream 4, which supports electrical resistors R1 and R2. Sample heating is enabled by a resistor with four loops, representing 90^0 of the circumference, or with both resistors comprising the entire area of the furnace, that is 180^0 of the circumference.

The furnace is fitted with a thermocouple 5 connected to an electronic thermometer 6, which helps us establish and maintain a certain temperature in the furnace through an automatic control, meanwhile 7 is the cooling of samples during experimental determinations.

The principle of investigations on experimental plant designed and built in two stages involve mounting two testing samples arranged opposite on the disk circumference of the thermocouple, and each are connected to a thermo-tension collector.

Figure 5 shows how we positioning the thermocouple on the sample and the sample size. In figure 6 is the connection made to a thermocouple inside the furnace to connect to the thermo-tension collector.

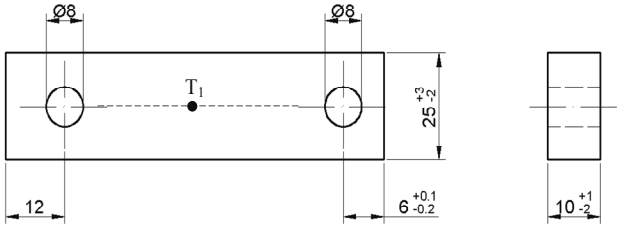

Figure 5. Thermocouple positioning in the experimental sample

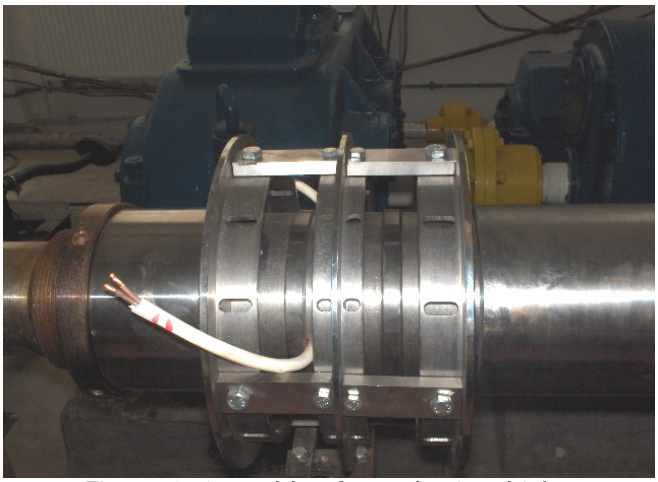

Figure 6. Assembly of samples in which a thermocouple is mounted

Electrical conductors from collector brushes of the thermo-tension are connected to a data acquisition system, connected with a computer, and allowing simultaneous determination and recording of temperature variations in the furnace for both type of evidence - inside or outside the furnace; evidence may be cooled in different environments, such as jets of air, water, ice tubes or fire extinguishers. In order to set the temperature of the coolant, we mounted a sample at the bottom of the which encloses a

thermocouple helping it to set up the average temperature at all speeds that will perform experimental tests, figure 7.
In order to take temperature inside and outside the furnace, the thermocouples used has small size and insignificant inertia, figure 8. The aim was to build thermocouples that would not disturb heat flow; so we are using some thermocouple characterized by high thermoelectric power. The wire of 0.5 mm diameter was placed inside the opening made in material δ = 0.8 mm. In figure 9 it is shown a scheme of a thermocouple for the sample temperature measurement.

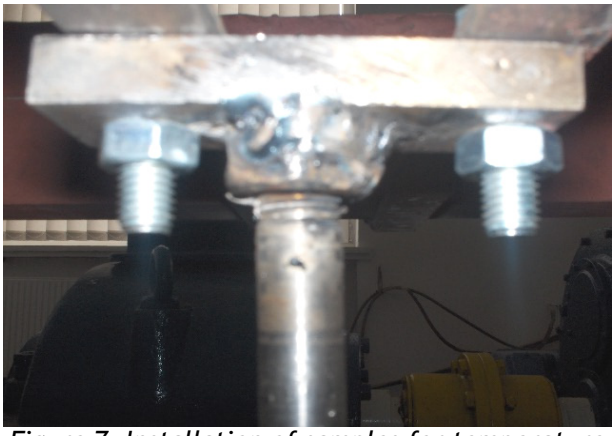

Figure 7. Installation of samples for temperature determination of the cooling environment

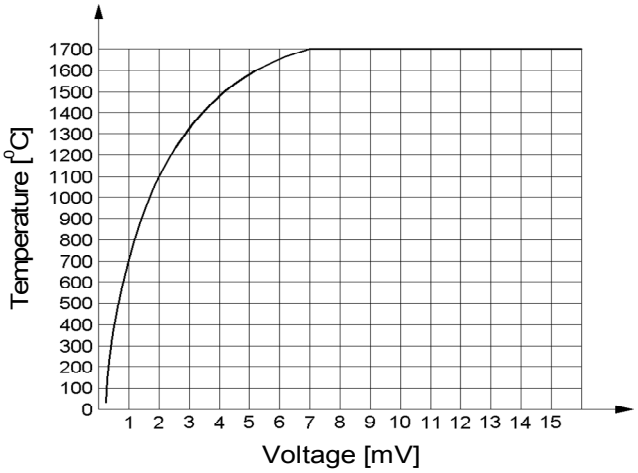

Figure 8. Diagram inertia response of the thermocouples used

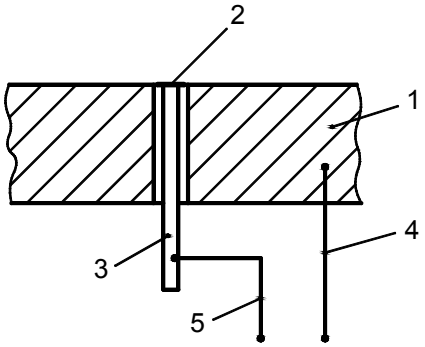

Figure 9. The scheme of a thermocouple for the sample temperature measurement
1- sample; 2- surface of the termocouples, 3- termocouple wire; 4- thermocouple wire connection; 5- sample wire connection

Figure 10 describes the thermo-tensions collector system used in experimental plants, as well as its design scheme with links to data acquisition system. In this figure the main components are:
1 - coupling couple;
2 - copper rings mounted on isolated discs textolit;
3 - carbon brushes;
4 - thermotension colector;
5 - connecting band;
6 - box connections;
7 - PC desk computer with an acquisition system.

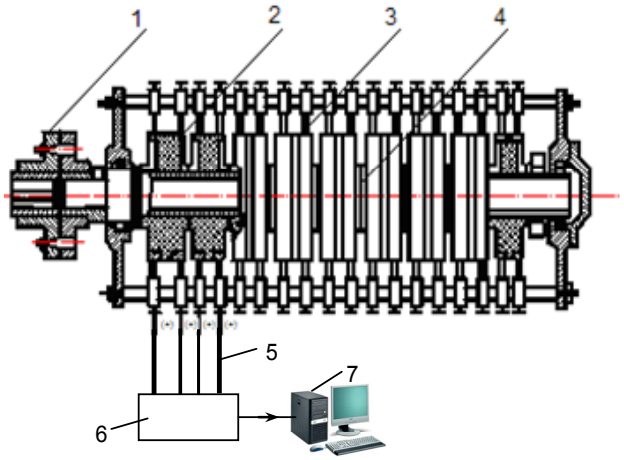

Figure 10. The design scheme of the thermotension colector with links to data acquisition system

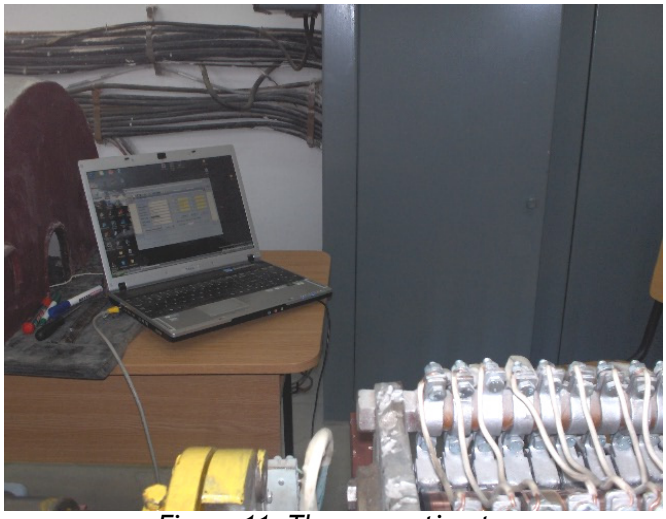

Figure 11. The connection to a data acquisition system

The software enables the system to store the experimental data as databases, from where they are processed and converted into temperature charts, [9]. The level and evolution of the thermal stresses caused by the temperature fields are determined by the diagrams recorded, representing the cyclical variations of the variable temperature fields which appear in the samples [3], [9].
Batch of samples is subjected to regimes of loading, aiming at the emergence of the first thermal fatigue cracks.
In order to reduce the number of load cycles to appear facelift thermal fatigue cracks can be admitted as evidence temperature is as high as possible and rapid cooling and steep.

To do this requires that speed electric motor can be change from minimum 100 rot/min, up to the maximum possible 1450 rot/min, this being achieved by means of a rheostat.

EXPERIMENTAL DETERMINATIONS

Allure of diagram presented in figure 12 confirms the theory found in the literature and thus validate the proposed model and experimental system developed for determining the thermal fatigue test machine in the fixed and mobile parts made of different internal combustion engines composition.

Variations of temperature fields of the samples have been recorded in very small time intervals, which indicate that the system accurately modelling the real situation inside combustion engines.

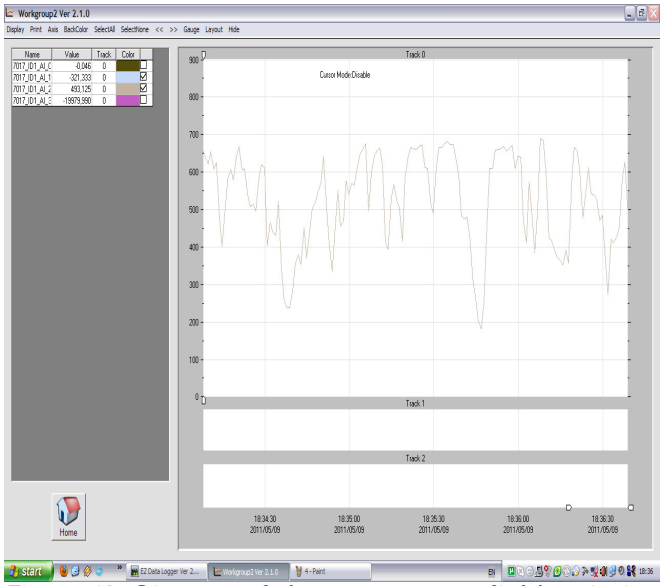

Figure 12. Diagram of the temperature field variation in the sample

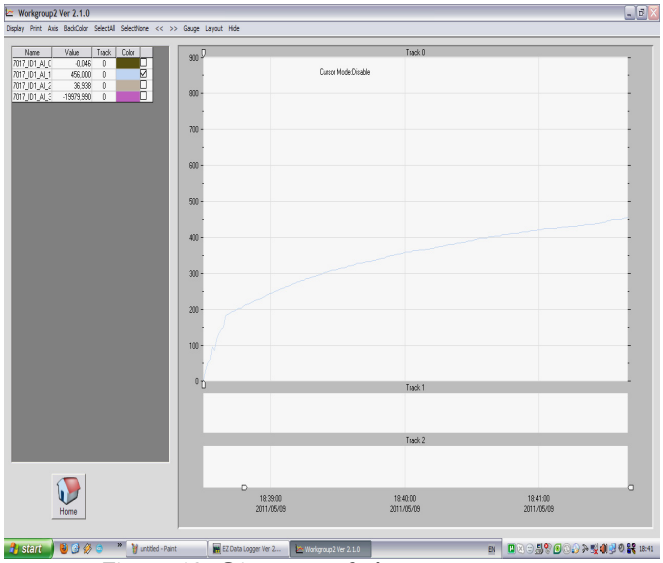

Figure13. Diagram of the temperature inside the furnace

Figure 13 diagram shows the evolution of the temperature inside the furnace to the start of experimental facility. When starting the system, temperature increases from zero to the value of 900^{0}C after which it maintained at this value during the experiments.

In the diagram shows a sequence only includes increasing the temperature up to 450^{0}C value.

This model confirms that the proposed experimental plant is well designed and built the wiring, which allows conducting experiments under optimal conditions.

CONCLUSIONS

The experimentally obtained temperature charts confirms the existence of variable temperature fields in the sample mounted in the experimental installation.

The temperature variation chart shows that its rate of change is of the order of seconds, consistent with the engine working cycle. The temperature charts allow the evaluation of the variable temperature fields and the determination of the associated thermal stresses. Their knowledge allows us to make a comparison with those determined by numerical methods, commonly used in the design of the machine parts fitted in the internal combustion engines.

The experimental facility meant to study thermal fatigue was designed and build based on concepts and laboratory modeling methods currently available in the literature and was validated following results.

On the other hand, these experiments are used to study the resistance at thermal fatigue of the component parts of internal combustion engines.

The findings may open the way for creating materials with high resistance to thermal fatigue, allowing the development of high performance parts fitting in the automotive engines.

REFERENCES

[1.] *BOTEAN, A., The study of the thermo-mechanical stresses spark ignition engine using modern method of study, Research report, Td2 cod CNCSIS 230, 2005, Bucharest*

[2.] *COFFIN, L.Jr., Prediction parameters and their application to high temperature low-cycle fatigue, Proceedings of second International Conference Fracture, Brington, London, 1969, pp.43-54*

[3.] *GARDYNSKI, L. (1995). Investigation of temperature fluctuations of diesel engine piston, Technical University of Lublin, Poland, pp.108-116.*

[4.] *HALFORD, G., Low cycle thermal fatigue, Edited by Hetnarski R., Elsevier Science Publisher B.V. 1987*

[5.] *KEREZSI, B.B, KOTOUSOV, A., PRINCE, J.W.H., Experimental apparatus for thermal shock fatigue investigations, International Journal Pressure Vessels and Pipping, 2000*

[6.] *MILLER, D., PRIEST, R., Material response to thermal-machanical strain cycling. High temperature fatigue- properties and prediction, Elsevier Applied Science, pp. 113-175, 1987*

[7.] *NITTA, A., KUWABARA, K., Thermal-mechanical faligue failure and life prediction. High temperature creep-fatigue, Elsevier Applied Science, pp. 203-222, 1988*

[8.] PINCA, C. JOSAN, A., Experimental plant for laboratory research of thermal fatigue phenomenon, WSEAS International Conference, Cambridge, UK, 2012, pp. 73-78.

[9.] PINCA, C. JOSAN, A., Determination of the variable temperature fields in the cylinder head of a spark ignition engine, Precedings of the 22nd International DAAAM Symposium, Vol. 22, No.I, Viena, Austria, 2011, pp. 605-606

[10.] SILVA, F.S.,- Fatigue on engines pistons-a compendium of case studies, Engineering Failure Analysis 13, Portugal, 2005, pp. 480-492

ACTA TECHNICA CORVINIENSIS - Bulletin of Engineering

ISSN: 2067-3809 [CD-Rom, online]

ACTA TECHNICA CORVINIENSIS – Bulletin of Engineering
Tome VI (Year 2013) – FASCICULE 3 [July–September]
ISSN 2067–3809

[1.] Guo ZHONGHOU, [2.] Shi YAN

THE RESEARCH ON THE RISK MANAGEMENT MECHANISM OF NATIONAL DEFENSE ECONOMY

[1.] DEPARTMENT OF NATIONAL DEFENSE ECONOMY, MILITARY ECONOMY ACADEMY – WUHAN, CHINA

ABSTRACT: Since entering the new century, the world's political, economic and military environment has undergone profound changes. Particularly since 2008, the global financial crisis spread, affecting and threatening the security of China's national defense economy. Therefore, strengthening the national defense economic risk management (risk management), constructing the risk management mechanism of the national defense economy, and enhancing a strong "firewall" for defending against the threat, is becoming a profound implications from historical experiences as well, and a timely measures for promoting the national defense economic development faster and better and for ensuring the national security. With the rapid development of economic globalization and promotion of the new military revolution, national defense economy is increasingly affected from the impact of the political, economic and military situations domestic and abroad.
KEYWORDS: national defense economy, risk management, mechanism

INTRODUCTION

With the rapid development of economic globalization and promotion of the new military revolution, national defense economy is increasingly affected from the impact of the political, economic and military situations domestic and abroad.

The sources of risk to the economy diverse to a higher degree, the speed that risk turns into a crisis becomes faster, and the impact of the crisis on national defense economy changes more violent. As President Hu Jintao pointed out, this is a time full of huge potential and dynamic development, also with all kinds of difficulties and risks; and this is a time of both rare opportunities and severe challenges.

We must take advantage of this period of important strategic opportunities, strengthening the national defense and economic construction, establishing and enhancing the national defense economic risk management mechanism, and improving the defense economic ability to cope with the risk.

THE MAIN PROBLEMS OF CHINA'S NATIONAL DEFENSE ECONOMIC RISK MANAGEMENT

In response to the international financial crisis, a series of measures of the national defense economy risk management are fruitful. But we must notice that the consciousness of the risk management in the individual departments or micro-economic organizations is relatively weak.

Moreover, the economic risk management mechanism has not to be established for the national defense yet, either the methods and means of crisis management is not perfect.

Specifically speaking:

- ***The awareness of importance of the national defense economic risk management is not clear enough.***

Currently, concerning the awareness on the issues of national security, someone still remains only in the military fields. However, in other areas such like political, economic, cultural, science and technology, and information fields, this kind of security awareness is limited either. With less sense of the risk, their theoretical study lags. As far as this financial crisis, this situation manifests in the following aspects:

First of all, we are lack of any awareness about the normality of the national defense economic risk and the inevitability of the financial crisis. It turns out that, through hundreds of years, expansion and contraction always alternatively occur in a circle during the market economy running course. However, from April 1991 to March 2001, the United States economy continued to grow for 120 months, so that some economists believe that the economic cycle has been flattened.

Consequently, during 2000 to 2002, when the United States appeared the capital expense cycle and real estate cycle again; and in 2007 when China's macroeconomic appeared the phenomenon that the assets expansion and inflation coexist which is rare during 10 years; and in 2008 when the fourth quarter of GDP growth had been below the potential growth more than 3 percentage points, many people still held to a blind optimistic hope on that economic situation, thinking the economic development momentum is good, but the outbreak of crisis is on a small probability.

However, the final result proved that the outbreak of the financial crisis became a solid evidence of the theoretical research on the economic cycle once again.

Next, we are short of cognition concerning the severity and destructiveness of the financial crisis on the economic crisis and the national defense. Some people believe that the national defense economy is dominated by plans. As long as a proper regulation, the risk can be reduced to the lowest point, and probably will not have much effect. But in fact, at present, under the circumstances that the economic globalization is advancing, China's market economy system is developing, and the civil-military parties are tending to integrate, the national defense is facing more risk resources. Further, the risk is more likely turning into a crisis, and then its development would be faster. Although the defense economy has followed relatively strict regulations, plans and policies, it was not able to completely avoid the venture and protect itself.

Thirdly, for the economic endogenous risk of the national defense, there is not much awareness. The outbreak of the financial crisis this time, has given us a profound revelation that is there exist several structural inconsistencies such like low investment structure of the national defense, outward and internal imbalance of the national defense industry, high proportion of the maintaining expenditure in the total defense spending, etc. These potential threats are normally difficult to detect. Yet once triggered by the financial crisis or other external incentives, it can lead to serious consequences. Especially in current, in China, for the science and technology of national defense industry is under adverse circumstances with weak independent innovation ability, inadequate key technology, and deficient strategic resources reserves; we should pay closer attention to the deeper conflict within the national defense economy and do a further analysis on it.

- ***The preparation for responding to the financial crisis is inadequate.***

Due to the lack of risk management awareness, some relevant departments often deny the normal risk management, which causes a lack of preparation for the despondence to the crisis. So when the crisis broke out, it leads to a series of passiveness.

First of all, the ability to accurately identify and capture the warning signs is not capable enough. Before the crisis occurred the "warning signs" would appear repeatedly. If these signs are recognized, given attention to and effectively addressed, so that many crises would be prevented before they occur. This is the best way to resolve the crisis. For example, during 2000-2006, before the outbreak of this financial crisis, the United States real estate market rose to more than 90%. If we can catch these signs, and put a certain prevention measures, it is quite possible to significantly reduce our losses from financial crisis.

Moreover, the national defense departments are lack of targeted response plans to the economic crisis.

Data shows that an effective contingency plans system can reduce the loss to 6% of the result from a non-emergency system. In October 2008, in order to avoid and reduce the United States financial crisis' impact on China, the Central Bank and the relevant regulatory bodies have developed the plans; the Regulators have strengthened the prudential supervision of financial institutions and services improving the ability to resist crisis. While in the area of national defense economy, it has not yet constructed an appropriate planning system, so that when the international financial crisis had a negative impact on China's national defense economy, with a rush we were unable to grasp the very opportunity to response to it very well. At the same time, as spreading the financial crisis caused a more complex international circumstance, which further exposed the disorder and shortage of the emergency planning system of every national defense department.

Thirdly, the emergency reserves in response to the financial crisis are short. On one hand, on the financial reserves respect, the State has not set up a special fund for the military national defense production enterprises and the small and medium complete enterprises, yet the local financial support was relatively limited either, resulting in some big and tough financial trouble for these enterprises. On the other hand, on the material reserves aspect, such as minerals, food, and other strategic materials, some are repeatedly stored, yet some are missing or insufficient; even the quality of those reserves is difficult to meet the standards. When an emergency or crisis occurs, the country is not able to control the number and distribution of the demanding materials as a whole.

- ***The system to deal with the crisis and implement the national defense economic risk management is not perfect enough.***

At present, China's national defense and economic risk management system are fairly far behind the requirements of normalizing risk management.

At first, the subject of the national defense economy risk management is a blank. While the State has established a special temporary risk management agency in response to the financial crisis, but this agency is on a temporary and uncertain side; and its running mechanism is difficult to maintain for a long time. To normalize the national defense economic risk management, there must be clear responsibilities respectively taken by each unit, department and individual. Some issues must be distinctly researched and reasoned like which work requires dedicated, standing agencies to engage in the national defense economic risk management, and what kind of task needed specific person in charge of.

Secondly, there is a lack of an auxiliary decision-making body for doing national defense economic risk research. Currently, there are not a large number of the experienced and decision-making "brains" in the national defense economic risk management. Then, just relying on the experience, knowledge and wisdom of the minority to make decision, there will inevitably be errors. Particularly, during more than 20 years after implementing market economy in our country, we often fail to recognize the present economic situation domestic and abroad due to the

short of experience in the field of the macroeconomic management, including economic management of national defense. Even the worse, at that time, it may cause failure on development policy making by just taking reference from the developed countries and acting like them.

Thirdly, we are lack of the personnel with professional skills on the risk management. In response to the crisis and handle the risk, it requires that the policy makers and managers must be fully competent with relatively good comprehensive quality. National Defense economy refers to the risk management of military and civil, two essential areas. It needs a number of trained professional risk managers. But the truth is that, many managers are not accepted the knowledge of special and systematic risk management and emergency response during their training. They know much less about the awareness of crisis, meanwhile their capabilities to manage the national defense economic risk need to be strengthened.

□ ***The national defense economic risk management mechanism is yet perfect.***

Owing to the complex and diverse national defense economic risk, there are several crisis-affected sectors. And as the national defense economy has a strong connection with the national economy, we should take used of a more systematic and scientific running mechanism to response to the crisis. Currently, in terms of the establishment of the mechanism, there exist following two issues:

- *On one hand, there is a lack of a whole process of the risk management mechanism including identification, analysis, early warning, control and handling. At present, in the economic management of national defense, there are still some problems remaining unresolved as who collects the information about the risk, what information can be collected, how can collect accurate information, and to whom to submit these collected information; In the risk analysis process, it mainly uses qualitative analysis, yet quantitative, scientific and accurate analysis is relatively insufficient; In the disposal process, it is still remaining in a less normative state in auxiliary decision-making, resource management, command and coordination, and rehabilitation.*
- *On the other hand, there is a lack of linkage and coordination mechanism of risk management. At present, in China's defense economic risk management, even though the vertical emergency disposal mechanism of all emergency management sectors is more than perfect, the duties division in horizontal level is not clear enough. The overlapping duties and the discrepancy of management coexist without a unified coordination.*

The division, collaboration, and communication mechanism as well as the running program of nation, army, and local authorities haven't yet institutionalized. The information from all parties is isolated with a less sharing which leads in a difficult unification on action and resources. Also there are certain difficulties in coordination in the interests.

THE PRELIMINARY DESIGN OF RISK MANAGEMENT MECHANISM OF CHINA'S NATIONAL DEFENSE ECONOMY

In the new stage of the new century, we must be based on the state of society, nation and the military intelligence, focusing our eyes on the long run risk management mechanism of the national defense economy, drawing on the international experience and lessons of financial crisis, to establish and strengthen the risk management mechanism of the national defense economy.

□ ***To develop a monitoring index system of risk management mechanism.***

From the perspective of the development of financial crisis and transmitting methods towards the national defense economy as well as the risk of the defense economy itself, the following factors can be considered in the development of risk monitoring index system.

First, it's necessary to strengthen monitoring the structure index of defense industry. The following factors should be taken into consideration in judging the risk of defense industry:

1.) *The structure of energy consumption. It refers to the dependence of defense industry on resources and energy, namely the issues as to how many industries are established on the basis of energy intensive consumption and how many industries would give rise to the shortage of national recourses and even to the deterioration of environment.*
2.) *The structure of industrial benefits. It refers to the issues as to how many related industries suffer losses, operational difficulties and profits decline.*
3.) *Regional structure. It refers to the issues as to whether the defense industry resources excessively concentrate on a certain area.*
4.) *The structure of industry. It refers to the issues as to whether the state or regional industrial structures are similar, causing excessive competition on small size and at low level, and further leading to a serious imbalance of resource allocation and loss of resources.*
5.) *The structure of technology. It refers to the technological capability, the quality of personnel, technological innovations and the proportion of defense industries in traditional industrialization.*

Second, it's necessary to strengthen monitoring the index of national defense economic strength:

1.) *Per capita level of national defense economy. Per capita GDP is an important symbol to measure the national and regional economic development. Similarly, per capita level of defense economy represents the development of defense economy. The risk revealed by a low level of per capita is much more dangerous than the low level of total amount. Besides the per capita national defense expenditure, and the per capita stock of defense assets, much attention should be given to the per capita index of other important strategic resources such as food, fuel, steel.*

2.) *Economic growth rate. The economic growth is a critical foundation of defense economic development, which shows the diffusion index for the national defense.*
3.) *The contribution rate of science and technology. This rate reveals the security of national defense, which also occupies an important place in the economic development. The more powerful the economic strength of a national defense is, the higher the contribution rate of science and technology will be, and the higher the contribution rate of science and technology of the national defense becomes.*
4.) *The ratio of the resource and labor-intensive industries to the knowledge and technology-intensive industries. This index reflects the modernization level of defense industry as a whole.*
5.) *The benefits of national defense economic. As far as the defense economy, it mainly refers to the benefits level of defense science and technology industry, the benefits level of defense expenditures. The low economic benefits show that the defense economy itself is under a serious risk and crisis.*

Third, it is necessary to strengthen the capacity of national fiscal and financial monitoring. National fiscal and financial capacity is the most important support of national defense economy:

1.) *The stability of exchange rate, as the Yuan's exchange rate to the dollar's, or to the Euro's. The exchange rate fluctuations do not fully reflect the actual change in the value of the RMB. But with the development of economic globalization, the status of the exchange rate is gradually improving compared with the rate of inflation, which is a sign of a financial crisis.*
2.) *The capital adequacy ratio of financial institutions. The strength of the financial institution lies on the quantity of its own capital. If the capital adequacy ratio falls below 8%, there would be a lower anti-risk capability and thus to cause a financial crisis.*
3.) *The revenue share of GDP indicates that the national fund raising ability is the essential support of national defense economy.*
4.) *The national debt pressures. When the debt is too heavy, it can cause an unstable macro economy.*

Fourth, it is necessary to strengthen the monitoring capacity of national defense economy towards foreign parties, including:

1.) *The level of foreign trade on military industry. It is a representative of defense economic development as a whole. However, the growing competition in international market, and the devaluation of currency and stable currency policy will bring some risks on the defense industries and enterprises.*
2.) *The resilience to external environment. It refers to the issues as to whether the competitive mechanism is perfect or not; whether the modern enterprise system is already set up or not; and whether we are capable to adapt to the changes in the world economic environment or not.*
3.) *The crisis index of international trade liberalization. It refers to the issues as to whether the trade liberalization would cause a loss for the national strategic reserve resources or not, leading to an excessive consumption of the natural and environmental resources.*

By tracking and monitoring the above indicators, coupled with modeling analysis, we will be able to judge the defense economic index, fluctuation degree, security status as well as the main risk, and to raise an alarm and thus to adjust the development policies of national defense economy in order to prevent and control the crisis.

□ ***To set up a risk management system for national defense economy.***

The defense economic risk, involving several aspects as multiple subjects, multilevel coordination, and broad coordination tasks, needs an urgent action to construct an authoritative, efficient, responsive, and highly integrated monitoring and early-warning systems, in order to ensure that the monitoring and early-warning capacity can be developed on the basis on a reliable organization.

At first, it is necessary to establish a defense economic risk management institution at national level. It can be set as a "National Strategic Early-Warning Leading Group" which consists of the leaders from relevant state ministries and committees and military departments. And it is suggested to build a strategic early warning center, with a subordinate national financial risk early-warning center.

The defense economic risk management office is regarded as one of the branches of the center. This office is a civil-military integrated institution running in a unified way. It is composed of the staff from some functional sections in the military and government agencies. Moreover, it is responsible for the some aspects of principles and policies, regulations and laws related to the defense economic security, the defense budget and the risk monitoring of major construction projects, as well as the integrated coordination of the risk management and disposal. Further, it is also in charge of publishing financial risk early-warning for national defense.

Secondly, it is necessary to establish risk monitoring institutions in all departments. These institutions will be responsible for reporting the information and research results concerning the defense economic security to the national defense economic risk management office which is especially set up for the monitoring and early warning of the defense economic security.

After an initial comprehensive analysis of all the information and research results about defense economic security, the office will submit the outcome to the leading agency. Each professional risk monitoring institution can publish the economic risk warning within its own field. At the same time, as for the information about significant and unexpected economic risks of national defense, the office can directly submit them to the national defense

economic and security crises management lead agency.

Thirdly, in accordance with the designed risk monitoring index system of defense economy, personnel are assigned to risk information acquisition and analysis at all levels, so that the work of the risk information acquisition and analysis could cover every index, and the risk information can be collected and submitted according to the procedure of this system.

- ***To enhance national defense crisis disposal capacity-building.***

Working on identifying and early warning risk system is to avoid crisis. However, some crisis emerges unexpectedly; therefore enhancing our ability on disposing national defense crisis contributes a vital aspect to strengthen the national defense economic risk management.

First of all, for national economic crisis occurs rather unexpectedly, which rarely left us time to get prepared. Under such circumstance we should perfect the crisis disposal preplan. From the detailed content, and based on the forecast and analysis of the defense economic security situation, we should draw up the crisis emergency preplan considering the aspects of situation judgment, response force, treatment measures, communication and coordination, etc. in order to make the preparation work effectively and targeted. Meanwhile, with full and thorough consideration on international security environment and the national defense strength, we need to work practically to focus on the most complex and difficult situation and formulate a set of effective measures in accordance with the principles of easy to prepare, easy to operate to ensure a calm and rapid response under the emergency situation.

Secondly, it is necessary to improve the emergency mechanism. It can be divided into two types: the first case is the plan that matches the risk disposition. We can find out the matched plan for the current crisis from the plans stock, and then evaluate the very plan to select the best, efficient and reliable one to respond to the crisis. If the alternative plan dissatisfies the requirements, then there would be a decision-making session for modification of the alternative plan, and then re-assess and adjustment, until it finally meets the requirements. The other case is the risk disposal lacking of an arranged plan. As long as the crisis occurs, the security risk management authority of defense economy should work out a rapid processing scheme for experts to evaluate, and then submit it to the National Defense Security Committee for decision-making. Meanwhile, the risk management authorities and departments at all levels should formulate their own disposal plan on the basis of the scheme.

Thirdly, we should enhance the crisis decision-making capacity of the decision-making bodies. To improve the communication and coordination ability of the decision-making bodies is to ensure establishing a rapid information communication, resource allocation and policy issuing mechanism when making decisions; it is necessary to cultivate large numbers of comprehensive personnel with higher quality of adaptability, authority, and coordination ability for crisis decision-making, to strengthen the importance of the crisis decision-making think tank, and keep them remain their relatively independence, to avert "Follow suit decisions" or "Echo decisions"; and to establish a supporting system of national defense crisis decision, which is capable of quick and reliable simulation analysis for crisis situations, and of improving the efficiency of the decision.

- ***To strengthen the theoretical study on the national defense economic risk.***

In order to better improve the national defense economic risk management, the state and the military should regularly organize regular research activities and make full use of the resourceful economic and strategic research institutions' outcomes both from military and civil parties to compile the Report on the National Defense Economic Risk Assessment and study on the issues of the national defense economic security policy, as well as focusing more attention on the national defense economic security monitoring and early warning. In the meaning time, we should also utilize information from the state and military intelligent agencies as well as the national security monitoring and early warning systems to enhance multiple communication and coordination mechanisms, and further improve the system of joint meetings, regular meetings, and information reporting to form a high-efficiency interaction mechanisms with close connection and flexible coordination to ensure that the national defense economic risk management information proceeds smoothly into the decision-making process.

REFERENCES

[1.] *Lisa Meulbroek. (2002). The Promise and Challenge of Integrated Risk Management, Risk Management and Insurance Review, Vol. 5,No.1 .*

[2.] *Peter Mangold. (1999). National Security and International Relations. London and New York: Routledeg.*

[3.] *Neu C. R., Charles Wolf. (1995). The Economic Dimensions of National Security. National Defense Research Institute, RAND and United States Dept. of Defense Office of the Secretary of Defense: Scientific and Technical Documents Publishing House.*

ACTA TECHNICA CORVINIENSIS – Bulletin of Engineering

ISSN: 2067-3809 [CD-Rom, online]

ACTA TECHNICA CORVINIENSIS - BULLETIN of ENGINEERING

ISSN: 2067-3809 [CD-Rom, online]

ACTA TECHNICA CORVINIENSIS - BULLETIN of ENGINEERING

ISSN: 2067-3809 [CD-Rom, online]

copyright © UNIVERSITY POLITEHNICA TIMISOARA,
FACULTY OF ENGINEERING HUNEDOARA,
5, REVOLUTIEI, 331128, HUNEDOARA, ROMANIA
http://acta.fih.upt.ro

ACTA TECHNICA CORVINIENSIS – Bulletin of Engineering
Tome VI (Year 2013) – FASCICULE 3 [July–September]
ISSN 2067–3809

[1.] P. Bala Anki REDDY, [2.] N. Bhaskar REDDY

MHD FREE CONVECTION FLOW WITH VARIABLE VISCOSITY AND THERMAL DIFFUSIVITY ALONG A MOVING VERTICAL PLATE EMBEDDED IN A POROUS MEDIUM

[1.] FLUID DYNAMICS DIVISION, SCHOOL OF ADVANCED SCIENCES, VIT UNIVERSITY, VELLORE 632014, INDIA
[2.] DEPARTMENT OF MATHEMATICS, S.V. UNIVERSITY, TIRUPATI-517502, A.P. INDIA

ABSTRACT: This paper investigates a study of the flow of a viscous incompressible fluid along a heated vertical porous plate, taking into account the variation of the viscosity and thermal diffusivity in the presence of the magnetic field. The governing partial differential equations of the flow field are transformed into ordinary differential equations by means of similarity transformation. The resultant equations are solved numerically using Runge-Kutta fourth order method along with shooting technique. The effects of variable thermo-viscous parameters, magnetic parameter, permeability parameter and suction parameter on the velocity, temperature, skin-friction coefficient and Nusselt number are obtained and discussed in detail.
KEYWORDS: Variable viscosity, thermal diffusivity, magnetic field and porous medium

INTRODUCTION

Natural convection flows driven by temperature differences are of great interest in a number of industrial applications. Buoyancy is also of importance in an environment where differences between land and air temperature can give rise to complicated flow patterns, and in enclosures such as ventilated and heated rooms and reactor configurations. Natural convection flows driven by temperature differences have been studied extensively. For example, Pohlhausen [11] first studied the steady free convection flow past a semi-infinite vertical plate by integral method. But the similarity solution to steady free convection flow past a semi-infinite vertical plate was presented by Ostrach [10], who solved the ordinary non-linear equations by a numerical method. Siegel [17] was the first to study the transient free convection flow past a semi-infinite vertical plate by integral method. The same problem was studied by Gebhart [3] by an approximate method.

In all the above studies, the free convection flow along a vertical flat plate was restricted, in general, to the case where the temperature difference between the plate and the fluid is small, so that the fluid properties may be taken as constant. For the fluids, which are important in the theory of lubrication, the heat generated by the internal fiction and the corresponding rise in temperature do affect the viscosity and thermal diffusivity of the fluid and they can no longer be regarded as constant. The physical properties of fluids such as viscosity and thermal diffusivity may change significantly with temperature. The temperature dependent property problem is further complicated by the fact that the properties of different fluids behave differently with temperature. Different relations between the physical properties of fluids and temperature are given by Kays and Grawford [8]. Mehta and Sood [9] have shown that when this effect is included, the flow characteristics may be substantially changed compared to the constant viscosity case. The influence of variable viscosity on the laminar boundary layer flow and heat transfer due to a continuously moving flat plate is examined by Pop et al. [12]. Kafoussias and Williams [7] investigated the effect of temperature-dependent viscosity on free-forced convective laminar boundary layer flow past a vertical isothermal plate. Hossain and Munir [4] analyzed a two-dimensional mixed convection flow of a viscous incompressible fluid of temperature dependent viscosity past a vertical plate. Elbashbeshy and Ibrahim [2] investigated the steady free convection flow with variable viscosity and thermal diffusivity along a heated vertical plate.

Hydromagnetic flows and heat transfer have become more important in recent years because of its varied applications in agriculture, engineering and petroleum industries. The free convection flow with variable viscosity and thermal diffusivity along a vertical plate in the presence of magnetic field has been studied by Elbashbeshy [1]. The effect of temperature dependent viscosity and thermal conductivity on unsteady MHD convective heat transfer past a semi-infinite vertical porous plate was studied by Seddek and Salama [16].

The heat transfer problem from different geometries embedded in porous media has many practical applications in industrial and technological fields such as geothermal reservoirs, drying of porous solids, thermal insulation, and enhanced oil recovery, packed-bed catalytic reactors, cooling of nuclear reactors and under ground energy transport. Raptis [13] considered mathematically the case of time-varying two-dimensional natural convection flow of an incompressible, electrically conducting fluid along an infinite vertical porous plate through a porous medium. Raptis et al. [14] analyzed hydromagnetic free convection flow through a porous medium between two parallel plates.

However the impact of variable viscosity and thermal diffusivity of a hydromagnetic free convection flow along a vertical porous plate embedded in a porous medium has received little attention. Hence an attempt is made to study the effects of variable viscosity and thermal diffusivity on a steady two-dimensional free convection flow of a viscous incompressible electrically conducting fluid along a vertical porous plate embedded in a porous medium.

The governing equations are transformed by using similarity transformation and the resultant dimensionless equations are solved numerically using the Runge-Kutta fourth order method with shooting technique. The effects of various governing parameters on the velocity, temperature, skin-friction coefficient and Nusselt number are shown in figures and tables and analyzed in detail.

MATHEMATICAL ANALYSIS

A steady two-dimensional laminar free convection flow of a viscous incompressible electrically conducting fluid along a moving semi infinite vertical flat plate embedded in a porous medium is considered. The flow is assumed to be in the x-direction, which is taken along the plate and y-axis normal to the plate. A uniform magnetic field is applied in the direction perpendicular to the plate. The fluid is assumed to be slightly conducting, and hence the magnetic Reynolds number is much less than unity and the induced magnetic field is negligible in comparison with the applied magnetic field. It is further assumed that there is no applied voltage, so that the electric field is absent. All the physical properties of the fluid are assumed to be constant except for the fluid viscosity, which varies exponentially with the fluid temperature, the thermal conductivity which varies linearly with the fluid temperature and the density variation in the body force term in the momentum equation where the Boussinesq's approximation is invoked. Under these assumptions, the conservation equations of the laminar boundary layer flow under consideration are

Continuity equation

$$\frac{\partial u}{\partial x}+\frac{\partial v}{\partial y}=0 \qquad (1)$$

Momentum equation

$$\rho\left(u\frac{\partial u}{\partial x}+v\frac{\partial u}{\partial y}\right)=\frac{\partial}{\partial y}\left(\mu\frac{\partial u}{\partial y}\right)+\rho g(T-T_\infty)-\sigma B_0^2 u-\frac{\mu}{K'}u \qquad (2)$$

Energy equation

$$u\frac{\partial T}{\partial x}+v\frac{\partial T}{\partial y}=\frac{\partial}{\partial y}\left(\alpha\frac{\partial T}{\partial y}\right) \qquad (3)$$

where u and v are the velocity components in the x- and y- directions respectively, ρ - the density of the fluid, μ - the variable dynamic coefficient of viscosity, g - the gravitational acceleration, T - the temperature of the fluid, T_∞ - the temperature far away from the plate, σ - the electrical conductivity of the fluid, B_0 - the magnetic induction, K' - the permeability of the porous medium and α - the variable thermal diffusivity of the fluid.

The boundary conditions for the velocity and temperature fields are

$$u=U_0,\ v=v_0(x),\ T=T_w \ \text{ at } \ y=0$$
$$u\to 0,\ T\to T_\infty \ \text{ as } \ y\to\infty \qquad (4)$$

where U_0 is the uniform velocity, $v_0(x)$ - the velocity of suction at the plate and T_w - the temperature of the plate.

The mass conservation equation (1) is satisfied by the stream function $\psi(x,y)$

$$u=\frac{\partial\psi}{\partial y},\ v=-\frac{\partial\psi}{\partial x} \qquad (5)$$

To transform equations (2) and (3) into a set of ordinary differential equations, the following dimensionless variables are introduced:

$$\eta=y\sqrt{\frac{U_0}{2\nu x}},\ \psi=\sqrt{2\nu x U_0}\,f(\eta),\ \theta(\eta)=\frac{T-T_\infty}{T_w-T_\infty},$$
$$Gr=\frac{g\beta(T_w-T_\infty)2x}{U_0^2},\ M=\frac{\sigma B_0^2\,2x}{\rho U_0},$$
$$K=\frac{2\upsilon x}{K'U_0},\ Pr=\frac{\upsilon}{\alpha_0},\ \upsilon=\frac{\mu_0}{\rho},\ \alpha=\frac{k}{\rho c_p} \qquad (6)$$

where θ is the non-dimensional temperature function, Gr - the thermal Grashof number, M - the magnetic field parameter, K - the permeability parameter, Pr - the Prandtl number, υ - the kinematic viscosity, α_0 - the thermal diffusivity at temperature T_w, μ_0 -the viscosity at temperature T_w, k - the thermal conductivity and c_p - the specific heat at constant pressure.

The variations of viscosity and thermal diffusivity with the dimensionless temperature are written in the form (Ibrahim and Ibrahim [5], Slattery [18])

$$\frac{\mu}{\mu_0}=e^{-\beta\theta} \qquad (7)$$

and

$$\frac{\alpha}{\alpha_0}=1+\gamma\theta \qquad (8)$$

where β and γ are the parameters depending on the nature of the fluid.

In view of equations (6)-(8), the equations (2) and (3) transform into

$$f'''+f''\left[e^{\beta\theta}f-\beta\theta'\right]+Gr\theta e^{\beta\theta}-(Me^{\beta\theta}+K)f'=0 \qquad (9)$$

$$\theta'' + \left(\frac{Pr\, f}{1+\gamma\theta}\right)\theta' + \left(\frac{\gamma}{1+\gamma\theta}\right)(\theta')^2 = 0 \qquad (10)$$

The corresponding boundary conditions are

$$f = f_w,\ f' = 1,\ \theta = 1 \text{ at } \eta = 0$$

$$f' = 0,\ \theta = 0 \text{ as } \eta \to \infty \qquad (11)$$

where f is the dimensionless stream function, $f_w = -v_0\sqrt{\frac{2x}{\upsilon U_0}}$ is the dimensionless suction velocity and prime denotes differentiation with respect to the variable η.

SOLUTION OF THE PROBLEM

The non-linear governing boundary layer equations (9) and (10) together with the boundary conditions (11) are solved numerically by using Runge-Kutta fourth order technique along with shooting method. First of all, higher order non-linear differential equations (9) and (10) are converted into simultaneous linear differential equations of first order and they are further transformed into initial value problem by applying the shooting technique (Jain et al. [6]).

The resultant initial value problem is solved by employing Runge-Kutta fourth order technique. The step size $\Delta\eta = 0.05$ is used to obtain the numerical solution with five decimal place accuracy as the criterion of convergence.

From the process of numerical computation, the skin-friction coefficient and the Nusselt number are also obtained and are presented in a tabular form.

RESULTS AND DISCUSSIONS

The parameters of the flow β, γ and Pr can be taken as follows (H. Schlichting [15], E.M.A. Elbashbeshy [1]): for air: - 0.7 ≤ β ≤ 0, 0≤ γ ≤ 6, Pr = 0.733. The effects of magnetic field parameter M, permeability parameter K, β, γ, thermal Grashof number Gr and suction parameter f_w on the velocity are shown in Figures 1-6.

It is observed that the velocity decreases as the magnetic parameter increases (Figure 1). It is because that the application of transverse magnetic field will result in a resistive type force (Lorentz force) similar to drag force which tends to resist the fluid flow and thus reducing its velocity. Also, the boundary layer thickness decreases with an increase in the magnetic parameter.

The parameter K as defined in equation (6) is inversely proportional to the actual permeability K' of the porous medium. An increase in K will therefore increase the resistance of the porous medium (as the permeability physically becomes less with increasing K') which will tend to decelerate the flow and reduce the velocity. This behavior is evident from Figure 2.

From Figure 3, it is clear that the velocity near to the vertical plate (η = constant) increases as β increases (the viscosity of air decreases). But an opposite effect is noticed at a certain distance from the plate ($\eta_0 \cong 1$). Figure 4 shows that the velocity in the fluid increases as γ increases (the thermal diffusivity of air increases) for fixed values of β. Moreover, the rise in the magnitude of the velocity is quite significant in the present case, showing that the volume rate of flow at a section perpendicular to the plate increases with an increase in γ.

The thermal Grashof number Gr signifies the relative effect of the thermal buoyancy force to the viscous hydrodynamic force in the boundary layer.

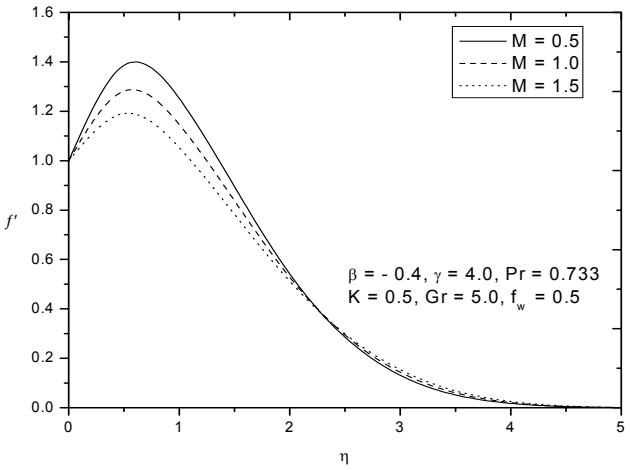

Figure 1. Velocity profiles for different values of M

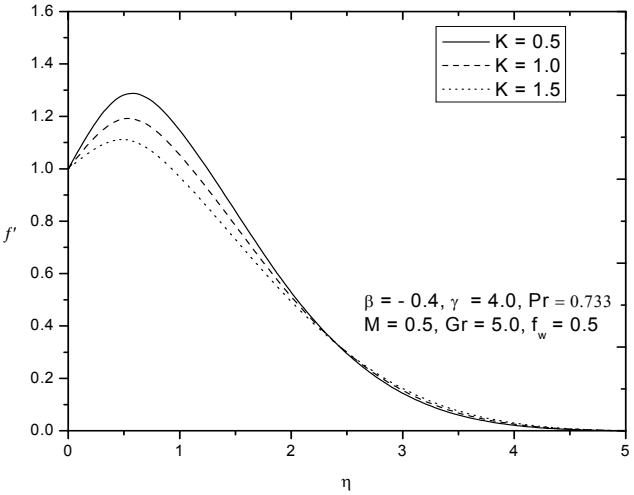

Figure 2. Velocity profiles for different values of K

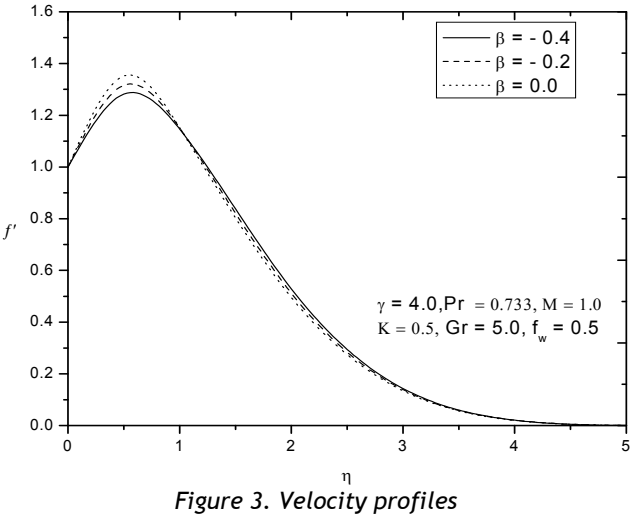

Figure 3. Velocity profiles for different values of B

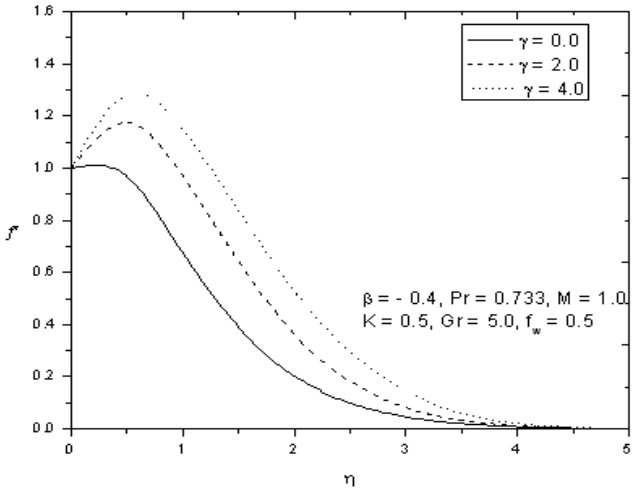

Figure 4. Velocity profiles for different values of y

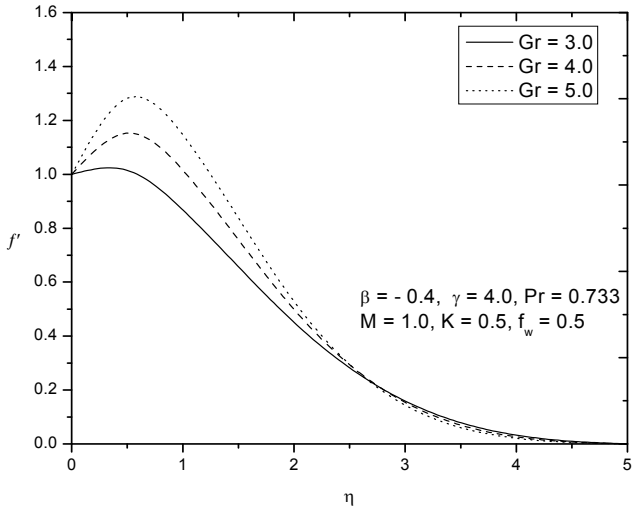

Figure 5. Velocity profiles for different values of Gr

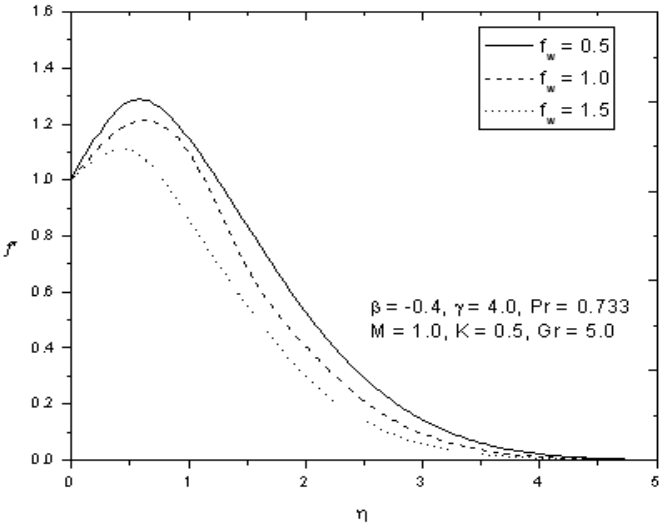

Figure 6. Velocity profiles for different values of f_w

As expected, from Figure 5, it is observed that there is a rise in the velocity due to the enhancement of thermal buoyancy force. Here, the positive values of Gr correspond to cooling of the plate. Also, as Gr increases, the peak values of the velocity increases rapidly near the porous plate and then decays smoothly to the free stream velocity.

From Figure 6, it is noticed that an increase in the suction parameter results in a decrease in the velocity.

The effects of magnetic field parameter M, permeability parameter K, β, γ, thermal Grashof number Gr and suction parameter f_w on the temperature are shown in Figures 7-12.

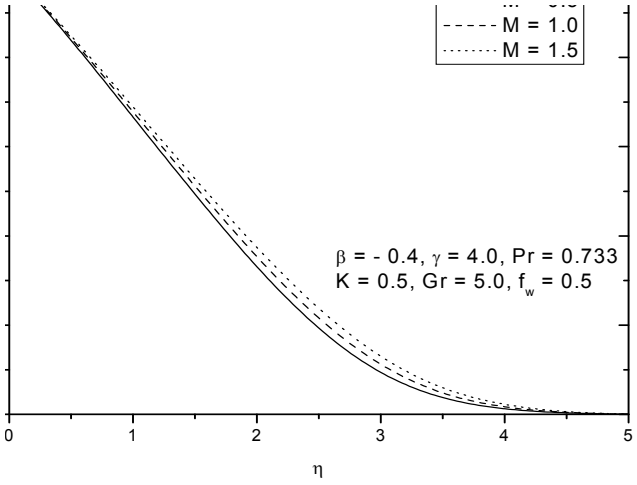

Figure 7. Temperature profiles for different values of M

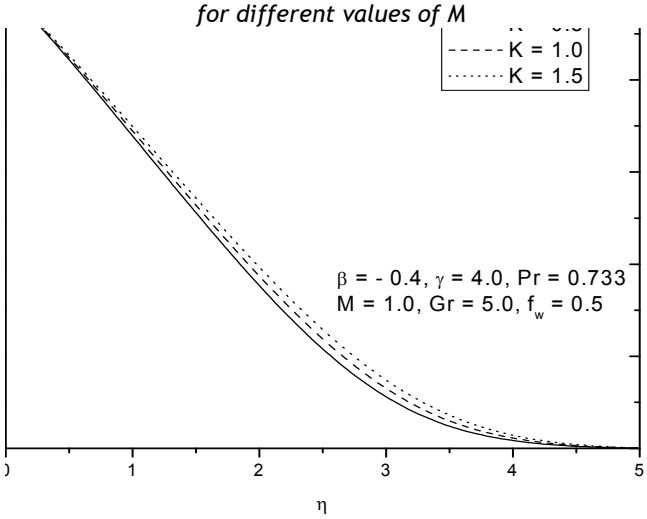

Figure 8. Temperature profiles for different values of K

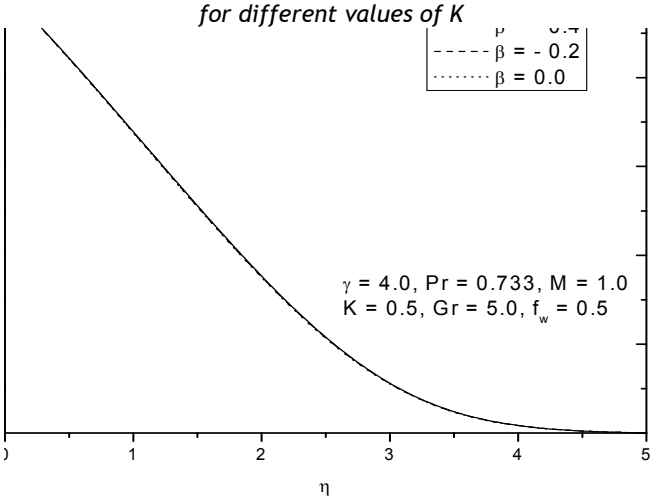

Figure 9. Temperature profiles for different values of B

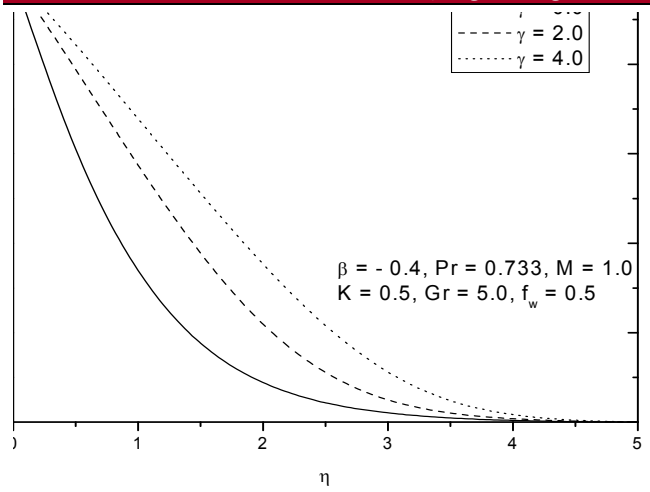

Figure 10. Temperature profiles for different values of γ

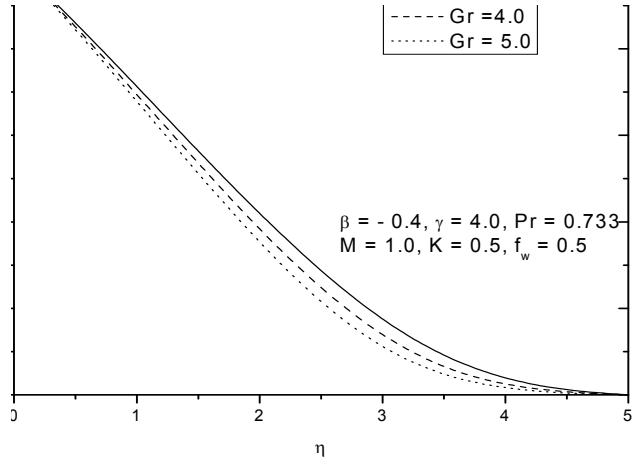

Figure 11. Temperature profiles for different values of Gr

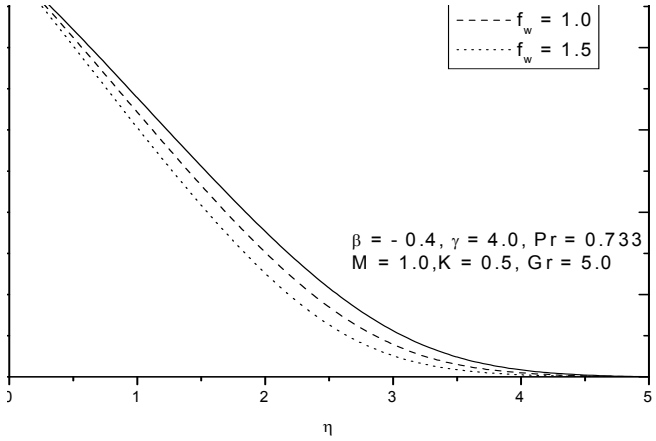

Figure 12. Temperature profiles for different values of f_w

It is observed that greater magnetic parameter causes a rise in the temperature (Figure 7). An increase in the permeability parameter causes a rise in the temperature. This is obvious from Figure 8. From Figure 9, it is noticed that as β increases, the temperature decreases and the decrement is very small.

Figure 10 reveals that the temperature in the fluid increases as γ increases (the thermal diffusivity of air increases) for fixed values of β. Moreover, in this case, the rise in the magnitude of the temperature is quite significant. It is seen that an increase in the Grashof number results in a decrease in the temperature (Figure 11).

Figure 12 illustrates that an increase in the suction parameter results in a decrease in the temperature.

Table 1. Skin-friction coefficient C_f and Nusselt number Nu for Pr = 0.733.

B	γ	M	K	Gr	f_w	C_f	Nu
-0.4	4	1.0	0.5	5.0	0.5	1.1398	0.3009
-0.2	4	1.0	0.5	5.0	0.5	1.3508	0.3022
-0.4	2	1.0	0.5	5.0	0.5	0.8967	0.4102
-0.4	4	2.0	0.5	5.0	0.5	0.6051	0.2832
-0.4	4	1.0	1.0	5.0	0.5	0.8579	0.2917
-0.4	4	1.0	0.5	4.0	0.5	0.7108	0.2875
-0.4	4	1.0	0.5	5.0	1.0	1.0135	0.3415

The effects of the β, γ, M, K, Gr and f_w on the skin-friction coefficient and Nusselt number are shown in Table 1. It is seen that, as β or K or Gr increases, the skin-friction coefficient as well as the Nusselt number increases.

Also, as γ increases, the skin-friction coefficient increases, whereas the Nusselt number decreases. Further, as M increases, there is a fall in both the skin-friction coefficient and Nusselt number. It is observed that as f_w increases the skin-friction coefficient decreases, whereas the Nusselt number increases.

Acknowledgement

I would like to acknowledge Dr. N. Bhaskar Reddy, Professor of Mathematics, S.V.University, Tirupati (A.P), India for fruitful discussion on the subject of this paper.

REFERENCES

[1.] B. Gebhart, Transient natural convection from vertical elements, J. Heat transfer, 83Cs (1961), 61-70.

[2.] E.M.A. Elbashbeshy, Free convection flow with variable viscosity and thermal diffusivity along a vertical plate in the presence of the magnetic field, International Journal of Engineering Science, 38(2000), 207-213.

[3.] E.M.A. Elbashbeshy, F.N. Ibrahim, Steady free convection flow with variable viscosity and thermal diffusivity along a vertical plate, J. Phys. D. Appl. Phys. 26(1993), 2137-2143.

[4.] M. Hossain, S. Munir, Mixed convection flow from a vertical plate with temperature dependent viscosity, Int. J. Therm. Sci., 39(2000), 173-183.

[5.] F.N. Ibrahim, E.I. Ibrahim, Proc. Marh. Phys. Soc. Egypt No 57(1984), .145-57.

[6.] M.K. Jain, S.R.K. Iyengar, R.K. Jain, Numerical Methods for Scientific and Engineering Computation, Wiley Eastern Ltd., New Delhi, India(1985).

[7.] N.G. Kafoussias, E.W. Williams, The effect of temperature-dependent viscosity on free-forced convective laminar boundary layer flow past a vertical isothermal plate, Acta Mechanica, 110(1995), 123-137.

[8.] W.M. Kays, M.E. Grawford, Convective Heat and Mass Transfer, McGraw-Hill, New York (1980).

[9.] K.N. Mehta, S. Sood, Transient free convection flow with temperature dependent viscosity in a fluid saturated porous medium, Int. J. Eng. Sci., 30(1992),1083-1087.

[10.] S. Ostrach, An analysis of laminar free convection flow and heat transfer about a flat plate parallel to the direction of the generating body force, NACA Report-TR1111 (1953), 63-79.

[11.] E. Pohlhausen, Der Warmeaustausch zwischen festen korpen and Flussigkeiten mit Kleiner Reibung und Kleiner Warmeleitung, ZAMM, 1(1921), 115-121.

[12.] I. Pop, R.S.R. Gorla, M. Rashidi, The effect of variable viscosity on flow and heat transfer to a continuous moving flat plate, Int. J. Eng. Sci.,30(1992), 1-6.

[13.] A. Raptis, Flow through a porous medium in the presence of magnetic field, Int. J Energy Res., 10(1986), 97-101.

[14.] A. Raptis, C. Massalas, G. Tzivanids, Hydromagnetic free convection flow through a porous medium between two parallel plates, Phy. Lett.,90A (1982), 288-289.

[15.] H. Schlichting, Boundary Layer Theory, Mc Graw-Hill, New York (1968).

[16.] M.A. Seddek, F.A. Salama, The effects of temperature dependent viscosity and thermal conductivity on unsteady MHD convective heat transfer past an infinite porous moving plate with variable suction, J. Computational Materials Sci., 40 (2007), 186-192.

[17.] R. Seigel, Transient free convection from a vertical flat plate, J. Heat Transfer, 80 (1958), 347-359.

[18.] J.C. Slattery, Momentum, Energy and Mass Transfer in Continua. McGraw Hill, New York (1972).

ACTA TECHNICA CORVINIENSIS – Bulletin of Engineering

ISSN: 2067-3809 [CD-Rom, online]

ACTA TECHNICA CORVINIENSIS – Bulletin of Engineering
Tome VI (Year 2013) – FASCICULE 3 [July–September]
ISSN 2067–3809

[1.] Jozef PETRÍK, [2.] Jana KADUKOVÁ, [3.] Pavol PALFY, [4.] Dana IVÁNOVÁ, [5.] Hedviga HORVÁTHOVÁ

THE QUALITY OF pH MEASUREMENT PROCESS

[1-5.] TECHNICAL UNIVERSITY OF KOŠICE, FACULTY OF METALLURGY, DEPT. OF INTEGRATED MANAGEMENT, SLOVAKIA

ABSTRACT: The value of pH is an important quality control parameter measured in industry and research. The quality of the measurement process can be evaluated in the same manner as any manufacturing process. The aim of submitted work is to analyze the quality of pH measurement. MSA, analysis of uncertainty, t-test and ANOVA were used. Four appraisers measured pH of 10 solutions of HCl and HNO_3. The pH meter GRYF 208L with standard electrode THETA 90 HC 113 were used as measurement equipment. Analyzed the process of pH measurement is capable according to MSA. The fine discrimination and high accuracy of used equipment and high pH variability of measured solutions are reasons of high process capability. Low value of index %AV witness good competence of all appraisers. Positive effect of appraisers on the capability was confirmed by t-test and ANOVA.
KEYWORDS: measurement, pH, acids, capability, uncertainty

INTRODUCTION

The value of pH is an important quality control parameter used in metallurgy, chemistry, food processing, pharmaceutical production and environmental control. It is commonly measured by calibrated pH meters.

It is one of the most frequent and relatively simple measurement methods. Like in any test of material properties, there is an obvious requirement for reliability of measurement results, which is unthinkable without sufficient quality of the measurement process.

The quality of the measurement process can be evaluated in the same manner as any manufacturing process. The measurement process takes place in the measurement system. The aim of the measurement system in accordance with the standard STN EN ISO 10012:2004 [1] is to regulate hazard that the measurement equipment or measurement process could provide incorrect results. Incorrect results negatively affect the final quality of products followed by economic or moral damages (e.g. the loss of producer's image).

Although, from experience, we can suppose that confirmed measurement equipment will still be accurate at the end of confirmation status, there is an obvious danger of equipment misuse. The misuse can result from incorrect measurement method, measurement environment or incompetent appraisers.

Metrological confirmation comprises measuring equipment calibration and verification. Metrological confirmation shall be designed and implemented to ensure that the metrological characteristics of the measuring equipment meet the metrological requirements for the measurement process [1].

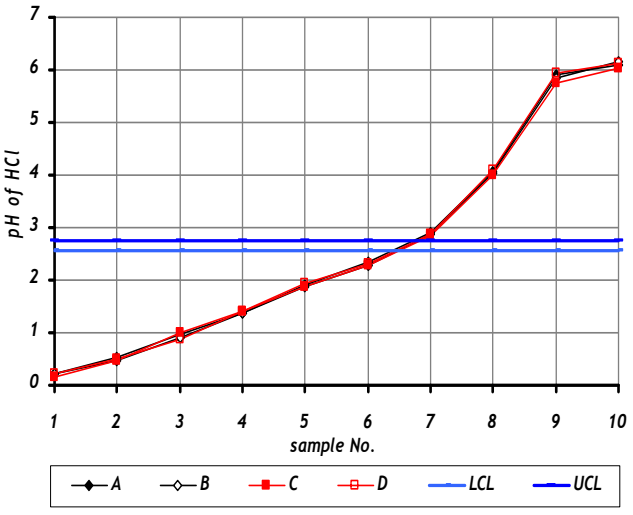

Figure 1.a: The average control chart, HCl

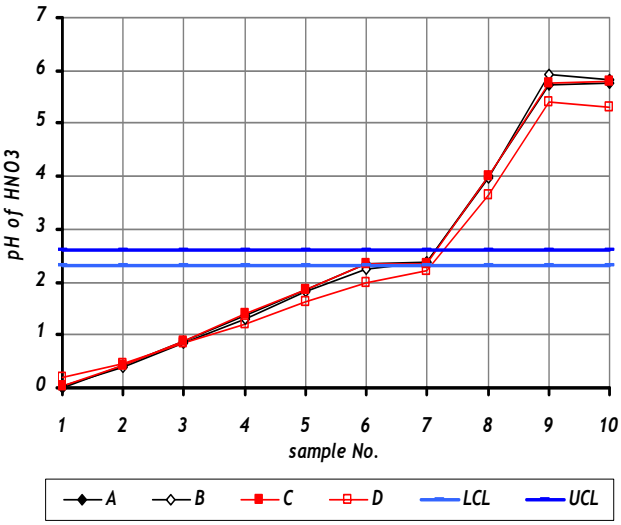

Figure 1.b: The average control chart, HNO3

Calibration is a set of operations that establish, under specified conditions, the relationship between values of quantities indicated by a measuring instrument or measuring system and the corresponding values realized by standards (certified reference materials CRM, buffers)[2].

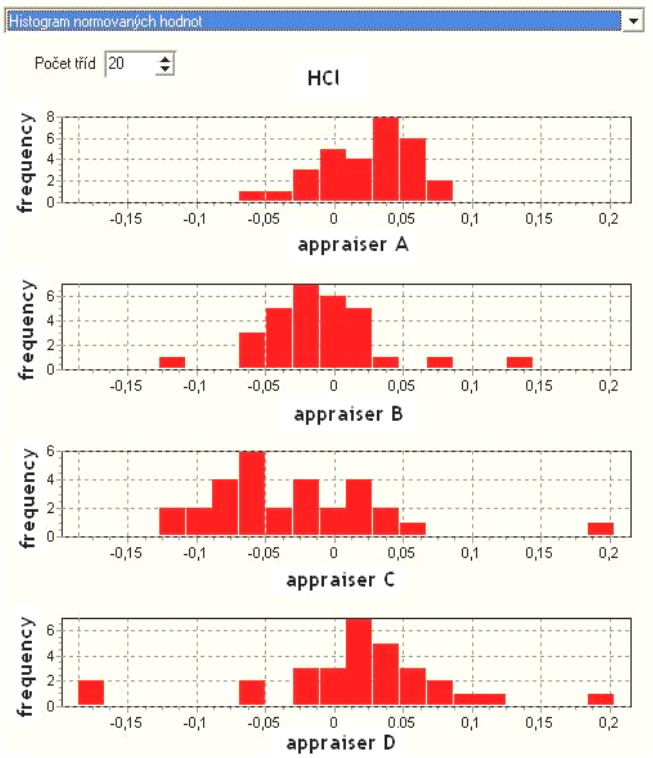

Figure 2.a. The normalized histogram, HCl

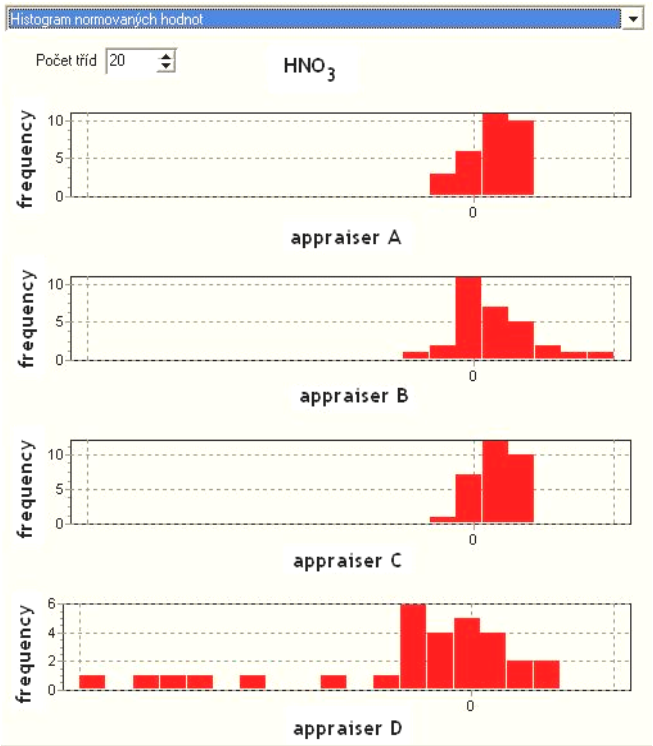

Figure 2.b. The normalized histogram, HNO_3

A perfect measurement would provide the true value of a quantity; nevertheless the true value is indeterminable in reality because a perfect measurement cannot be performed. The estimation of the true value is the finally corrected result. The measurement uncertainty is a parameter that characterizes the dispersion of the values that could reasonably be attributed to the result of measurement. Testing laboratories shall have and shall apply procedures for estimating uncertainty of measurement or calibration [3].

The aim of submitted work is to analyze the quality of pH measurement of water solutions of two acids (HCl and HNO_3) by evaluation of the measurement process capability by MSA method and by analysis of uncertainty. The results were validated using t-test and analysis of variance (ANOVA).

EXPERIMENTAL

The pH of ten samples with various HCl and HNO_3 concentrations prepared in agreement with calculation (calculated pH in Table 1 and Table 2) was measured by routine method by four appraisers (A, B, C, D) in 3 trials.

Table 1.a. The values of "measured pH", the standard deviation SD, statistical standard uncertainty u_A, normality, outliers and the error of repeatability r_{rel}. The values of pH, HCl.

	1	2	3	4	5
calculated pH	0	0.5	1.0	1.5	2.0
measured pH	0.198	0.489	0.947	1.383	1.908
SD of measured pH	0.039	0.042	0.085	0.041	0.039
u_A (n = 12)	0.011	0.012	0.025	0.017	0.011
normality (p)	0.076	0.369	0.014	0.323	0.418
outliers	1	0	0	0	0
r_{rel} (%)	75.6	24.5	40.1	9.4	5.8
	6	7	8	9	10
calculated pH	2.54	2.84	4.0	6.0	6.0
measured pH	2.307	2.875	4.045	5.863	6.111
SD of measured pH	0.039	0.073	0.057	0.100	0.071
u_A (n = 12)	0.011	0.021	0.016	0.029	0.021
normality (p)	0.052	0.106	0.513	0.526	0.214
outliers	0	1	0	0	0
r_{rel} (%)	4.8	9.4	4.4	5.3	3.8

Table 1.b. The values of "measured pH", the standard deviation SD, statistical standard uncertainty u_A, normality, outliers and the error of repeatability r_{rel}. The values of pH, HNO_3.

	1	2	3	4	5
calculated pH	0	0.5	1.0	1.5	2.0
measured pH	0.646	0.142	0.583	1.242	1.904
SD of measured pH	0.093	0.044	0.075	0.108	0.158
u_A (n =12)	0.027	0.013	0.022	0.031	0.046
normality (p)	0	0.004	0	0	0
outliers	0	1	1	1	1
r_{rel} (%)	40.3	41.0	35.0	31.3	32.1
	6	7	8	9	10
calculated pH	2.54	2.84	4.0	6.0	6.0
measured pH	2.288	2.333	3.942	5.708	5.675
SD of measured pH	0.217	0.069	0.237	0.267	0.302
u_A (n =12)	0.063	0.020	0.068	0.077	0.087
normality (p)	0	0	0	0.002	0
outliers	1	0	2	1	3
r_{rel} (%)	33.2	9.0	21.7	19.1	19.2

The pH meter GRYF 208L (the range of measurement 0-14 pH, range of adjustment N (for pH 7) ± 1.8 pH, range of adjustment S (for pH 4) ± 0,8 pH, the accuracy of measurement ± 0.01 pH ± 1 dig. with

standard electrode THETA 90 HC 113 were used as measurement equipment. The equipment was in accordance with standard STN 99 9000:1997 [4]. Two working buffers - reference materials with a nominal value pH 7 and pH 4 were used for calibration. The temperature of samples varied in range 24.1-26.1°C for HCl and 26.2-27.5°C for HNO_3. The temperature 25°C was designated for adjustment and calibration of equipment.

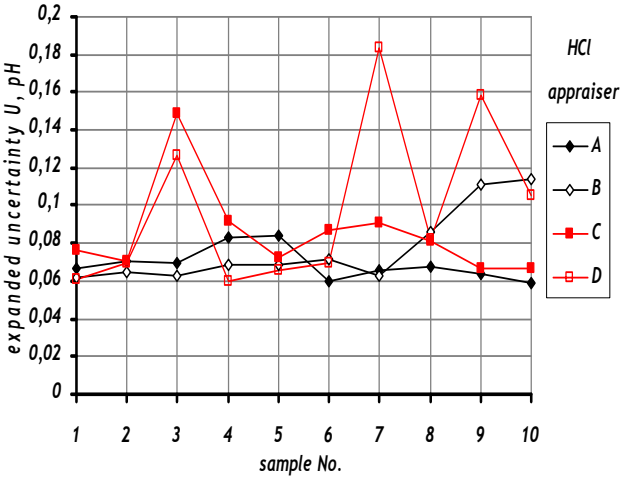

Figure 3a. The expanded uncertainty U of particular appraisers, HCl

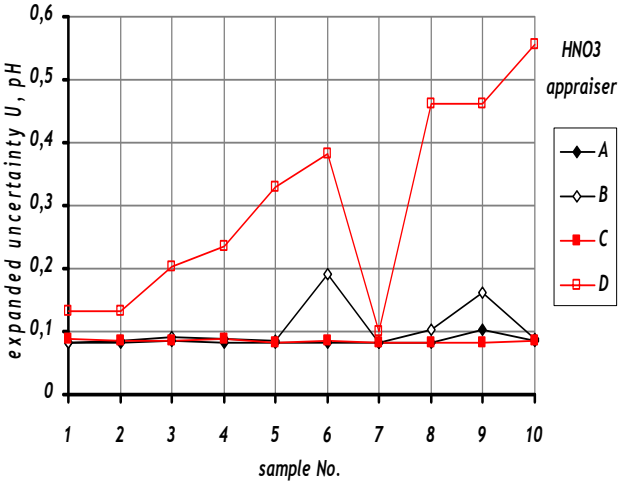

Figure 3b. The expanded uncertainty U of particular appraisers, HNO_3

The Measurement Systems Analysis (MSA) was originally designed for the engineering industry. If is used outside its intended scope - in chemical analysis, it is needs to regard the peculiarities of both areas with a different approach, traditions and object of interest (the part in engineering - a solution in chemistry).

MSA is not standardized yet but is recommended in the reference manuals for the automotive industry. It helps to conform with ISO/TS 16 949:2009 [5] requirements, as well as AIAG standards. MSA is an experimental and mathematical method of determining how much the variation within the measurement process contributes to the overall process variability. If the analyzed measurement system (consists of measurement equipment, parts, environment, method, appraisers…) is capable, it is likely that the measurement process, taking place in it is capable, as well. The capability is the ability of the system or process to realize a product that will fulfill the requirements for that product.

The analysis of variance (ANOVA) is one of MSA methods. Its advantages are that it is capable of handling any experimental set-up, can estimate the variance accurately and extracts more information from the experimental data. The disadvantages are the complex numerical computations and users required to have a certain degree of statistical knowledge to interpret the results. Simpler method of MSA, GRR (gauge repeatability and reproducibility) is an approach which will provide an estimate of both repeatability and reproducibility for a measurement system.

This approach will allow the measurement system's variation to be decomposed into two separate components, repeatability and reproducibility. However, variation due to the interaction between the appraiser and the part/gage is not accounted for in the analysis [6].

The calculation of capability by GRR method was carried out in accordance with [6] using the software Palstat CAQ (significance level α = 0.01 and confidence level α = 0.01 ≈ 5.15 σ).

The uncertainty of measured pH values was calculated in accordance with the standard [4]

$$u = \sqrt{u_A^2 + u_{\Delta s}^2 + u_{\Delta pHi}^2 + u_z^2} \qquad (1)$$

The values in Table 1 are the results of all 3 trials of all 4 appraisers (number of measurements n = 12). The "measured pH" is the average value of 3 trials of all 4 appraisers, "SD of measured pH" is the standard deviation of 3 trials of all 4 appraisers. The first source of uncertainty is statistical uncertainty u_A, calculated by formula (2); n = 3 for 3 trials of particular appraiser or n = 12 for 3 trials × 4 appraisers.

$$u_A = \frac{SD}{\sqrt{n}};\ n = 12 \qquad (2)$$

$u_{\Delta s}^2$ *- function of the difference between the measured value of pH and value of pH of calibration*

$$u_{\Delta s}^2 = \frac{\Delta s(\ pH - pH_s\ )}{s \cdot \chi} \qquad (3)$$

$\Delta s, s$ *- functions of temperature, listed in the standard [4]*

pH *- average pH (3 trials)*

pHi *- pH of certified reference material (buffer)*

$\chi = \sqrt{3}$ *for assumed rectangular distribution.*

$$u_{\Delta pHi} = \frac{\Delta pHi\,\alpha(t - \Theta)}{s \cdot \chi} \qquad (4)$$

$\Delta pHi \approx 4$ *for ordinary pH-meter and glass electrode*

α = 0.1984 mVK^{-1}

t *- temperature of measurement*

Θ *- temperature of calibration*

s *- function of temperature, listed in standard, [4]*

$\chi = \sqrt{3}$ *for assumed rectangular distribution.*

The source of uncertainty that is not specified in the standard [4] is connected with discrimination (resolution) δ_z = 0.01 pH of used pH meter [7].

$$u_z = \delta_z \cdot 2\sqrt{3} = 0.29\delta_z \quad (5)$$

The effort devoted to determining other eventual sources of measurement uncertainties was proportional to the importance of the measurement results. Their detailed determination is unjustifiable on technical grounds.

Expanded uncertainty

$$U = u \times k \quad (6)$$

The coverage coefficient k = 2

The uncertainties and coverage factors could be calculated using other methods [7], as well.

r_{rel} is relative repeatability (the error of repeatability)

$$r_{rel} = \left(\frac{pH_{max} - pH_{min}}{AVER} \right) \times 100\% \quad (7)$$

RESULTS AND DISCUSSION

The error of repeatability is inversely proportional to pH. The value of error for HNO_3 is higher than that for HCl.

The normality was determined by Freeware Process Capability Calculator software, using Anderson - Darling test ($p \geq 0.07$ for a file with a normal distribution). The standard methods of MSA assume normal probability distribution. If normality of the file is not confirmed, the measurement system error is overestimated. The statistical outliers would indicate that the process is suffering from special causes (disturbances) and is out of statistical control.

The normality and the outliers were evaluated for files, involving the results of all measurements of one sample (n = 12). On one hand, all files of HCl have a normal distribution an only two files contain outliers; on the other hand, the normality was not confirmed for all files of HNO_3 and eight samples contained 1-3 outliers (Table 1, Table 2).

The first step of MSA is the analysis of the equipment resolution - to estimate whether the discrimination (the value of the smallest scale graduation of equipment) is sufficient.

A general rule of thumb is that the discrimination ought to be at most one tenth of the process variation [6]. If we compare the value of discrimination δ_z = 0.01 pH with values of standard deviation ("SD of measured pH", Table 1), the resolution of used equipment is terminal.

The measurement system ought to be under statistical control before capability is assessed. The process is under control if all ranges are between control limits of the range control chart. If one appraiser is out of control, the method used differs from the others (appraiser D). The average control chart (X-bar control chart) provides an indication of "usability" of the measurement system. The area within the control limits represents the measurement sensitivity ("noise"). If one half or more of the averages falls outside the control limits, then the measurement system should be considered adequate to detect variation between the levels of pH. Analyzed system has sufficient sensitivity - all measurements for HCl and 87.5 % measurements for HNO_3 are outside the control limits (Figure 1).

Table 2. a. The paired t-test comparing the means of two groups - the average value of pH measured by particular appraiser and "measured pH" - average value of 4 appraisers.HCl, p - values.

appraiser	1	2	3	4	5
A	0.2546	0.0912	0.6176	0.7193	0.6473
B	0.8319	0.2212	0.6038	0.372	0.3415
C	0.06	0.3393	0.2691	0.7313	0.4954
D	0.4387	0.0001	0.2548	0.3508	0.2474
	6	7	8	9	10
A	0.3367	0.5346	0.4524	0.3591	0.7357
B	0.6013	0.9477	0.7533	0.6412	0.2241
C	0.2886	0.6896	0.1374	0.1075	0.1199
D	0.4315	0.8373	0.2667	0.2774	0.5933

Table 2. b. The paired t-test comparing the means of two groups - the average value of pH measured by particular appraiser and "measured pH" - average value of 4 appraisers. HNO_3, p - values.

appraiser	1	2	3	4	5
A	0.2649	0.9259	0.5607	0.4153	0.4413
B	0.018	0.3188	0.6151	0.8693	0.7061
C	0.5087	0.8785	0.6364	0.3642	0.5145
D	0.0145	0.4109	0.6854	0.2185	0.1608
	6	7	8	9	10
A	0.3508	0.3245	0.4939	0.8452	0.6057
B	0.9248	0.3261	0.6171	0.1926	0.3943
C	0.4172	0.5763	0.4797	0.7494	0.5226
D	0.1317	0.0265	0.1362	0.1271	0.1123

Table 3. A paired t-test comparing the means of two groups - the average value of pH measured by particular appraiser, p values.

appraiser	HCl			HNO_3		
	A	B	C	A	B	C
B	0.0496	-	-	0.8832	-	-
C	0.0165	0.3280	-	0.5377	0.8376	-
D	0.6625	0.1048	0.1046	0.0170	0.0322	0.0179

The number of distinct categories ("ndc", based on Wheeler's discrimination ratio) is connected with the resolution of equipment. It indicates the number of various categories, which can be distinguished by the measurement systems. It is the number of non-overlay 97 % confidence intervals, which cover the range of expected variability of product.

The ndc ≥ 5 for capable processes, the processes with ndc between 2-5 may be conditionally used for rough estimations. Ndc for HCl is 48.6 and for HNO_3 is 20.5. Value of ndc and analysis of the average control chart demonstrate sufficient sensitivity of the measurement system for variability of measured value.

%EV index represents cumulative influence of measurement equipment, measuring method and environmental conditions on the variability. It is a function of average range of trials of all appraisers. The value of %EV is 2.69 % for HCl and 4.9 % for HNO_3.

Whereas standardized measurement method and equipment with valid confirmation status were used,

only the resolution of equipment and the environment (variation of ambient temperature) could affect the value of %EV index.
%AV index represents the influence of appraisers on the variability. It is a function of the maximum average appraiser difference. The value of %AV is 1.15 % for HCl and 4.78 % for HNO_3. Low value of index confirms competence of appraisers.
%GRR index represents the process capability in practice. For acceptable measurement system %GRR < 10 %, %GRR > 30 % is considered not acceptable.
Analyzed measurement system and also the process carried out within it are acceptable - capable because %GRR is 2.90 % for HCl and 6.85 % for HNO_3.
%PV index is a function of the range of the pH values of particular samples. It is sensitive to variability between samples pH. The value of %PV indirectly defines suitability of equipment for specific measurement. %PV above 99 % suggests extremely accurate, above 90 % suitable, above 70 % satisfactory and above 50 % inaccurate equipment. Because %PV is 99.96 % for HCl and 99.77 %, for HNO_3, used equipment is extremely accurate for both acids in respect of variability between the pH of samples.
Normalized histogram - histogram plot is a graph that displays the frequency distribution of the gage error of appraisers who participated in the study.
The graph provides a quick overview how the error, i.e. difference between an observed value and reference value (samples average) is distributed. As can be seen in Figure 2a, the differences of bias (systematic error - the difference between the peak of histogram peak and zero) and variability (random error - the width of histogram) between appraisers for all measurements are negligible for HCl. The results of appraiser B have minimum variability and are best centered. As can be seen in Figure 2b, the differences between appraisers A-B-C are low, the variability of appraiser D is superior to others in the measurement of HNO_3.
As far as the analysis of uncertainty, the relation between the average value of pH and expanded uncertainty U of the result is ambiguous and depends on appraisers, Figure 3. The uncertainty moderately increases with increasing of "measured pH" (Table 1) for appraises B, D and decreases for appraisers A, C in measurement of HCl. It also moderately increases with increasing of "measured pH" for appraises A, B, C and intensively increases for appraiser D in measurement of HNO_3.
A paired t-test comparing the means of two groups (significance level $\alpha = 0.01$) was used for evaluation of particular appraisers quality e. i. difference between the values of particular appraiser and "measured pH" - average value of 4 appraisers (Table 1). The difference is statistically significant for $p \leq 0.05$. Table 2 summarizes that except for one sample of HCl (appraiser D) and three samples of HNO_3 (two appraiser D, one appraiser B) the differences were not statistically significant. It confirms low value of %AV index as well as low difference between competence of particular appraisers.
The comparison of the average pH values of particular appraisers by paired t-test (3 trials, all samples) are in Table 3. The differences are statistically significant between appraisers A-B and A-C are for HCl and between appraiser D and others appraisers for HNO_3.
According to a single factor analysis of variance (ANOVA) the influence of appraiser on the measured values of pH is not statistically significant for both acids ($p = 0.9999$ for HCl and 0.9955 for HNO_3).
Four appraisers measured the pH of distilled water H_2O and five water solutions: hydrochloric acid HCl, sodium hydroxide NaOH, sodium bicarbonate $NaHCO_3$, acetic acid CH_3COOH and citric acid $C_6H_8O_7$ by routine method in accordance with standard [4], the capability of the process was comparable to abovementioned results (%GRR = 6.44 %) [8].
The capability of pH measurement is better than that of comparable measurement processes as a rule. For example, measurement process of foundry sand properties (compression strength RC2, shearing strength RT2 and mold permeability) was analyzed. It was capable of permeability (%GRR = 7.47 %) but not acceptable for RC2 (%GRR = 37.9 %) and conditionally acceptable for KT2 (%GRR = 23.49 %) [9].

CONCLUSIONS

1. Analyzed process of pH measurement is capable of both acids.
2. The fine discrimination (scale interval) and high accuracy of used equipment, high pH variability of measured solutions are reasons of high process capability.
3. Low value of index %AV proves good competence of all appraisers.
4. The influence of final pH and appraiser on expanded uncertainty of the results of measurement is inexpressive.
5. The t-tests and ANOVA confirmed minor influence of appraiser on the result of measurement.
6. The results of appraiser D show some distance from the results of others appraisers.
7. The lower capability of the measurement process of HNO_3 can be affected be other than normal probability distribution of the results.

ACKNOWLEDGEMENTS

This work was supported by the Slovak Grant Agency for Science VEGA 1/0672/10 and 1/0134/09

REFERENCES

[1.] ISO 10 012:2003, Measurement management systems - Requirements for measurement processes and measuring equipment.
[2.] International Vocabulary of Basic and General Terms in Metrology, ISO, Geneva, 1993.
[3.] ISO/IEC 17025:2005, General requirements for the competence of testing and calibration laboratories.
[4.] STN 99 9000:1997, Meranie pH vo vodných prostrediach (in Slovak).
[5.] ISO 16 949:2009, Quality management systems. Particular requirements for the application of ISO 9001:2008 for automotive production and relevant service part organizations.
[6.] Measurement systems analysis (MSA), 4th edn. Chrysler Group LLC, Ford Motor Company, General Motors Corporation, 2010.

[7.] Dietrich, E.: Es geht auch einfach. Messunsicherheit in Analogie zur Prüfmittelfähigkeit bestimmen, QZ Magazine, No. 3, Vol. 46, 2001, p. 264 (in German).

[8.] Petrík, J. Kaduková, J.: The capability of pH measurement process, Transaction of the Universities of Košice, No. 2, Vol. 20, 2010, p. 44

[9.] Petrík, J. - Gengeľ, P.: The capability of green sand mold strength and mold permeability process. Acta Metallurgica Slovaca, No. 2, Vol. 15, 2009, p. 86.

ISSN: 2067-3809 [CD-Rom, online]

ACTA TECHNICA CORVINIENSIS – Bulletin of Engineering
Tome VI (Year 2013) – FASCICULE 3 [July–September]
ISSN 2067–3809

[1.] Gunjan CHUGH

IMAGE STEGANOGRAPHY TECHNIQUES: A REVIEW ARTICLE

[1.] BANASTHALI VIDYAPITH, RAJASTHAN, INDIA

ABSTRACT: In today's world, since the rise of internet most of the communication and information sharing is done over the web. With the increasing unauthorized access of confidential data, information security is of utmost importance. Thus, a big issue now a day is to reduce the chances of information detection during transmission. Cryptography deals with encryption of message but its presence arouse suspicion about the communication, on the other hand, Steganography hides the existence of message in such a way that no one can even guess about the communication going on between two parties. Due to rapid development in both computer technologies and Internet, the security of information is regarded as one of the most important factors of Information Technology and communication. A large variety of Steganographic techniques exists for hiding data in digital images. In this paper, an overview on Steganography is presented and it also covers different existing techniques on Image Steganography and their relative strong and weak points. Steganography benefits and applications are also discussed.
KEYWORDS: Cover Image, Stego Image, Cryptography, Steganography

INTRODUCTION

Most of the time, users on the internet have to send, share or receive confidential information [1].

Due to rapid development in both computer technologies and Internet, the security of information is regarded as one of the most important factors of Information Technology and communication. Attacks on confidential data, unauthorized access of data have crossed the limits. Accordingly, we need to take measures which protect the secret information [2,3]. Steganography has emerged as a powerful and efficient tool which provides high level for security particularly when it is combined with encryption [4]

The general idea of hiding some information in digital content has a wider class of applications that go beyond steganography. The techniques involved in such applications are collectively referred to as information hiding. Two special cases of information hiding include digital watermarking and Fingerprinting. Watermarking can be used to provide copyright protection by extending the cover source with some extra information which can later be extracted and can be used for variety of purposes like copyright protection and control.

Digital watermarking has become an active and important area of research, and development and commercialization of watermarking techniques is being deemed essential to help address some of the challenges faced by the rapid proliferation of digital content [5].

In Fingerprinting, different customers are given different and specific marks embedded in the copies of their work. It helps to identify those customers who violate the licensing agreement when they transmit property to other groups illegally [4].

Steganography vs Cryptography

It is often thought that communications may be secured by encrypting the traffic, but this has rarely been adequate in practice [6]. Cryptography deals with the encryption of text to form cipher (encrypted) text using a secret key. However, the transmission of cipher text may easily arouse attackers suspicion, and the cipher text may thus be intercepted, attacked or decrypted violently. In order to overcome the shortcomings of cryptographic techniques, an important sub-discipline of information hiding i.e Steganography has been developed as a new covert communication means in recent years. It transfers message secretly by embedding it into a cover medium with the use of information hiding techniques [7].

Steganography, hides the existence of message such that intruder can't even guess that communication is going on and thus provides a higher level of security than cryptography. Both cryptographic and steganographic systems provide secret communications, but they are different in terms of system breaking. If the intruder can read the secret message, then a cryptographic system is broken. However, a steganographic system is considered broken if the intruder can detect the existence or read the contents of the hidden message.

If the intruder suspects a specific file or steganography method even without decoding the message, a steganographic system will be considered to have failed. Thus, steganographic systems are

more fragile than cryptography systems in terms of system failure. [8]

Steganography

The word Steganography comes from the Greek origin, means "concealed (covered) writing". The word 'steganos' means "covered or protected" and 'graphie' means "writing" [9]. Steganography is thus, not only the art of information hiding, but also the art and science of hiding the fact that communication is even taking place.[10]

Due to the prohibition and restriction imposed by the government on cryptographic systems, Steganographic technologies are a very important part of the future of Internet security and privacy on open systems such as the Internet. Thus, Steganographic research is thus, primarily driven by the lack of strength in the cryptographic systems on their own and the desire to have complete secrecy in an open-systems environment.

Steganography hides secret data in another file in such a way that only the recipient knows that such a message even exists. Neither Cryptography nor Steganography are sufficient, but using both technologies together can add multiple layers of security and provides a very acceptable amount of privacy for anyone connecting to and communicating over these systems. [11]

The goal of steganography is to avoid drawing suspicion to the transmission of the secret message. On other hand, steganalysis is a way of detecting possible secret communication using against steganography. That is, steganalysis attempts to defeat steganography techniques. It is based on the fact that hiding information in digital media alters the carriers and introduces unusual signatures or some form of degradation that is visible to the human eye. Thus, it is crucial that a steganography system to ascertain that the hidden messages are not detectable [7].

Reasons for rapid growth of interest in Steganography

1.) Restrictions imposed on the availability of encryption service by various governments have encouraged people to take a move towards the methods through which messages can be embedded in cover sources.

2.) Publishing and broadcasting industries have become interested in techniques for hiding encrypted copyright marks and serial numbers in digital films, audio recordings, books and multimedia products

STEGANOGRAPHY HISTORY

Information hiding is a science which dates back to 1499, and it has long history. It has been used in various forms for 2500 years. It has found use in military, diplomatic, personal, spies, ruler, governments etc. Steganography has been widely used, including in recent historical times and the present day. Some known examples include:

□ ***Past***

Early steganography was messy. Before phones, before mail, before horses, messages were sent on foot. If you wanted to hide a message, you had two choices: have the messenger memorize it, or hide it on the messenger. While information hiding techniques have received a tremendous attention recently, its application goes back to Greek times.

- according to Greek historian Herodotus, the famous Greek tyrant Histiaeus, while in prison, used unusual method to send message to his son-in-law. He shaved the head of a slave to tattoo a message on his scalp. Histiaeus then waited until the hair grew back on slave's head prior to sending him off to his son-in-law. Herodotus provides the first records of steganography in Greece [13].
- to communicate Greeks would etch the message they wished to send into the wax.
- coating of a wooden tablet. The tablet would then be transported to the recipient who would read the message, then re-melt the wax to etch their reply. In order to communicate in secret, the army would remove the wax completely, carve the secret message into the wood, and re-coat the tablet with wax [13].
- Messages were also written on envelopes in the area covered by postage stamps to avoid the possible detection of the message.

□ ***Present***

In today's generation, as most of the people often transmit images, audio over the internet, so most of the Steganographic system's uses multimedia objects like image, audio and video as cover sources to hide the confidential data [14]. So, on the basis of this, steganography is divided into four categories:

1. Text Steganography
2. Image Steganography
3. Audio/Video Steganography
4. Protocol Steganography

□ ***Future***

Steganalysis can be defined as process to crack the cover object in order to get the hidden data. In general terms, it is known as Hacking i.e. unauthorized access of data during transmission. Future perspective of steganography lies on combining steganography with cryptography to achieve a higher level of security such that even if intruder detects the hidden message, he/she will not be able to decode it [14] .

STEGANOGRAPHY CLASSIFICATION

When we talk of digital steganography, we mean to say that, digital media's like Image, Audio /Video, Protocol are used as innocent covers for hiding secret confidential messages.

Almost all digital file formats can be used for steganography, but the formats that are more suitable are those with a high degree of redundancy. Redundancy can be defined as the bits of an object that provide accuracy far greater than necessary for the object's use and display [16]. The redundant bits of an object are those bits that can be altered without the alteration being detected easily [6]. Image and audio files especially comply with this requirement, while research has also uncovered other file formats that can be used for information hiding. Figure 1 shows the four main categories of file formats that can be used for steganography. [2]

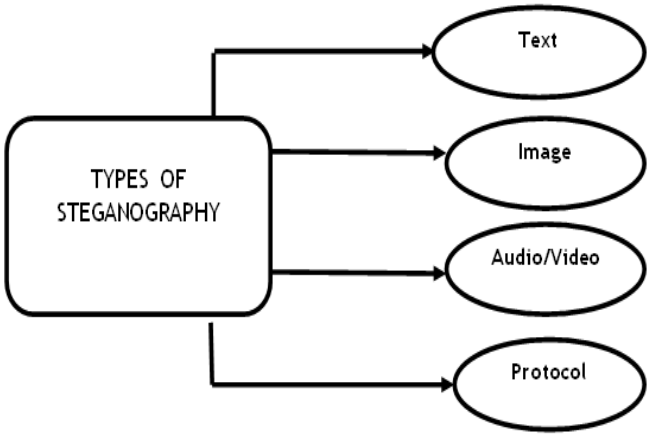

Figure 1: Classification of different types of Steganography

- ***Hiding information in text:***

Information can also be hidden in text files. The most popular method was to hide a secret message in every nth letter of every word of a text message [2]. A variety of different techniques exist of hiding data in text files. Text steganography using digital files is not used very often since text files have a very small amount of redundant data.

- ***Hiding information in images:***

Images are very popular cover source for digital steganography because of the large amount of redundant bits present in the digital representation of an image. This paper will focus on hiding information in images in the next sections.

- ***Hiding Information in Audio Files:***

Audio files can also be used for hiding secret data. One different technique unique to audio steganography is masking, which exploits the properties of the human ear to hide information unnoticeably. A faint, but audible, sound becomes inaudible in the presence of another louder audible sound [2].This property creates a channel in which to hide information.

The larger size of meaningful audio files makes them less popular to use than images [17].

- ***Hiding Information in Protocols:***

The term protocol steganography refers to the technique of embedding information within messages and network control protocols used in network transmission [16]. In the layers of the OSI network model there exist covert channels where steganography can be used [19].

An example of where information can be hidden is in the header of a TCP/IP packet in some fields that are either optional or are never used. A paper by Ahsan and Kundur provides more information on this.[18, 2]

IMAGE STEGANOGRAPHY

The standard concept of "What You See Is What You Get (WYSIWYG)" which we encounter sometimes while printing images does not always hold true. Images can be more than what we see with our Human Visual System (HVS); hence, they can convey more than merely 1000 words [20].

The confidential data that is embedded should be of adequate quality in order to make it imperceptible and indecipherable.

In addition, the technique employed should facilitate the use of a high payload by the diligent embedding of more data in a given cover image [21].

BASIC CONCEPT

Steganography is a two-step process:

- *Step 1) Creating a stego image which is a combination of message and carrier*
- *Step 2) Extracting the message image from the stego image.*

Variations are in the techniques that are used to generate the stego image using the carrier and the message image. [21]

On the sender side, a Cover image is selected and then message is hidden using a secret key and message embedding algorithm. Secret key is basically used to find out the pseudorandom pixel locations where the data will be hidden. Secret key is to be shared between sender and receiver.

Thus, it works as password such that even if someone breaks the algorithm then also the message can't be extracted until he/she knows the secret key. Stego image is obtained as output (as shown in Figure 2).

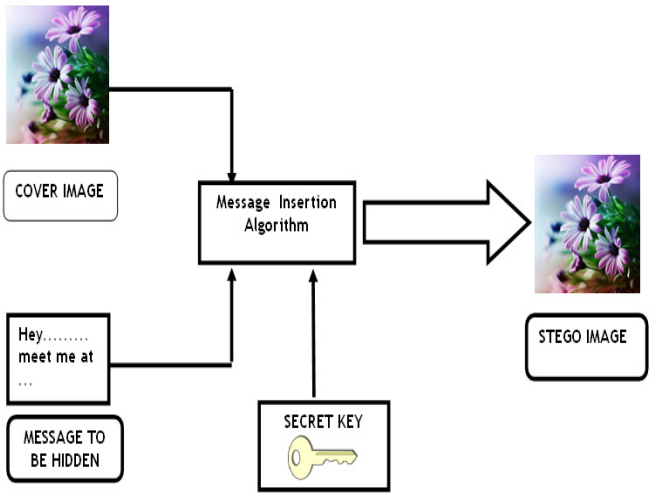

Figure 2: Image Steganography : Message Insertion

On the receiver side, Stego image is taken as input and by using the same secret key and message retrieval algorithm, message is extracted(as shown in Figure 3).

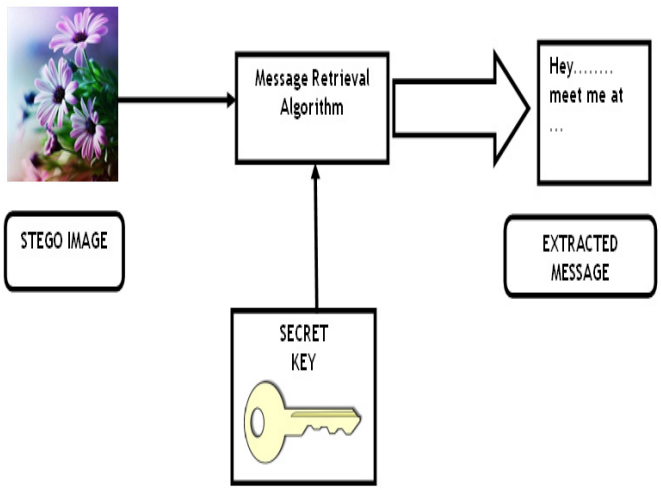

Figure 3: Image Steganography : Message Retrieval

FACTORS AFFECTING A STEGANOGRAPHIC SYSTEM

The effectiveness of any Steganographic method can be visualized by comparing Stego Image (Image after inserting message) with the Cover Image (Image before message insertion). Thus, some factors that determines how efficient and powerful a technique is are as follows:

1.) ***Robustness**: Robustness refers to the ability of embedded data to remain intact if the stego-image undergoes transformations, such as linear and non-linear filtering, addition of random noise, sharpening or blurring, scaling and rotations, cropping or decimation, lossy compression [8].*

2.) ***Imperceptibility**: The invisibility of a steganographic algorithm is the first and foremost requirement, since the strength of steganography lies in its ability to be unnoticed by the human eye. The moment that one can see that an image has been tampered with, the algorithm is compromised[22]*

3.) ***Payload Capacity**: It refers to the amount of secret information that can be hidden in the cover source. Watermarking, needs to embed only a small amount of copyright information, on the other side, steganography aims at hidden communication and therefore requires sufficient embedding capacity [22].*

4.) ***PSNR (Peak Signal to Noise Ratio)**: It is the ratio between the maximum possible power of a signal and the power of corrupting noise that affects the fidelity of its representation [23, 24]. This ratio is often used as a quality measurement between the original and a compressed image. The higher the PSNR, the better the quality of the compressed image.*

5.) ***MSE (Mean Square Error)**: Mean Squared Error is the average squared difference between a reference image and a distorted image. An Image steganography technique is efficient if it gives low MSE. It is computed pixel-by-pixel by adding up the squared differences of all the pixels and dividing by the total pixel count [25].*

6.) ***SNR (Signal to Noise Ratio)**: It compares the level of a desired signal to the level of background noise. It is defined as the ratio of signal power to the noise power [26].*

7.) ***NCC (Normalized Cross-Correlation)**: Normalized cross-correlation can be used to determine how to register or align the images by translating one of them. NCC is one of the methods used for template matching, a process used for finding incidences of a pattern or object within an image[27]*

8.) ***BER (Bit Error Rate)**: The bit error rate or bit error ratio (BER) is the number of bit errors divided by the total number of transferred bits during a studied time interval [28].*

IMAGE STEGANOGRAPHY CLASSIFICATION

There are two popular schemes used for image steganography (shown in Figure 4): spatial domain embedding and transform domain embedding. Most of the steganographic techniques either use spatial domain or transform domain to embed the secret message [21].

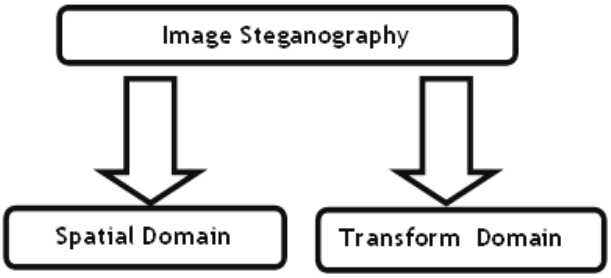

Figure 4: Image Steganography Classification

□ ***Spatial Domain***

In spatial domain scheme, the secret messages are embedded directly [10]. It embeds information in the intensity of the pixels [3]. We try to find out some areas or data that can be modified without having any significant effects on this cover file (Cole, 2003). Therefore, a secret message can be embedded by replacing the redundant or insignificant parts of a cover file with secret message bits, without adding any significant noise to this cover file (Kipper, 2004). [10]. The Least Significant Bit (LSB) substitution is the most commonly used spatial domain technique. In LSB substitution technique the least significant bit of each pixel of the cover is replaced by the secret message bits. Hiding images using LSB substitution techniques can be found in [21].

□ ***Transform Domain***

Transform Domain embeds information in frequency domain of previously transformed image [3]. Transform (frequency) domain techniques hide secret data in significant parts of the cover file. Therefore, frequency domain techniques are considered more robust to attacks than spatial domain techniques. Hence, most of robust steganographic systems known today rely on frequency domain techniques. There are many transforms used to map a signal into the frequency domain.

Discrete cosine transform (DCT), discrete wavelet transform (DWT), and discrete Fourier transform (DFT) are methods used as mediums to embed secret data in digital images. However, when we add a slight noise or secret data to some frequency domain components, it changes the whole image rather than changing only this part of the image. Thus, secret and embedded data will be spread across the entire image and will not be concentrated on one certain area or region [10].

DIFFERENT IMAGE STEGANOGRAPHY TECHNIQUES

□ ***LSB (Least Significant Bit) method** [8, 29, 30]*

It is one of the most common and easiest methods for message hiding. In this method, message is hidden in the least significant bits of image pixels .Changing the LSB of the pixels does not introduce much difference in the image and thus the stego image looks similar to the original image. In case of 24-bit images three bits of pixel can be used for LSB substitution as each pixel has separate components for red, green and blue.

Advantages:

1.) Simplest and easiest to implement.

2.) Chances of message insertion are 100%.

Drawbacks:

1.) *Not vulnerable to different attacks.*
2.) *Intruder can easily guess and change the LSB's of the image pixels, thus original message gets destroyed.*
3.) *Causes some distortion in the original image*
4.) *Scaling, rotation, cropping, addition of noise, or lossy compression to the stego-image will destroy the message*

□ ***Masking and Filtering*** *[8,29,30]*

Basically, this method is used for 24-bit and grey scale images. It is similar to placing watermarks on the image. Steganography only hides the information where as watermarks becomes part or attribute of the image. This method is more robust than LSB in terms of some image processing like - compression, cropping which makes it suitable in lossy JPEG images. Masking images involves changing the luminance of the masked area.

Advantages:

1.) Immune to image manipulation
2.) Robust technique

Drawbacks:

This method is mostly used for only 24 bit and grey scale images.

□ ***Parity Checker Method*** *[31]*

In this method, concept of even and odd parity is used. '0' is inserted at pixel value when it contains odd parity i.e. no. of 1's in the binary value of pixel must be odd Similarly, '1' is inserted at pixel value if it contains even parity i.e. no. of 1's in the binary value of the pixel must be even. If the corresponding parity does not exist at pixel location for 0 or 1 then it is made by adding or subtracting 1from the pixel value. For retrieval of message, if odd parity is present, then '0' is the message bit and if even parity is present, then '1' is the message bit.

Advantages:

1.) *Increases chances of message insertion.*
2.) *Steganalysis is difficult because whole pixel is used instead of particular bits as used by LSB method.*
3.) *Difference between cover image and stego image is difficult to be observed by naked eye.*

Drawbacks:

1.) *If intruder changes the LSB, then parity also changes and thus the method fails.*
2.) *In some situations when odd or even parity not present, then it can be made by both +1 or -1. So, it creates confusion, which one to choose.*

□ ***Gray Level Modification (GLM)*** *[15]*

In this technique, gray level values of the image pixels are modified. It provides one-to one mapping between the binary data and the selected pixels in an image. A set of pixels are selected from the image. First, all odd selected pixels are made even by changing gray level by one unit. Then, a comparison is made by selecting first bit from the message and first bit of the pixel.

If the first bit is even (0) then all pixels have even gray level and are not modified at all. But if the first bit is odd (1) then gray level of the pixel is decremented by one unit to make its value odd. Thus, Gray Level of all the pixels is modified accordingly.

Advantage:

Effective method as it can store as many bits as the size of the image

Drawback:

If LSB is damaged or changed by the intruder, then there is no concept of odd or even pixels and the method no longer works.

□ ***Pixel value Differencing (PVD) technique*** *[32]*

In this method, Wu & Tsai, selected two consecutive pixels for embedding the message. By checking the difference between two consecutive pixels ,payload of Wu and Tsai method is determined and it serves as basis to find out whether the two pixels belongs to an edge area or smooth area.

If the difference is large, it means pixels belong to an edge area and more secret data can be embedded at this location. On the other hand, if difference is small, it means pixels belong to smooth area and less secret data can be embedded at this place.

If the original difference value is unequal to the secret message, then the two consecutive pixels are directly adjusted so that the difference value can stand for the secret data [34].

Advantages:

1.) *Works better than LSB which directly embed secret data without considering the difference between the two pixels.*
2.) *Stego images produced are very much similar to the original image.*

Drawbacks:

1.) *Considerable stego image distortion can occur when the PVD method adjusts the two consecutive pixels in order to hide the secret data in the difference value.*
2.) *Falling off boundary problem may occur when the two consecutive pixels are located in extreme edge or smooth areas or when the values of two consecutive pixels form a contrast.*

□ ***Algorithms and Transformations***

This technique hides data in mathematical functions that are often used in compression algorithms. The idea of this method is to hide the secret message in the data bits in the least significant coefficients [33]. The advantage that JPEG images have over other formats is Compression. Using JPEG compression methods, high color quality images can be stored in relatively small files. JPEG images use the discrete cosine transform to achieve compression [29]. In addition to DCT, images can be processed with fast Fourier transformation and wavelet transformation. Other image properties such as luminance can also be manipulated.

Hidden information can be scattered through out the cover image using Patchwork and similar techniques such as spread spectrum methods. These approaches may help protect against image processing such as cropping and rotating, and they hide information more thoroughly than by simple masking.

By using redundant pattern encoding, a small message may be painted many times over an image so that if the stego image is cropped, there is a high probability that the watermark can still be read. A

large message may be embedded only once because it would occupy a much greater portion of the image area [29].

Advantages:

1.) Increases robustness, by using redundant pattern encoding i.e there is higher chance that message will be available after image manipulation.
2.) Message can easily be hidden in high colour quality JPEG images as they use DCT lossy compression transform.
3.) It also increases probability that only the intended receiver will be able to decode the message as message is encrypted and scattered through out the image.[3]

Drawbacks:

1.) This method uses frequency domain techniques such as cosine transform, wavelet transform and Fourier transform which are not so easy to implement.
2.) As using this technique, message is spread through out the image, so adding a slight noise may change the whole image rather than only the parts where data is hidden.

BENEFITS OF STEGANOGRAPHY [11]

1. Cryptography only encrypts the message and thus provides a clue to the intruder that communication is going on. Steganography on the other hand conceals the existence of message in some cover source, such that no one can guess that message is being hidden in some cover source.
2. Watermarking, another useful concept can also be implemented using Steganography. Watermarking can be used to provide copyright protection by extending the cover source with some extra information. Steganography can be used to maintain the confidentiality of valuable information to protect the data from possible sabotage, theft.
3. In today's world, all the transactions, shopping, banking, reservations are done over the web so it is very much essential to keep confidential information secret like credit card numbers, debit cards and personal bank accounts. All this can easily be done by hiding these confidential data in a cover source using digital Steganography.

DRAWBACKS OF STEGANOGRAPHY [17]

1. Steganography hides a message, but if someone knows the message is there, the message can be read. To avoid this, cryptography combined with steganography is used. For example, the message could be encrypted before it is hidden. Therefore, even if the message is found, it cannot be read.
2. If someone suspects that Steganography is being used, hidden message can be destroyed. For example, if data is hidden within an image, the message is usually inserted into the least significant bits. Therefore, if the bit composition changes even slightly, the message is destroyed.
3. Another limitation is due to the size of the medium being used to hide the data. Message should be hidden in such a way that it requires minimum changes in cover source in which it is embedded.

APPLICATIONS [8]

□ ***Secret Communication***

Using Steganography, two parties can communicate secretly without anyone knowing about the communication. Cryptography, only encode the message but its presence is not hidden and thus draws unwanted attention, Steganography, thus, on the other hand, hides the existence of message in some cover media. Steganography provides us with [35]:

1. Potential capability to hide the existence of confidential data
2. Hardness of detecting the hidden (i.e., embedded) data
3. Strengthening of the secrecy of encrypted data

□ ***Copyright Protection***

This is basically related to watermarking i.e a secret message is embedded in the image which serves as the watermark and thus identify it as an intellectual property which belongs to a particular owner.

□ ***Feature Tagging***

Features such as captions, annotations, name of the individuals in a photo or location in a map can be embedded inside an image. Copying the stego image also copies all of the embedded features and only parties who possess the decoding stego key will be able to extract and view the features [9].

□ ***Digital Watermarking***

This is one of the most important applications of Steganography. It basically embeds a digital watermark inside an image. Digital watermarks may be used to verify the authenticity or integrity of the carrier signal or to show the identity of its owners. It is prominently used for tracing copyright infringements and for banknote authentication [35]

□ ***Use by terrorists***

Steganography at a large scale can also be used by terrorists, who hide their secret messages in innocent, cover sources to spread terrorism across the country. Rumours were spread about terrorists using steganography when the two articles titled "Terrorist instructions hidden online" and "Terror groups hide behind Web encryption" were published in newspaper. Other media worldwide cited these rumours many times, especially after the terrorist attack of 9/11, without ever showing proof.[36]

□ ***Other Applications***

Steganography is widely used in areas such as Military, Banking, Market Applications to provide secure communication between the parties. In Industries, Steganography is widely used as a mechanism to prevent piracy. It is also used in biometrics for providing secure and robust biometrics system

CONCLUSIONS

In this paper, an overview on Steganography is described. How Steganography differs from cryptography is also discussed. In the former, message is hidden in the cover source where as in the later message is only encrypted but it is visible during the transmission. Different techniques on image steganography with their relative pros and cons such as Least Significant Bit (LSB), Making and Filtering, Parity Checker Method, Gray Level

Modification (GLM) method are also discussed. The paper also covers steganography benefits, drawbacks and different applications such as secret communication, copyright protection, digital watermarking.

REFERENCES

[1.] *Arvind Kumar and Km. Pooja "Steganography- A Data Hiding Technique", International Journal of Computer Applications (0975 - 8887) ,Volume 9- No.7, November 2010*

[2.] *T. Morkel , J.H.P. Eloff and M.S. Olivier "An Overview of Image Steganography"*

[3.] *Amanpreet Kaur, Renu Dhir, and Geeta Sikka "A New Image Steganography Based On First Component Alteration Technique" (IJCSIS) International Journal of Computer Science and Information Security,Vol. 6, No. 3, 2009*

[4.] *Nagham Hamid, Abid Yahya, R. Badlishah Ahmad and Osamah M. Al-Qershi "Image Steganography Techniques: An Overview" International Journal of Computer Science and Security (IJCSS), Volume (6) : Issue (3) : 2012*

[5.] *Mehdi Kharrazi, Husrev T. Sencar and Nasir Memon "Image Steganography : Concepts and Practices "Polytechnic University, Brooklyn, NY 11201, USA*

[6.] *Fabien A. P. Petitcolas, Ross J. Anderson and Markus G. Kuhn "Information Hiding A Survey"Proceedings of the IEEE, special issue on protection of multimedia content, 87(7):1062{1078, July 1999.*

[7.] *Ankita Agarwal " Security Enhancement Scheme for Image Steganography using S-DES Technique" International Journal of Advanced Research in Computer Science and Software Engineering , Volume 2, Issue 4, April 2012*

[8.] *Adel Almohammad "Steganography-Based Secret and Reliable Communications: Improving Steganographic Capacity and Imperceptibility" A thesis submitted for the degree of Doctor of Philosophy, Department of Information Systems and Computing , Brunel University, August, 2010.*

[9.] *Rajkumar Yadav "Study of Information Hiding Techniques and their Counterattacks: A Review Article" , International Journal of Computer Science & Communication Networks, Vol 1(2), 142-164, Oct-Nov 2011*

[10.] *Angela D. Orebaugh " Steganalysis: A Steganography Intrusion Detection System" , George Mason University*

[11.] *Bret Dunbar, "A detailed look at Steganographic Techniques and their use in an Open- Systems Environment", SANS Institute InfoSec Reading Room, SANS Institute 2002*

[12.] *Jagvinder Kaur, Sanjeev Kumar "Study and Analysis of Various Image Steganography Techniques" IJCST Vol. 2, Issue 3, September 2011*

[13.] *www.ims.nus.edu.sg/Programs/imgsci/files/memon/sing_stego.pdf "Image Steganography and Steganalysis*

[14.] *Samir K Bandyopadhyay, Debnath Bhattacharyya[1], Debashis Gangul[1], Swarnendu Mukherjee[1] and Poulami Das[1] "A Tutorial Review on Steganography" University of Calcutta, Senate House, 87 /1 College Street, Kolkata - 700073 , [1]Computer Science and Engineering Department, Heritage Institute of Technology, Anandapur, Kolkata - 700107 , IC3-2008*

[15.] *Ahmad T. Al-Taani and Abdullah M. AL-Issa "A Novel Steganographic Method for Gray-Level Images" International Journal of Computer and Information Engineering 3:1 2009*

[16.] *W Bender, D. Gruhl, N. Morimoto, and A. Lu, "Techniques for data hiding," IBM Systems Journal, Vol. 35, No. 3 and 4, pp. 313-336, 1996.*

[17.] *Eric Cole "Stego Marking Packets to Control Info. Leakage on TCP/IP Based Networks"*

[18.] *Rengarajan Amirtharajan, Aishwarya G, Madhumita Rameshbabu, John Bosco Balaguru Rayappan, "Optimum Pixel & Bit location for Colour Image Stego- A Distortion Resistant Approach", International Journal of Computer Applications (0975 - 8887),Volume 10- No.7, November 2010*

[19.] *Abbas Cheddad " Strengthening Steganography in Digital Images" ,School of Computing and Intelligent Systems, Faculty of Engineering, University of Ulster, Magee*

[20.] *Abbas Cheddad, JoanCondell, KevinCurran, PaulMcKevitt "Digital image steganography: Survey and analysis of current methods" Signal Processing 90 (2010) 727-752*

[21.] *Saurabh V. Joshi ,Ajinkya A. Bokil, Nikhil A. Jain, Deepali Koshti "Image Steganography Combination of Spatial and Frequency Domain" International Journal of Computer Applications (0975 - 8887) Volume 53- No.5, September 2012*

[22.] *T. Morkel 1, J.H.P. Eloff 2, M.S. Olivier " An Overview of Image Steganography", Information and Computer Security Architecture (ICSA) Research Group ,Department of Computer Science, University of Pretoria, 0002, Pretoria, South Africa*

[23.] *http://en.wikipedia.org/wiki/Peak_signal-to-noise_ratio "Peak Signal to Noise Ratio"*

[24.] *http://wiki.answers.com/Q/What_is_psnr_in_steganography "PSNR in Steganography"*

[25.] *http://tdistler.com/iqa/algorithms.html "Mean Square Error"*

[26.] *http://en.wikipedia.org/wiki/Signal-to-noise_ratio "Signal-to-Noise Ratio"*

[27.] *http://www.mathworks.in/help/images/examples/registering-an-image-using-normalized-cross-correlation.html "Normalized Cross Co-relation"*

[28.] *http://en.wikipedia.org/wiki/Bit_error_rate "Bit-Error Rate"*

[29.] Neil F Johnson, Sushil Jajodia, "Exploring Stenography: Seeing the Unseen", IEEE Computer, Feb 1998, pp 26-34.

[30.] Rajkumar Yadav "Analysis of Incremental Growth in Image Steganography Techniques for Various Parameters" Int. J. Comp. Tech. Appl., Vol 2 (6),1867-1870, NOV-DEC 2011

[31.] Rajkumar , Rahul Rishi , Sudhir Batra " A New Steganography Method for Gray Level Images using Parity Checker" International Journal of Computer Applications (0975 – 8887) Volume 11– No.11, December 2010

[32.] Chung-Ming Wang , Nan-I Wu , Chwei-Shyong Tsai , Min-Shiang Hwang, "A high quality steganographic method with pixel-value differencing and modulus function" J. Syst. Software (2007), doi:10.1016/j.jss.2007.01.049

[33.] Khan, Mohammed Minhajuddin , "Steganography"

[34.] G.Rupesh Kumar "Steganography", Seminar Report, Balaji Institute of technology and Sciences, Deptt. of Computer Science and Engg. Narsampet, Warangal, March 2011

[35.] Applications of Steganography http://www.datahide.com/BPCSe/applications-e.html

[36.] http://en.wikipedia.org/wiki/Steganography

ISSN: 2067-3809 [CD-Rom, online]

ACTA TECHNICA CORVINIENSIS – Bulletin of Engineering
Tome VI (Year 2013) – FASCICULE 3 [July–September]
ISSN 2067–3809

[1.] K. K. ALANEME, [2.] M. O. BODUNRIN

MECHANICAL BEHAVIOUR OF ALUMINA REINFORCED AA 6063 METAL MATRIX COMPOSITES DEVELOPED BY TWO STEP – STIR CASTING PROCESS

[1-2.] DEPARTMENT OF METALLURGICAL AND MATERIALS ENGINEERING, FEDERAL UNIVERSITY OF TECHNOLOGY, AKURE, NIGERIA

ABSTRACT: Among metallic matrices, Aluminum based matrix remains the most explored metal matrix material for the development of MMCs. This is primarily due to the broad spectrum of properties offered by aluminum based matrix composites at low processing cost. The mechanical behavior of aluminum alloy (6063) - alumina particulate composites developed using two step stir casting was investigated. AA 6063 - Al_2O_3 particulate composites having 6, 9, 15, and 18 volume percent of Al_2O_3 were produced. It is observed that AA 6063/Al_2O_{3p} composites having low porosity levels (≤ 3.51 %porosity) and a good uniform distribution of the alumina particulates in the matrix of the AA 6063 were produced. The tensile strength, yield strength, and hardness increased with increase in alumina volume percent while the strain to fracture and fracture toughness decreased with increasing volume percent alumina.
KEYWORDS: stir casting; AA6063-Al_2O_3, fracture toughness, tensile properties, porosity

INTRODUCTION

The viability of developing simple, cost effective and technically efficient processing routes for the production of metal matrix composites (MMCs) is currently being explored by materials researchers from most developing countries [1 - 2]. The motivation for research in MMCs development is its attractive properties and higher performance potentials over traditional metals and alloys [3 - 4]. Some of the desirable properties of MMCs include high specific strength and stiffness, better high temperature performance, and low thermal expansion [5-6]. Among metallic matrices, Aluminum based matrix remains the most explored metal matrix material for the development of MMCs. This is primarily due to the broad spectrum of properties offerred by aluminium based matrix composites at low processing cost [6]. Currently, Aluminum based matrix composites are applied in the design of a wide range of components for use in aerospace technology, defense, electronic heat sinks, solar panel substrates, antenna reflectors, automotive drive shaft fins, explosion engine components, and sports equipment among others [6 - 7].

Deriving optimized properties from any selected Al based matrix composite requires a sound knowledge of the material behavior of the composite which is influenced by such factors as the base Al alloy composition, the manufacturing process, the reactivity between the reinforcement and the matrix, the size, morphology and volume fraction of the reinforcement [8 - 10].

The current research work is an effort to study the mechanical behaviour of AA (6063)/ Al_2O_{3p} composites produced using two step stir casting process. AA 6063 is processed in large quantities at lower costs in many developing countries but its potentials for use as Al alloy matrix for composite development has not been explored as extensively as the other age hardenable Al alloy series such as the AA 6061, AA 7075, and AA 2024 series [8, 11 - 12].

MATERIALS AND METHODS. Materials

The materials utilized in the present study are 100 percent chemically pure alumina (Al_2O_3) particles having a particle size of 28 μm and Aluminum 6063 alloy which served as the matrix. The composition of the Aluminum 6063 alloy is shown in Table 1.

Table 1: Chemical Composition of the Aluminum Alloy 6063 (AA 6063)

Si	Fe	Cu	Mn	Mg
0.45	0.22	0.02	0.03	0.50

Zn	Cr	Ti	Al
0.02	0.03	0.02	Bal.

Methods

☐ ***Stir Casting***

The quantity of Aluminium (6063) alloy and alumina (Al_2O_3) particles required to produce composites having 6, 9, 15, and 18 volume percent alumina were evaluated using charge calculations. The alumina particles were initially preheated at a temperature of 250^{0}C for 5minutes to help improve wettability with the AA 6063 alloy. The AA 6063 ingots were charged into a gas-fired crucible furnace and heated to a temperature of 750^{0}C ± 30^{0}C (above the liquidus temperature of the alloy) and the liquid alloy was

then allowed to cool in the furnace to a semi solid state at a temperature of about 600^{0}C.
The preheated alumina was added at this temperature and stirring of the slurry was performed manually for 5 minutes. The composite slurry was then superheated to 720^{0}C and a second stirring performed using a mechanical stirrer. The stirring operation was performed at a speed of 300 rpm for 10 minutes to help improve the distribution of the alumina particles in the molten AA 6063.
An external temperature probe (thermocouple) was utilized to monitor the temperature of the furnace. The molten composite was then cast into prepared sand moulds. Unreinforced AA 6063 were also prepared by casting for control experimentation.

□ ***Hardness Measurement***

The hardness of the composites was evaluated using a Vickers Hardness Tester (LECO AT 700 Microhardness Tester). Prior to testing, the surface of the composite test specimens of sizes 25 × Ø20 mm were subjected to grinding and polishing operation to obtain a flat and smooth surface finish. A direct load of 50gf (490.3 mN) was then applied on the specimens for 10 seconds and the hardness readings evaluated following standard procedures.
Multiple hardness tests were performed on each sample and the average value taken as a measure of the hardness of the specimen.

□ ***Density Measurement***

The density measurements were carried out to determine the porosity levels of the samples. This was achieved by comparing the experimental and theoretical densities of each volume percent Al_2O_3 reinforced composite.
The experimental density of the samples was evaluated by weighing the test samples having dimensions of 20 mm diameter and 220 mm length using a high precision electronic weighing balance with a tolerance of 0.1mg. The measured weighs in each case was divided by the volume of the respective samples.
The theoretical density of composite was evaluated by using the rule of mixtures given by:

$$\rho_{AA\frac{6063}{Al_2O_{3p}}} = Vol._{AA6063} \times \rho_{AA6063} + Vol._{Al_2O_3} \times \rho_{Al_2O_3} \quad (2.1)$$

where, $\rho_{AA\frac{6063}{Al_2O_{3p}}}$ *= Density of Composite,*

$Vol._{AA6063}$ *= Volume fraction of AA 6063,*

ρ_{AA6063} *= Density of AA 6063,*

$Vol._{Al_2O_3}$ *= Volume fraction Al_2O_3, and*

$\rho_{Al_2O_3}$ *= Density of Al_2O_3.*

The percent porosity of the composites was evaluated using the relations [12]:

$$\% \text{ porosity} = \{(\rho_T - \rho_{EX}) \div \rho_T\} \times 100\% \quad (2.2)$$

where, ρ_T *=Theoretical Density (g/cm^3),*

ρ_{EX} *= Experimental Density (g/cm^3)*

□ ***Tensile Testing***

Room temperature uniaxial tension tests were performed on round tensile samples machined from the monolithic alloy and the composites with dimensions of 6 mm diameter and 30 mm gauge length.
The testing was performed using an instron universal testing machine operated at a constant cross head speed of 1mm/s; and the procedure adopted was in conformity with ASTM E8M - 91 standards [13]. Three repeat tests were performed for each test condition to guarantee reliability of the data generated.
The tensile properties evaluated from the stress-strain curves developed from the tension test are - the ultimate tensile strength (σ_u), the 0.2% offset yield strength (σ_y), and the strain to fracture (ε_f).

□ ***Fracture Toughness, K_{1C}***

Circumferential notch tensile (CNT) specimens were prepared for the evaluation of fracture toughness in accordance with Alaneme [14]. The CNT specimens were machined with gauge length of 30mm, specimen diameter of 6mm (D), notch diameter of 4.5mm (d) and notch angle of 60^0.
The specimens were then subjected to tensile loading to fracture using an instron universal testing machine. The fracture load (P_f) obtained from the CNT specimens' load - extension plots were used to evaluate the fracture toughness using the empirical relations by Dieter [15]:

$$K_{1C} = P_f / (D)^{3/2} [1.72(D/d) - 1.27] \quad (2.3)$$

Where, D and d are respectively the specimen diameter and the diameter of the notched section. The validity of the fracture toughness values was evaluated using the relations in accordance with Nath and Das [16]:

$$D \geq (K_{1C} / \sigma_y)^2 \quad (2.4)$$

A minimum of two repeat tests were performed for each treatment condition and the results obtained were taken to be highly consistent if the difference between measured values for a given treatment condition is not more than 2%.

□ ***Microstructure***

The microstructural investigation was performed using a Datteng Software-Driven Metallurgical Microscope. The specimens for the optical microscopy were polished using a series of emery papers of grit sizes ranging from 500µm - 1500µm; while fine polishing was performed using polycrystalline diamond suspension of particle sizes ranging from 10µm - 0.5µm with ethanol solvent. The specimens were etched using 1HNO_3: 1HCl solution by swabbing in accordance with Yussof et al [17] before microstructural examination was performed using the optical microscope.

RESULTS AND DISCUSSION. Microstructure

Figure 1 shows representative optical micrograph for the 9 and15 volume percent Al_2O_3 reinforced AA 6063 composites. It is observed that the Al_2O_3 particulates are visible and a good dispersion of the particulates in the AA 6063 matrix is evident. This is a good indicator of the efficiency of the production technique.

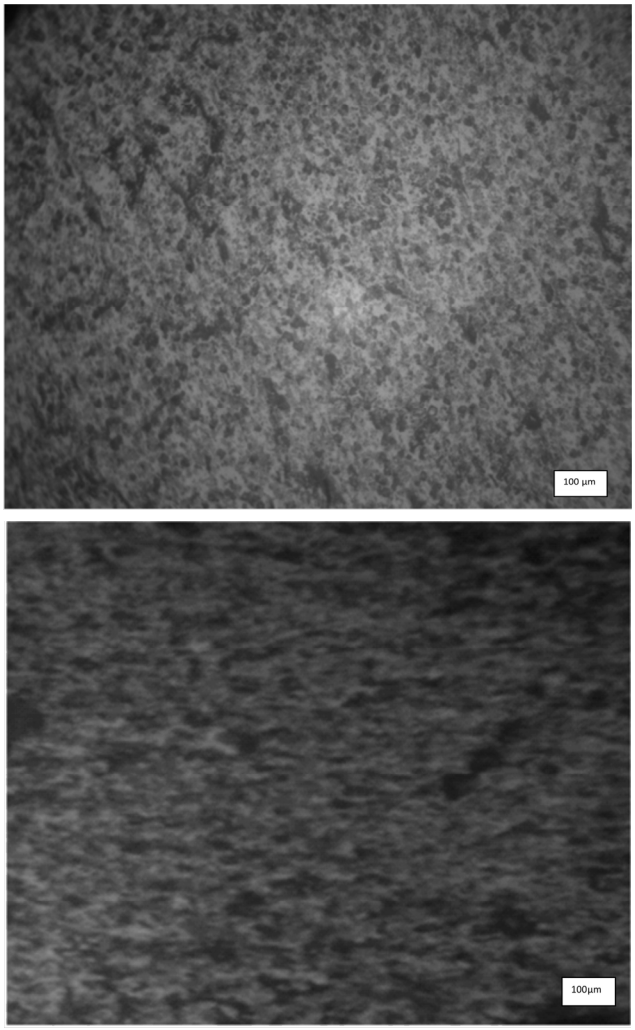

Figure 1: Representative Micrographs for (a) AA 6063 - 9 vol% Al_2O_3, and (b) AA 6063 - 15 vol% Al_2O_3

Percent Porosity

The results of the percent porosity of the composites are presented in Table 2. It is observed that slight porosities exist in the produced composites since the experimental densities are lower than the theoretical densities. It is however encouraging that the percent porosities are between 1.08 - 3.51% which is within the acceptable range of 4% porosity reported in literature as the maximum permissible in cast metal matrix composites [18-19].

Table 2: Percent Porosity and Hardness data for the AA 6063 – Al_2O_3 Composites

Materials Samples	Theoretical Density (g/cm^3)	Experimental Density (g/cm^3)	% Porosity	Hardness (VHN)
0%	2.70	2.68	0.74	40.3 ± 0.2
6%	2.76	2.69	2.54	40.5 ± 0.1
9%	2.79	2.74	1.79	41.4 ± 0.4
15%	2.85	2.75	3.51	43.6 ± 0.2
18%	2.87	2.77	3.48	45.1 ± 0.3

The low porosity levels are attributed to the two - step stirring process adopted for producing the composites. The manual mixing operation performed in the semi-solid state helps to break the surface gas layers and to spread the liquid metal onto the surface of the particles. It also reduces the surface tension between the AA 6063 melt and the particles to facilitate easier wetting and mixing of the alumina particulates in the melt.

The mechanical stirring employed at the liquidus state helps in reducing the sedimentation of alumina particles by virtue of their higher density ($3.95g/cm^3$); and also improve the dispersion of the alumina particulates.

Mechanical Properties

The variation of hardness with volume percent Al_2O_3 is also presented in Table 2. It is observed that the hardness increases with increase in volume percent Al_2O_3. This trend is due to an increase in the proportion of the hard Al_2O_3 particulates in the composites, which increases the composites resistance to indentation in comparison to the monolithic alloy [18].

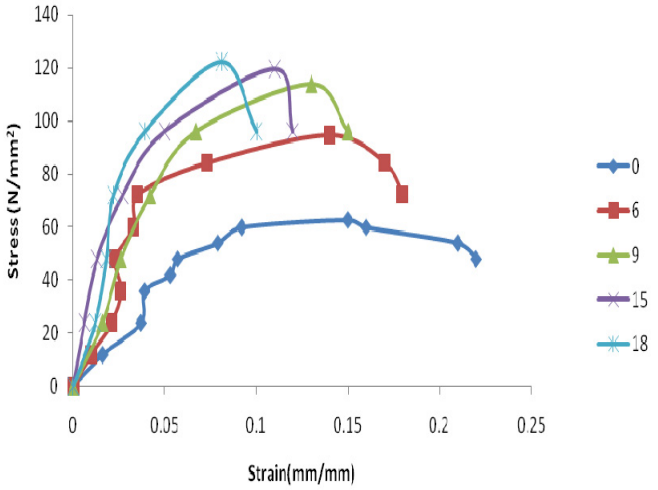

Figure 2: Tensile Stress - Strain curves of the AA 6063 - Al_2O_3 Composites.

The stress-strain plots of the composites are presented in Figure 2; while the variation of ultimate tensile and yield strengths and strain to fracture are presented in Figures 3 - 4. It is observed from the stress - strain plots that the monolithic alloy has the largest plastic strain and also exhibits the least resistance to plastic deformation judging from its relatively lower flow stress in comparison with the composites.

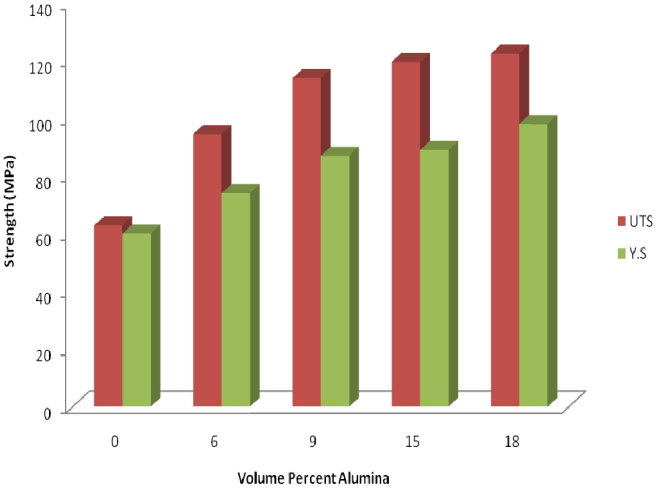

Figure 3- Variation of Ultimate Tensile and Yield Strengths in the Composite with increase in Volume percent alumina reinforcement.

Figure 3 shows clearly that the ultimate tensile and yield strengths of the composites increases with increase in volume percent alumina.

The observed trend is in conformity with observations in most hard particulate reinforced metal matrix composites [20-21]. The strengthening mechanisms has been well reported by Chawla and Shen [22] who attributed it to increased load sustaining capacity of the composite with increase in the volume percent of the hard particulates; and the increased resistance to dislocation movement by the particulates.
The resulting thermal mismatch between the high expansion metallic matrix and the low expansion ceramic particulates results in the generation of dislocations at the reinforcement/matrix interface upon cooling, contributing to an increase in dislocation density in the composites with increasing particulate content [22 - 23].

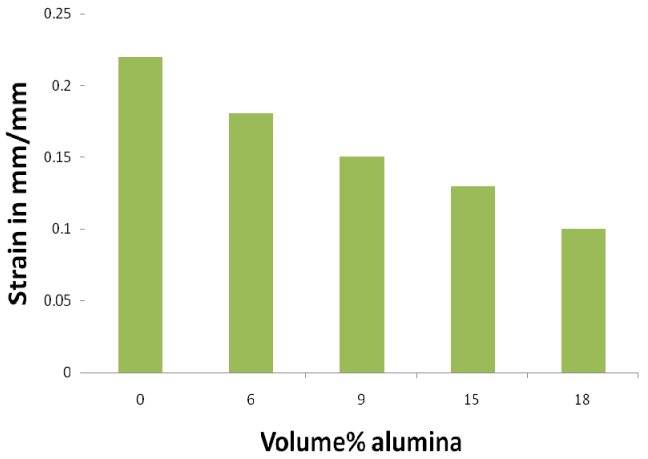

Figure 4: Variation of Strain to fracture with increase in volume percent alumina particulates

The strains to fracture for the composites (Figure 4) are observed to decrease with increase in volume percent alumina; and the values are observed to be less than 0.19 (19%). The increased matrix/ particulate interfaces with increase in volume percent alumina leads to an increase in the potential sites for void nucleation or micro-crack formation. The uneven plastic strain at the interface facilitates the nucleation of voids or micro-cracks [22-24].

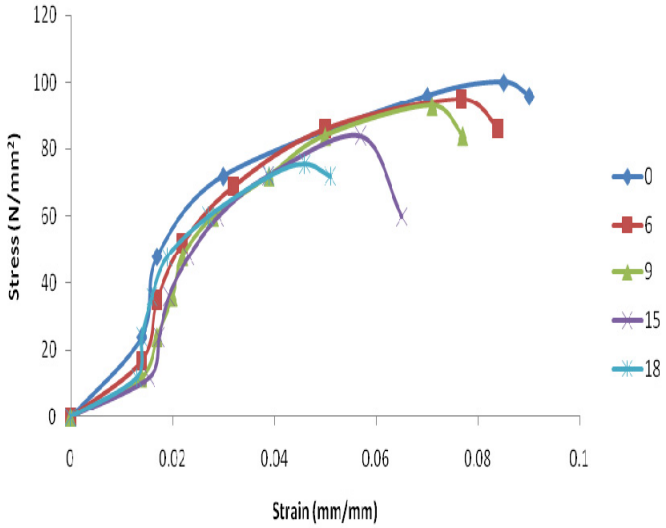

Figure 5: Stress - Strain curves for the CNT tests on the AA 6063 - Al_2O_3 Composites

The fracture loads utilized for the evaluation of the fracture toughness were derived from the stress - strain plots of the circumferential notch tensile specimens (Figure 5).

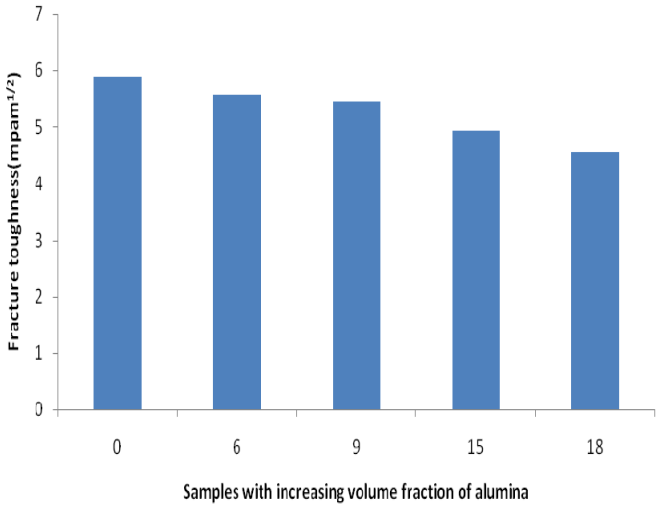

Figure 6: Variation of Fracture Toughness with increase in volume percent of alumina particulates

The variation of fracture toughness of the composites with increase in Al_2O_3 volume percent is presented in Figure 6. The results were taken to be reliable because the requirement for nominal plain strain condition was met with the specimen diameter of 6mm since the relation $D \geq (K_{1C}/\sigma_y)^2$ [16] was utilized to test for the validity of the K_{1C} values evaluated from the CNT testing.
The fracture toughness (which is a measure of the composites resistance to crack propagation) was observed to decrease with increase in volume percent of Al_2O_3 which is consistent with the trend in most hard particle reinforced metal matrix composites [22, 25-26].
The increased sites (particles, particle/matrix interfaces, and particle clusters) for crack nucleation with increasing volume percent of the Al_2O_3 were responsible for the observed trend [26 - 27]. The fracture micro-mechanism may be due to particulate cracking, interfacial cracking or particle debonding [27 - 28]. Generally, the fracture toughness values obtained for the composites were found to be comparable to that of Al matrix composites processed under similar conditions [29-30].

CONCLUSIONS

From the results of this research investigation, It has been established that low porosity levels less than 3.6% is observed in AA 6063/Al_2O_{3p} composites developed by the two step stir casting process adopted in this research.
The tensile strength, yield strength, and hardness values of the composites increased with increase in alumina volume percent while the strain to fracture and fracture toughness decreased with increasing volume percent alumina.
The mechanical properties obtained from the AA 6063/Al_2O_{3p} composites developed compares favorably with that of other aluminum based alumina reinforced composites reported in literature.

REFERENCES

[1.] Soboyejo W. Mechanical Properties of Engineered Materials. New York: Marcel Dekker Inc., 2003.

[2.] Miracle, DB. Metal Matrix Composites-From Science to technological significance. Composites Sci and Tech 2005; 65(15-16): 2526-2540.

[3.] Anilkumar H. C., Hebbar H. S. and Ravishankar K. S. Mechanical Properties of Fly Ash Reinforced Aluminium Alloy (Al 6061) Composites. International Journal of mechanical and Materials Engineering 2011; 6 (1):41-45

[4.] Adiamak, M. Selected Properties of Aluminium Base Composites reinforced with intermetallic Particles, Journal of Achievemnets in Materials and Manufacturing Technology, 2006, 14 (1-2): 43-47.

[5.] Alaneme, K. K. Influence of Thermo-mechanical Treatment on the Tensile Behaviour and CNT evaluated Fracture Toughness of Borax premixed silicon carbide reinforced Aluminium (6063) Matrix Composites, International Journal of Materials and Mechanical Engineering, 2012, 7(1): 96 - 100.

[6.] Veeresh Kumar GB, Rao, CSP, Selvaraj N, Bhagyashekar MS. Studies on Al (6061) and 7075 - Al203 Metal Matrix Composites. J of Minerals & Matls Charac & Eng 2010; 9(1): 43-55.

[7.] Natarajan, N., Vijayarangan, S. and Rajendran, I. Fabrication, testing and thermal analysis of metal matrix composite brake drum. International Journal of Vehicle Design 2007, 443(4): 339-359.

[8.] Chawla V, Manoj S, Dwivedi D D, Lakhvit S. Development of Aluminium Based SiC Particulate Metal Matrix Composite 2009; J of Minerals & Matls Charac & Eng 2009; 8(6): 455-467.

[9.] Zamri, Y.B., Shamsul, J.B. and Amin, M.M. Potential of palm oil clinker as reinforcement in aluminium matrix composites for tribological applications, International Journal of Mechanical and Materials Engineering 2011; 6 (1): 10-17.

[10.] Cocen U, Onel K. Ductility and Strength of extruded SiCp/ aluminium alloy composites. Comp Sci and Tech 2002; 62: 275-282.

[11.] Christy T V, Murugan N, Kumar S. A Comparative study on the microstructures and Mechanical Properties of Al 6061 alloy and the MMC Al 6061/TiB2/12p. J Minrls and Matls Charac & Eng 2010; 9(1): 57-65.

[12.] Alaneme, K. K. and Aluko, A. O. Production and Age - hardening Behaviour of Borax Pre-mixed SiC Reinforced Al-Mg-Si alloy Composites developed by Double Stir Casting Technique, The West Indian Journal of Engineering, 2012, 34(1/2): 80 - 85.

[13.] ASTM E 8M . Standard Test Method for Tension Testing of Metallic Materials (Metric) in Annual Book of ASTM Standards. Philadelphia: ASTM; 1991.

[14.] Alaneme, K. K. Fracture Toughness (K_{1C}) Evaluation for Dual Phase low alloy Steels Using Circumferential Notched Tensile (CNT) Specimens, Materials Research, 2011, Vol. 14, No. 2, doi: 10.1590/S1516- 14392011005000028

[15.] Dieter G E. Mechanical Metallurgy, SI Metric Ed. Singapore: McGraw- Hill; 1988.

[16.] Nath S K, Das U K. Effect of Microstructure and Notches on the Fracture Toughness of Medium Carbon Steel. J Naval Archi & Marine Eng 2006; 3: 15 - 22.

[17.] Yussof Z, Ahmad K.R and S.B., Jamaludin Comparative Study of Corrosion Behavior of AA 2014/15vol%Al_2O_{3p} and AA2009/20Vol% SiCw, Portugaliae Electrochemica Acta, Volume 26, 2008, Pp 291-301.

[18.] Kok M. Production and Mechanical Properties of Al_2O_3 particle Reinforced 2024 Aluminium Composites, Journal of Materials Processing Technology. Volume 16, 2005, Pp. 381-387.

[19.] Hizombor M, Mirbagher S.M.H and Abdideh, Casting of A356/ TiB_2p Composite Based on the TiB_2p/ CMC / PPS MORTAR., Volume 18, 2010, Roznov pod Radhostem, Czech Republic, EU.

[20.] Dobrzanski L.A, Kremzer M., Nagel A. Aluminium EN Al-SiC Alloy Matrix Composite Reinforced by Al_2O_3 Preform, Achieves of Materials Science and Engineering, Volume 28, Issue 10, 2007, Pp 593-596.

[21.] Kumar S. and Theatan J.A., Production and Characterization of Aluminium Fly Ash Composites using stir Casting Method, B. Tech Thesis, National Institute of Technology, Pourkela. 2008.

[22.] Chawla N, Shen Y. Mechanical Behavior of Particle Reinforced Metal Matrix Composites. Advanced Engineering Materials 2001; 3(6): 357 - 370.

[23.] Ehsani R, Seyed Reihani S M. Aging Behaviour and Tensile Properties of Squeeze Cast Al 6061/ SiC Metal Matrix Composites. Scientia Iranica 2004; 11(4): 392-397.

[24.] Sharma S C, Girish B M, Kamath R, Satish B M. Fractography, Fluidity and Tensile Properties of Aluminium/Hematite Particulate Composites. J Matls Eng & Perf 1999; 8(3) 310 - 314.

[25.] Garcia-Romero A M, Egizabal P, Irisarri A M., Fracture and Fatigue Behaviour of Aluminium Matrix Composite Automotive Piston. Appl Compos Mater 2010; 17:15-30.

[26.] Perez.Ipina J E, Yawny A A, Stuke R, Gonzalez Oliver C. Fracture Toughness in Metal Matrix Composites. Materials Research 2000; 3(3): 74 - 78.

[27.] Mohammed M. Ranjbaran, Low Fracture Toughness in Al 7191-20%SiCp Aluminium Matrix Composite. European Journal of Scientific Research, Vol. 41, No. 2, 2010, Pp. 261-272.

[28.] Mortensen, A. A Review of the Fracture Toughness of Particle Reinforced Aluminium Alloys. Proc Int Conf Fabrication of Particulates Reinforced Metal Composites, Quebec, Canada 1999; 217 - 233.

[29.] Milan M T, Bowen P. Tensile and Fracture Toughness Properties of SiCp reinforced al alloys: Effects of Particle Size, Particle volume fraction and matrix strength, Journal of Materials Engineering and Performance 2004; 13(6) 775 - 783.

[30.] Alaneme, K. K. and Aluko, A. O. Fracture Toughness (K_{1C}) and Tensile Properties of As-Cast and Age-Hardened Aluminium (6063) - Silicon Carbide Particulate Composites, Scientia Iranica, Transactions A: Civil Engineering (Elsevier), 19(4), pp. 992 - 996.

ACTA TECHNICA CORVINIENSIS - Bulletin of Engineering

ISSN: 2067-3809 [CD-Rom, online]

ACTA TECHNICA CORVINIENSIS – Bulletin of Engineering
Tome VI (Year 2013) – FASCICULE 3 [July–September]
ISSN 2067–3809

[1.] Ali Asghar Fathollahi FARD

STEP VOLTAGE WITH MICROCONTROLLER TO REDUCE TRANSFORMER IN RUSH CURRENT

[1.] FACULTY OF ENGINEERING, MULTI MEDIA UNIVERSITY, MALAYSIA

ABSTRACT: When a transformer is energized by the supply voltage, a high current called transient inrush current which it may raise to ten times of the transformer full load current could be drawn by the primary winding. This paper discusses a microcontroller circuit with the intention of controlling and limiting the inrush current for a transformer by the method of ramping up the supply voltage feeding to the transformer primary. Simulations and the experimental results show a significant reduction of inrush current when the ramping up voltage is applied to the three-phase transformer load. Inrush current could be almost eliminated if choosing a correct switching step rate.
KEYWORDS: Transformer inrush current, Zero-crossing on sine wave, Triac/SCR, Microcontroller

INTRODUCTION

Inrush current is a serious problem that plagues almost every electrical equipment and electrical machineries, especially those which are inductive in nature such as transformers, switching power supplies and synchronous/induction motors. In transformer study, a phenomenon which engineers always encounter, amount of produced inrush current can be very large, many times larger than the transformer full-load current rating. Inrush current can produce mechanical stress to the transformer, damaging to transformer windings, it often affect the power system quality, may disrupt the operation of sensitive electrical loads due to voltage dips, and also maloperation cases of transformer protection relays sometimes happen. Therefore, it is a very serious that has to be tackled by electrical engineers all over the world [1,2].

There are a few methods that are used to protect transformer against inrush current. Most of these methods do not exactly eliminate inrush current but they reduce the current to a level which is safe for the equipment. A well-known method is a passive method which is done by using Negative Temperature Coefficient thermistors. Controlled switching, and sequential phase energization also are the other methods to eliminate the inrush current caused by the transformer primary windings [1,2]. The simplified equation often used to calculate the peak value of the first cycle of inrush current in Amps is as follows:

$$I_{inrush} = \frac{\sqrt{2}V}{\sqrt{(\omega \cdot L)^2 + R^2}} \left[\frac{2B_N + B_R - B_S}{B_N} \right] \qquad (1)$$

Where:V = Applied voltage involts, L = Air core inductance of the transformer windings inohms, B_R = Remnant flux density of the transformer core in Tesla, B_S = Saturation flux density of the core material in Tesla, B_N = Normal rated flux density of the transformer core in Tesla [3]. As the equation shows applied voltage V is an effective part of the formula and its magnitude will change the amount of inrush current remarkably.

Voltage ramping up method to increase the transformer primary voltage gradually is suggested in this paper. The gradually increase of supply voltage is injected to the transformer primary in few cycles, until the full amount of the transformer rated voltage is connected. By the help of power electronic components and amicrocontroller the method works in such that a percentage of the supply voltage is firstly injected to the primary of transformer, then, the amount of the injected voltage is gradually increased to the full voltage value after maximum of 20 cycles or 1000 mili- seconds time period counted in 50 Hz supply. The microcontroller is assisted by a zero-crossing detecting circuit to synchronise switching times, and sending pulses to the power electronic elements thetriacs/SCRs, capable of switching on/off the main supply voltage to the transformer load. Initial switching tests,and simulations by software NI Multisim have been successfully done to help the experiment research. The suggested method is generally more expensive and is complicated due to usage of active components.

This work implements an 8052based microcontroller to trigger three power electronics elements Triacs/SCRsas switches to turn on a three-phase transformer. High voltage section of the three-phase power supply is isolated from the low voltage microcontroller circuitry by optocouplers, and a zero-

crossing detector works in tandem with the microcontroller to synchronise the switching of the Triacs/SCRs so that the timing and triggering of the voltage ramping is coordinated [4].

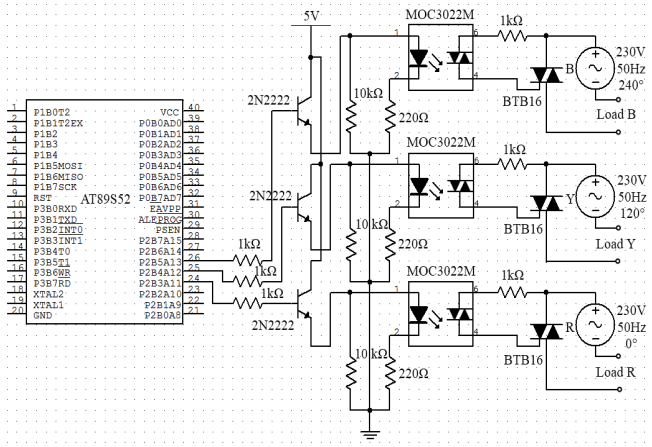

Figure 1: Microcontroller, optocouplers and triacs circuit

The microcontrollers entirely programmed in assembly with the MCS51 Assembly Language. Figure 1 shows the circuit of the microcontroller and the basic components required for the work provided by NI Multisim 11.0 software.

INITIAL TESTING AND TRIGGERING

The zero-crossing detector circuit sends pulses for the positive and negative zero-crossings to the microcontroller. The microcontroller then reads these pulses and it will wait for the last negative zero-crossing and trigger the triacs on the next zero-crossing. For the triggering of the three-phase supply voltage in this research work, a stage triggering method is employed.

The method is to start triggering triacs from the zero-crossings happen at the angle of 90° on the waveform of the supply voltage or when the first cycle of the waveform reaches its peak value. For this triggering method, step rates voltage of 5%, 10%, 20%, and 50% are applied.

Table 1 refers information on triggering on the voltage sine wave, and figure 2 shows the results of NI Multisim 11.0 simulation on starting angle of 90° for single phase switching.

Table 1: Summary of triggering

Triggering at 90° of voltage wave				
Step-rate (%)	5	10	20	50
No. of cycles to full voltage	20	10	5	2

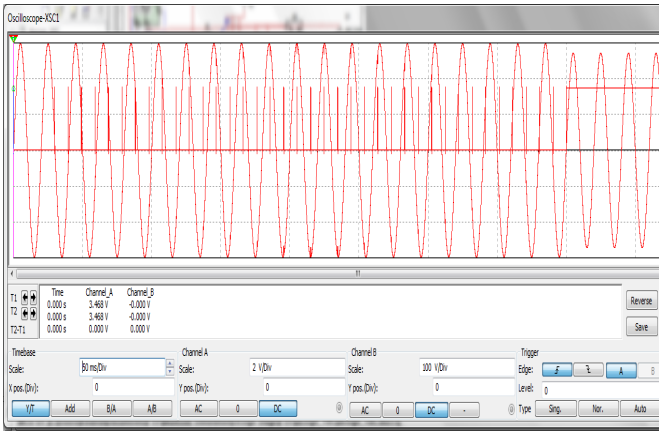

Figure 2: Starting angle of 90° for single phase switching

For the 50 Hz supply voltage, one full cycle of the ac waveform takes 20ms to be completed. Initially, the first phase of three-phase (Aphase) is triggered by a certain time delay according the step-rate chosen. A 50% step-rate has a time delay of 10ms after the zero-crossing is detected. This 10ms time delay is generated in the assembly programming by using loops, which is a conventional but an effective way of generating a time delay.

For the second phase (Bphase), an interrupt timer is being set to count an interval of 6.667 ms after each triggering of the first phase, as the second phase lags the first phase by 120° and it translates into 6.667ms of real time to reach its peak point.

For the third phase (Cphase), the similar method is used to trigger the supply voltage but this time a different interrupt timer is being utilised.

The output voltages for all the step rates were observed to the switching pulses from the microcontroller to insure accurate switching control of stepping ramping voltage for the three-phase transformer before actual experiments of the inrush currents effects.

INRUSH CURRENT TESTS ON TRANSFORMERS

Inrush current tests were conducted with three single-phase 1 kVA transformers which were connected in star in the primary. The inrush current effect tests firstly were conducted with direct-on-line connection to the supply voltage. This should serve as the initial value to compare with the resulting inrush currents with the use the stepping ramping voltage control afterwards.

A lot of trials were done in order to get the highest possible inrush current resulted from the energization of the transformers at 0° of the supply voltage sine wave,and existence of the maximum value of initial core fluxeswhich is counted as the worst case of producing inrush current in the transformer [5].

The highest inrush current for the primary wye connected three-phase transformer 3×1 kVA rating was obtained to be 86A as shown in Figure 3, and the steady state current of this transformer was found to be around 2A as it is shown in figure 4.

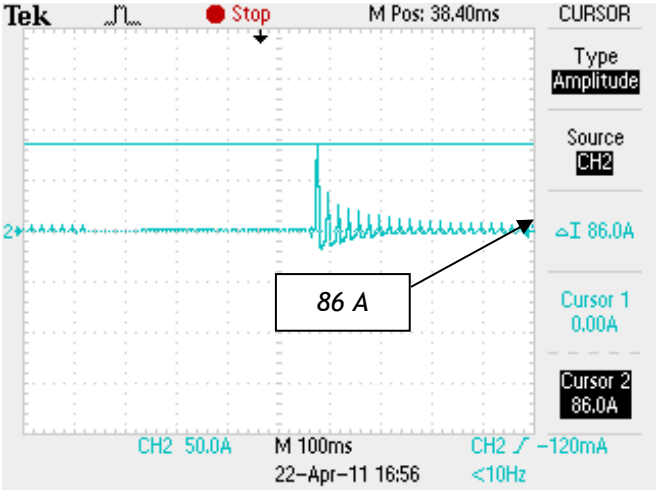

Figure 3: Highest recorded of inrush current for 3×1 kVA transformers

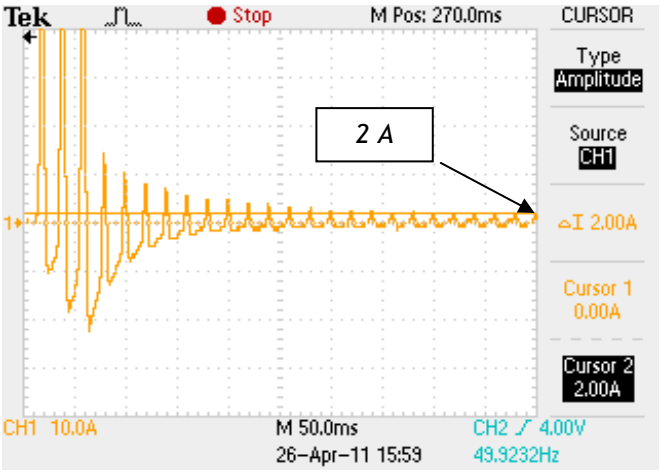

Figure 4: The value of steady state current for 3×1 kVA transformers

In the next step of the work, using the microcontroller ramping voltage circuit in order to reduce the magnitude of inrush current, after series of tests were done, the followings are the results captured by the digital oscilloscope.For the step starting angle of 90° on voltage sine wave and 5% step rateof ramping up voltage shown in figure 5, inrush current was found to be peaking at 70.4A highest. No significant inrush current suppression was observed from the inrush current previous value of 86A.

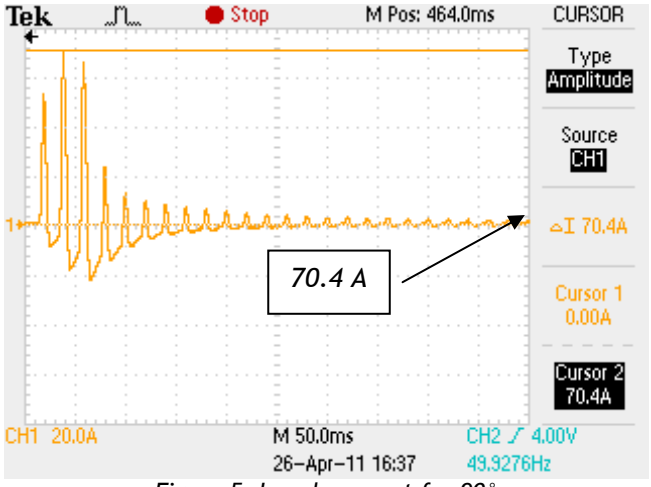

Figure 5: Inrush current for 90° and 5% switching

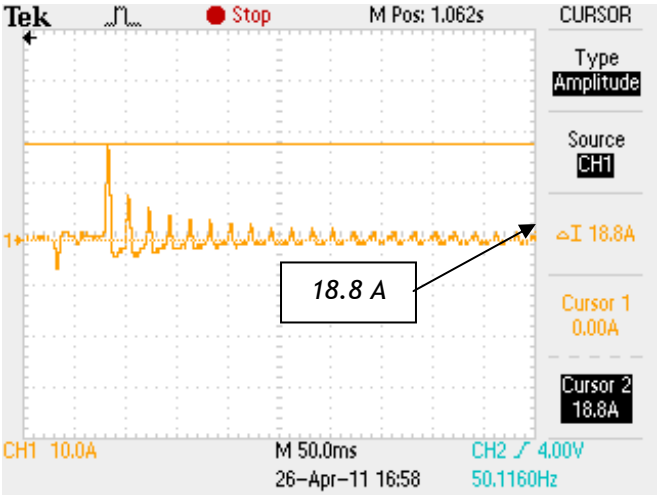

Figure 6: Inrush current for 90° and 20% switching

For the step starting angle of 90° on voltage sine wave and 20% step rate of ramping up voltage, inrush current was found to be dropped to 18.8A highest. A significant suppression of inrush current was observed from the inrush current previous value of 86A to lower value of 18.8A shown in figure 6.

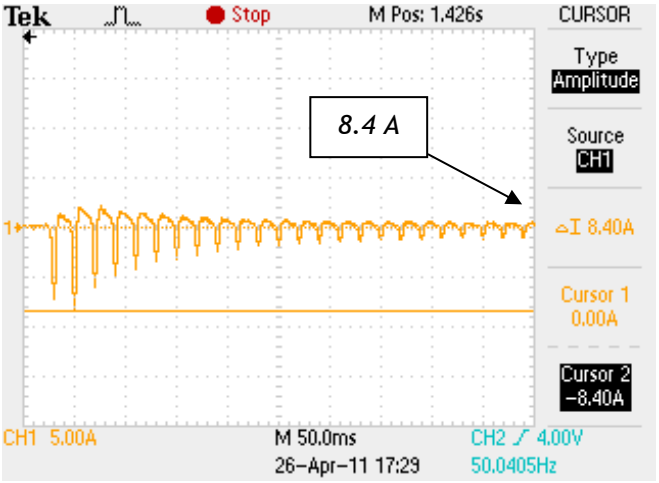

Figure 7: Inrush current for 180° and 50% switching

Lastly, as shown in figure 7 for the step starting angle of 90° on voltage sine wave and 50% step rate of ramping up voltage, the amount of inrush current also has been dropped to 8.4 A.

FINDINGS AND DISCUSSION

At a glance, it seemed that the controlled triggering through voltage ramping up technique is able to reduce the inrush current of a three-phase transformer load up to certain extent. However, the reduction in the inrush current was not so significant until at least 20% step rate in 90° angle on voltage sine wave. The control value of inrush current obtained was peaking at 86A after many trials were done. Basing with the 86A inrush current, a direct comparison was made with the results which were written in Table 2.

Table 2: Reduction in inrush current with controlled triggering on supply voltage (initial record of maximum inrush current was 86 A)

Energization at 90° of voltage sine wave				
Step rate (%)	5	10	20	50
Peak inrush current (A)	70.4	67.2	18.8	8.4

CONCLUSIONS

The method of switching control on three-phase supply voltage is achievable by use of a microcontroller, and some standard electronics components such as Triac/SCR, optocoupler and zero-crossing detector IC.

For transformers loads, the switching with control on the three-phase supply voltage to ramping up can limit inrush current when the step rate is kept relatively high, that is a rate equal or larger than 20%. Though the circuit has not been tested on an AC motor, another type of inductive load, it is believed that switching three-phase ramping voltage can effectively start a ac motor as a soft starter. This is due to the fact that voltage is gradually increased until very low starting current for the motor is observed. The circuit is deemed successful for the

fact that the control switching of a three-phase supply voltage is possible with the help of a microcontroller, and it can effectively limit transformer inrush current when there is no failure in triggering and microcontroller pulses.

REFERENCES

[1] *J.H Brunke, and K.J. Frohlich: Elimination of transformer inrush currents by controlled switching I. Theoretical considerations, IEEE Transactions on power delivery, vol.16, no.2, pp.276-280, Apr 2001.*

[2] *Yu Cui, Sami G. Abdulsalam, Shiuming Chen, and WilsunXu: A Sequential Phase Energization Technique for Transformer Inrush Current Reduction Part I: Simulation and Experimental Results, IEEE Transactions on power delivery, vol. 20, no. 2, 2005.*

[3] *Fahrudin Mekic, Ramsis Girgis, ZoranGajic, and Ed teNyenhuis: Power Transformer Characteristics and Their Effect on Protective Relays, 33rd Western Protective Relay Conference, Oct. 2006.*

[4] *B. Somanathan Nair, and S. R. Deepa: The Triode AC Switch in Solid State Devices, New Delhi India, PHI Learning Pvt. Ltd., 2010.*

[5] *Fathollahi Fard Ali Asghar, and K. P. Basu: A new design for point on wave switching with microcontroller to minimize transformer inrush current, IEEEconference: Electrical Energy and Industrial Electronic Systems EEIES 2009, Penang Malaysia, Dec 2009.*

ISSN: 2067-3809 [CD-Rom, online]

ACTA TECHNICA CORVINIENSIS – Bulletin of Engineering
Tome VI (Year 2013) – FASCICULE 3 [July–September]
ISSN 2067–3809

[1.] G.NAGARAJU, [2.] J.V.RAMANA MURTHY, [3.] K.S.SAI

STEADY MHD FLOW OF MICROPOLAR FLUID BETWEEN TWO ROTATING CYLINDERS WITH POROUS LINING

[1.] DEPARTMENT OF MATHEMATICS, GITAM UNIVERSITY, HYDERABAD CAMPUS,RUDRARAM, MEDAK DIST (A.P) - 506004, INDIA
[2.] DEPARTMENT OF MATHEMATICS, NIT, WARANGAL (A.P) -506004, INDIA
[3.] DEPARTMENT OF MATHEMATICS, MACHILIPATNAM ENGINEERING COLLEGE, MACHILIPATNAM, KRISHNA DISTRICT, AP, INDIA

ABSTRACT: The steady flow of an electrically conducting, incompressible micropolar fluid in a narrow gap between two concentric rotating vertical cylinders, with porous lining on inside of outer cylinder, under an imposed axial magnetic field is studied. Beavers and Joseph slip condition is taken at the porous lining boundary. The velocity profiles, coefficient of skin friction on the cylinders are calculated. The effects of Hartmann number, the porous lining thickness parameter, coupling number, couple stress parameters and Reynolds number on azimuthal velocity, micro-rotation component and coefficient of skin friction on cylinders are depicted through graphs.
KEYWORDS: Micropolar fluid; Magnetic field; porous lining; Skin friction; Angular velocity; micro-rotation vector

INTRODUCTION

Micropolar fluids are fluids with microstructures. They belong to a class of fluids with a non-symmetric stress tensor. Micropolar fluids consist of rigid, randomly oriented spherical particles with their own spins and micro-rotations, suspended in a viscous medium. The concept of micro-rotation was proposed by Cosserat and Cosserat in the theory of elasticity [1]. In the middle of the 1960s, Condiff and Dahler [2] and Eringen [3] applied the concept to describe fluids with microstructures. Recently, a comprehensive text book on micropolar fluids has been published [4]. Physical examples of micropolar fluids can be seen in ferrofluids [5], blood flows [6, 7], bubbly liquids [8], liquid crystals [9], and so on, all of them containing intrinsic polarities. Thus, micropolar fluid mechanics is not a useless generalization of the Navier-Stokes model, but is a physically relevant model that has many applications. Flows through and past porous media with finite thickness are of relevance in many industrial applications like lubrication and tapping of solar energy. The control of shearing stress is important in the design of rotating machinery like totally enclosed fan cooled motors and lubrication industry in which centrifugal force plays a major role.

Channabasappa et al [10] have examined the effect of porous lining thickness on velocity vector and shear stresses at the wall of inner and outer cylinders for the flow between two rotating cylinders. Sai [11] has studied the steady motion of an electrically conducting, incompressible viscous liquid in a narrow gap between two concentric rotating vertical cylinders in presence of an imposed magnetic field and he has presented the velocity profiles graphically. Bathaiah et al [12] have studied the viscous incompressible, slightly conducting fluid flow between two concentric rotating cylinders with non-erodable and non conducting porous lining on the inner wall of the outer cylinder under the influence of radial magnetic field of the form given in Hughes and Young and they have shown the effect of magnetic parameter, porous lining thickness, the ratio of the velocities of the cylinders, the slip parameter on velocity and temperature distributions graphically. Beavers and Joseph [13] studied the flow of a viscous fluid in a channel bounded below by a naturally permeable wall. Ramamurthy [14] have obtained the velocity distribution and magnetic field for a viscous incompressible conducting fluid between two coaxial rotating cylinders under the influence of radial magnetic field. Singh et al [15] have investigated the impulsive motion of a viscous liquid contained between two concentric circular cylinders in the presence of radial magnetic field. Mahapatra [16] studied the unsteady motion of an incompressible viscous conducting liquid between two porous concentric circular cylinders in presence of a radial magnetic field. Subotic et al [17] have obtained the analytical solutions for the flow and temperature fields in an annulus with a porous sleeve between two rotating cylinders and they studied the effects of Darcy number, Brinkman number and porous sleeve thickness on the velocity profile and temperature distribution. Ranganna et al [18] have studied the stability analysis of laminar flow between two long concentric circular rotating cylinders with non-erodible porous lining on the outer wall of the inner cylinder and he has shown the effect of porous lining thickness on critical Taylor

number graphically. Kamel [19] has studied the creeping motion of a polar fluid in the annular region between the two eccentric rotating cylinders. He depicted the dependence of the velocity components and the spin on the coupling number and the length ratio graphically. Meena et al [20] have studied the flow of a viscous incompressible fluid between two eccentric rotating porous cylinders with small suction/injection at both the cylinders and they have presented stream lines and pressure plots graphically. Borkakati et al [21] have examined the steady flow of an incompressible electrically conducting fluid between two coaxial cylinders in presence of radial magnetic field and they plotted graphically the heat transfer rate from the cylinders against the Hartmann number.

Srinivasacharya et al [22] have studied the steady flow of incompressible and electrically conducting micropolar fluid flow between two concentric porous cylinders and they have presented the profiles of velocity and micro-rotation components for different micropolar fluid parameters and magnetic parameter. Pontrelli et al [23] studied the steady flow of an Oldroyd-B fluid between two porous concentric circular cylinders. They found velocity by numerically solving a system of nonlinear ODEs obtained from the equation of motion and constitutive equations and the effects of non-Newtonian parameters on velocity and on shear stress are shown through graphs.

Fetecau et al [24] studied the velocity fields corresponding to the motion of an incompressible second grade fluid due to longitudinal and torsional oscillations of an infinite circular cylinder.

In this paper, we study the steady incompressible electrically conducting micropolar fluid flow between two concentric rotating cylinders with porous lining in the presence of an axial magnetic field.

FORMULATION AND SOLUTION OF THE PROBLEM

Consider an incompressible micropolar fluid between two concentric circular cylinders of radii a and b (a<b). The inner and outer cylinders are rotating with constant angular velocities Ω_1 and Ω_2 respectively.

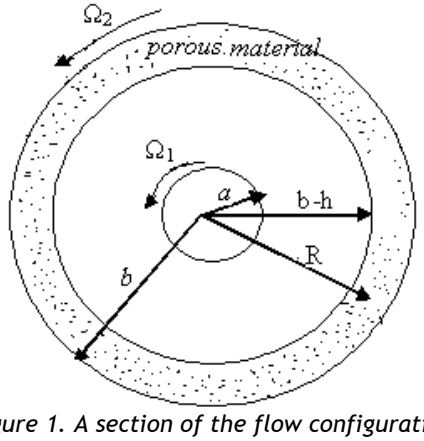

Figure 1. A section of the flow configuration

There is a non-erodible porous lining of thickness h on the inside of the outer cylinder. The flow is generated due to the rotation of these cylinders. The flow is subject to a constant magnetic field B_0 along the axis of the cylinders and no external electric field is applied. We assume that the induced magnetic field is much smaller than the externally applied magnetic field. Assume that the magnetic Reynolds number is very small, so that induced magnetic field and electric field produced by the motion of the electrically conducting fluid are negligible. The physical model of the problem is shown in Figure 1.

Choose the cylindrical polar coordinate system (R, θ, Z) with origin at the centre of the cylinder and Z axis along the axis of the cylinder and with (e_r, e_θ, e_z) as unit base vectors. Neglecting body forces and body couples, the field equations governing the micropolar fluid dynamics are:

$$\nabla_1 \cdot Q = 0 \qquad (1)$$

$$\rho Q.\nabla_1 Q = -\nabla_1 P + \kappa \nabla_1 \times l - (\mu + \kappa) \nabla_1 \times \nabla_1 \times Q + J \times B \qquad (2)$$

$$\rho j Q.\nabla_1 l = -2\kappa l + \kappa \nabla_1 \times Q - \gamma \nabla_1 \times \nabla_1 \times l + (\alpha + \beta + \gamma) \nabla_1 (\nabla_1 \cdot l) \qquad (3)$$

where Q is velocity vector, l is micro rotation vector, P is the fluid pressure, ρ and j are the fluid density and micro-gyration parameter, and {μ, κ}and {a, B, γ}are viscosity and gyro viscosity coefficients. The current density J, magnetic field B and electric field E are related by Maxwell's equations

$$\nabla_1 \times E = \frac{\partial B}{\partial t}, \quad \nabla_1 \cdot B = 0, \quad \nabla_1 \times B = \mu' J, \quad \nabla_1 \cdot J = 0$$

$$\text{and } J = \sigma_e (E + Q \times B)$$

where ∇_1 is the dimensional gradient, σ_e is electrical conductivity and μ' is the magnetic permeability. By nature of the flow, the velocity and micro-rotation components are axially symmetric and depend only on radial distance. Hence we assume that the velocity, micro-rotation vectors and the magnetic field are of the form

$$Q = V(r)\, e_\theta,\ l = C(r)\, e_z,\ B = B_0\, e_z \qquad (4)$$

Hence J×B simplifies to $J \times B = -\sigma_e B_0^2 Q$.

We introduce the following non-dimensional scheme

$$q = \frac{Q}{b\Omega_2}, \quad r = \frac{R}{b}, \quad v = \frac{l}{\Omega_2}, \quad p = \frac{P}{\rho b^2 \Omega_2^2}, \quad v = \frac{V}{b\Omega_2},$$

$$C = \frac{C}{\Omega_2} \quad r_0 = \frac{a}{b}, \quad \lambda = \frac{\Omega_1}{\Omega_2},$$

$$v_B = \frac{V_B}{b\Omega_2}, \quad e = \frac{h}{b}, \quad \sigma = \frac{b}{\sqrt{K}} \qquad (5)$$

Using (5) in (2) and (3) we get the equations for the flow in the following form

$$Re q.\nabla q = -Re \nabla p + c \nabla \times v - \nabla \times \nabla \times q - M^2 q \qquad (6)$$

$$\varepsilon q.\nabla v = -2s v + s \nabla \times q - \nabla \times \nabla \times v + \frac{1}{\delta} \nabla (\nabla \cdot v) \qquad (7)$$

where the non-dimensional parameters viz. Reynolds number Re, Hartmann number M, cross viscosity parameter or coupling number c, couple stress parameters s and δ and gyration parameter ε are defined by

$$Re = \frac{\rho b^2 \Omega_2}{\mu + \kappa}, \quad M = \sqrt{\frac{\sigma_e B_0^2 b^2}{\mu + \kappa}}, \quad c = \frac{\kappa}{\mu + \kappa}, \quad \varepsilon = \frac{\rho j b^2 \Omega_2}{\gamma},$$

$$s = \frac{\kappa b^2}{\gamma}, \quad \delta = \frac{\gamma}{\alpha + \beta + \gamma} \qquad (8)$$

The velocity and micro-rotation are choosen in the form

$$q = v(r)e_\theta \quad \text{and} \quad v = C(r)e_z \tag{9}$$

Substituting (9) in (6) and comparing the components along e_r, e_θ directions, we get

$$\frac{dp}{dr} = \frac{v^2}{r} \tag{10}$$

$$-c\frac{dC}{dr} + D^2 v - M^2 v = 0 \tag{11}$$

where $D^2 = \frac{d^2}{dr^2} + \frac{1}{r}\frac{d}{dr} - \frac{1}{r^2}$

Similarly using (9) in the equation (7), the axial direction component yields the following equation for micro-rotation C.

$$-2sC + s\left(\frac{dv}{dr} + \frac{v}{r}\right) + \left(\frac{d^2C}{dr^2} + \frac{1}{r}\frac{dC}{dr}\right) = 0 \tag{12}$$

Eliminating $\frac{dC}{dr}$ value from (11) and (12) we get the following equation for v as

$$D^4 v - \left(M^2 + (2-c)s\right)D^2 v + 2sM^2 v = 0$$

This can be expressed as

$$\left(D^2 - \lambda_1^2\right)\left(D^2 - \lambda_2^2\right)v = 0 \tag{13}$$

where

$$\lambda_1^2 + \lambda_2^2 = M^2 + s(2-c) \quad \text{and} \quad \lambda_1^2\lambda_2^2 = 2sM^2$$

As q is finite between the interval $r_0 < r < r_1 = 1-e$, the solution of (13) can be written as

$$v(r) = a_1 I_1(\lambda_1 r) + a_2 K_1(\lambda_1 r) + a_3 I_1(\lambda_2 r) + a_4 K_1(\lambda_2 r) \tag{14}$$

The constants a_1, a_2, a_3 and a_4 can be found by using the no slip boundary condition on azimuthal velocity v and hyper-stick boundary condition on micro-rotation C. These conditions at the inner cylinder and at the porous lining of outer cylinder are explicitly given as below.

BOUNDARY CONDITIONS

The equations (14) is solved for the velocities v and C, and can be found by using the boundary conditions

$V = a\Omega_1$ at $R = a$

$V = V_B$ at $R = b-h$

$$l_\Gamma = \frac{1}{2} curl\, Q_\Gamma \quad \text{at } R=a \tag{15}$$

$$l_\Gamma = 0 \quad \text{at } R = b-h$$

where Γ represent the boundary of inner cylinder and V_B is the slip velocity obtained by using Beavers and Joseph condition

$$\frac{dV}{dR} = \frac{\alpha}{\sqrt{K}}\left(V_B - Q_D\right) \quad at\ R = b-h \tag{16}$$

a is the slip parameter, K is the porosity of the lining material, λ is the ratio of the angular velocities of the cylinders, Q_D is the Darcy velocity in the porous lining. In equation (16), the Darcy's velocity Q_D is given by the relation

$$Q_D = R\Omega_2 + \Phi \tag{17}$$

where $\Phi = \frac{K}{\mu}\frac{\int_0^{2\pi}\int_{b-h}^{b}\rho R\ \Omega_2^2\ (Rd\theta dR)}{\int_0^{2\pi}\int_{b-h}^{b}(Rd\theta dR)}$

which on simplification is given by

$$\Phi = \frac{2K\ \Omega_2^2\rho}{3\mu}\left(\frac{3b^2 - 3bh + h^2}{2b - h}\right) \tag{18}$$

The expression for Φ, as given above, is the one considered by Channabasappa et al [10]. In relation (17), the two terms on RHS arise due to the rotation of the porous medium along with the outer cylinder. Using the four boundary conditions of (15) in non-dimensional form for velocity and micro-rotation components, we get the following equations

$$\begin{gathered} a_1 I_1(\lambda_1 r_0) + a_2 K_1(\lambda_1 r_0) + a_3 I_1(\lambda_2 r_0) + a_4 K_1(\lambda_2 r_0) = \lambda r_0 \\ a_1\Delta_1 + a_2\Delta_2 + a_3\Delta_3 + a_4\Delta_4 = \Delta_5 \\ a_1\Delta_6 + a_2\Delta_7 + a_3\Delta_8 + a_4\Delta_9 = 2sc\lambda \\ a_1\Delta_{10} + a_2\Delta_{11} + a_3\Delta_{12} + a_4\Delta_{13} = 0 \end{gathered} \tag{19}$$

where: $\Delta_1 = \alpha\sigma I_1(m_1) - \frac{I_1(m_1)}{1-e} - \lambda_1 I_2(m_1)$

$$\Delta_2 = \alpha\sigma K_1(m_1) - \frac{K_1(m_1)}{1-e} + \lambda_1 K_2(m_1)$$

$$\Delta_3 = \alpha\sigma I_1(m_2) - \frac{I_1(m_2)}{1-e} - \lambda_2 I_2(m_2)$$

$$\Delta_4 = \alpha\sigma K_1(m_2) - \frac{K_1(m_2)}{1-e} + \lambda_2 K_2(m_2)$$

with $m_1 = \lambda_1(1-e)$ and $m_2 = \lambda_2(1-e)$

$$\Delta_5 = \frac{3\alpha\sigma^2(e-1)(e-2)(1-c) + 2\alpha\, Re\left(e^2 - 3e + 3\right)}{3\sigma(2-e)(1-c)}$$

$$\Delta_6 = \left(sc + \lambda_1^2 - M^2\right)\left(\frac{2I_1(\lambda_1 r_0)}{r_0} + \lambda_1 I_2(\lambda_1 r_0)\right)$$

$$\Delta_7 = \left(sc + \lambda_1^2 - M^2\right)\left(\frac{2K_1(\lambda_1 r_0)}{r_0} - \lambda_1 K_2(\lambda_1 r_0)\right)$$

$$\Delta_8 = \left(sc + \lambda_2^2 - M^2\right)\left(\frac{2I_1(\lambda_2 r_0)}{r_0} + \lambda_2 I_2(\lambda_2 r_0)\right)$$

$$\Delta_9 = \left(sc + \lambda_2^2 - M^2\right)\left(\frac{2K_1(\lambda_2 r_0)}{r_0} - \lambda_2 K_2(\lambda_2 r_0)\right)$$

$$\Delta_{10} = \left(sc + \lambda_1^2 - M^2\right)\left(\frac{2I_1(m_1)}{1-e} + \lambda_1 I_2(m_1)\right)$$

$$\Delta_{11} = \left(sc + \lambda_1^2 - M^2\right)\left(\frac{2K_1(m_1)}{1-e} - \lambda_1 K_2(m_1)\right)$$

$$\Delta_{12} = \left(sc + \lambda_2^2 - M^2\right)\left(\frac{2I_1(m_2)}{1-e} + \lambda_2 I_2(m_2)\right)$$

and $\Delta_{13} = \left(sc + \lambda_2^2 - M^2\right)\left(\frac{2K_1(m_2)}{1-e} - \lambda_2 K_2(m_2)\right)$

The linear systems of equations in (19) are solved numerically using Mathematica for the four constants a_1, a_2, a_3, and a_4 for various values of micropolar parameters.

SKIN FRICTION

The constitutive equation for stress tensor is given by

$$T_{ij} = -P\delta_{ij} + (2\mu + \kappa)e_{ij} + \kappa\varepsilon_{ijm}(\omega_m - l_m) \tag{20}$$

where **ω** is the vorticity vector, e_{ij} is shear rate tensor, δ_{ij} is the Kronecker delta and ε_{ijm} is the alternating symbol. From equation (20), we get

$$\bar{T}_{r\theta} = \frac{dv}{dr} - (1-c)\frac{v}{r} - c\,C \tag{21}$$

where $\bar{T}_{r\theta} = \dfrac{T_{r\theta}}{\Omega_2 (\mu + k)}$ is the non dimensional stress.

Hence the coefficient of skin friction on the inner and outer cylinders is given by

$$C_f = \frac{2T_{r\theta}}{\rho U^2} \text{ at } R=a \text{ and } R=b-h \qquad (22)$$

where U = Characteristic velocity = $b\Omega_2$

This can be written in the following non-dimensional form as

$$C_f = \frac{2\bar{T}_{r\theta}}{Re} \text{ at } r=r_0 \text{ and } r=1-e \qquad (23)$$

TORQUE

The torque acting on the cylinders about the common axis of the cylinders is given by

$$\tau = (T_{r\theta} \times 2\pi R) \times R \,. \qquad (24)$$

Hence the non dimensional torque on inner and outer cylinders are calculated as

$$\bar{\tau}_{in} = 2\pi r_0^2 \, \bar{T}_{r\theta}\big|_{r = r_0}$$

and

$$\bar{\tau}_{out} = 2\pi (1-e)^2 \, \bar{T}_{r\theta}\big|_{r=1-e} \qquad (25)$$

RESULTS AND DISCUSSIONS

The velocity filed is considered along tangential (azimuthal) direction only. In fact we can start with nonzero radial velocity and come to conclude that it should vanish by considering continuity equation and the condition that there is no suction on the walls. (See Channabasappa, Umapathy and Nayak [10].)

We have investigated the effects of the Hartmann number M, the porous lining thickness parameter e, Reynolds number Re, coupling number c and couple stress parameter s on azimuthal velocity v, micro-rotation velocity C and the coefficient of skin friction at the inner and outer cylinders are numerically obtained and are depicted through Figures 2 to 19. The azimuthal velocity v and Micro-rotation velocity C are computed for different values of M and e.

Figures 2-7 shows the azimuthal velocity v and micro-rotation velocity C against distance r for different values of M at a fixed value of porous lining thickness parameter e = 0.1, 0.3, 0.4. We have observed that v decreases as e increases and C increases as e increases. Both v and C decrease as M increases. It is observed that the nature of velocity profiles v is increasing with distance where as the nature of rotation C is increasing and decreasing as M increases. But for small values of M, C is decreasing with r. When M takes large values, the values of C are near to zero. i.e rotation of the particles can be neglected.

The Figures 2, 4 and 6 of velocity v are in good agreement with the results obtained by Bathaih and Venugopal [12] and Subotic and Lai [17], when there is no applied magnetic field (the curve with M =0.0001 indicates almost no magnetic field). Figures 8 and 9 give the velocity profiles v and C for different values of c. From this it is clear that an increase in coupling parameter c increases the values of both the velocities v and C. i.e. if micro-polarity of the fluid increases, the velocity v and micro-rotation C will also increase. In Figures 10 and 11 the velocity profiles v and C plotted against Re. From this it is clear that an increase in Re increases both the velocities.

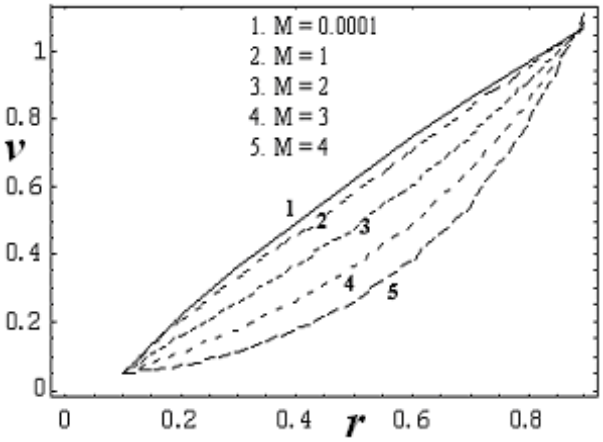

Figure 2. Variation of v with r at e = 0.1

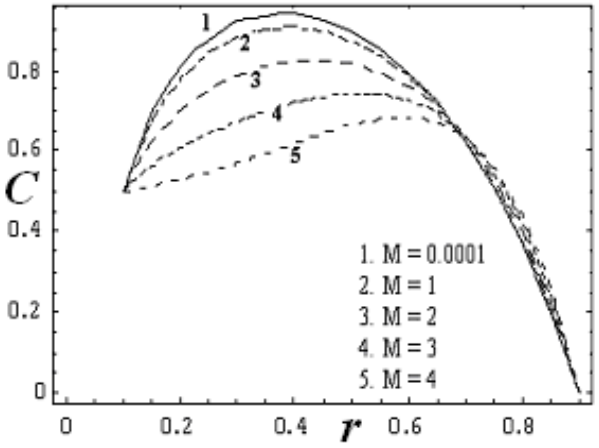

Figure 3. Variation of C with r at e = 0.1

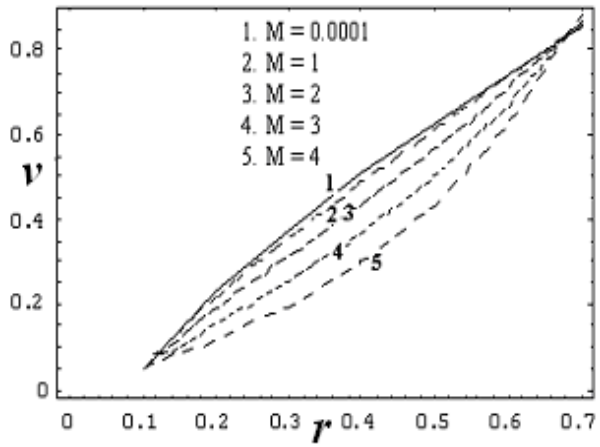

Figure 4. Variation of v with r at e = 0.3

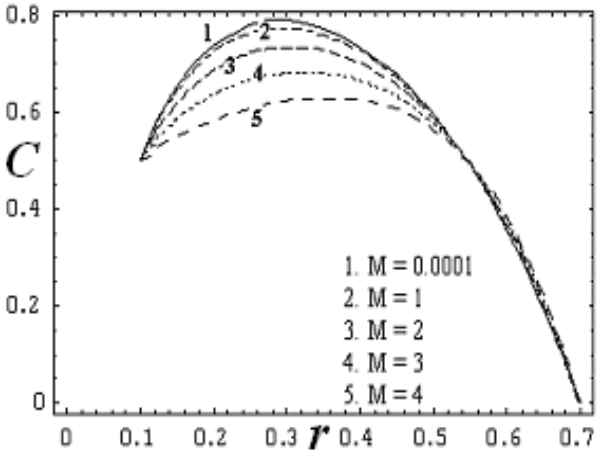

Figure 5. Variation of C with r at e = 0.3

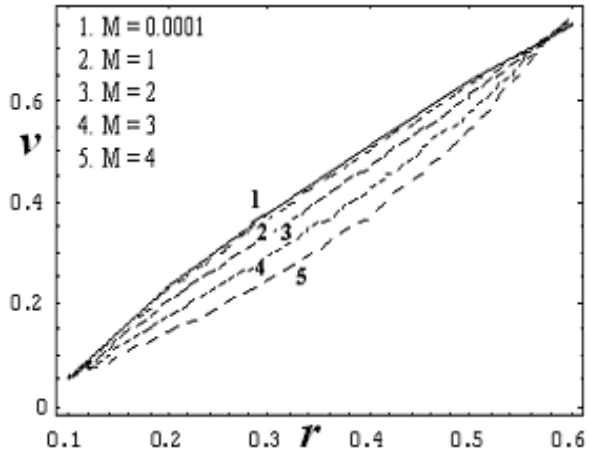

Figure 6. Variation of v with r at e = 0.4

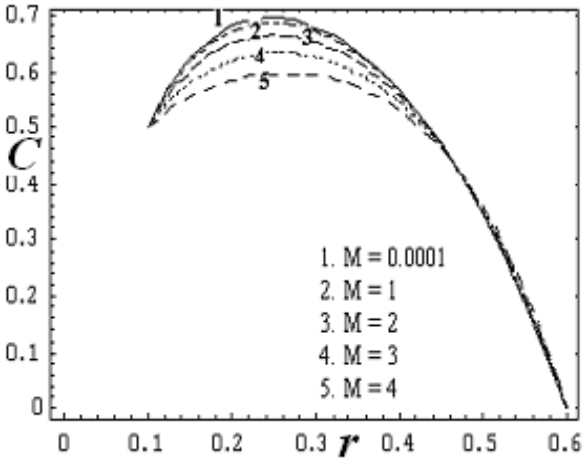

Figure 7. Variation of C with r at e = 0.4

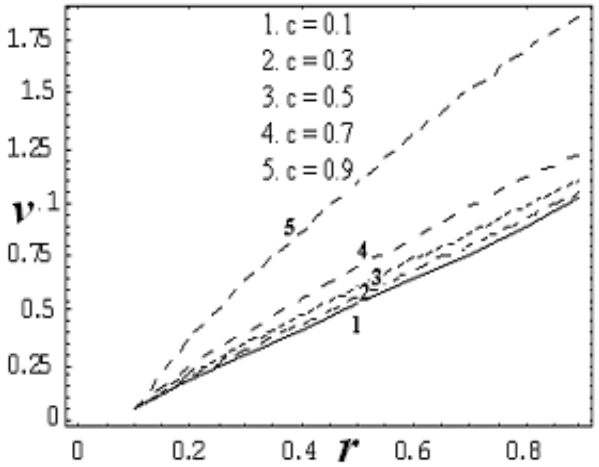

Figure 8. Variation of v with r

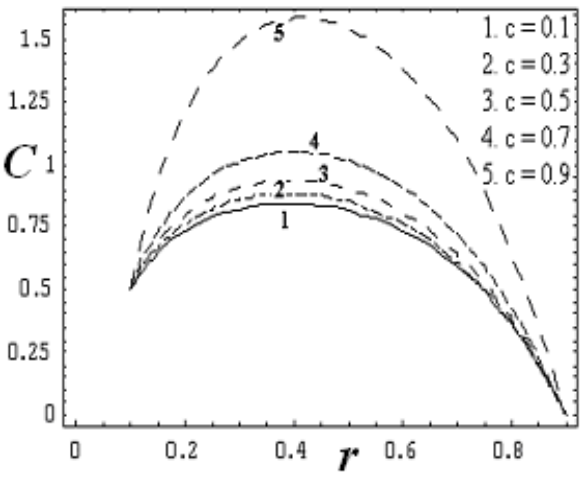

Figure 9. Variation of C with r

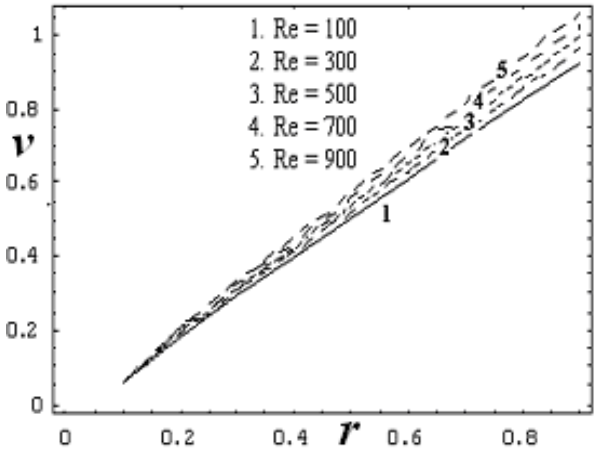

Figure 10. Variation of v with r

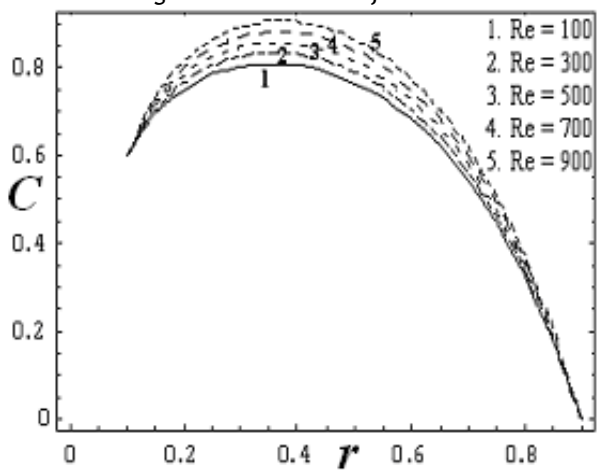

Figure 11. Variation of C with r

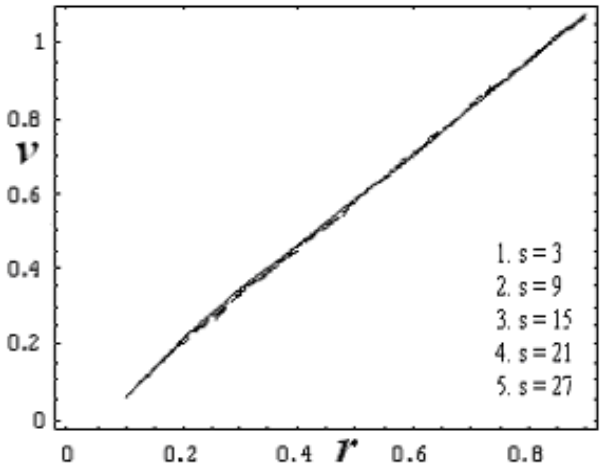

Figure 12. Variation of v with r

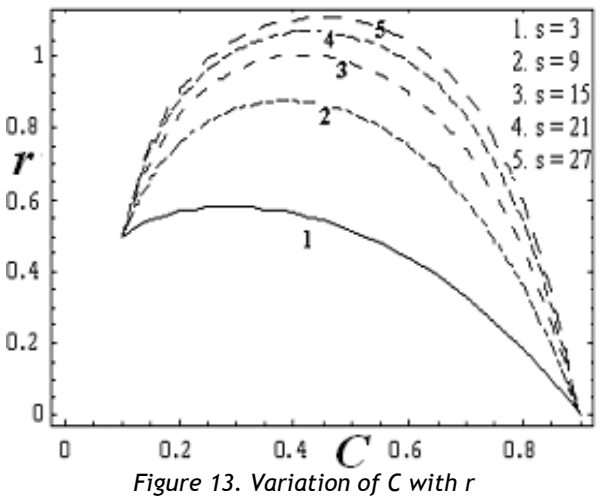

Figure 13. Variation of C with r

Figures 12-13 we have seen that as the couple stress parameter s increases both the velocities v and C are increasing. But the effect of s on the values of v is not very significant. i.e., the variation in the values of s does not result in much variation in the values v.
Figures 14-16 show the variation the coefficient of skin friction $C_f\big|_{in}$ *at the inner cylinder against c for different values of M, Re, s.*
We observe that $C_f\big|_{in}$ *decreases with increasing values of M, Re, s whereas in Figures 17-19, the skin-friction* $C_f\big|_{out}$ *at the outer cylinder increases with increasing values of M, Re, s.*

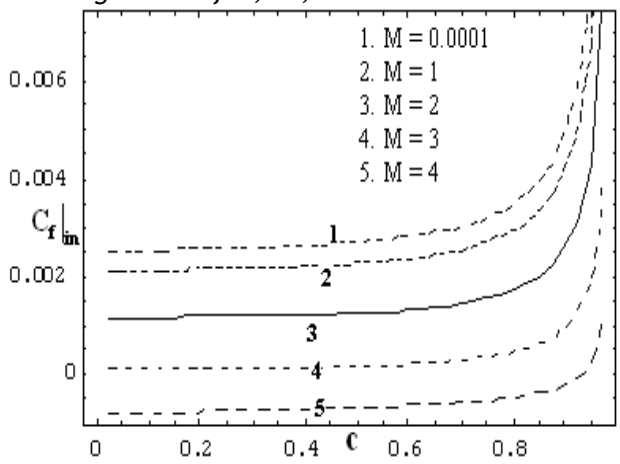

Figure 14. Variation of $C_f\big|_{in}$ *with c*

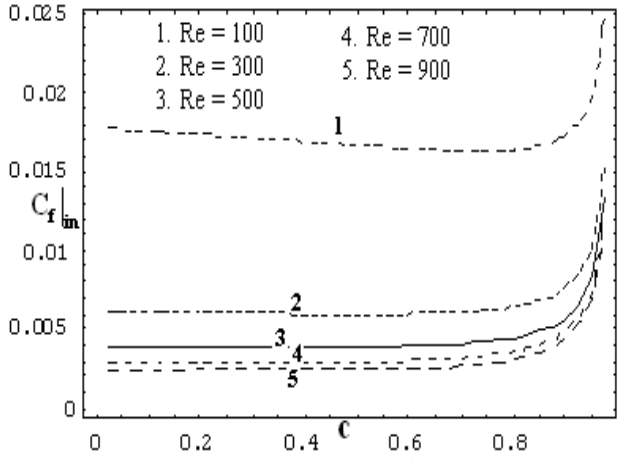

Figure 15. Variation of $C_f\big|_{in}$ *with c*

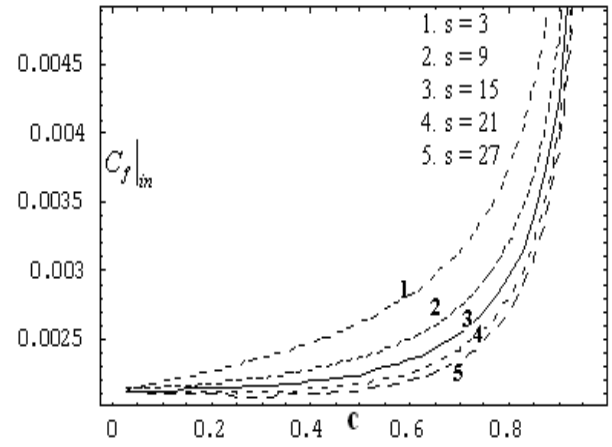

Figure 16. Variation of $C_f\big|_{in}$ *with c*

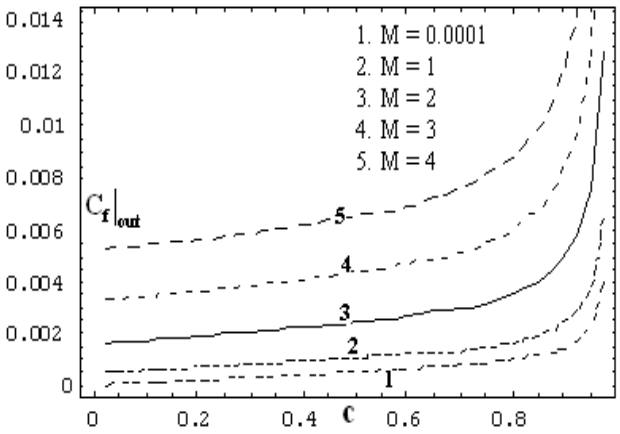

Figure 17. Variation of $C_f\big|_{out}$ *with c*

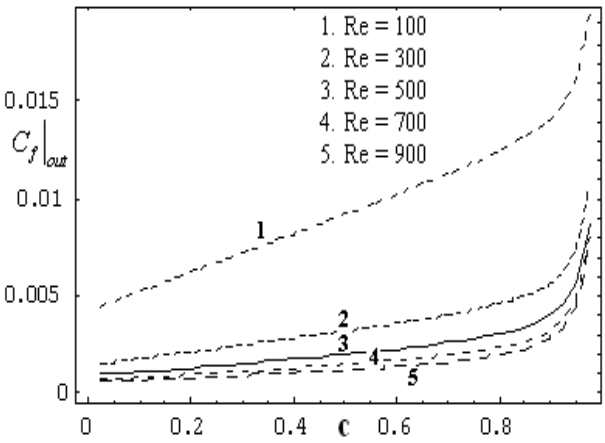

Figure 18. Variation of $C_f\big|_{out}$ *with c*

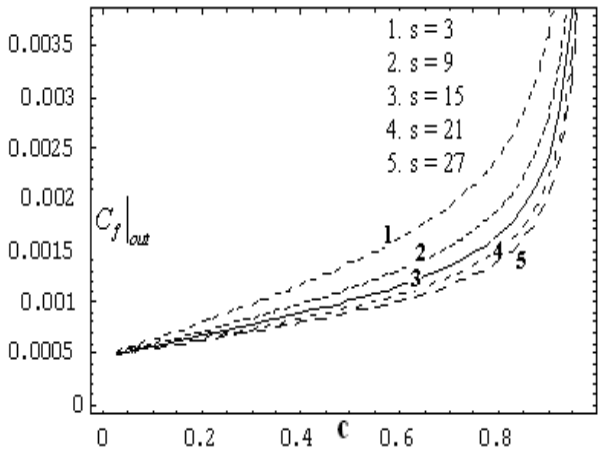

Figure 19. Variation of $C_f\big|_{out}$ *with c*

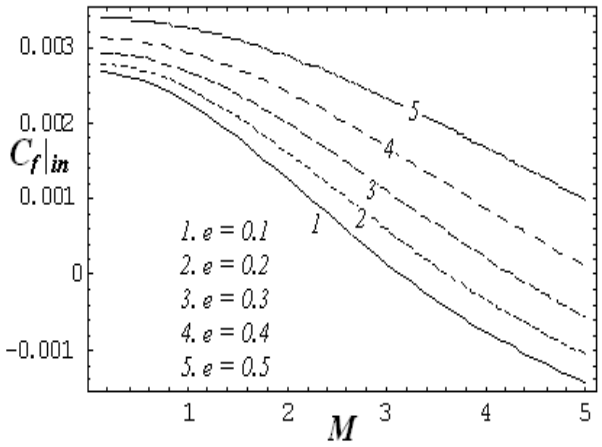

Figure 20. Variation of $C_f\big|_{in}$ *with e*

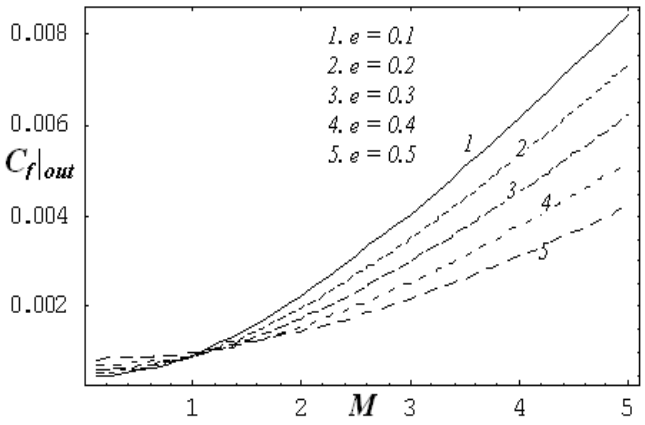

Figure 21. Variation of $C_f|_{out}$ with e

Figures 20-21 show the variation of the coefficient of skin friction at inner and outer cylinders against M for different values of e.

We observe that $C_f|_{in}$ increases, whereas $C_f|_{out}$ decreases with increasing values of e. These results are in correlation with the results of Bathiah and Venugopal [12].

CONCLUSIONS

In this paper, the effect of axial magnetic field on micropolar fluid flow due to steady rotation of concentric cylinders with inner porous lining is examined. It is observed that

1. *Micro-polarity of the fluid affects the velocity but couple stress parameter can not affect the velocity profiles*
2. *As magnetic field strength increases velocity decreases and micro-rotation of the particles decreases and there by skin friction decreases at inner cylinder and increases at outer cylinder*
3. *As porous lining thickness increases, the skin friction at the inner cylinder increases and at the outer cylinder decreases.*

REFERENCES

[1.] E. Cossera and F. Cosserat, Theorie des Corps Deformables. (A. Hermann, Paris) (1909).

[2.] D.W. Condiff and J.S. Dahler, Fluid mechanical aspects of anti-symmetric stress, Phys. Fluids, 7, 842-854, (1964).

[3.] A.C. Eringen, Theory of micropolar fluids, J. Math. Mech, 16, 1-18, (1966).

[4.] G.Lukaszewicz, "Micropolar fluids theory and applications", Birkhauser, Boston, (1999).

[5.] R.E. Rosensweig, Ferrohydro-dynamics, Cambridge University Press, Cambridge, (1985).

[6.] M.A. Turk, N.D. Syvester and T. Ariman, Amicrocontinuum model of blood with deformable cells, ASME Biomechanics symposium (Edited by Y.C. Fung and J.A.Brighton), (1973).

[7.] Bugliarello G., Sevilla J., Velocity distribution and other characteristics of steady and pulsatile blood flow in glass tubes, Biorheology, 7, 85-107, (1970).

[8.] A.C. Eringen, Theory of thermo-microstretch fluids and bubbly liquids, Int. J. Eng. Sci. 28, 133-143, (1990).

[9.] P.G. de Gennes and J. Prost, The Physics of Liquid Crystals, 2nd ed. Oxford University Press, Oxford, (1993).

[10.] M.N. Channabasappa, K.G.Umapathy and I.V. Nayak, Effect of porous lining on the flow between two concentric rotating cylinders, Proc. Indian Acad. Sci., 88 A III, 163-167, (1979).

[11.] K.S. Sai, MHD flow between two rotating cylinders with porous lining, Rev. Roum. Phys, 30, 119-125, (1985).

[12.] D. Bathaiah and R. Venugopal, Effect of porous lining on the MHD flow between two concentric rotating cylinders under the influence of a radial magnetic field, Acta. Mech, 44, 141-158, (1982).

[13.] G.S. Beavers and D.D. Joseph, Boundary conditions at a naturally permeable wall, J. Fluid. Mec, 30,197-207, (1967).

[14.] P. Ramamurthy, Flow between two concentric rotating cylinders with a radial magnetic field, Phys. Fluids 4, 1444, (1961).

[15.] D. Singh and Syed Ali Tahir Rizvi Unsteady motion of a conducting liquid between two infinite coaxial cylinders, Phys.Fluids, 7,760-761, (1964).

[16.] J.R. Mahapatra, A note on the unsteady motion of a viscous conducting liquid between two porous concentric circular cylinders acted on by a radial magnetic field, Appl. sci. res, 27, 274-282, (1973).

[17.] M. Subotic and F.C. Lai, Flows between rotating cylinders with a porous lining, J. of Heat Transfer, 130, 102601(1-6), (2008).

[18.] M.N. Chinnabasappa, G. Ranganna and B. Rajappa, Stability of couette flow between rotating cylinders lined with porous material-I, Indian J.Pure Appl.Math, 14 (6), 741-756, (1983).

[19.] M.T. Kamel, Flow of a polar fluid between two eccentric rotating cylinders, J. of Rheol., 29 (1), 37-48, (1985).

[20.] S. Meena, P. Kandaswamy and Lokenath Debnath, Hydrodynamic flow between two eccentric cylinders with suction at the porous walls, Int. J math. maths sci,25 (2),93-113, (2001).

[21.] A.K. Borkakati and I. Pop, MHD Heat transfer in the flow between two coaxial cylinders, Acta Mech., 51, 97-102, (1984).

[22.] D. Srinivasacharya and M. Shiferaw Numerical solution to the MHD flow of micropolar fluid between two concentric porous cylinders, Int. J. of Appl. Math. Mech, 4(2), 77-86, (2008).

[23.] G. Pontrelli and R.K. Bhatnagar, Flow of a viscoelastic fluid between two rotating circular cylinders subject to suction or injection, Int. J for Numer. Methods in Fluids, 24, 337-349, (1997).

[24.] C. Fetecau and Corina Fetecau, Starting solutions for the motion of a second grade fluid due to longitudinal and torsional oscillations of a circular cylinder, Int. J of Engg. sci, 44, 788-796, (2006).

ACTA TECHNICA CORVINIENSIS - Bulletin of Engineering

ISSN: 2067-3809 [CD-Rom, online]

ACTA TECHNICA CORVINIENSIS - BULLETIN of ENGINEERING

ISSN: 2067-3809 [CD-Rom, online]

ACTA TECHNICA CORVINIENSIS - BULLETIN of ENGINEERING

ISSN: 2067-3809 [CD-Rom, online]

copyright © UNIVERSITY POLITEHNICA TIMISOARA,
FACULTY OF ENGINEERING HUNEDOARA,
5, REVOLUTIEI, 331128, HUNEDOARA, ROMANIA
http://acta.fih.upt.ro

ACTA TECHNICA CORVINIENSIS – Bulletin of Engineering
Tome VI (Year 2013) – FASCICULE 3 [July–September]
ISSN 2067–3809

[1.] Martin KOVÁČ, [2.] Ivan BURANSKÝ

EXPERIMENTAL DETERMINATION OF MILLING MODEL FOR THIN-WALLED PARTS

[1,2.] SLOVAK UNIVERSITY OF TECHNOLOGY, FACULTY OF MATERIALS SCIENCE AND TECHNOLOGY IN TRNAVA, INSTITUTE OF PRODUCTION TECHNOLOGIES, CENTRE OF EXCELLENCE 5 AXIS MACHINING, J. BOTTU 25, 917 24 TRNAVA, SLOVAKIA

ABSTRACT: An article deals with the experimental determination of milling model for thin-walled parts. The determination of milling model is one of basic characteristics for calculating cutting forces and chip thickness. The calculation of milling model is analytically and numerically by finite element method. Experiment is performed with modal hammer. With modal hammer is determined dynamic elasticity for work-piece and tool. In the first section is summarized the basic knowledge of thin-walled parts. Inn experimental part is described Frequency Response Function and application of this technique. The last part of this work is to evaluate the experiment, which compared different techniques to determinate milling model during machining thin-walled parts.
KEYWORDS: thin walled parts, milling, milling model, frequency response function, rigidity

INTRODUCTION

The thin-walled parts are widely used in the aviation, aeronautics, automotive and energetic industry. Due to its shapes and low rigidity thin-walled parts easily deform during the milling process. The thin-walled structures are very easy to deform under the cutting force, which will influence to surface quality and accuracy. In finishing milling process, the thickness of the parts is reducing progressively, which makes it even more difficult to control the accuracy of machining. A lot of significant work was done in the predicting the deformation of thin-walled parts. Most researchers reflect that elastic deformation caused by the cutting force is the main factor of part deflection. The main topic of these scholars is to establish cutting forces, use finite element method for simulate the milling process or predict the deformation of the thin-walled parts.The thin-walled plates are that the thickness h is smaller than the minimal dimension of middle plane b, i.e. (1/80~1/100)b<<h<<(1/8~1/5)b [1]. Very flexible components are considered to have a wall thickness thinner than 5 mm and an axial depth of cut larger than 30 mm [2]. Budak and Altintas [2] view the tool and part as elastic figures and they investigated the error of peripheral milling process. The deformations in milling operations have been done several researches [3],[4]. Ratchev [4] investigate the compensation strategy specifically focused on force induced errors in milling. The finite element method for calculation of the deformation thin-walled parts and NC compensation method was done by Ning [5]. Liu [6] studied milling model especially rigid work-piece and flexible tool. Flexible work-piece a rigid tool of the milling process was done and describe by Seguy [7]. Dynamic milling model, flexible work-piece and flexible tool, was described in [8].In this paper, the milling model for thin-walled part is analyzed and set. Rigidity of tool and thin-walled part in bending is solved by analytically and numerically.

RIGIDITY OF TOOL AND THIN-WALED PART BENDING

Technological set rigidity is concerned with resistance to elastic deformations. Its influence in machining especially appears in the issue of accuracy in machining due to the occurrence of vibration [9]. According to various authors, rigidity in bending can be defined as follows: according to [10] the solid rigidity means it is resistant to elastic deformation. With respect to the theory of elasticity and rigidity, in the rigidity k we usually determine: solid rigidity k as a relation of Fy force and y deflection. Where y deflection is in the direction of Fy force action. The rigidity of parts and construction is evaluated via a k rigidity coefficient, which is defined as the ratio of the part load value and deformation. We can speak about specific rigidities like, rake rigidity, bending rigidity, torsion stiffness and joint rigidity. In machining we are chiefly interested in bending rigidity, which can be expressed as follows:

$$k = \frac{F_y}{y} \qquad (1)$$

where k [N.m^{-1}] is coefficient of bending rigidity, F [N] is loading force, y [m] is size of deflection.

RIGIDITY OF THIN-WALED PART IN BENDING

Technological set rigidity refers to resistance to elastic deformations and its influence on machining. It is especially found in the work of [9]: machining accuracy, vibration origin. In general, there is the principle that the increased rigidity of a tool and work-piece set prevents vibration from occurring in machining. The rigidity and mass of the tool and work-piece determine the vibration frequency. Thin-walled part rigidity cause changes in the cutting

process because of material takeoff in the form of a chip. To determine rigidity, it is necessary to locate the thin-walled part bending. The bending can be determined analytically or numerically via finite element method. However, the analytical determination of a thin-walled part deflection is quite demanding. Therefore, y deflection of the thin-walled par was determined by finite element method. The thin-walled part was exposed to the load of F solitary force. The wall deflection was measured at the point of the loading force. According to [1] the smallest deflection is in the point (position one) of the load force F (Figure 1) and the greatest deflection is in the point (position two) of the load force F (Figure 2). After the determination of static rigidity via finite element method, the part dimensions were as follows: height x width x thickness, 80x80x10 to 1 mm. The grey color depicts the wall restrain. The load force F acted on the point 75 mm, 40 mm (in the middle of the part) and in the other case, it acted on the point 75 mm, 100 (on the edge of a part).

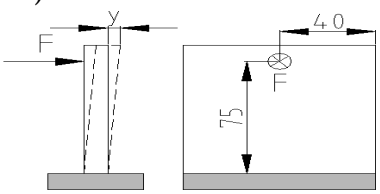

Figure 1. Load force activity in the middle of wall

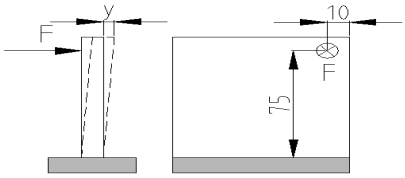

Figure 2. Load force activity on the edge of a wall

The simulation of plate bending was carried out in the environment of the Inventor Pro 2010 software. The load force F was 1 N. For material was chose EN AW 6082 aluminum alloy. The material density was $2.710.10^3$ $kg.m^{-3}$. Its Young's modulus of elasticity was 68,9 GPA and its Poisson's ratio was 0,33. The simulations results for a plate with 1 mm thickness are shown in Figure 3 and 4. Subsequently, the rigidity was calculated as follows (1).

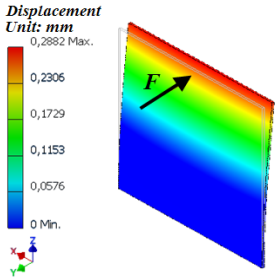

Figure 3. Plate bending by load force acting in the midle of a plate

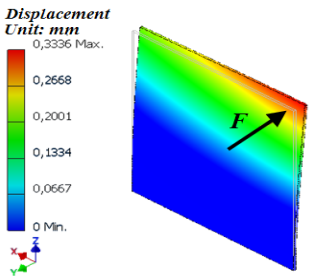

Figure 4. Plate bending by load force acting on the edge of a plate

The graph (Figure 5) shows that the thicker the wall, the greater the rigidity. Comparing the graphs (Figure 5 and 6), we can state there is a different rigidity value in the same wall thickness. This is the result of the F load force position.

If the tool has a higher rigidity than the part, then the chosen work-piece will be the vibrating element in the tool - work-piece set. Therefore, it is essential to investigate the tool rigidity so as to confirm that tool rigidity is greater than work-piece rigidity and it will as consequence not deform in experiments.

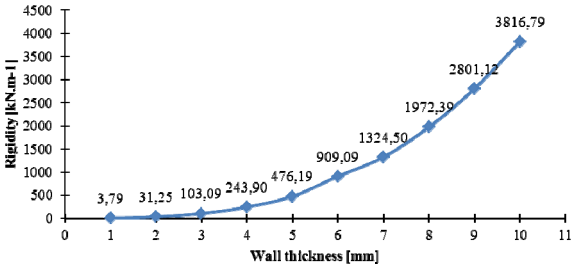

Figure 5. Dependence of wall static rigidity on wall thickness - force in the middle of the wall

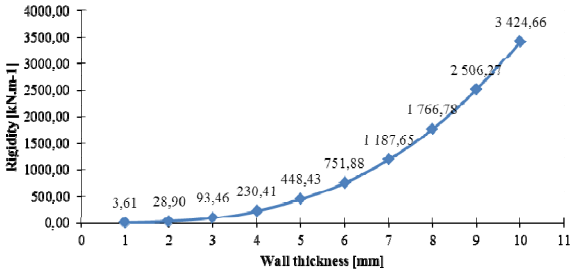

Figure 5. Dependence of wall static rigidity on wall thickness - force on the edge of the wall

RIGIDITY OF THE TOOL IN BENDING

Tool rigidity can be dealt with both analytically and numerically. In terms of an analytical calculation we need to be able to calculate tool deflection, which is defined by the relation (2), and the following: attaching of shank as a solid restrain, consistent section upon the whole length, joined load is replaced by a solitary force, force has its load point in the tool axis. Tool deflection calculates:

$$y = \frac{FI^3}{aEJ} \qquad (2)$$

where y[mm] is tool deflection, a is coefficient, whose value depends on the conditions of support load (solitary force, joined load) and on the way of support position, for inclusion a = 3. F [N] is solitary load, l [m] is length of tool overhang, E is Young's modulus of elasticity, J [m^4] is quadratic moment for the circular section and is calculated as follows:

$$J = \frac{\pi D^4}{64} \qquad (3)$$

then the rigidity of toll can be expressed as follows:

$$k = \frac{F}{y} = 3\frac{EJ}{l^3} \qquad (4)$$

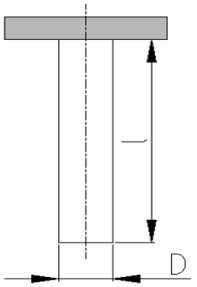

Figure 6. Diameter if D tool and tool overhang l

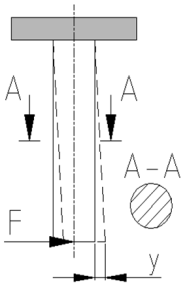

Figure 7. Tool bending y [mm] and load by solitary force F [N]

Tool bending y and tool load by a solitary force F is illustrated in (Figure 6). The grey colour depicts the

tool restrain. Tool diameter is D = 20 mm. Tool ovehang is l = 60 mm (Figure 6 and 7) and force is F = 1 N. The tool bending is calculated according to relation (2) and tool rigidity in bending is analytically calculated according to relation (4).
The simulation result of the tool bending developed in the Inventor Pro 2010 program is shown in Figure 8. Tool rigidity is obtained analytically and numerically in Table 1.

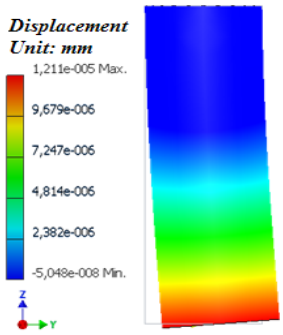

Figure 8. Tool bending in Invertor Pro 2010

Table 1. Tool rigidity

	Analytically	Numerically
Rigidity	65449.84 kN/m	82576.38 kN/m

The work-piece rigidity of 10 mm thickness part's is 3816.79 kN/m and for 1 mm thickness is rigidity 3.79 kN/m. The tool rigidity is numerically 82576.38 kN/m. With respect to the comparison of tool and work-piece rigidity, we can see than tool rigidity is twice as great as work-piece rigidity. Therefore, we can state that the tool has a higher resistance to elastic deformation.

EXPERIMENTAL DETERMINATION OF MILLING MODEL USING FRF

The assessment of stability for machine tool, tool and work-piece is possible use vibration test. Modal hammer is one of possibilities how to get vibration to the system. With modal hammer is obtaining Frequency Response Function (FRF). With this parameter we set natural frequency, damping ratio, stability diagram, milling model etc. For measurement of FRF is needed to determine place on work-piece and tool. In this place is a piezoelectric sensor. Hit with modal hammer have to be against piezoelectric sensor. The scheme of work-piece with piezoelectric sensor and modal hammer is pictured in Figure 9. The grey colour depicts the workpiece restrain.

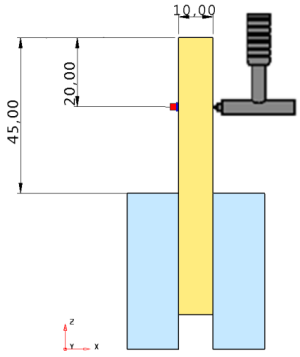

Figure 9. Scheme of FRF measurment of work-piece

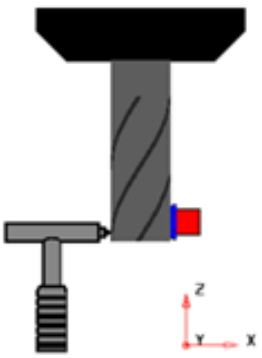

Figure 10. Scheme of FRF measurment of tool

Same measurement of FRF was use on the tool with diameter 20 mm and tool owerhang from tool holder 50 mm (Figure 10). Measurement was carried out in two directions X and Y of work-peiece and tool.

FRF MEASUREMENT CHARACTERICTICS

During milling process about stability of machining decides the spindle. However, in case of milling thin wall structures decides about stability of machining the work-piece. This fact is possible to identify the excitation of thin walled-structured by FRF characteristic (Figure 11). Those characteristics are depended on driver frequency and location of measurement. Vertical axis indicates dynamic elasticity of system (m/N). Horizontal axis is frequency (Hz). A visual inspection of the FRF shows different natural frequencies for tool and work-piece. For us is important first shape of natural frequency which determines the stability of milling process.

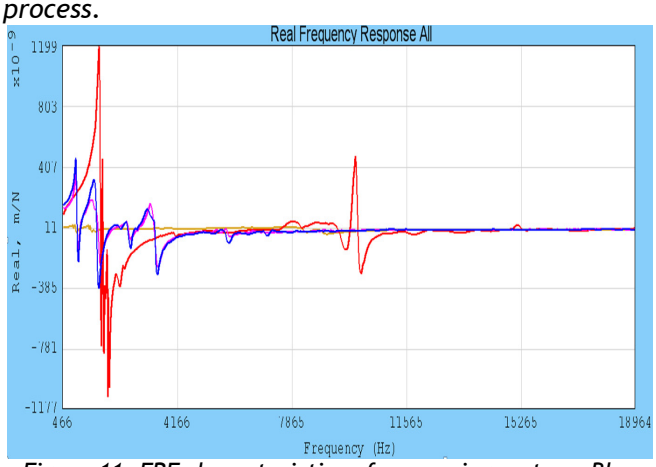

Figure 11. FRF characteristics of measuring system. Blue and purple line is corresponds to tool. Red line is work-piece in the X direction (10 mm thickness). Brown line is work-piece in the Y direction (80 mm length).

FRF characteristics of clamped tool in the spindle are shown blue and purple color. Both lines are almost identical, because the tool is geometrically symmetric component. Positive dynamic elasticity of tool is 433.10^{-9} m/N. FRF characteristics for clamped work-piece is very clear. Dynamic elasticity of thin walled part in Y direction is lower than tool. It means good rigidity in Y direction (80 mm length). Dynamic elasticity in X direction is huge (1199.10^{-9} m/N) as you can see on figure eleven. Rigidity in X direction of thin walled part is poor. The same conclusion was done with analytical and numerical methods. According to these claims is easy determine milling model. Milling model for thin walled parts is considered as single-degree-of-freedom spring-damper vibration system in one direction X.

SINGLE-DEGREE-OF-FREEDOM MILLING MODEL

An elastic work-piece and rigid tool represent a dynamic model of thin-walled part milling. The tool has a large diameter and good rigidity. The tool does not deform during the milling process or the deformation is very small and negligible in comparison to the work-piece.
In this model, the work-piece vibrates and this vibration results in waved machined surface. In this model of thin-walled part milling with single-degree-of-freedom is shown in Figure 12.

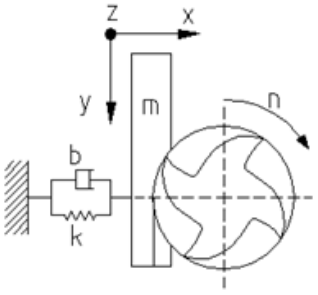

Figure 12. Single-degree-of freedom milling model

The structure is assumed to be flexible in the x direction, while the feed is parallel to the y direction. The dynamic model is defined by the following equation:

$$m\ddot{x}(t)+b\dot{x}(t)+kx(t)=Fx(t) \quad (5)$$

where: x [mm] is deflection in x-axis, b is the damping, k is the stiffness, and Fx(t) [N] is the cutting force in the x direction. According to linear cutting law, the x component of the force is given by:

$$Fx(t)+ap\sum_{j=1}^{z} [(Kr\cos\varphi j - Kt\sin\varphi j)\, hj(t)] \quad (6)$$

whereap[mm] is axial depth of cut, φj [°] is the angular position of the cutting edge, Kt and Kr [-] are thespecific tangential and radial cutting coefficient, and hj(t) [mm] is chip thickness.

CONCLUSIONS

The experimental determination of milling model for thin-walled parts is proposed. Milling model is given by numerical and finite element methods. For thin walled-part is characteristic different rigidity during milling process. Different deflection on work-piece is proposed and we can state there is a different rigidity value in the same wall thickness. With respect to the comparison of tool and work-piece rigidity, we can see than tool rigidity is twice as great as work-piece rigidity. Therefore, we can state that the tool has a higher resistance to elastic deformation. In x direction the work-piece rigidity is poor. Work-piece vibrates and this vibration results in waved machined surface. Thin-walled parts determine the stability of milling. Milling model for thin-walled parts is important to identify and calculate the cutting force or chip thickness.

Acknowledgements

1/0250/11 - Investigation of dynamic characteristics of the cutting process in 5 - axis milling in conditions of Centre of Excellence of 5 - axis machining.

REFERENCES

[1] *Aijun, T., Zhanqiang, L. 2007, Deformations of thin-walled plate due to static end milling force. Journal of materials processing technology.[Online] 15. December 2007. www.elsevier.com/locate/jmatprotec*

[2] *Budak, E., Altintas, Y. 1995, Modeling and avoidance of static form errors in peripheral milling of plates. [Online] 4.4 1995. [Date: 2. 9. 2010.] ww.scincedirect.com*

[3] *Budak, E., 2006. Analytical models for high performance milling. Part I. Cutting forces, structural deformations and tolerance integrity, Int. J. Mach. Tools. Manuf. 46, 1478-1488.*

[4] *Ratchev, S., Liu, S., Becker, A.A., 2005. Error compensation strategy in milling flexible thin-wall parts. J. Mater. Process. Technol. 162-163, 673-681.*

[5] *Ning, H., Zhigang, W., Chengyu, J., et al., 2003. Finite element method analysis and control stratagem for machining deformation of thin-walled components. J. Mater. Process. Technol. 139, 332-336.*

[6] *Liu, X. W., Cheng,K., Webb, D. 2002.Prediction and simulation on the machining Dynamics and instability in peripheral milling. American Society for Precision Engineering.[Online] 2002. http://www.aspe.net/publications/Annual_2002/PDF/POSTERS/4proc/ 2mach/865.PDF..*

[7] *Seguy, S., Dessein, G., l Arnaud, L. 2009. On the stability of high-speed milling with spindle speed variation. The International Journal of Advanced Manufacturing Technology.[Online] 2009.[Dátum: 15. 12 2009.]http://www.springerlink.com/content/nv7413 71272x8058/fulltext.pdf.ISSN 0268-3768 (Print) 1433-3015 (Online).*

[8] *Adetoro, O. B., Wen, P.H., W. M. Sim, R. Vepa. 2009. Stability Lobes Prediction in Thin Wall Machining. Proceedings of the World Congress on Engineering.[Online] Vol I., 2009a. http://www.iaeng.org/publication/WCE2009/WCE2009_pp520-525.pdf.*

[9] *Janáč, A. 1971.The field of vibrationless cutting conditions by machining of clamped shafts. Bratislava, 1971.Dissertation thesis.*

[10] *Peterka, J. 1995. Issue of drills torsion rigidity, Trnava: MTF STU, 1995. Dissertation thesis*

ACTA TECHNICA CORVINIENSIS - Bulletin of Engineering

ISSN: 2067-3809 [CD-Rom, online]

ACTA TECHNICA CORVINIENSIS – Bulletin of Engineering
Tome VI (Year 2013) – FASCICULE 3 [July–September]
ISSN 2067–3809

[1.] Bogdan Cornel BENEA

STUDY REGARDING THE EFFECT OF BIODIESEL ON DIESEL ENGINE EMISSION

[1.] "TRANSILVANIA" UNIVERSITY, BRASOV, ROMANIA

ABSTRACT: This paper analyzes effect of biodiesel on engine power, fuel consumption, emissions: nitrogen oxides (NOx) and particulate matter (PM) while the effective power is maintain constant. Biodiesel is a renewable, alternative diesel fuel of domestic origin derived from a variety of fats and oils by a transesterification reaction. Considering global energy policies, more and more governments try to increase the usability of biodiesel for powering motor vehicles. Cars manufacturing companies and private users are reluctant in using biodiesel, especially in current engines. Because of this, it is difficult to achieve the targets of increases the usage of biodiesel in ICE. There is a lack of knowledge on emissions of an engine what is fueled with biodiesel. An advantage of biodiesel is its potential to significantly reduce most regulated exhaust emissions, including particulate matter (PM), with the exception of nitrogen oxides (NO_x).
KEYWORDS: diesel engine, biofuel, emission, NO_x, particulate matter

INTRODUCTION

The fuel used for motor vehicles are subject to regulation EN-590. One of the most important restrictions is sulfur content (max 0.001% since 1 January 2009) and it had economical consequence for oil companies and on final fuel price. Together with the fluctuating price of oil price and with reducing of taxes for biofuels has opened the way for the use of biodiesel and a way to reduce the price of transport.
The technical definition of biodiesel is a fuel suitable for use in compression ignition (diesel) engines that is made of fatty acid monoalkyl esters derived from biologically produced oils or fats including vegetable oils, animal fats and microalgal oils.
When biodiesel is produced from these types of oil using methanol fatty acid methyl esters (FAME) are produced. Biodiesel fuels can also be produced using other alcohols, for example using ethanol to produce fatty acid ethyl esters, however these types of biodiesel are not covered by EN 14214 which applies only to methyl esters i.e. biodiesel produced using methanol. [1]
Considering global energy policies, more and more governments try to increase the usability of biodiesel for powering motor vehicles. Cars manufacturing companies and private users are reluctant in using biodiesel, especially in current engines. Because of this, it is difficult to achieve the targets of increases the usage of biodiesel in ICE. There is a lack of knowledge on emissions of an engine what is fueled with biodiesel.
Biodiesel fuels have a higher lubricity than conventional fuels, but they can contribute to the formation of deposits, the degradation of filters materials, depending on their degradability, their glycerol content, and their cold flow properties and on other quality specifications [2].
Biodiesel fuels also have a potential to reduce chemical emissions. The effect depends on the engine's type, engine speed, load, ambient condition. According Euro 5 emissions standard, NOx and PM emissions were reduced to 0.18 g/km and 0.005 g/km. Use of biodiesel can help to meet these limits. For this, automakers would have to adapt their engines for operation with biodiesel, which involve additional cost.

Table 1 - Ranges of the specifications of the fuels

Specifications	Biodiesel	Diesel
Density (15^0C) (kg/m^3)	870 - 895	810 - 860
Visosity (40^0C)(cSt)	3.5 - 5.5	2 - 3.5
Cetane number	45 - 65	40 - 55
Cloud point (^0C)	-5 - 10	-20 - 0
Lower heating value (MJ/kg)	36.5 - 38	42.5 - 44
Water content (mg/kg)	0 - 500	0
Sulfur content (mg/kg)	0	15 - 500

Engine performance

At partial loads, the output power of an engine fueled with biodiesel is the same as for diesel fuel.
The driver press more the accelerator to obtain the same power.

At full load or for the same pedal position of accelerator, the output power is lower.
Kaplan et al. [3] compared sunflower-oil biodiesel and diesel fuels at full and partial load. After tests they determined that power and torque values fall between 5 and 10%. Cetinkaya at al. [4] compared pure waste-oil biodiesel and diesel fuels and achieved a decrease of power and torque by 3 - 5%.
Other authors report an increase of power and torque when using biodiesel. Altiparmak et al [5] obtain a increase of torque by 6.1% when used a blend with 70% tall-oil biodiesel. They explained this by high cetane number, high values of density and viscosity of biodiesel fuel (922 kg/m^3, 7.1cSt at 40^{0}C).
In the literature are offered several reasons to explain the difference between lost of power and torque compared with calorific value, most related to viscosity.

Nitric oxides

FEV report [6] concludes NOx emission increases with biodiesel content until maximum 8% for B100. Schumaher at al. [7] tested a 200 kW engine with B10, B20, B30 and B40 soybean-oil biodiesel. They observed an increase in NOx emissions with 15% for B40.
An explanation for the increase in NOx emissions can be higher cetane number for biodiesel.
After laboratory experiment with different heavy-duty engines (without EGR) US EPA [8] has determined an equation with an accuracy of 95%.

$$\frac{NO_x}{NO_{xD}} = e^{0.0009794\%B} \qquad (1)$$

An explanation for the increase of NO_x when using biodiesel is advancing combustion process due to physical defining characteristics (viscosity, density, compressibility).

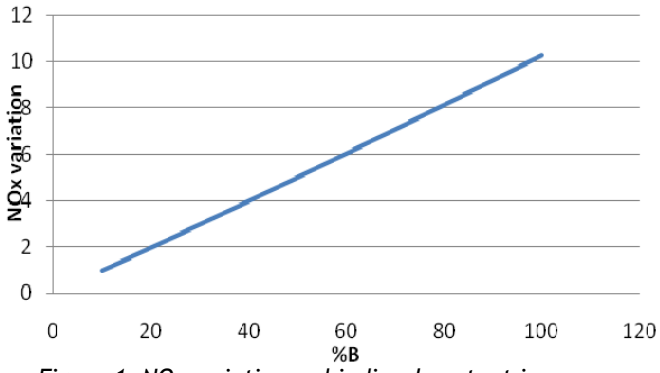

Figure 1. NO_x variation as biodiesel content increases

Effect of physical properties on the advance injection can be seen on mechanical injection pumps. When biodiesel is injected, the pressure increase is faster because smaller compressibility and also propagation speed is higher. Due to the high viscosity, the pressure losses are lower injection pump, resulting in a linear increase in pressure.
As a result, the injector needle rises faster, achieving a higher injection advance.
And tests that remained at the start of fuel injection were observed an increase in NO_x emissions. One reason is due to higher flame temperature adiabatic temperature increase, either due to reduced heat dissipation by radiation as a consequence of low particulate emissions.
Other explanations for the increase in NO_x emissions: high cetane number and greater availability of oxygen when using biodiesel.
To reduce NO_x emissions when replace diesel with biodiesel fuels is necessary to modify the law injection, to delay the moment when injection start. It prefers a delay in injection to maintain the NO_x emissions at the diesel limits, although the advantage of lower soot emissions disappears.

Particulate matter and smoke opacity

Using biodiesel instead of diesel fuel a decrease of PM emissions is observed.
The results of several tests were collected by EPA [8] who has determined an equation with 95% accuracy.

$$\frac{PM}{PM_D} = e^{-0.006384\%B} \qquad (2)$$

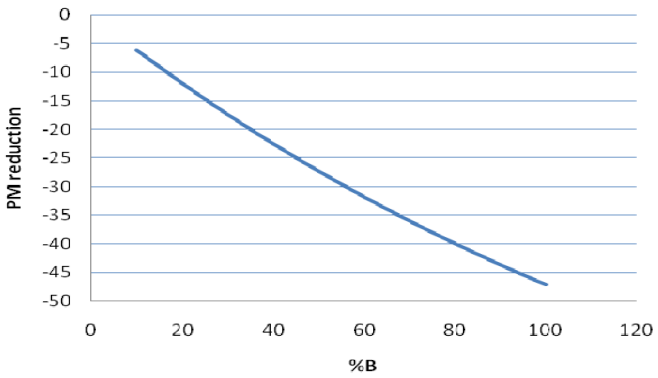

Figure 2. Mean reduction in PM emissions as the biodiesel content increases

There are several ways to explain the reduction when biofuels is used:

- *Oxygen content from biofuels molecule ensuring more complete combustion and oxidation of PM already formed;*
- *Biodiesel need a lower stoichiometric ratio, which reduces the likelihood of a rich mixture;*
- *Absence of aromatics in biofuels, which are considered precursors to soot;*
- *Because larger injection advance, the soot spend a long time in the presence of oxygen and high temperature, which contributes to their oxidation;*
- *The different structure of soot between diesel and biodiesel fuels;*
- *Biofules have 0 sulfur content and prevent sulfate formation which is a significant component of PM.*

Hydrocarbons

The EPA review [8] shows a 70% reduction with pure biodiesel according with equation (3).

$$\frac{HC}{HC_D} = e^{-0.011195\%B} \qquad (3)$$

Several reasons have been proposed to explain the decrease in HC emissions when is used biofuels:

- *Oxygen content from biofuels molecule ensuring more complete and cleaner combustion;*
- *Higher cetane number of biodiesel reduces the auto ignition delay;*

- Even biofuels is less volatile as diesel fuels, diesel fuels has final point of distillation higher. Final fraction of diesel fuels may not vaporize completely, resulting in unburned hydrocarbons;

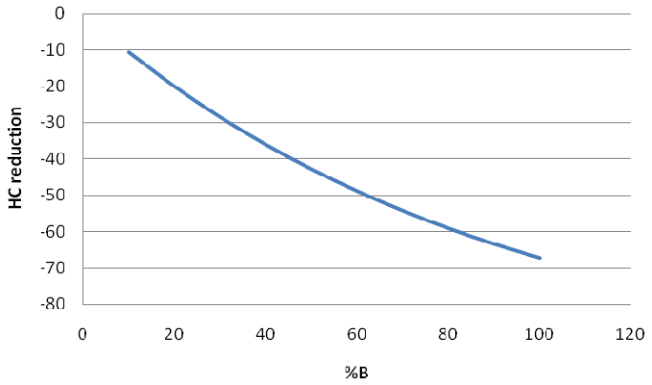

Figure 3. Mean reduction of HC emissions as biodiesel content increases

Carbon monoxide

A decrease in CO emissions when substituting diesel fuel with biodiesel can be observed. After revising several works, EPA [8] proposed equation (4) for general trend.

$$\frac{CO}{CO_D} = e^{-0.006561\%B} \qquad (4)$$

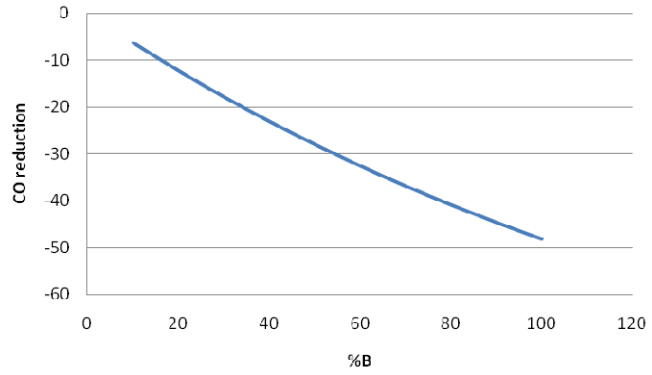

Figure 4. CO reduction as the biodiesel content increases

Several reasons have been proposed to explain the decrease in HC emissions when is used biofuels:

- Oxygen content from biofuels molecule ensuring more complete combustion;
- Higher cetane number of biodiesel reduces the probability of fuel-rich zone formation;
- The advanced injection and combustion when using biofuels may also justify the CO reduction with this fuel.

CONCLUSIONS

The following general conclusions could be proposed:

- At partial loads, the output power is identical, fuel consumption increases to compensate the lower calorific power;
- NO_x emissions increase because the injection process is advanced with biodiesel;
- When biodiesel is used, it is obtained a reduction of soot. Oxygen content and no aromatic substances leading to this decrease;
- HC and CO emissions are significantly reduced by using biodiesel. A more complete combustion caused by the presence of oxygen can cause this reduction.

REFERENCES

[1.] http://en.wikipedia.org/wiki/EN_14214
[2.] Waynick JA. Characterization of biodiesel oxidation and oxidation products. USA SouthWest Research Institute 2005 [Project 08-10721].
[3.] Kaplan C, Arslan R, Surmen A. Performance characteristics of sunflower methyl esters as biodiesel. Energy Sources 2006;Part A 28:751-5.
[4.] Cetinkaya M, Ulusay Y, Tekın Y, Karaosmanoglu F. Engine and winter road test performances of used cooking oil originated biodiesel. Energy Convers Manage 2005;46:1279-91.
[5.] Altiparmak D, Deskin A, Koca A, Guru M. Alternative fuel properties of tall oil fatty acid methyl ester-diesel fuel blends. Bioresource Technol 2007;98:241-6.
[6.] FEV Engine Technology. Emissions and performance characteristics of the Navistar T444E DI engine fuelled with blends of biodiesel and low sulphur diesel. Final report to National Biodiesel Board 1994.
[7.] Schumacher LG, Borgelt SC, Hires WG, Fosseen D, Goetz W. Fueling diesel engines with blends of methyl ester soybean oil and diesel fuel. 1994. Available on line: www.missouri.edu/_pavt0689/ASAED94.htm
[8.] Assessment and Standards Division (Office of Transportation and Air Quality of the US Environmental Protection Agency). A comprehensive analysis of biodiesel impacts on exhaust emissions, 2002; EPA420-P-02-001.

ACTA TECHNICA CORVINIENSIS – Bulletin of Engineering

ISSN: 2067-3809 [CD-Rom, online]

ACTA TECHNICA CORVINIENSIS - BULLETIN of ENGINEERING

ISSN: 2067-3809 [CD-Rom, online]

ACTA TECHNICA CORVINIENSIS - BULLETIN of ENGINEERING

ISSN: 2067-3809 [CD-Rom, online]

copyright © UNIVERSITY POLITEHNICA TIMISOARA,
FACULTY OF ENGINEERING HUNEDOARA,
5, REVOLUTIEI, 331128, HUNEDOARA, ROMANIA
http://acta.fih.upt.ro

ACTA TECHNICA CORVINIENSIS – Bulletin of Engineering
Tome VI (Year 2013) – FASCICULE 3 [July–September]
ISSN 2067–3809

[1.] Daniel OSTOIA, [2.] Liviu MIHON, [3.] Arina NEGOIȚESCU, [4.] Adriana TOKAR

ASPECTS REGARDING CONSTRUCTIVE MODIFICATION TO ENGINES FULFILL THE EURO 5 AND EURO 6 DEMANDS TO PASSENGER CAR

[1.] "POLITEHNICA" UNIVERSITY, TIMIȘOARA, ROMANIA

ABSTRACT: The increase of the environment pollution generated by the internal combustion engines the vehicles are equipped with, represent a desideratum both for the manufacturers and for those who use them. The problems generated by this pollution are complex and their causes are various. The paper presents some aspects regards the main constructive modification to engine to achieved regulation adopted by European Commission in sector of automotive industry: air quality regulations (Euro 5 and Euro 6), fuel efficiency and CO_2 regulation. Some engine which equipped passenger car, has major constructive modification to main components of the engine, but it is necessary to complete with some auxiliary components which mean cumulative costs of the engine.
KEYWORDS: pistons, intake manifold, blow by gases

INTRODUCTION

The increase of the environment pollution generated by the internal combustion engines the vehicles are equipped with, represent a desideratum both for the manufacturers and for those who use them. The problems generated by this pollution are complex and their causes are various. In the last decade much of legislation regard air quality has forced technology developments at automotive industry as means to make constructive modifications to the major source of pollution to passenger car. The constructive modifications to the engines are different to diesel engine comparative to spark ignition engine and the costs to achive at this performances are bigger to diesel engine. In this paper are presented some constructive modifications to fulfill the EURO 5 and EURO 6 to diesel engine.

THE RESEARCH METHOD

In this paper are presented some constructive modifications which are maked to the intake manifold and to theblow-by gases recirculation equipment, modifications which are realized on diesel engine.

The major problems to diesel engine concerning to pollution are some aspects regarding to the burning process into the combustion chamber. The mixture air/diesel fuel must be optimum to every operating mode.

For example to the diesel engine for passenger car to achive this goal, the pistons of the engine don't have valve pockets, this measures lead to reduction of space stagnation and the improved the gases flow circulation. The circular motion of the mixture air-fuel is very important to make optimum combustion. The cooling of the pistons are realized with the cooling duct into the piston, the suplimentary cooling are maked with oil which are circulated into cooling duct (Figure 1).

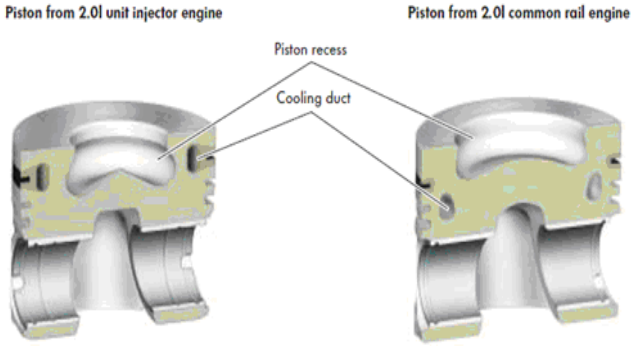

Figure 1. Constructive differences at piston engines [7]

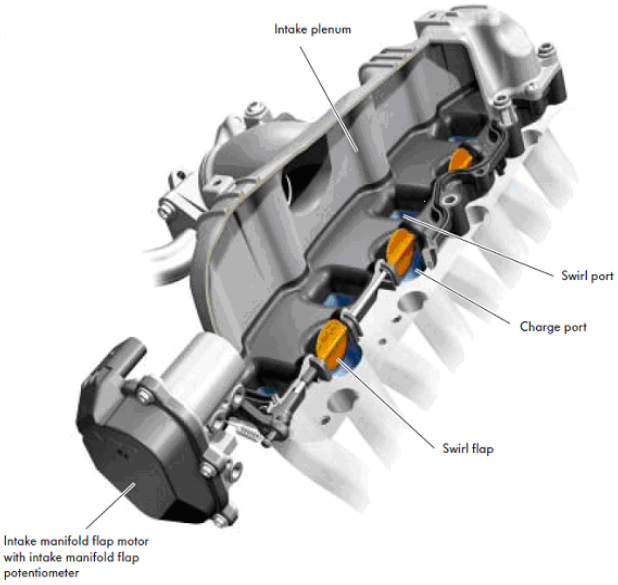

Figure 2. Intake manifold with swirl flap [7]

The pistons are cavity in to the direction of fuel injection and are more flat compared with pistons from unit injector engine. The mixture air-fuel is more homogeneous in this case and the unburning particles are less than comparative unit injector engine.
In the intake manifold it is a swirl flap, which are generated a swirl motion to the intake air by rotation engine. The motion of swirl flap is generated by a sliding rod. The command is generated by electronic unit control (Figure 2).
This swirl flap are closed when the engine are running to low load and low rotation (Figure 3).

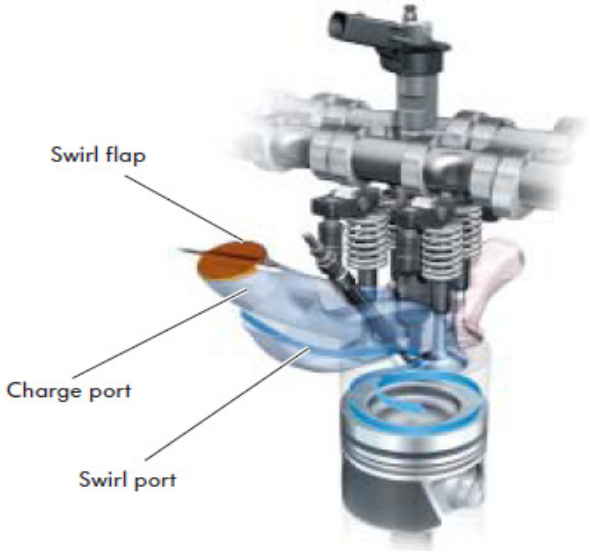

Figure 3. The swirl flap close [7]

In the function of engine the swirl flap are continue adjusted with the rotation engine. There is an optimum position for swirl flap for every operation domain to obtain an optimum combustion. After 3000 rpm the swirl flap are opened, the air circulation is optimum for this operation domain. (Figure 4).

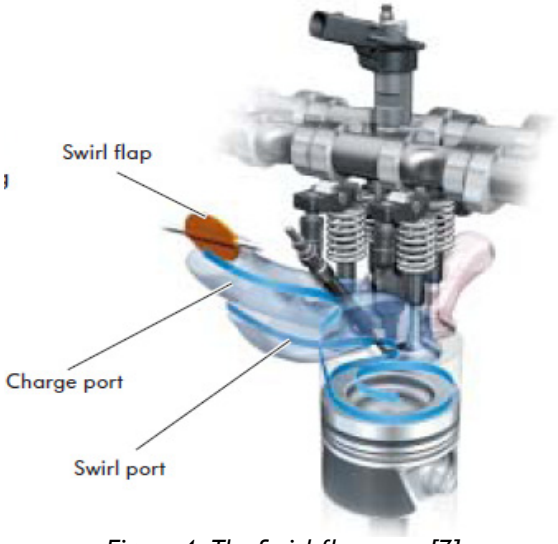

Figure 4. The Swirl flap open [7]

In to the combustion internal engines there is a circulation of the gases between combustion chambers and the crankcase. This circulation are generated by the differences pressure of this volumes, this gases are called blow-by gases. The blow-by gases are containing oil which haven't must burned because generate environmental damage.
The environmental requirements create the need to separation of oil vapors. The oil separation is created by a gradual separation in this case only a few quantity of oil are burned. The oil separation is realized in three steps:

- *rough oil separation*
- *fine oil separation*
- *air damping volume.*

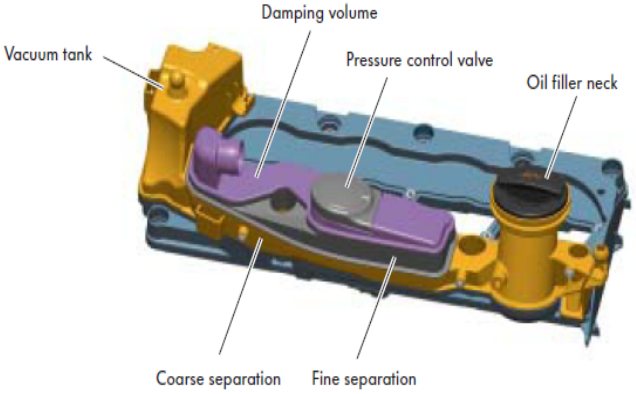

Figure 5. Crankes volume ventilation [7]

The rough oil separation are generated by oil collection volumes (Figure 6).

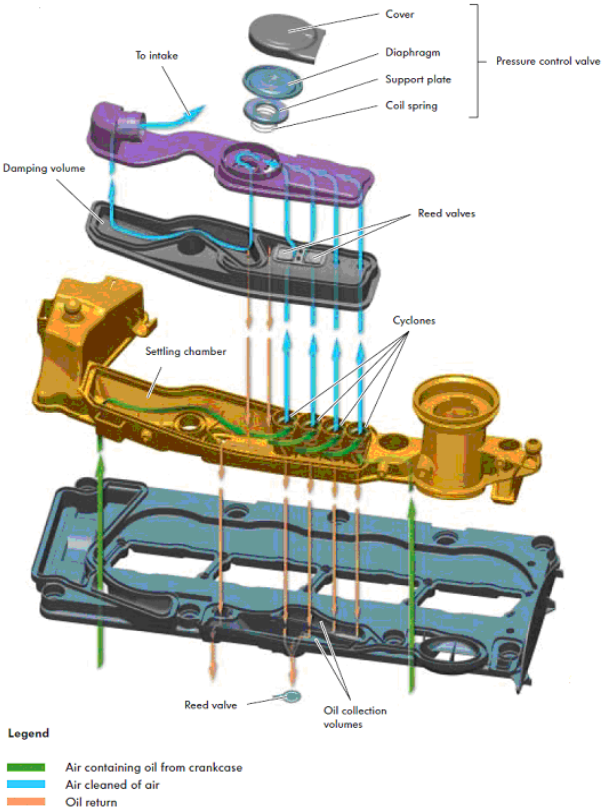

Figure 6. The rough oil separation [7]

The fine oil separaton are generated by four cyclones which are working function by the pressure level between volumes (Figure 7). Function of centrifugal forces the oil vapors are separated by cyclones.
For the engine ventilation it is necessary to control the blow-by gases pressure. The systems are composed by a diaphragm and pressure springs which are open or closed functions the blow-by gases pressure (Figure 8).

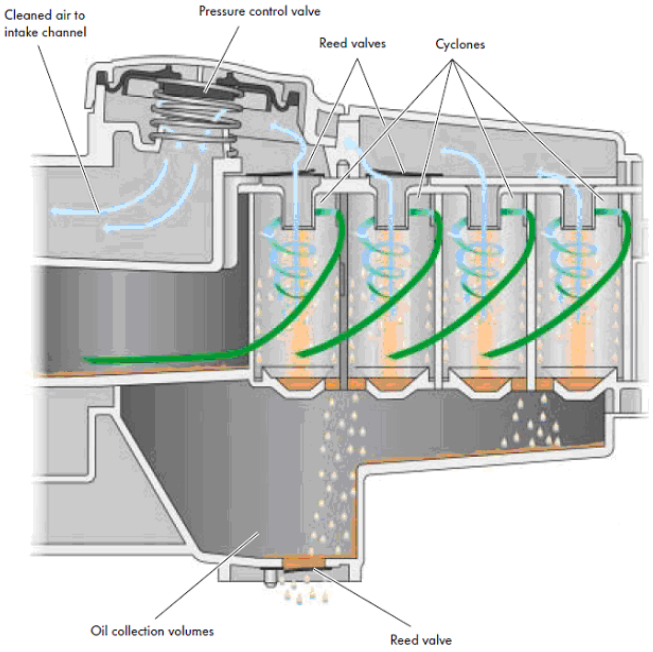

Figure 7. The fine oil separation [7]

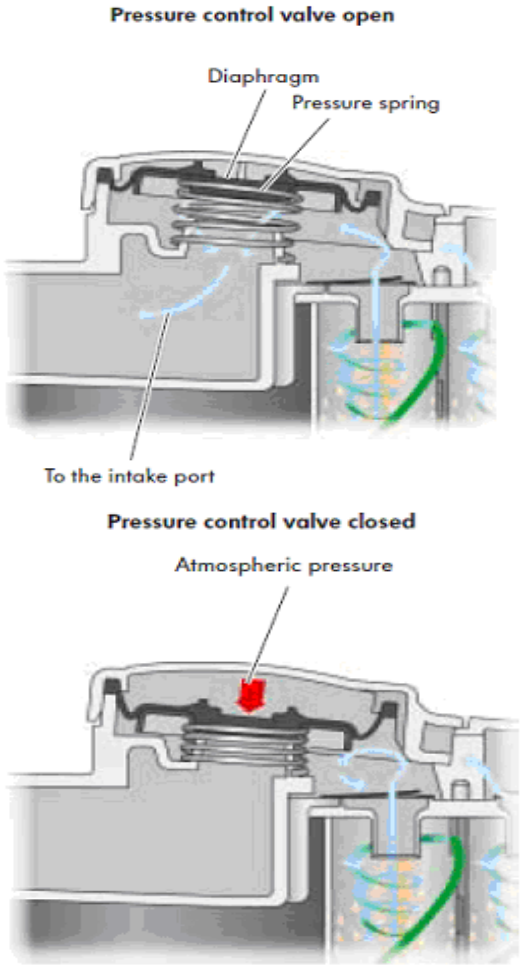

Figure 8. Pressure control valve [7]

To avoid the turbulent circulation of blow-by gases it is necessary to have a damping chamber, which reduces the kinetic energy of these gases and realized a small separation of oil (Figure 9).

These constructive changes must be together with other modifications which are for example: engine calibration, optimized fuel injection system, exhausted gases recirculation (EGR), cooled EGR, advanced turbocharger, intercooler, DPF.

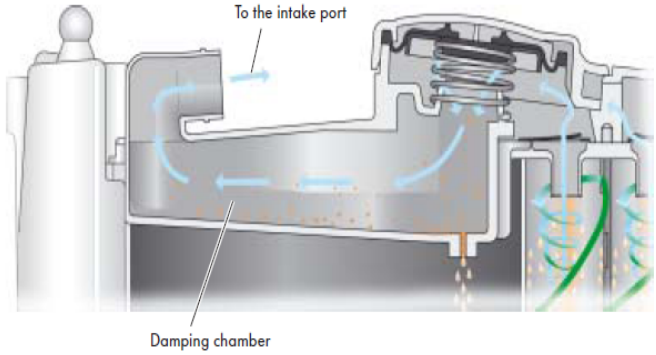

Figure 9. Damping chamber [7]

The optimum formula of constructive changes to fulfill Euro 5 or Euro 6 must be adjusted with vehicle mass and cylinder volume (Figure 10) to obtained a lower CO_2 emission.

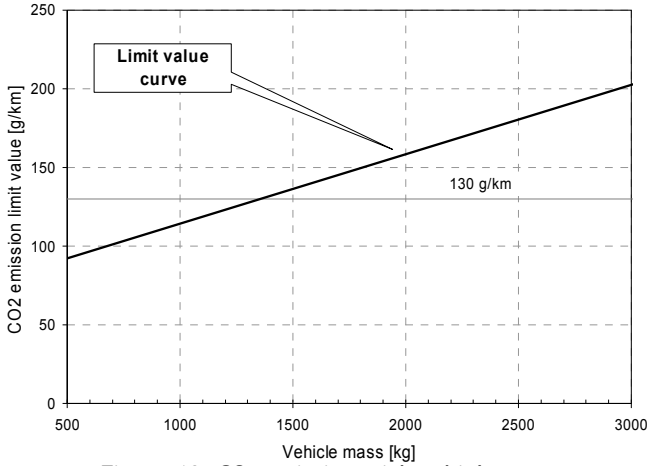

Figure 10. CO_2 emission with vehicle mass [Source: EU Commission]

Vehicle technical specification often evolves around regulation, and the cost impact is not immediately clear. The following example concerning the cost impact of the move towards Euro-IV compliance illustrates how complex the cost impact could be, and how dangerous it can be to generalise the cost impact of several possible technical solutions. All of the prices indicated are merely reflections of the relative cost of such systems, and depending on applications may vary; they also assume that all of these

CONCLUSIONS

By analyzing the accomplished researches regarding the constructive modifications from the diesel engine fulfill Euro 5 and Euro, results the following conclusions:

- *It is necessary to make constructive changes to pistons engine in correlation with optimization mixing air-fuel;*
- *The blow-by oil gases recirculation is important cu be controlled, because vapors of the oil which reach in to the combustion chambers increase the pollution degree;*
- *The blow-by oil gases are together with the wear of the sealing element;*

This constructive modification apply to diesel engine fulfill Euro5 and Euro 6 is just a part of the modifications, because to achieve this objectives is necessary to complete with a complex injection

system with a after treatment noxes systems, but every engine must be analyzed because there is not a general solution for every type of engine.

REFERENCES

[1.] *Ostoia, D. Studies and researches of the formation control of mixture and burning and the influence of behaviour in work to the combustion chamber in correlation with pollution conditions to the diesel engines., Doctoral theses 2006, University Politehnica of Timisoara*

[2.] *Iorga, D., Mekki, C., Ostoia D., The connection between the state parameters and smoke degree of a direct injection diesel engine, Zilele Academice Timișene, Ediția a VII-a, Simpozion "Omul și mediu"*

[3.] *Ostoia, D., Negoitescu, A.,S., A study regarding the combustion chambers behavior in corelation with emitted noxe sot diesel engines,576-578, The 30th Annual Congres of the American Romanian Academy of Arts and Sciences , The Academy of Economic studies of Moldova july 5-10, 2005*

[4.] *Mădăras L, Ostoia Daniel., Holotescu S., The influence of loses diesel engine combustion chambers to mechanical indicate work at idle characteristic, The Third Edition of the French - Romanian Colloquim COFRET 2006*

[5.] *www.ihs.com*

[6.] *ec.europa.eu*

[7.] *VW- training service*

ISSN: 2067-3809 [CD-Rom, online]

ACTA TECHNICA CORVINIENSIS – Bulletin of Engineering
Tome VI (Year 2013) – FASCICULE 3 [July–September]
ISSN 2067–3809

[1.] Daniela FLOREA, [2.] Dinu COVACIU, [3.] Ion PREDA, [4.] Janos TIMAR

COMPARATIVE ANALYSIS OF THE MOVING OBSERVER KINEMATICS IN THE URBAN ROAD NETWORK

[1-4.] TRANSILVANIA UNIVERSITY OF BRAŞOV, ROMANIA

ABSTRACT: The parameters that describe the urban road traffic are related to the speed evolution on certain routes. In order to make a good quality analysis is mandatory to have good quality data. That means one of the most important activity is the data acquisition, which involve the selection of the appropriate methods and devices. Using a database build in years, it was possible to compare the distribution of speed frequency for a moving observer in our city, before and after some major changes in the road network architecture.
KEYWORDS: moving observer, kinematic, speed, road network, statistical analysis

INTRODUCTION

During the last three years (2010 - 2012) many changes were made in the road network of the Brasov city and these lead to changes in the traffic parameters. Part of these changes consists in converting signalized intersections into roundabouts, also the speed limit was increased from 50 km/h to 60 km/h, so it is expected to obtain reduced stop times and higher values for mean speed. Starting from 2008, in the Department of Automotive and Transport Engineering of Transilvania University it was build a database with kinematic data collected using the Moving Car Observer method. This paper is based on a study conducted using the data collected during these years.

The goal of the study was to highlight the changes in the travel speed of individual vehicles. Such information may be useful for estimating the level of noise or chemical pollution caused by the road traffic [[4.]], or for estimating the effect of the traffic on the vehicle itself. This study was made from a "microscopic" point of view, and this means that it was analyzed the movement of the vehicle as entity, not the traffic flow. However, since the individual vehicle is driven in the same conditions as all the other vehicles in the flow, it can be assumed that the average values determined for a vehicle traveling many times on a certain routes are valid also for other vehicle on the same routes.

The concepts used in the traffic flows theory [[3.]] were extended to the microscopic analysis of the driving, for an extended urban network instead of the analysis of a particular road segment. The statistic indicators used to describe the spot speed distributions are used to describe also the distribution of the moving observer speed.

THEORETICAL ASPECTS

The key statistics used in the traffic theory to describe the speed distributions are [[6.]]:

- Average speed (time mean speed);
- Standard deviation - the average difference between the measured speed and the mean speed;
- 85^{th} percentile speed V85 - the speed below which 85% of the vehicles are traveled;
- Median speed V50 (50^{th} percentile speed) - the speed that equally divides the distribution of the spot speeds;
- Pace - a 20 km/h increment in speeds that encompasses the highest proportion of observed speeds. The literature [[6.]] recommends a 10 miles/hour increment and we converted this value into 20 km/hour; an increment of 16 km/h looks more closed to the recommended value, however the experimental results revealed similar values and the same conclusions with both values of the pace intervals.

The mean speed, the median speed and the pace are all measures of the central tendency, describing the approximate middle or center of the distribution. The standard deviation is a measure of dispersion, describing the extent to which data spreads around the center of the distribution.

Formulas used for calculation of the above indicators are as follows:

- Average speed: $$\bar{v} = \frac{\sum_i f_i v_i}{N} \qquad (1)$$

where $\bar{v}$ is the average speed, f_i is the frequency of observations in the speed group i, v_i is the middle value of speed in the group i and N is the total number of observations;

- Standard deviation: $$s = \sqrt{\frac{\sum (v_i - \bar{v})^2}{N-1}} \qquad (2)$$

where s is the standard deviation, v_i is the value of the speed i, $\bar{v}$ is the average speed, and N is the number of observations.

The median speed, as well as the 85th percentile and 15th percentile speeds (V85 and V50) are determined graphically, using the diagram of the cumulative frequency distribution. The pace can be found also from diagram, moving a horizontal line of the established length along the left side of the curve, on the diagram of frequency distribution, until the right end of the line meet the right side of the curve. A measure of both central tendency and dispersion is the percentage of vehicles travelling within the pace speeds. This can be found also graphically using both the frequency distribution and cumulative frequency distribution curves.

DATA ACQUISITION AND PROCESSING TECHNIQUES

The data were collected using GPS receivers with a sampling rate of 1 Hz. This means that one record is saved at every second. Each record includes information about time and the vehicle position (longitude, latitude and altitude). The method was described in previous work [[1.], [4.]] and it was extensively used in traffic studies in the last years. Basically, it is the moving car observer method, where the car is equipped with GPS receiver as data acquisition device. One of the great advantages of using GPS devices is the easy of installation and use.

Each record is stored sequentially in a text file, or in an XML field in a GPX file, depending by the device used [[2.]]. Each record corresponds to a speed observation, according to the theory presented above. The sampling rate of 1 Hz is accurate enough for statistical analysis of the travel speed. The output file from the GPS receiver is downloaded on a PC using a custom CAD application written for AutoCAD and described in detail in the book [[2.]], where are given also more information on the accuracy of the devices and methods that can be used for GPS data acquisition.

The routes used as reference in this study are presented in Figure 1 using dedicated map viewing software and in Figure 2 as AutoCAD drawing. On these routes, three intersections previously signalized with traffic lights were converted into roundabouts. The data collected are grouped in two categories: before and after changes of the road network. The length of the routes is between 4.2 and 5.3 km.

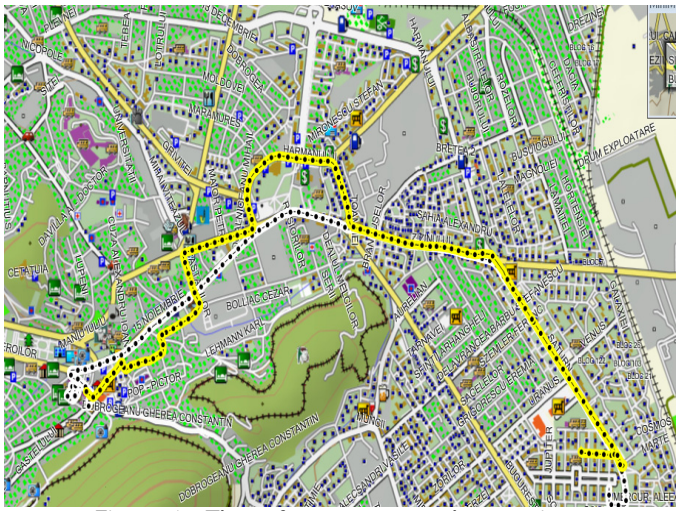

Figure 1 - The reference routes shown using map software (MapSource)

The first phase of processing data consists in importing the text file in the CAD environment, draw the track(s) and generate the diagrams of speed and/or acceleration as function of time and space (example in Figure 3).

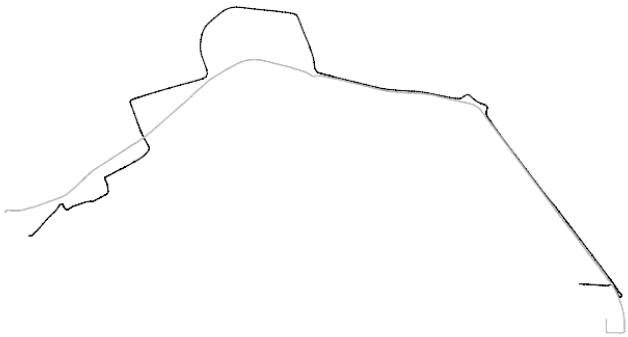

Figure 2 - The reference routes represented in AutoCAD

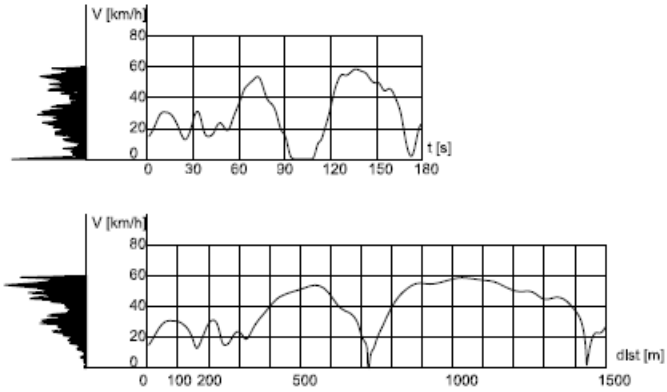

Figure 3 - Example of speed versus time (top) and speed versus space (bottom) diagrams for a track

In Figure 3 the side diagrams represents the frequency distribution of speed. These diagrams are presented here for one single track. When the all the tracks are added together on the same diagram, the frequency distribution looks like in Figure 4.

The next action is to generate the diagram of cumulative frequency distribution, starting from the diagram shown in Figure 4. It is used a custom function written in Lisp, which browse through the curve reading the coordinates of each vertex, then calculate the percentage of each speed group. Each speed group in this analysis has a 2 km/h range. The result of this action is the curve shown in the bottom part of Figure 5 and Figure 6. The horizontal axis is for the speed values, the vertical axis is for the speed percentage.

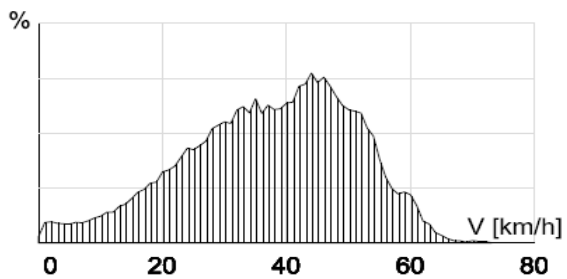

Figure 4 - Frequency distribution for speed/space diagram

The 85th percentile, 50th percentile and 15th percentile speeds can be easily extracted from the curve: a horizontal line starts from the percentile value on the vertical axis, and then the line is

extended until it intersects the curve. From the intersection point a new line is created down to the horizontal axis. The distance from the origin of the diagram to the last intersection point is the value of the percentile speed.

The pace is more difficult to be obtained graphically, even using the CAD environment. A good solution is to calculate the pace interval analytically, comparing the number of observations for all the possible pace intervals. The input values are the vertices of the curve representing the frequency distribution (top diagram in Figure 5 and Figure 6).

RESULTS

The data collected before implementing the changes in the road network were used to generate the diagrams in Figure 5. It can be observed that the value of V85 is 50.49 km/h. Since V85 is recommended to be the value of the speed limit, it can be stated that the limit of 50 km/h was a good choice at that time. The median speed V50 was found at 37.58 km/h.

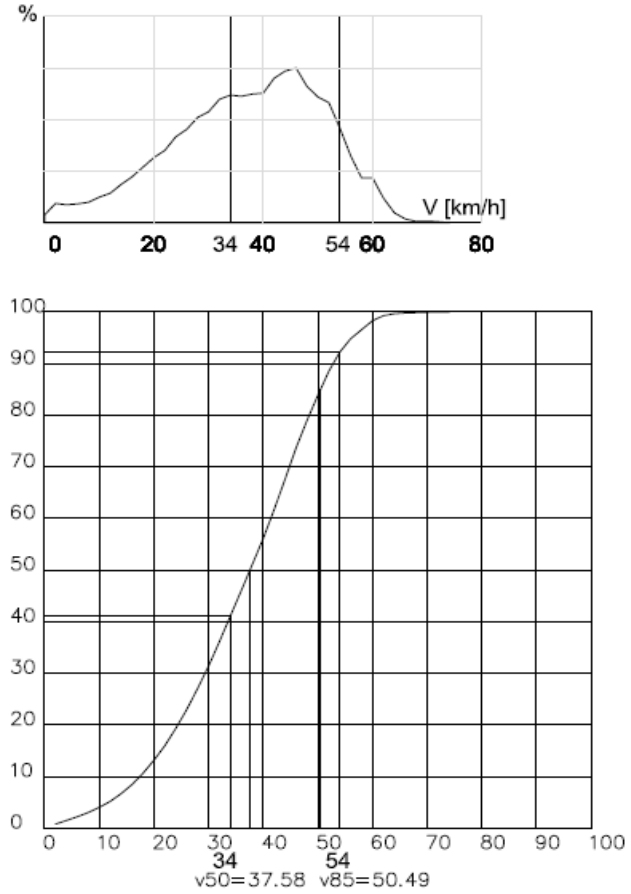

Figure 5 - Frequency distribution and cumulative frequency distribution (before changes in the road network)

After upgrading the road network, the same routes were traveled in order to collect new data, which are summarized in the diagrams in Figure 6. The new value of V85 is 52.69 km/h, not far from the previous V85, even if the speed limit is now 60 km/h. This means that a higher speed limit don't lead automatically to higher travel speeds inside the urban network. V50 is now 37.51, practically the same value as before.

The general aspect of the frequency distribution curve is not changed dramatically (Figure 7); it is mainly flattened, having a lower mode (modal speed: the single value of speed that is most likely to occur) and little higher values on both sides of the curve. The area inside the curve is almost the same, since the traffic volumes are similar.

The pace interval was found to be the same in both cases: between 34 and 54 km/h, but with different percents of measured speed values. The percent vehicles within the pace can be ascertained from the cumulative frequency diagram, by measuring the vertical distance between the intersection of curve with the two pace limits. This means that 51% and 45% respectively of the measured speeds are in the interval of 34 - 54 km/h, with a standard deviation of approximately 10 km/h.

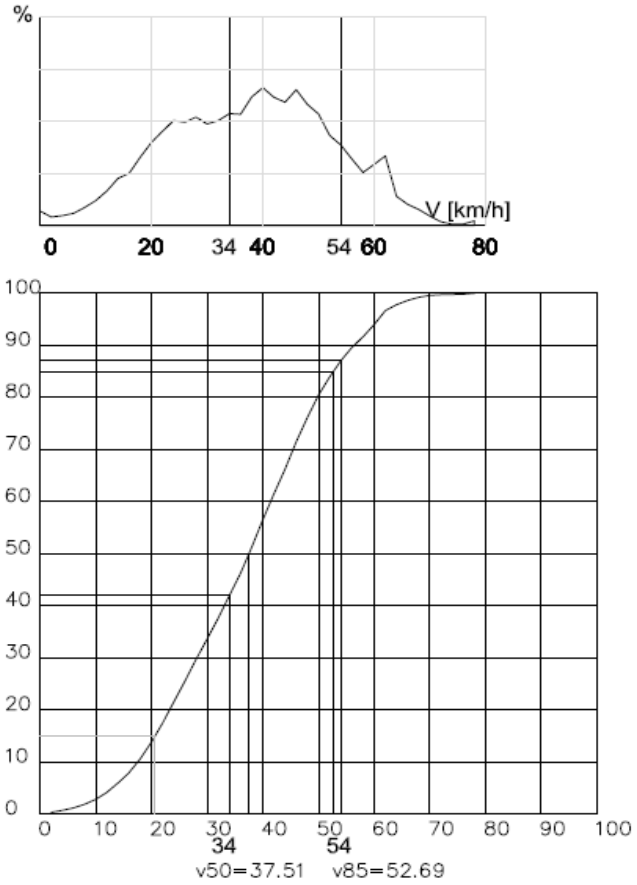

Figure 6 - Frequency distribution and cumulative frequency distribution (after changes in the road network)

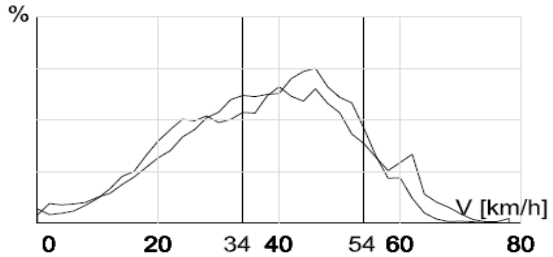

Figure 7 - Frequency distribution before and after changing the road network

The 85th and the 15th percentile speeds can be used to roughly estimate the standard deviation of the distribution [[6.]]. The formula for this estimation is:

$$s_{est} = \frac{V85 - V15}{2} \quad (3)$$

resulting a value for the standard deviation of 16.52 km/h for measurements taken before changes in the road network and 16.02 km/h after.

Table 1 - Summary of results

	Before	After
Average speed (km/h)	37.14	37.71
V15 (km/h)	17.45	20.65
V50 (median speed) (km/h)	37.58	37.51
V85 (km/h)	50.49	52.69
Modal speed (mode) (km/h)	46	40 and 46
Pace interval (from-to, km/h)	34 - 54	34 - 54
Percent vehicles within the pace	51	45
Standard deviation (km/h)	13.7	14.86

The results are summarized in Table 1. It can be noted that there are two values for modal speed - two speed values are most likely to occur, equally - 40 km/h and 46 km/h. As the number of observations will be increased, most probably the modal speed will be somewhere between these two values.
The average speed here is the space mean speed, as the observations are extracted from the diagram of speed as function of distance travelled.
The values for standard deviation of the measured speeds calculated from the precise experimental determinations (values given in Table 1) are close to the values estimated above using formula (2).

CONCLUSIONS

The study on which this paper is based was made from the point of view of the individual vehicles moving through an urban road network. Having a database built in time, about five years with tens of tracks recorded per year, with different vehicles on few routes (but not just a single route), the results can be extended to all individual vehicles in the network.
The goal was to make a comparative analysis of driving parameters before and after some major changes in the road network. The main changes were the conversion of three intersections that were initially signalized with traffic lights into roundabouts, and the increase of the speed limit from 50 km/h to 60 km/h.
It was expected that these changes will cause an increase of the average speed and an increase of the number of vehicles moving with higher speeds - a higher value of V85. The 85th percentile speed was increased indeed, but with a small difference from the previous value. Before changes the V85 value was close to the speed limit, but after the changes were implemented the new value is less than the new speed limit (see Table 1). This led us to the conclusion that the changes in the speed limit do not affect the traffic fluency too much.
The space mean speed, the median speed (V50) and the pace are almost the same. The most important increase is of the 15th percentile speed, and this means that there are less road segments where the vehicles move with low speeds - like in the queues at intersections.
In this study it was not taken into account the time to destination, or the distance traveled to destination, neither the duration while the vehicles are stationary.

Acknowledgements

This paper is supported by the Sectoral Operational Programme Human Resources Development (SOP HRD), financed from the European Social Fund and by the Romanian Government under the contract number POSDRU POSTDOC-DD, ID 59323.

REFERENCES

[1.] Covaciu, Dinu; Florea, Daniela; Preda, Ion; Timar, Janos; Using GPS Devices For Collecting Traffic Data; SMAT2008 International Conference, Craiova, 2008.
[2.] Covaciu, Dinu; Use of GPS and CAD in Vehicle Dynamics Study; VDM Verlag, Saarbruecken, ISBN: 978-3-639-35589-5, 2011.
[3.] Florea, Daniela; Managementul traficului rutier, Ediția a II-a (Road Traffic Management, Second Edition), Editura Universității Transilvania din Brașov, ISBN 973 -9474-55-1, 2000.
[4.] Florea, Daniela; Cofaru, Corneliu; Covaciu, Dinu; Timar, Janos; Data Acquisition Methods for Estimate the Noise Generated by the Road Traffic; 3rd WSEAS Conference on Urban Planning and Transportation UPT 2010, Corfu (Kerkyra), Greece, 2010.
[5.] Hobbs, F.D.; Traffic Planning & Engineering - Second Edition; Pergamon Press, 1979.
[6.] Roess, Roger P.; Prassas, Elena S.; McShane, William R.; Traffic Engineering, 3rd Edition, Pearson Prentice Hall, ISBN 0-13-142471-8, 2004.

ACTA TECHNICA CORVINIENSIS - Bulletin of Engineering

ISSN: 2067-3809 [CD-Rom, online]

ACTA TECHNICA CORVINIENSIS – Bulletin of Engineering
Tome VI (Year 2013) – FASCICULE 3 [July–September]
ISSN 2067–3809

[1.] G. SATYANARAYANA, [2.] Ch. VARUN, [3.] S.S. NAIDU

CFD ANALYSIS OF CONVERGENT-DIVERGENT NOZZLE

[1-3.] DEPARTMENT OF MECHANICAL ENGINEERING, MVGRCE, VIZIANAGARAM, 535005, (A.P.), INDIA

ABSTRACT: CFD is a branch of fluid mechanics that uses numerical methods and algorithms to solve and analyze problems that involve fluid flows. Computers are used to perform the calculations required to simulate the interaction of liquids and gases with surfaces defined by boundary conditions. In this thesis, CFD analysis of flow within Convergent-Divergent supersonic nozzle of different cross sections rectangular, square and circular has been performed. The analysis has been performed according to the shape of the supersonic nozzle and keeping the same input conditions. Our objective is to investigate the best suited nozzle which gives high exit velocity among the different cross sections considered. The application of these nozzles is mainly in torpedos. The work is carried out in two stages: 1.Modeling and analysis of flow for supersonic nozzles of different cross sections.2.Prediction of best suited nozzle among the nozzles considered. In this, initially modeling of the nozzles has been done in CATIA and later on mesh generation and analysis have been carried out in ANSYS FLUENT 12.0 and various contours like velocity, pressure, temperature have been taken and their variation according to different nozzles has been studied. Compared to square and circular nozzles, rectangular nozzle gives an increased velocity of about 23.93% and 24.47% respectively and an increased pressure drop of 22.93% and 23.97% respectively and an increased temperature drop of 42.56% and 43.68% respectively. It is found that fluid properties like velocity, pressure and temperature are largely dependent on the cross section of the nozzle which affects the flow within the nozzle and the extent of flow expansion.
KEYWORDS: convergent divergent nozzle

INTRODUCTION

Advances in computing technology, software and hardware have revolutionized the design process of engineering vehicles such as aircrafts, automobiles and ships. Many commercial software packages are being used in the design as well as analysis processes which not only save the lead time and costs of new designs, but also are used to study systems where controlled experiments are difficult or impossible to perform. In the area of fluid dynamics, there are many commercial Computational Fluid Dynamics (CFD) packages available for modeling flow in or around objects. Computational Fluid Dynamics (CFD) has been constantly developed over the past few decades and now both commercial and research codes can provide more and more robust and accurate results. Combined with the use of wind tunnel test data, CFD can be used in the design process to drive geometry changed instead of being used mainly as a design validation tool. Computational Fluid Dynamics (CFD) has become an integral part of the engineering design and analysis environment of many companies that require the availability to predict performance of new designs or processes before they are ever manufactured or implemented.

One of the most critical requirements for any CFD tool used for thermal applications is the ability to simulate flows along nozzles, turbines. Such challenging features has pressure gradients, shocks, velocity distribution, eddy location, stream line curvature, and stream wise vortices pose a challenge for computing. The small margins of improvement that are usually targeted in nozzle and turbines design today require precise tools capable of discerning small differences between alternate designs. Custom modeling tools that are based as simplified numerical methods and assumptions cannot provide accuracy that can be obtained with CFD, which offers mainly inherent advantages for ex: it offers quick and cheap solution and comparison to experimental solution and more accurate in comparison to empirical methods used in design. Accurate simulation of flows through the nozzle is important for prediction of velocity pattern and pressure pattern.

The current study aims analysis of flow through the nozzle and prediction of optimal axial clearance. Solution of flow along the nozzle involves only one phase of gas. Results are verified with the experimental data. As a part of project work nozzle studies carried out and with using same nozzle, axial gap / (Clearance determination) is analyzed. The results are in good agreement with the experimental ones.

MODELING OF THE COMPONENTS

Modeling the Supersonic Nozzle:

The coordinates are provided in Table 1, Table 2 for development of the 3D model of the supersonic

nozzle. For design purpose, the nozzle can be seen as an assembly of 3 separate sections operating in series a converging section, a throat and finally the diverging section. Different models of nozzles can be observed in Figure 1 to Figure 5.

Table 1: coordinates for end points of nozzle profile

Sl. No.	X (mm)	Y (mm)
1	4.000	0.000
2	5.000	1.000
3	5.000	2.854
4	6.810	9.191
5	14.639	17.129
6	25.915	23.387
7	37.497	27.252
8	54.685	32.100
9	78.997	32.100
10	63.282	28.688
11	38.482	23.303
12	29.197	19.638
13	23.628	15.216
14	21.553	11.526
15	20.525	5.000
16	20.525	1.000
17	21.525	1.000

Table 2: coordinates for arc centers

CENTERS	X (mm)	Y (mm)	RADIUS (mm)
C1	4.000	1.000	1.000
C2	17.000	2.854	12.000
C3	31.531	-7.360	29.750
C4	48.045	-29.780	57.589
C5	56.123	-47.842	77.370
C6	-47.118	-12.171	36.510
C7	39.334	1.158	21.079
C8	30.695	8.812	9.536
C9	50.985	2.284	38.556
C10	21.525	1.000	1.000

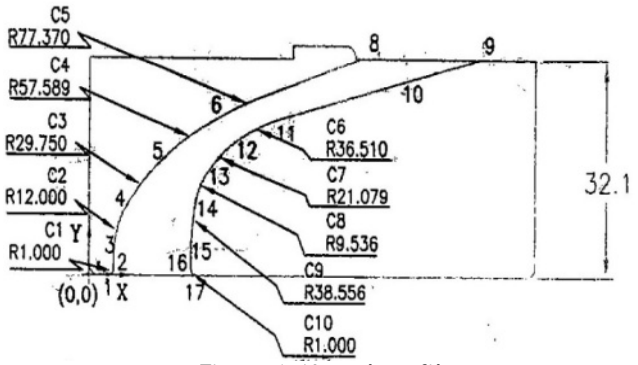

Figure 1: Nozzel profile

Figure 2: Geometry of rectangular bent nozzle

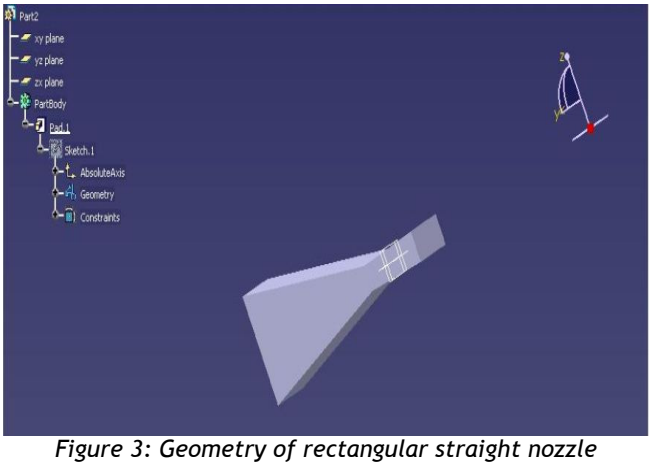

Figure 3: Geometry of rectangular straight nozzle

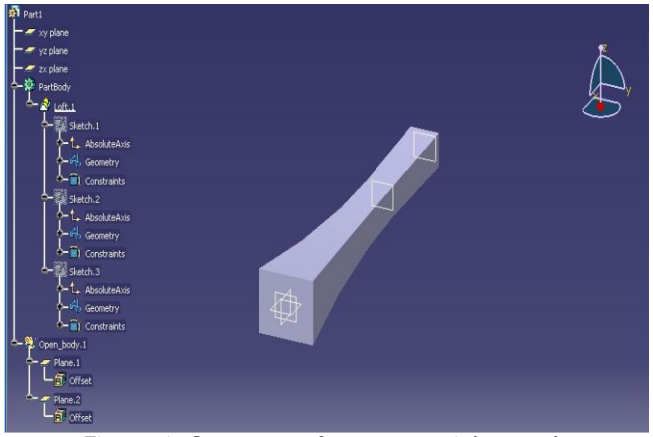

Figure 4: Geometry of square straight nozzle

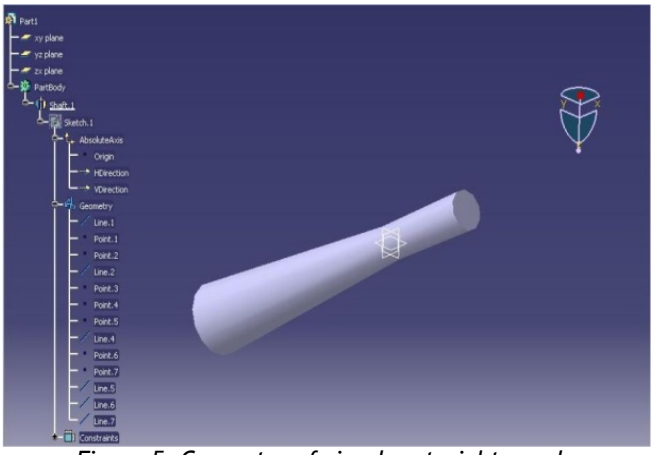

Figure 5: Geometry of circular straight nozzle

Conversion of nozzle geometry:

Taking the rectangular bent nozzle as reference and keeping the inlet, throat and exit areas and the axis length constant, three dimensional rectangular, square and circular straight nozzles geometries were generated.

Analysis of C-D nozzle:

The analysis and meshing is carried out in ANSYS FLEUNT software importing the conditions and the boundary values for the problem statement.

Meshing:

ANSYS FLUENT software is opened and the design file of C-D nozzle saved in CATIA is imported. And then the meshing of nozzle is done with inflation control is set to "Program Controlled" and the INLET, OUTLET and WALL named selections are defined and the meshing is updated.

Following this the scaling is done. Scale is set to mm. Grid created was changed to mm.

SOLVER AND MATERIAL SELECTION AND OPERATING CONDITION DEFINING

The solver is defined first. Solver is taken as Couple based and formulation as implicit, space as 3D and time as steady. Velocity formulation as absolute and gradient options as "Green gauss cell based" are taken. Energy equation is taken into consideration. The viscous medium is also taken. They analysis is carried using K-epsilon turbulence model.

The selection of material is done. Material selected is gas. The properties of gas taken as follows:

- *Density as Ideal gas*
- *C_p (Specific heat capacity) = 2034.6 J/Kg.K*
- *Thermal Conductivity = 0.0706 W/m.K*
- *Viscosity = 6.07 e-5 Kg/m.s*
- *Molecular Weight = 23.05 Kg/K.mol*

The analysis is carried out under operating condition of zero Pascal. Gravity is not taken into consideration.

BOUNDARY CONDITIONS

Nozzle Inlet:

Pressure inlet was taken as inlet for nozzle. The value of pressure is 8101325 Pascal. Initial gauge pressure was taken as 7898681 Pascal. Temperature was taken as 1583 K.

Nozzle Outlet:

The nozzle outlet is set as pressure outlet with a value of 13e5.

Controls Setup:

The solution controls are set as listed below:

- *Turbulence Kinetic Energy = 0.8*
- *Turbulence Dissipation rate = 0.8*
- *Turbulence Viscosity = 1*

The under relaxation factor was given as given.

Discretization Equation is selected as given:

- *Flow (Second order up wind)*
- *Turbulence Kinetic Energy (1st order upwind)*
- *Turbulence Dissipations rate (1st order upwind)*

Initialization:

Solution initialization is done. Initial value of velocity is taken as 186.3 m/s.

Temperature is taken as 1583 K.

Residual monitoring is done and convergence criteria are set up. The convergence criteria of various parameters are listed below.

Continuity	-	*0.001*
X Velocity	-	*0.001*
Y Velocity	-	*0.001*
Z Velocity	-	*0.001*

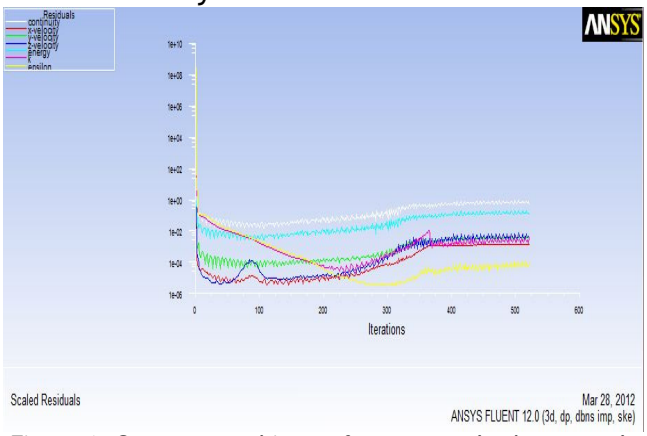

Figure 6: Convergence history for rectangular bent nozzle

The number of iterations is set up and iterations start.

The iterations continue till the convergence is reached and convergence history as shown in Figure 6 to Figure 9.

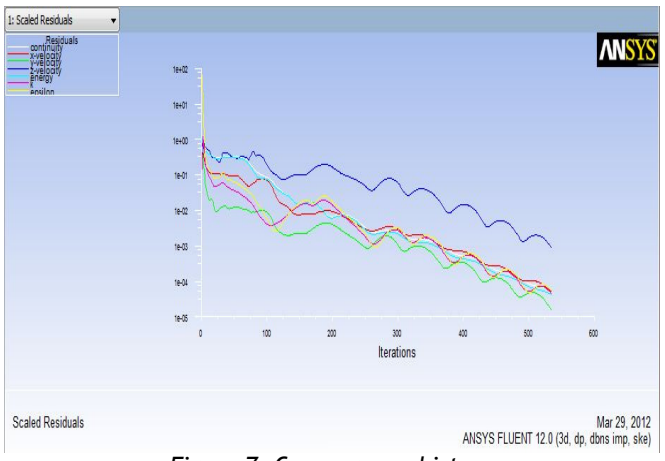

Figure 7: Convergence history for rectangular straight nozzle

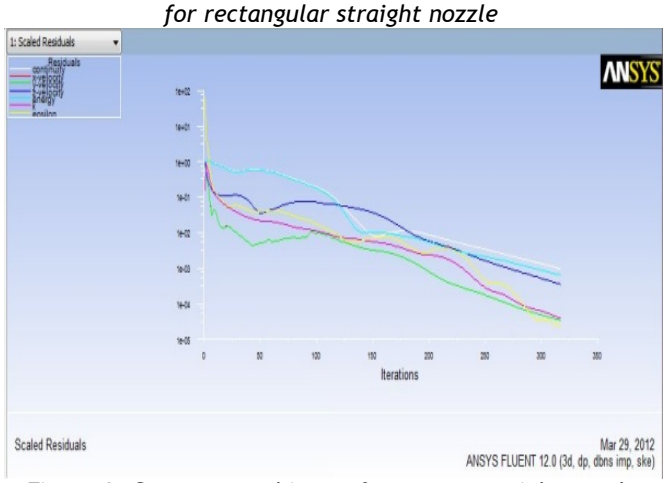

Figure 8: Convergence history for square straight nozzle

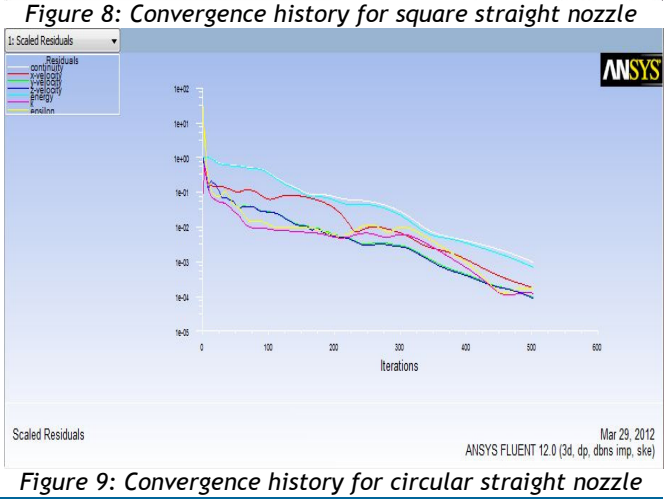

Figure 9: Convergence history for circular straight nozzle

THEORETICAL CALCULATIONS OF C-D NOZZLE

Properties of Gases:

- *GAMA of gases (γ)=1.27*
- *Thermal Conductivity [K]=0.0706 W/m.K*
- *Molecular Weight=23.05 Kg/K.mol*
- *Specific heat of gases (C_p)=2034.6 J/Kg.K*
- *Density treated as Ideal gas*
- *Gas constant (R) =432*
- *Viscosity=6.07e-5 Kg/m.s*

Boundary (Inlet/Exit) Conditions:

- *NPR (Nozzle Pressure Ratio) =6.16*
- *Inlet pressure= 80 bar*

- Exit pressure= 12.987 bar
- Inlet temperature=1583 K

Geometrical Parameters:

Throat area =2.85e-5 m^2

Given Inlet Mach number= 0.2

Mach number definition: M=V/C 1(a)

C is acoustic velocity

$$C = \sqrt{\gamma RT} \quad 1(b)$$

$$C = \sqrt{(1.27)(432)(1583)} = 931.931$$

Inlet Velocity is $\frac{V}{931.931} = 0.2$

V = 186.3 m/sec

Throat Pressure $\frac{P_T}{P_l} = \left(\frac{2}{n+1}\right) n/(n-1)$ 1(c)

P_T = 44.096 bar

Velocity at throat: P = ρRT 1(d)

$80x10^5 = \rho\ (432)\ (1583)$

$\rho = 11.698\ kg/m^3$

$$V_T = \sqrt{\frac{2n}{n-1} P_l V \left(1 - \left(\frac{P_T}{P_l}\right)^{\frac{n-1}{n}}\right)} = \quad 1(e)$$

$$= \sqrt{\frac{2\times 1.27}{0.27} \cdot \frac{80\times 10^5}{11.698}\left(1 - \left(\frac{44.096}{80}\right)^{\frac{0.27}{1.27}}\right)} = 874.78 m/sec$$

Velocity at exit:

$$V_E = \sqrt{\frac{2n}{n-1} P_l V_l \left(1 - \left(\frac{P_E}{P_l}\right)^{\frac{n-1}{n}}\right)} = \quad 1(f)$$

$$= \sqrt{\frac{2\times 1.27}{0.27} \cdot \frac{80\times 10^5}{11.698}\left(1 - \left(\frac{1}{6.16}\right)^{\frac{0.27}{1.27}}\right)} = 1436\ m/sec$$

So by the above results Exit Mach number is

$$M = \frac{V_e}{C} = \frac{1436}{931.931} = 1.54$$

Known relation, Mach number related with other parameters,

$$\frac{A_E}{A_T} = \frac{1}{M_{Exit}}\left[\frac{1 + \frac{(\gamma-1)}{2} M_{Exit}^2}{\frac{(\gamma+1)}{2}}\right]^{\frac{(\gamma+1)}{2(\gamma-1)}} \quad 1\ (g)$$

$$\frac{A_E}{A_T} = \frac{1}{1.54}\left[\frac{1 + \frac{0.27}{2}(1.54)^2}{\frac{2.27}{2}}\right]^{\frac{1.27}{2(0.27)}}$$

$$\frac{A_E}{A_T} = 1.255$$

So $A_{EXIT} = 0.3495\times 10^{-4} m^2$; $A_{THROAT} = 0.285\times 10^{-4} m^2$

RESULTS AND DISCUSSION

Results for nozzle:

Nozzle profile which is examined is considered in 3D. Flow through the nozzle for given input condition with velocity as 183.6 m/s and maximum output was observed as 1436 m/s such that Mach number is increased from 0.2 to 1.54 in which nozzle is acting as supersonic nozzle. The velocity contours of nozzle are plotted in Figure 10 to Figure 12. The pressure contours of nozzle is plotted in Figure 14 to Figure 17 and temperature contours of nozzle is plotted in Figure 18 to Figure 21. The velocity, temperature, Mach number and pressure variation along the nozzle is compared with theoretical calculation and with experimental too.

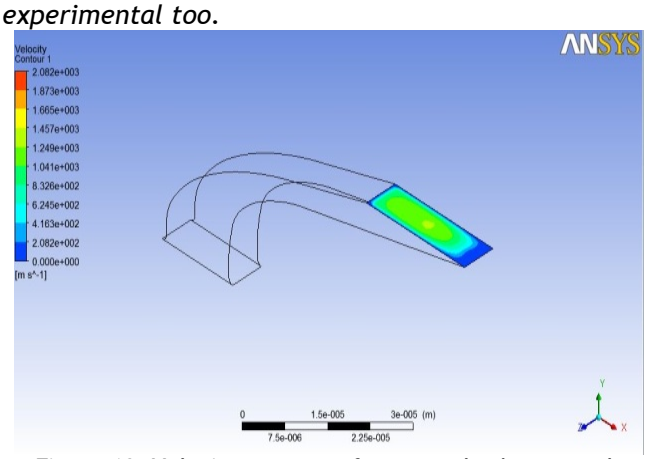

Figure 10: Velocity contour of rectangular bent nozzle

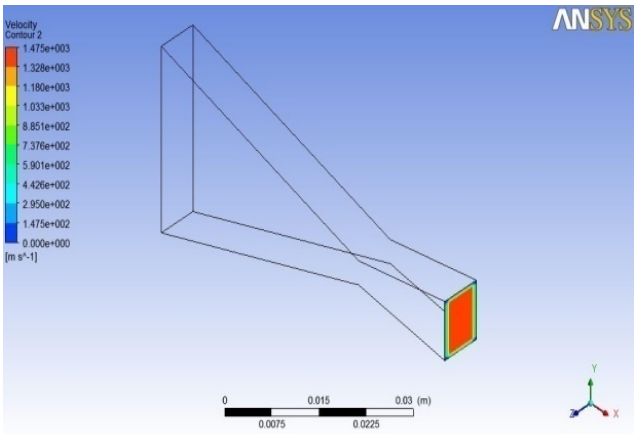

Figure 11: Velocity contour of rectangular straight nozzle

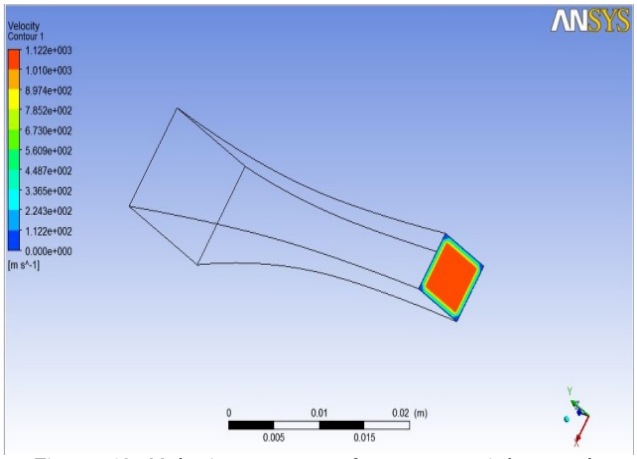

Figure 12: Velocity contour of square straight nozzle

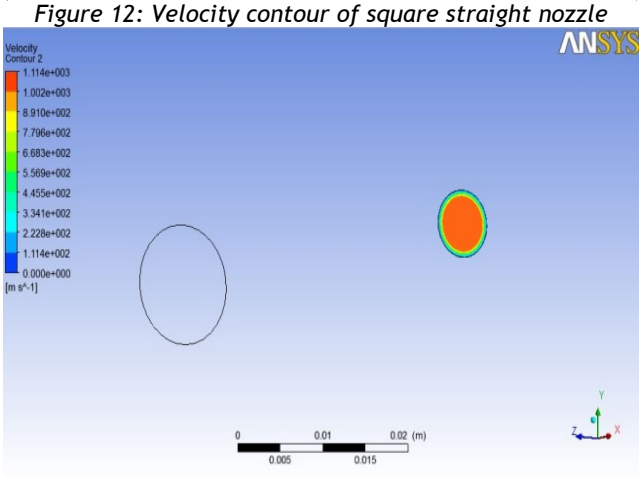

Figure 13: Velocity contour of circular straight nozzle

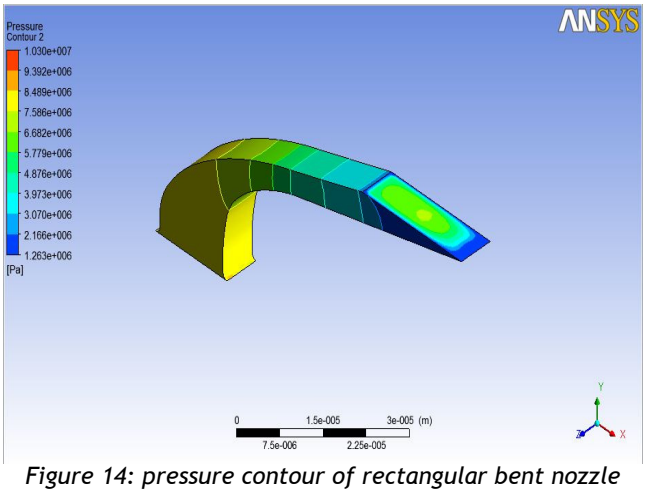

Figure 14: pressure contour of rectangular bent nozzle

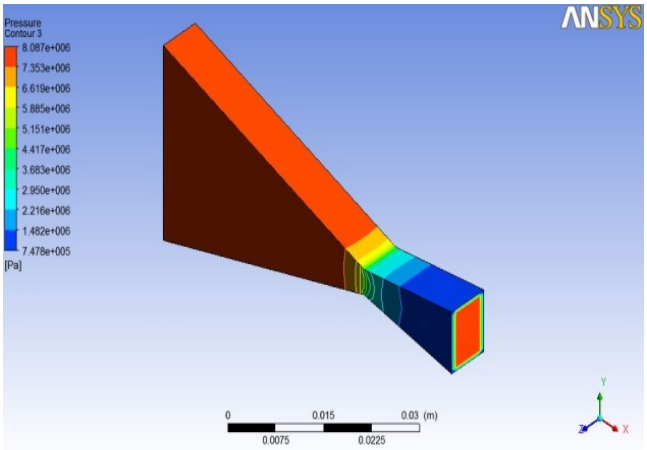

Figure 15: pressure contour of rectangular straight nozzle

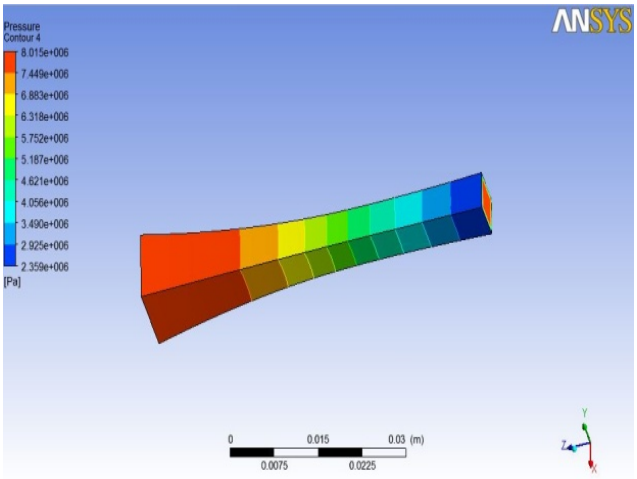

Figure 16: pressure contour of square straight nozzle

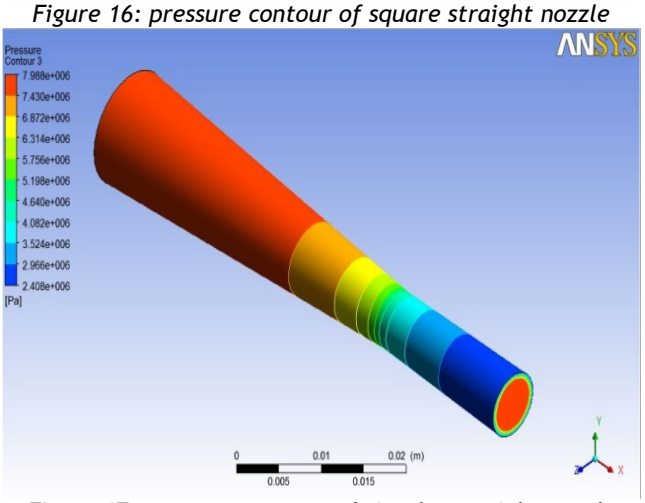

Figure 17: pressure contour of circular straight nozzle

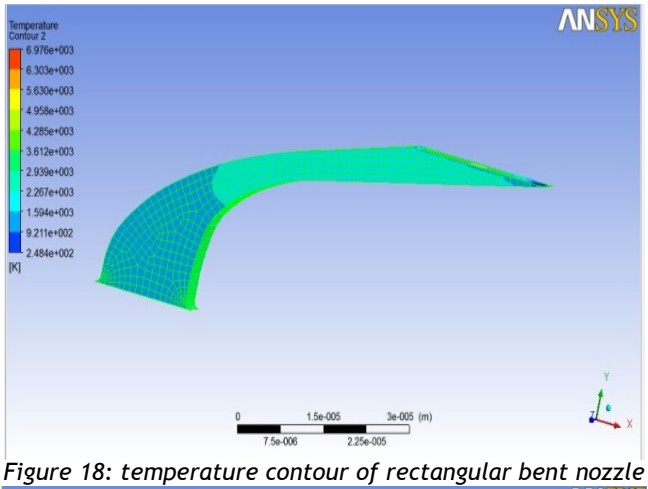

Figure 18: temperature contour of rectangular bent nozzle

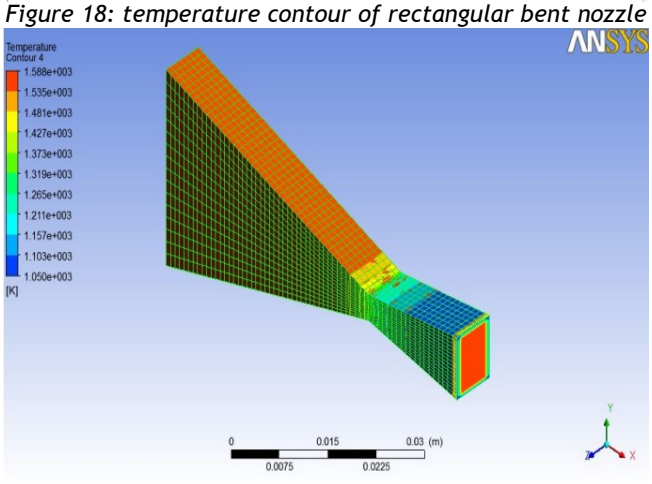

Figure 3.19: temperature contour of rectangular straight nozzle

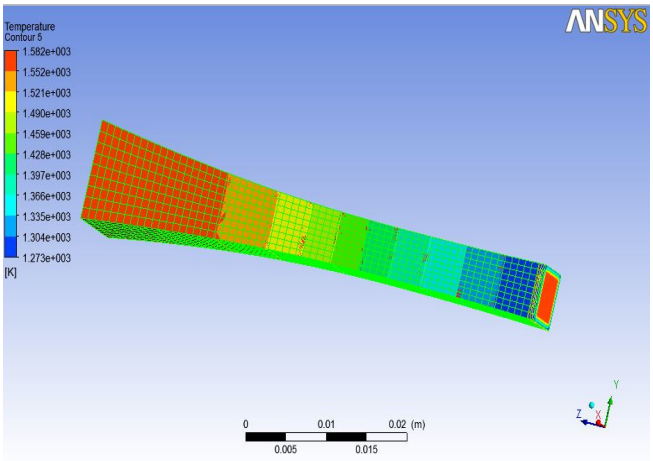

Figure 3.20: temperature contour of square straight nozzle

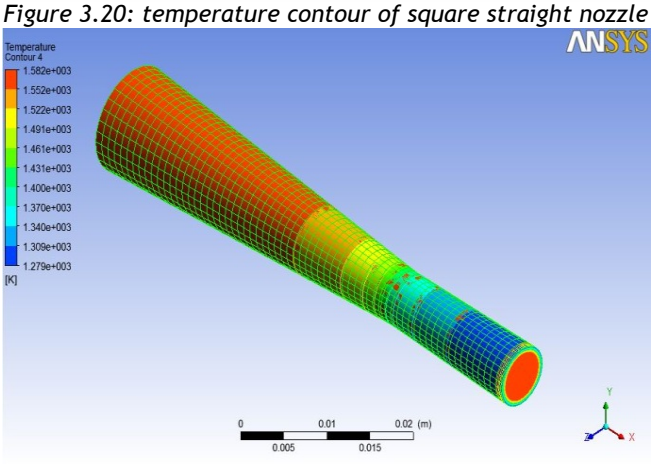

Figure 3.21: temperature contour of circular straight nozzle

These three results are good in agreement with each other.

Velocity contours:

By observing the velocity contours for rectangular bent in shape nozzle. Exit velocity and throat velocity and same as the theoretical calculations, and maximum incurred velocity is in this nozzle is ranging from the input value to 2082 m/s. For the same inlet and outlet condition and keeping the inlet, exit, throat area as like bent in shape rectangular nozzle is allowed to pass through straight in rectangular shape nozzle the maximum velocity incurred in this case is from inlet valve to 1475 m/s the same flow is allowed for straight in square shape nozzle the maximum velocity incurred is of range 1122 m/s. The same flow is allowed for straight circular in shape nozzle the maximum velocity incurred is of range 1114 m/s to minimum the machining cost of rectangular bent in shape nozzle, we can use straight in rectangular shape nozzle.

Pressure contours:

By pressure contours observation we conclude that maximum pressure incurred is of range 103 bar for bent rectangular shape. In straight rectangular nozzle maximum pressure will reach till the throat and drives to increase the exit velocity and in this pressure contours the maximum pressure incurred is of 80 bar. In straight square nozzle the pressure will not reach maximum length and velocity obtained is of range 1122 m/s at exit.

In circular straight shape nozzle maximum incurred pressure is of 79 bar and incurred maximum velocity is of 1114 m/s velocity at exit.

Temperature contours:

Temperature contours obtained for rectangular bent in shape is at range of 6976 K which is a very high value compared to the rectangular straight in shape nozzle. For exit velocity of 1475 m/s the maximum temperature value in the contours is 1588 K and impact of temperature reach till the throat is very high when compared to circular and square in shape nozzles.

CONCLUSIONS

From the investigation we have done, the following conclusions have been drawn.

- *CFD analysis has been done on Convergent-Divergent nozzles of different cross sections like rectangular, square and circular.*
- *It has been found that rectangular nozzle gives a velocity of 1475 m/s where as square nozzle gives a velocity of 1122 m/s and circular nozzle gives a velocity of 1114 m/s.*
- *Thus, rectangular nozzle gives an increased velocity of about 23.93% compared to square nozzle and about 24.47% compared to circular nozzle.*
- *Velocity increases when pressure drops. It has been found that rectangular nozzle gives a pressure drop of 73.392 bar where as square nozzle gives a pressure drop of 56.56 bar and circular nozzle gives a pressure drop of 55.8 bar.*
- *Thus, rectangular nozzle gives an increased pressure drop of about 22.93% compared to square nozzle and about 23.97% compared to circular nozzle.*
- *It has been found that rectangular nozzle gives a temperature drop of 538 K where as square nozzle gives a temperature drop of 309 K and circular nozzle gives a temperature drop of 303 K.*
- *Thus, rectangular nozzle gives an increased temperature drop of about 42.56% compared to square nozzle and about 43.68% compared to circular nozzle.*
- *Hence, it has been found from the results that rectangular nozzle gives high exit velocity, high pressure drop and high temperature drop along the nozzle compared to square and circular nozzles.*
- *Computational results are in good agreement with the experimental results of N.S.T.L. and also with the theoretical results published in the literature.*

Nomenclature

CO	*carbon monoxide*
HC	*hydro carbon*
NO_x	*oxides of nitrogen*
CO_2	*carbon dioxide*
HSU	*Hatridge smoke unit*
BTDC	*before top dead centre*
Y	*total percentages of uncertainty*

REFERENCES

[1] *A.A.Khan and T.R.Shem bharkar, "Viscous flow analysis in a Convergent-Divergent nozzle". Proceedings of the international conferece on Aero Space Science and Technology, Bangalore, India, June 26-28, 2008.*

[2] *H.K.Versteeg and W.Malala Sekhara, "An introduction to Computational fluid Dynamics", British Library cataloguing pub, 4th edition, 1996.*

[3] *David C.Wil Cox, "Turbulence modeling for CFD" Second Edition 1998.*

[4] *S.Majumdar and B.N.Rajani, "Grid generation for Arbitrary 3-D configuration using a Differential Algebraic Hybrid Method, CTFD Division, NAL, Bangalore, April 1995.*

[5] *Layton, W.Sahin and Volker.J, "A problem solving approach using Les for a backward facing-step" 2002.*

[6] *M.M.Atha vale and H.Q. Yang, "Coupled field thermal structural simulations in Micro Valves and Micro channels" CFD Research Corporation.*

[7] *Lars Davidson, "An introduction to turbulence Models", Department of thermo and fluid dynamics, Chalmers university of technology, Goteborg, Sweden, November, 2003.*

[8] *Kazuhiro Nakahashi, "Navier-Stokes Computations of two and three dimensional cascade flow fields", Vol.5, No.3, May-June 1989.*

ACTA TECHNICA CORVINIENSIS – Bulletin of Engineering

ISSN: 2067-3809 [CD-Rom, online]

ACTA TECHNICA CORVINIENSIS – Bulletin of Engineering
Tome VI (Year 2013) – FASCICULE 3 [July–September]
ISSN 2067–3809

Scientific Events in 2013

1. THE 5th INTERNATIONAL CONFERENCE ON GEARS WITH EXHIBITION – GEARS 2013
7 – 9 October, 2013, Garching (near Munich), GERMANY

The fifth international conference on gears and transmissions in Germany will become a broad platform for equipment manufacturers and producers and researchers of gear and transmission systems to present new solutions and their latest research results.

Climate change is one of the big issues in public discussion, in politics and industry. The conference will show, what the transmission and drive train industry can contribute to increase energy efficiency. Gears are vital in the efficiency of different applications. They transmit and vary torque between prime movers and applications.

There is still room for improvement, which will be demonstrated by the presenters. New concepts for drive trains of energy supply systems provide answers to the increasing demand for energy worldwide. These concepts must be introduced to global markets more quickly. Therefore, new designs are necessary and will be presented at the conference.

The state-of-the-art of industrial applications will be demonstrated at an exhibition beside the conference.

The conference will last three days, comprising keynote addresses and presentations in a series of plenary and parallel sessions. The official language of the conference will be English. No simultaneous translation will be provided. The conference program and the registration form will be available in June 2013.

Detailed informations here: www.vdi-gears.eu

2. THE 7th INTERNATIONAL SCIENTIFIC-PROFESSIONAL CONFERENCE – SB 2013 "CONTEMPORARY PRODUCTION PROCESSES, EQUIPMENT AND MATERIALS FOR WELDED CONSTRUCTIONS AND PRODUCTS"
23 – 25 October, 2013, Slavonski Brod, CROATIA

During last six meetings this conference had gathered number of experts and scientists who presented and introduced novelty in welding profession. Due to that, for the seventh time, organizers call everyone who can give their contribution to the area of welding technology and welding related techniques, automation and robotization in production of welded constructions, and all others that can, in any other way, give their contribution to development of welding practice, to present their scientific and professional knowledge and experiences.

This year, also, there will be the exhibition of welding devices, filler metals and equipment, and all presented papers will be published i the conference proceedings and CD media. We thank to all our present partners of this conference for their contribution and welcome you in Slavonski Brod.

Topics of interest for the conference should be related but not limited to the following thematic focuses:

- *New technologies and materials*
- *Welding processes*
- *Robotization and automation*
- *Pressure vessels*
- *Welding related techniques*
- *Manufacturing of welded construction*
- *Quality control of welded products*
- *Reliability and safety of welded productions and constructions*
- *Weldability of materials*
- *Filler metals*
- *Equipment for welding and welding related techniques*
- *Personnel and education in welding*

- *Metallurgy*
- *Ecology and occupational health*
- *Economical aspects of welding*

Detailed informations here: http://www.sfsb.hr/dtzsb/

3. FEDERATED CONFERENCE ON COMPUTER SCIENCE AND INFORMATION SYSTEMS – FedCSIS 2013
8 – 11 September, 2013, Kraków, POLAND

The 2013 Federated Conference on Computer Science and Information Systems cordially invites you to consider contributing an Event (conference, symposium, workshop, consortium meeting, special session). The FedCSIS multi-conference consists of a significant number of recurring Events, but proposals for new associated Events are welcome until January 14, 2013. The Events can run over any span of time within the conference dates, from half-day to three days.
The FedCSIS Events provide a platform for bringing together researchers, practitioners, and academia to present and discuss ideas, challenges, and potential solutions on established or emerging topics related to research and practice in computer science and information systems.
The Events will be selected based on the scientific/technical interest and/or their relevance to practitioners in their topics, the clarity of the proposal in addressing the requested information, the innovativeness of the Event topics, and the capacity in the FedCSIS multi-conference program.
Detailed informations here: www.fedcsis.org

4. INTERNATIONAL CONFERENCE on MATHEMATICAL MODELING in PHYSICAL SCIENCES - IC-MSQUARE 2013
1- 5 September, 2013, Prague, CZECH REPUBLIC

It is our pleasure to circulate the announcement of the 2nd International Conference on Mathematical Modeling in Physical Sciences, IC-MSQUARE 2013. The conference aims to promote the knowledge and the development of high-quality research in mathematical fields that have to do with the applications of other scientific fields and the modern technological trends that appear in them, these fields being those of Physics, Chemistry, Biology, Medicine, Economics, Sociology, Environmental sciences etc.
IC-MSQUARE-2013 topics encompass, but are not restricted to, the following areas:

- *mathematical modeling in Fundamental Physics*
- *evolutionary computation*
- *complex physical and technical systems*
- *software and computer complexes for experimental data processing*
- *qualitative modeling including fuzzy and iterative approaches to modeling*
- *nonlinear problems*
- *computational chemistry, biology, and biophysics*
- *new generation computing tools, distributed scientific computing*
- *computational modeling in engineering and science*
- *multiscale modeling, multiphysics modeling*
- *progress in discretization methods*
- *financial mathematics and mathematics in economics etc.*

You may find details of the Conference visiting the Conference website at http://www.icmsquare.net.

5. IV. CENTRAL EUROPEAN CONFERENCE ON LOGISTICS – CECOL 2013
5 – 7 November, 2013, Magdeburg, GERMANY

As a result of the scientific collaboration among higher education centers of the central European zone and three previous successful editions held in Miskolc, Hungary (2010), Częstochowa, Poland (2011), Trnava, Slovak Republic (2012) the Institute of Logistics and Material Handling Systems (ILM), belonging to the Faculty of Mechanical Engineering (FMB) is proud to announce that the 4th Central European Conference on Logistics (CECOL 2013) will be held in the city of Magdeburg, Germany, during November 5th-7th, 2013.
The CECOL 2013 will provide a high-level international platform for academicians and practitioners from all over the world, to present their research results and development activities in the broad field of logistics. This way, the organizing committee is pleased to invite prospective authors to submit their original manuscripts to the conference. Topics of interest for the conference should be related but not limited to the following thematic focuses:

1. *Modeling and simulation in logistics*
2. *Logistics process analysis and planning*
3. *Localization, navigation and communication in transportation and logistics*
4. *Manufacturing process and logistics networks simulations*
5. *Production planning and scheduling*
6. *Maintenance and robot implementation into the logistic processes*
7. *New teaching and research approaches in logistics*

For any further information, we recommend you the conference website: www.ilm.ovgu.de/cecol2013.

6. INDUSTRIAL ENGINEERING AND ENVIRONMENTAL PROTECTION
30th October, 2013, Zrenjanin, SERBIA

The conference provides forum for discussion and exchange of experiences between people from government, state agencies, universities and research institutions, and practitioners from industry.
Framework scientific topics of the conference:

1. *Process Technology*
2. *Engineering Environmental Protection and safety at work*

3. Manufacturing technologies and materials
4. Maintenance
5. Design and maintenance of process plants
6. Basic operations, machinery and processes
7. Computer technologies and engineering education
8. Biotechnology
9. Reengineering and project management
10. Process management
For any further information, we recommend you the website: http://www.tfzr.uns.ac.rs/ieep/index.php

7. THE 7th INTERNATIONAL CONFERENCE INTERDISCIPLINARITY IN ENGINEERING - INTER-ENG 2013
10 - 11th October, 2013, Tirgu Mures, ROMANIA

It is with great pleasure that the "Petru Maior" University of Tîrgu Mures - Faculty of Engineering in collaboration with Romanian Academy of Technical Sciences invites you to the International Conference Interdisciplinarity in Engineering INTER-ENG 2013. The conference will be jointly organized and hosted by the Department of Industrial Engineering and Management and the Department of Electrical Engineering and Computer Science of "Petru Maior" University of Tîrgu Mures.
The main theme of the Conference is announced as: "Advanced technologies for the next-generation manufacturing processes". The conference scope is to provide a professional and scientific forum for engineers and research scientists from universities, research centers and to present research works, contributions and recent developments as well as current practices in engineering. The INTER-ENG conference will also offer the opportunity for companies in engineering to present their products and services. This conference aims to bring together the researchers, scientists, professors, graduate students and civil society organizations and their representatives to share and to discuss theoretical and practical knowledge in the scientific environment. In this edition special attention will be given to young professional orientation to technical studies, that will be invited to participate in plenary sessions, but a Workshop will also be hold for both teachers and students from high schools, with the theme of Vocational education and training in engineering and industrial management.
The conference will promote dialogue on how to comprehend and develop advanced engineering technologies and achieve next-generation industrial manufacturing in the interdisciplinary context from different fields: mechanics, electronics, informatics, etc.
The Inter-Eng Conference drives innovation and enterprise, creating new technologies and developing applications and intellectual property for the benefit of the society. The event will develop thinking on modeling for future engineering technologies.
For any further information, we recommend you the INTER-ENG 2013 conference website: http://www.inter-eng.upm.ro/2013/

8. INTERNATIONAL ELECTRICAL ENGINEERING CONFERENCE FOR YOUNG RESEARCHERS - IEECYR2013
23 - 26 October, 2013, Cluj Napoca, ROMANIA

It is a great pleasure and an honor to extend you a warm invitation to attend the 2013 International Electrical Engineering Conference for Young Researchers organised by Technical University of Cluj-Napoca, to be held October 23-26, 2013 in Cluj-Napoca, Romania.
The role of Electric Engineering and Power Systems is becoming more and more important as most domains are directly dependent of it. Whether your interests are in Electrical Engineering, Power Systems, Computer Science, Telecomunications, Robotics or Automations join hundreds of fellow PhDs, young academic staff and researchers from throughout the world to engage in a focused, 2-day series of workshops, presentations, technical sessions and seminars covering the main topics of interests.
The conference will be held from 23rd to 26th of October, 2013 in Cluj-Napoca, the heart of Transylvania and the European Youth Capital (2015), Romania.
For any further information, we recommend you the conference website: http://www.ieecyr2013.org/

9. INTERNATIONAL CONFERENCE ON MECHANICAL, AUTOMOTIVE AND AEROSPACE ENGINEERING 2013 - ICMAAE '13
2 - 4 July, 2013, Kuala Lumpur, MALAYSIA

The Department of Mechanical Engineering, Faculty of Engineering, International Islamic University Malaysia is organizing this International Conference on Mechanical, Automotive and Aerospace Engineering to bring together researchers and engineering professionals from all over the globe to meet and deliberate in the beautiful green city of Kuala Lumpur, during the period July 2-4, 2013. The forum will also provide a platform for entrepreneurs to seek partnership with scientists and engineers and enhance commercialization of ideas, inventions and products.
Main topics include the general areas of:
- *Mechanical Engineering*
- *Aerospace Engineering*
- *Automotive Engineering*

For any further information, we recommend you the website: http://www.iium.edu.my/icmaae/2013

10. INTERNATIONAL CONFERENCE ON ENGINEERING & BUSINESS EDUCATION, INNOVATION AND ENTREPRENEURSHIP
18 - 21 October 2012, Sibiu, ROMANIA

Lucian Blaga University of Sibiu (LBUS) started to organize the Balkan Region Conference on Engineering Education (BRCEE) in 2003, with an important support from UNESCO International Centre for Engineering

Education. There were 2 very successful editions in 2003 and 2005 when participants from all over the world published scientific papers that were included in internationally recognized proceedings. In 2007, the year when Sibiu was declared European Capital of Culture, a joint conference was organized together with another international periodical conference organized by LBUS - MSE (Manufacturing Science and Engineering). In 2009 we decided to broaden the international dimension of the conference and we agreed, together with Hochschule Wismar, University of Technology Business and Design to organize the BRCEE together with the International Conference on Engineering and Business Education at the 2nd conference, the first one being organized in 2008 in Wismar, Germany.
Comprises three international events:
- *6th Balkan Region Conference on Engineering and Business Education*
- *5th International Conference on Engineering and Business Education*
- *4th International Conference on Innovation and Entrepreneurship*

For any further information, we recommend you the website: http://cedc.ro/conf.brcee/

11. INTERNATIONAL CONFERENCE "MATHEMATICAL METHODS IN ENGINEERING" - MME 2013
22 - 26 July, 2013, Porto, PORTUGAL

The International Conference "MATHEMATICAL METHODS IN ENGINEERING" will be held in the Institute of Engineering of the Polytechnic of Porto, Portugal, July 22-26, 2013. The aim of this conference is to bring together scientists and engineers to present and discuss some recent developments in the area of Mathematical Methods in Engineering. The conference is designed to maximize the involvement of all participants and will present the state of the art research and the latest achievements.
For any further information, we recommend you the website: http://www.dma.isep.ipp.pt/mme2013/

12. THE 13th INTERNATIONAL CONFERENCE "RESEARCH AND DEVELOPMENT IN MECHANICAL INDUSTRY" - RaDMI 2013
12 - 15 September, 2013, Kopaonik, SERBIA

The 13th International Conference "Research and Development in Mechanical Industry" - RaDMI 2013 will be held on 12-15. September 2013, in Kopaonik, Serbia.
TOPICS:
- *Research & development of manufacturing systems, tools & technologies, new materials & product design;*
- *Tribology;*
- *Maintenance and effectiveness of technical systems;*
- *Quality management, ISO 9000, ISO 14000, TQM and management in mechanical engineering;*
- *Application of information technologies and electronics in mechanical engineering:*
- *Transport systems and logistics and*
- *Application of mechanical engineering in other industrial fields.*

Website: http://www.RaDMI.org/

ACTA TECHNICA CORVINIENSIS - BULLETIN of ENGINEERING

ISSN: 2067-3809 [CD-Rom, online]

ACTA TECHNICA CORVINIENSIS – Bulletin of Engineering
Tome VI (Year 2013) – FASCICULE 3 [July–September]
ISSN 2067–3809

MANUSCRIPT PREPARATION – General Guidelines

These instructions are written in a form that satisfies all of the formatting requirements for the author manuscript. Please use them as a template in preparing your manuscript. Authors must take special care to follow these instructions concerning margins. The basic instructions are simple:

- *Manuscript shall be formatted for an A4 size page.*
- *The top and left margins shall be 25 mm.*
- *The bottom and right margins shall be 25 mm.*
- *The text shall have both the left and right margins justified.*

The original of the technical paper will be sent through e-mail as attached document (.doc, Windows 95 or higher). Manuscripts should be submitted to e-mail: redactie@fih.upt.ro, with mention "for **ACTA TECHNICA CORVINIENSIS – Bull. of Eng.**".*

STRUCTURE

The manuscript should be organized in the following order: Title of the paper, Authors' names and affiliation, Abstract, Key Words, Introduction, Body of the paper (in sequential headings), Conclusion, Acknowledgements (where applicable), References, and Appendices (where applicable).

THE TITLE

The title is centered on the page and is CAPITALIZED AND SET IN BOLDFACE (font size 14 pt). It should adequately describe the content of the paper. An abbreviated title of less than 60 characters (including spaces) should also be suggested.

AUTHOR'S NAME AND AFFILIATION

The author's name(s) follows the title and is also centered on the page (font size 11 pt). A blank line is required between the title and the author's name(s). Last names should be spelled out in full and succeeded by author's initials. The author's affiliation (in font size 11 pt) is provided below. Phone and fax numbers do not appear.

ABSTRACT

A nonmathematical abstract, not exceeding 200 words, is required for all papers. It should be an abbreviated, accurate presentation of the contents of the paper. It should contain sufficient information to enable readers to decide whether they should obtain and read the entire paper. Do not cite references in the abstract.

KEY WORDS

The author should provide a list of three to five key words that clearly describe the subject matter of the paper.

TEXT LAYOUT

The manuscript must be typed single spacing. Use extra line spacing between equations, illustrations, figures and tables. The body of the text should be prepared using Georgia or Times New Roman. The font size used for preparation of the manuscript must be 11 points. The first paragraph following a heading should not be indented. The following paragraphs must be indented 10 mm. Note that there is no line spacing between paragraphs unless a subheading is used. Symbols for physical quantities in the text should be written in italics.

FIGURES AND TABLES

Figures (diagrams and photographs) should be numbered consecutively using Arabic numbers. They should be placed in the text soon after the point where they are referenced. Figures should be centered in a column and should have a figure caption placed underneath. Captions should be centered in the column, in the format "Figure 1" and are in upper and lower case letters. When referring to a figure in the body of the text, the abbreviation "Figure" is used Illustrations must be submitted in digital format, with a good resolution. Table captions appear centered above the table in upper and lower case letters. When referring to a table in the text, "Table" with the proper number is used. Captions should be centered in the column, in the format "Table 1" and are in upper and lower case letters. Tables are numbered consecutively and independently of any figures. All figures and tables must be incorporated into the text.

EQUATIONS AND MATHEMATICAL EXPRESSIONS

Equation numbers should appear in parentheses and be numbered consecutively. All equation numbers must appear on the right-hand side of the equation and should be referred to within the text.

CONCLUSION

A conclusion section must be included and should indicate clearly the advantages, limitations and possible applications of the paper. Discuss about future work.

ACKNOWLEDGEMENTS

An acknowledgement section may be presented after the conclusion, if desired. Individuals or units other than authors who were of direct help in the work could be acknowledged by a brief statement following the text.

REFERENCES

References should be listed together at the end of the paper in alphabetical order by author's surname. List of references indent 10 mm from the second line of each references. Personal communications and unpublished data are not acceptable references.

***Journal Papers**: Surname 1, Initials; Surname 2, Initials and Surname3, Initials: Title, Journal Name, volume (number), pages, year.*

***Books**: Surname 1, Initials and Surname 2, Initials: Title, Edition (if existent), Place of publication, Publisher, year.*

***Proceedings Papers**: Surname 1, Initials; Surname 2, Initials and Surname 3, Initials: Paper title, Proceedings title, pages, year.*

ACTA TECHNICA CORVINIENSIS - BULLETIN of ENGINEERING

ISSN: 2067-3809 [CD-Rom, online]

Indexes & Databases

ACTA TECHNICA CORVINIENSIS – BULLETIN of ENGINEERING

*is accredited and ranked in the **"B+" CATEGORY** Journal by **CNCSIS – The National University Research Council's Classification of Romanian Journals (poz. 940)**. The Journal is a part of the **SCIPIO – The Romanian Editorial Platform.***

ACTA TECHNICA CORVINIENSIS – BULLETIN of ENGINEERING

is indexed and covered in the following databases and directories:

INDEX COPERNICUS – JOURNAL MASTER LIST

http://journals.indexcopernicus.com/

GENAMICS JOURNALSEEK Database

http://journalseek.net/

DOAJ – Directory of Open Access Journals

http://www.doaj.org/

EVISA Database

http://www.speciation.net/

CHEMICAL ABSTRACTS SERVICE (CAS)

A division of the American Chemical Society
http://www.cas.org/

EBSCO Publishing

http://www.ebscohost.com/

GOOGLE SCHOLAR

http://scholar.google.com

SCIRUS - Elsevier

http://www.scirus.com/

ULRICHSweb - Global serials directory

http://ulrichsweb.serialssolutions.com

getCITED

http://www.getcited.org

BASE - Bielefeld Academic Search Engine

http://www.base-search.net

Electronic Journals Library

http://rzblx1.uni-regensburg.de

Open J-Gate

http://www.openj-gate.com

ProQUEST Research Library

http://www.proquest.com

ACTA TECHNICA CORVINIENSIS - BULLETIN of ENGINEERING

ISSN: 2067-3809 [CD-Rom, online]

ACTA TECHNICA CORVINIENSIS
– BULLETIN of ENGINEERING

ACTA TECHNICA CORVINIENSIS
– BULLETIN of ENGINEERING
ISSN: 2067-3809 [CD-Rom, online]

http://acta.fih.upt.ro

ACTA TECHNICA CORVINIENSIS
BULLETIN OF ENGINEERING

ISSN: 2067-3809

fascicule 3
[July-September]

TOME VI
[2013]